Universitäts-Sternwarte
München

Radiative Transfer, Stellar Atmospheres and Winds

Five lectures (four hours each) within the IMPRS advanced course

Joachim Puls

University Observatory Munich

Radiative transfer, stellar atmospheres and winds

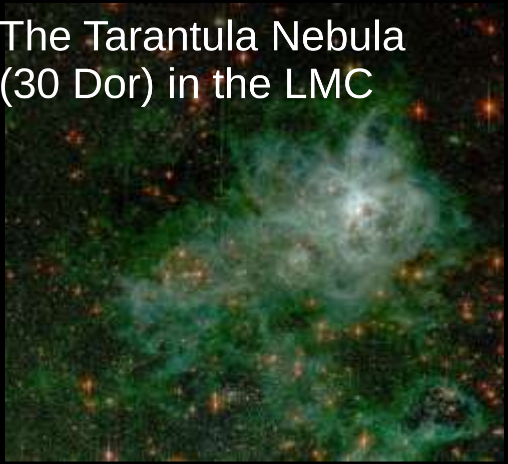

The Tarantula Nebula (30 Dor) in the LMC

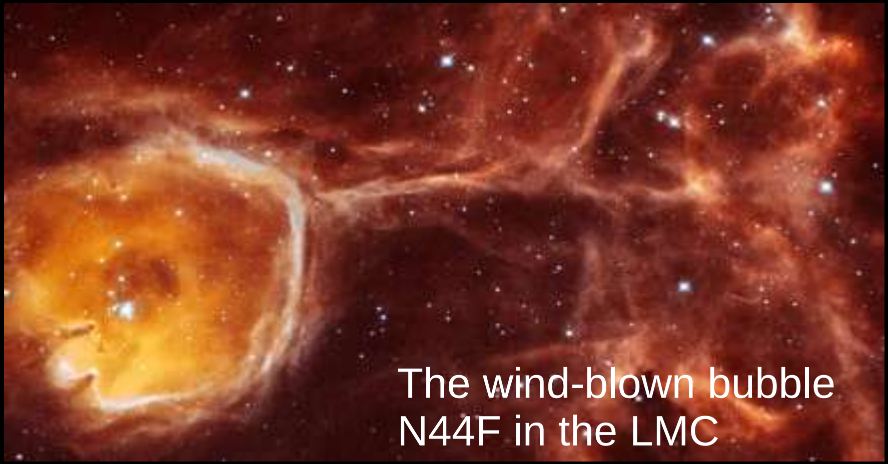

The wind-blown bubble N44F in the LMC

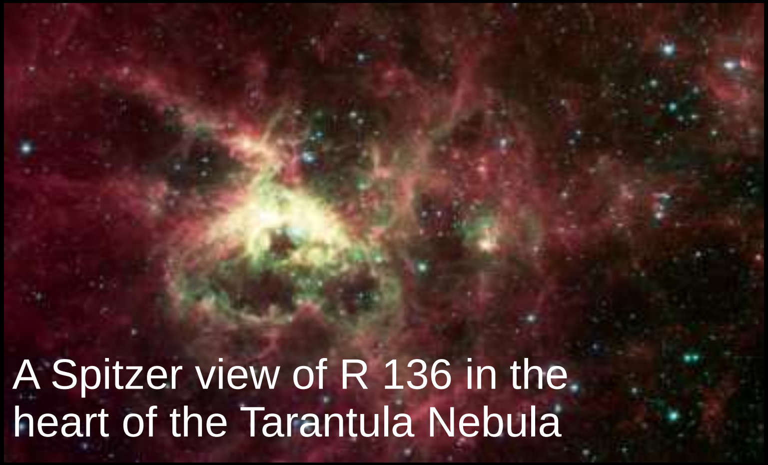

A Spitzer view of R 136 in the heart of the Tarantula Nebula

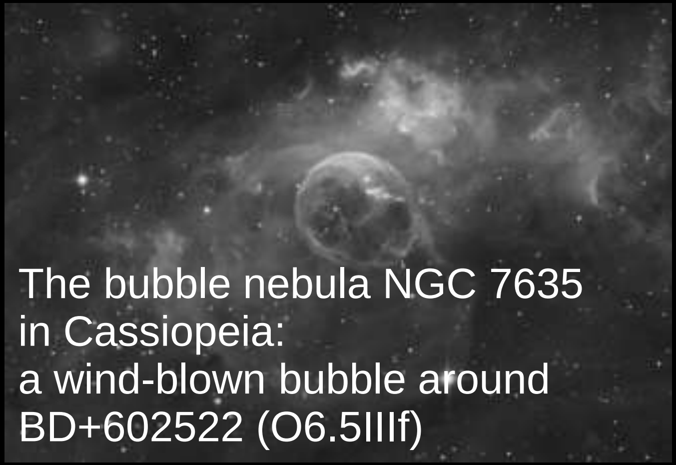

The bubble nebula NGC 7635 in Cassiopeia:
a wind-blown bubble around BD+602522 (O6.5IIIf)

Content

Literature

- Carroll, B.W., Ostlie, D.A., “An Introduction to Modern Astrophysics”, 2nd edition, Pearson International Edition, San Francisco, 2007, Chap. 3,5,8,9
- Mihalas, D., "Stellar atmospheres", 2nd edition, Freeman & Co., San Francisco, 1978
- Hubeny, I., & Mihalas, D., “Theory of Stellar Atmospheres”, Princeton Univ. Press, 2014
- Unsöld, A., "Physik der Sternatmosphären", 2nd edition, Springer Verlag, Heidelberg, 1968
- Puls, J., Herrero, A., Allende Prieto, C., “Stellar Atmospheres”, to be published in Encyclopedia of Astrophysics (Elsevier), 2024, arXiv:2409.03329
- Shu, F.H., "The physics of astrophysics, Volume I: radiation", University science books, Mill Valley, 1991
- Rybicki, G.B., Lightman, A., "Radiative Processes in Astrophysics", New York, Wiley, 1979
- Osterbrock, D.E., "Astrophysics of Gaseous Nebulae and Active Galactic Nuclei", University science books, Mill Valley, 1989
- Mihalas, D., Weibel Mihalas, B., “Foundations of Radiation Hydrodynamics”, Oxford University Press, New York, 1984
- Cercignani, C., "The Boltzmann Equation and Its Applications", Appl. Math. Sciences 67, Springer, 1987
- Kudritzki, R.-P., Hummer, D.G., "Quantitative spectroscopy of hot stars", Annual Review of Astronomy and Astrophysics, Vol. 28, p. 303, 1990
- Simon-Diaz, S., “A Modern Guide to Quantitative Spectroscopy of Massive OB Stars”. In: “Reviews in Frontiers of Modern Astrophysics; From Space Debris to Cosmology”, edited by Kabáth, P. et al., p. 155, Springer, 2020, arXiv:2001.04853

- Sobolev, V.V., “Moving envelopes of stars”, Cambridge: Harvard University Press, 1960
- Puls, J., “Radiative Transfer in the (Expanding) Atmospheres of Early-Type Stars, and Related Problems”, in: “Radiative Transfer in Stellar and Planetary Atmospheres”, edited by L. Crivellari, S. Simón-Díaz and A.J. Arévalo, Canary Islands Winter School of Astrophysics, Vol. XXIX, Cambridge University Press, 2019
- Kudritzki, R.-P., Puls, J., "Winds from hot stars", Annual Review of Astronomy and Astrophysics, Vol. 38, p. 613, 2000
- Puls, J., Vink, J.S., Najarro, F., "Mass loss from hot massive stars", Astronomy & Astrophysics Review, Vol. 16, ISSUE 3, p. 209, Springer, 2008
- Vink, J.S., “Theory and Diagnostics of Hot Star Mass Loss”, Annual Review of Astronomy and Astrophysics, Vol. 60, p. 203, 2022

Chap. 1 – Prelude

- cosmology, galaxies, dark energy, dark matter, …

What are stars good for?

- … and who cares for radiative transfer and stellar atmospheres?

- Remember
  - galaxies consist of stars (and gas, dust)
  - most of the (visible) light originates from stars
  - astronomical experiments are (mostly) observations of light: have to understand how it is created and transported

The cosmic circuit of matter

What are stars good for?

- ▸ Us!
- ▸ (whether this is really good, is another question...)

Joni Mitchell - Woodstock (1970!)

"… We are stardust

Billion year old carbon…"

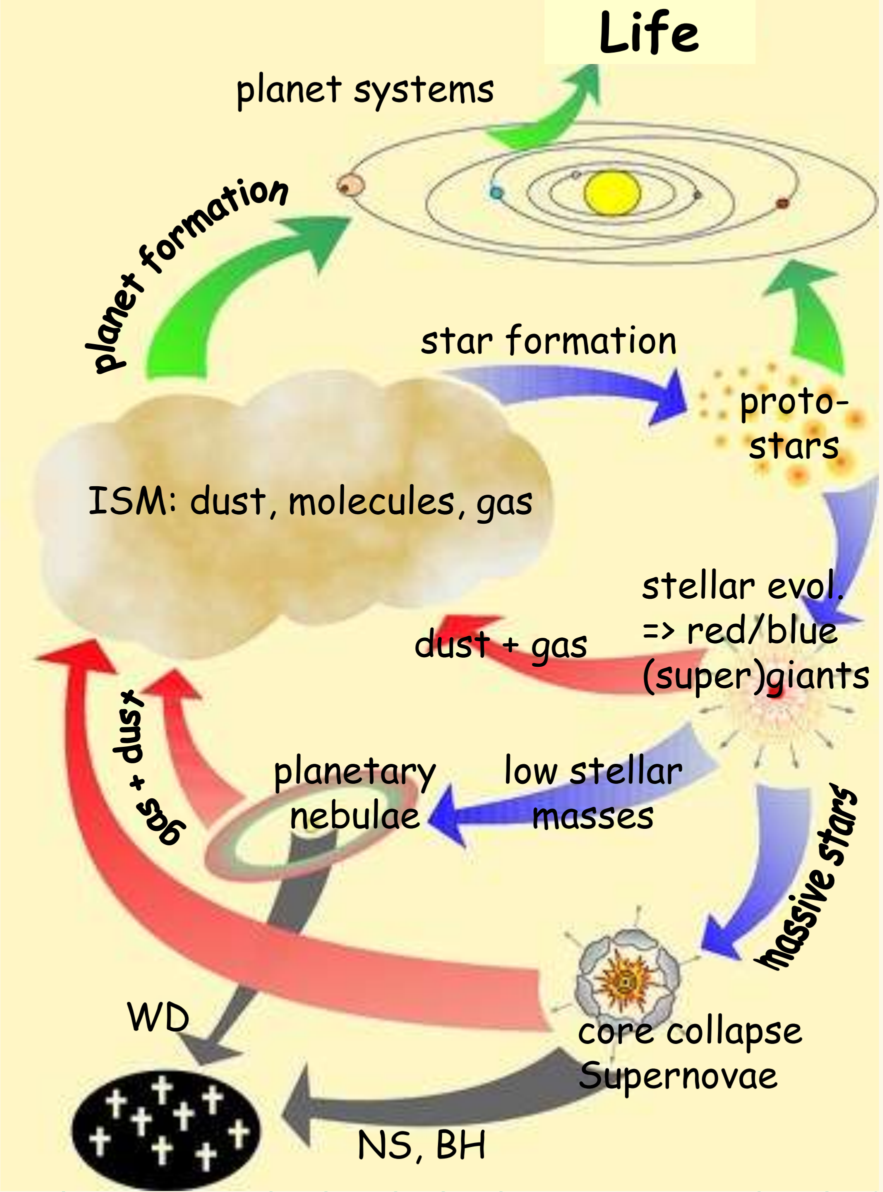

adapted from http://astro.physik.tu-berlin.de/~sonja/Materiekreislauf/index.html

First stars and reionization

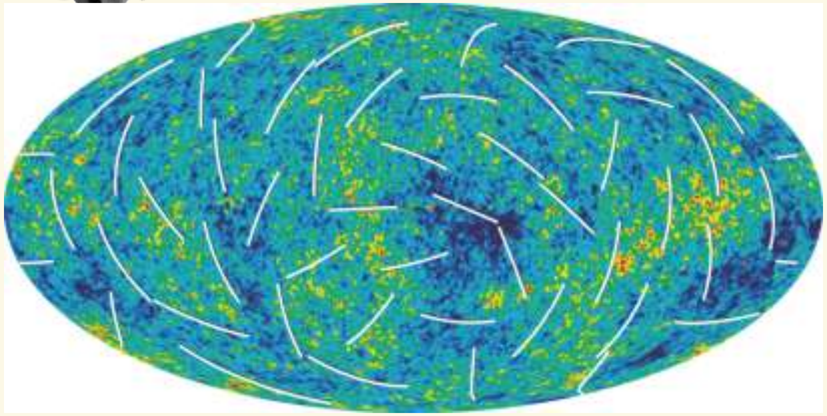

credit: NASA/WMAP Science Team

WMAP = Wilkinson Microwave Anisotropy Probe

color coding: ΔT range ± 200 μK, $\Delta T/T \sim$ few 10^{-5}

=> “anisotropy” of last scattering surface (before recomb.)

white bars: polarization vector

$\Rightarrow$ CMB photons scattered at electrons (reionzed gas)

[NOTE: newer data from PLANCK]

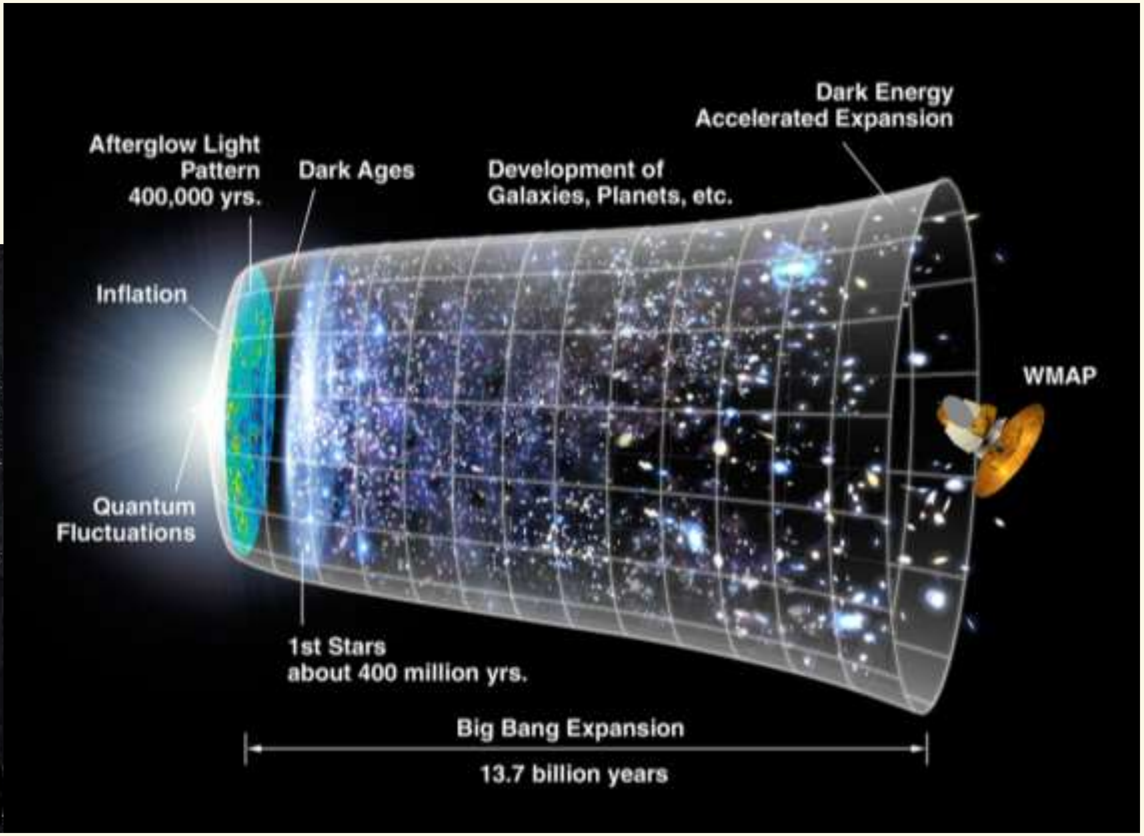

The first stars …

- cosmic reionization:
    - z=7.7 ± 0.8 (from PLANCK, assuming instantaneous reionization, state 2018)
    - z ≈ 11 (begin) to 7 (from WMAP)
- quasars **alone** not capable to reionize Universe at that high redshift, since rapid decline in space density for z > 3 (Madau et al.1999, ApJ 514, Fan et al. 2006, ARA&A 44)

Bromm et al. (2001, ApJ 552)

- (almost) metal free: Pop III
- very massive stars (VMS) with
  1000 $M_\odot$ > M > 100 $M_\odot$, L prop. to M, $T_{\rm eff}$ ~100 kK
- large H/He ionizing fluxes:
  10^{48} (10^{47}) H (He) ionizing photons
  per second *and solar mass*
- assume that primordial IMF is *heavy*, i.e., favours formation of VMS
- then VMS capable to reionize universe alone

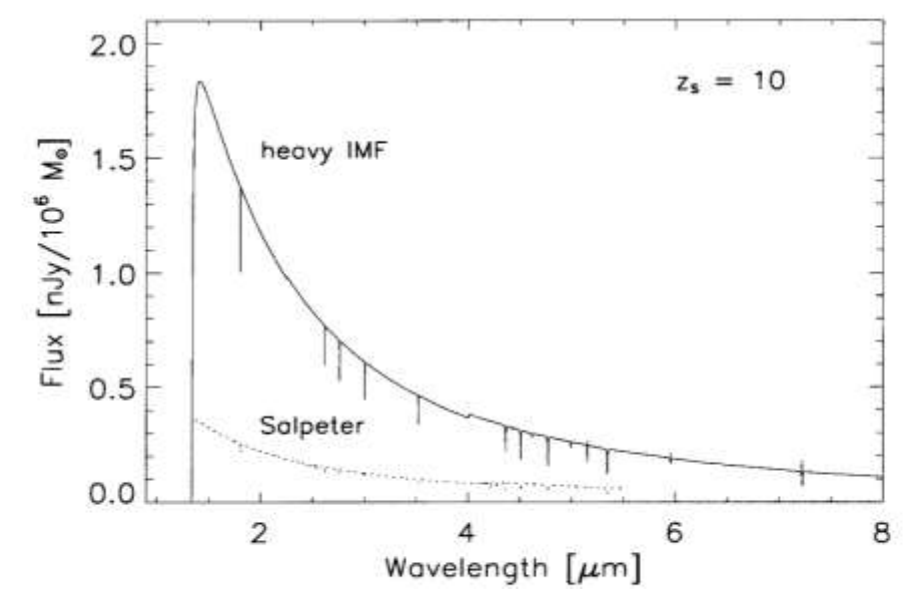

But: theoretical models indicate more typical masses around 40 $M_\odot$ (fragmentation!, Hosokawa et al. 2011), though (much) more massive stars might have formed as well

Present status: Massive stars important for reionization, but not exclusive

see also: Abel et al. 2000, ApJ 540; Bromm et al. 2002, ApJ 564; Cen 2003, ApJ 591; Furnaletto & Loeb 2005, ApJ 634; Wise & Abel 2008, ApJ 684; Johnson et al. 2008, Proc IAU Symp 250 (review); Maio et al. 2009, A&A 503; Maio et al. 2010, MNRAS 407; Weber et al. 2013, A&A 555

… and many more publications

… might be observable in the NIR

with a ≥ 30m telescope, e.g. via HeII λ1640 Å (strong ISM recomb. line)

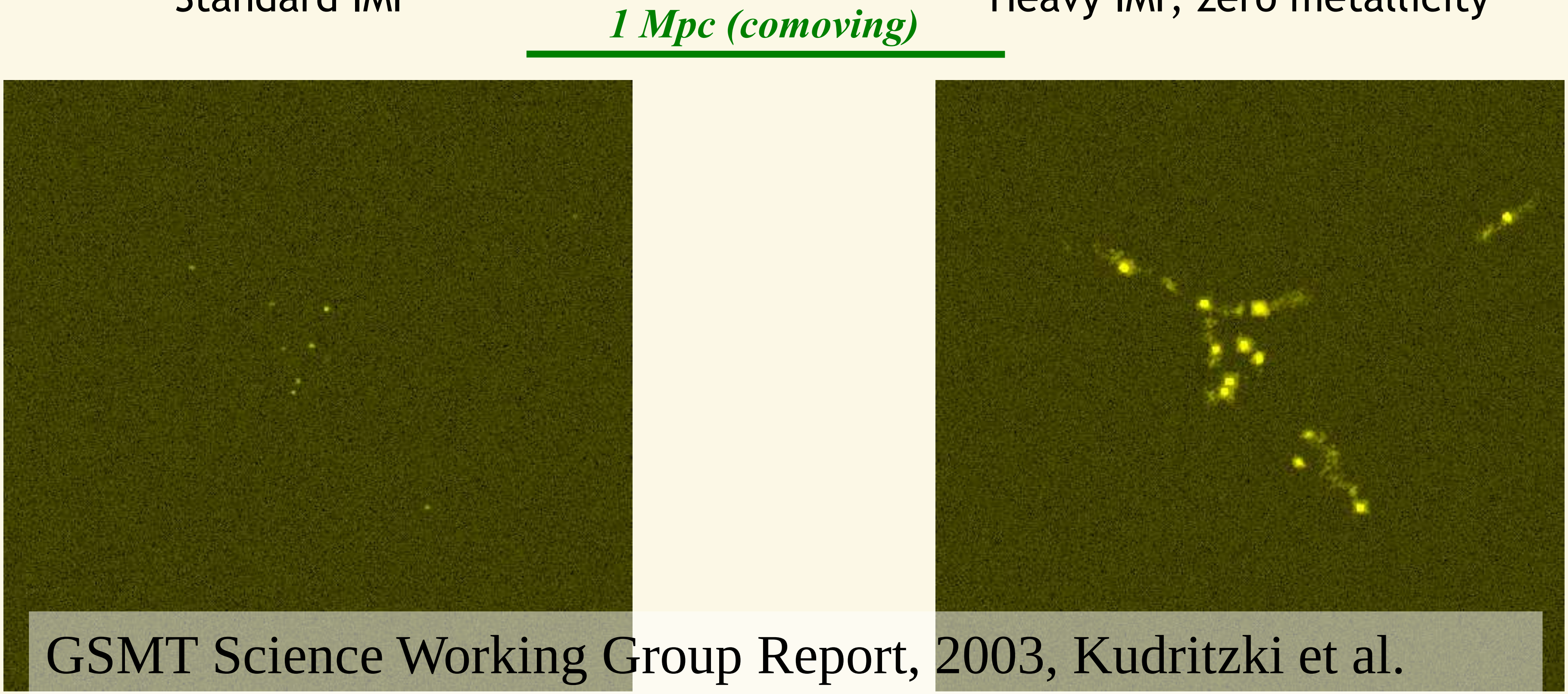

Standard IMF

Heavy IMF, zero metallicity

GSMT Science Working Group Report, 2003, Kudritzki et al.

http://www.aura-nio.noao.edu/gsmt_swg/SWG_Report/SWG_Report_7.2.03.pdf

(Hydro-simulations by Davé, Katz, & Weinberg)

As observed through 30-meter telescope R=3000, 10^5 seconds (favourable conditions, see also Barton et al., 2004, ApJ 604, L1)

Massive vs. ediate-/low-mass stars

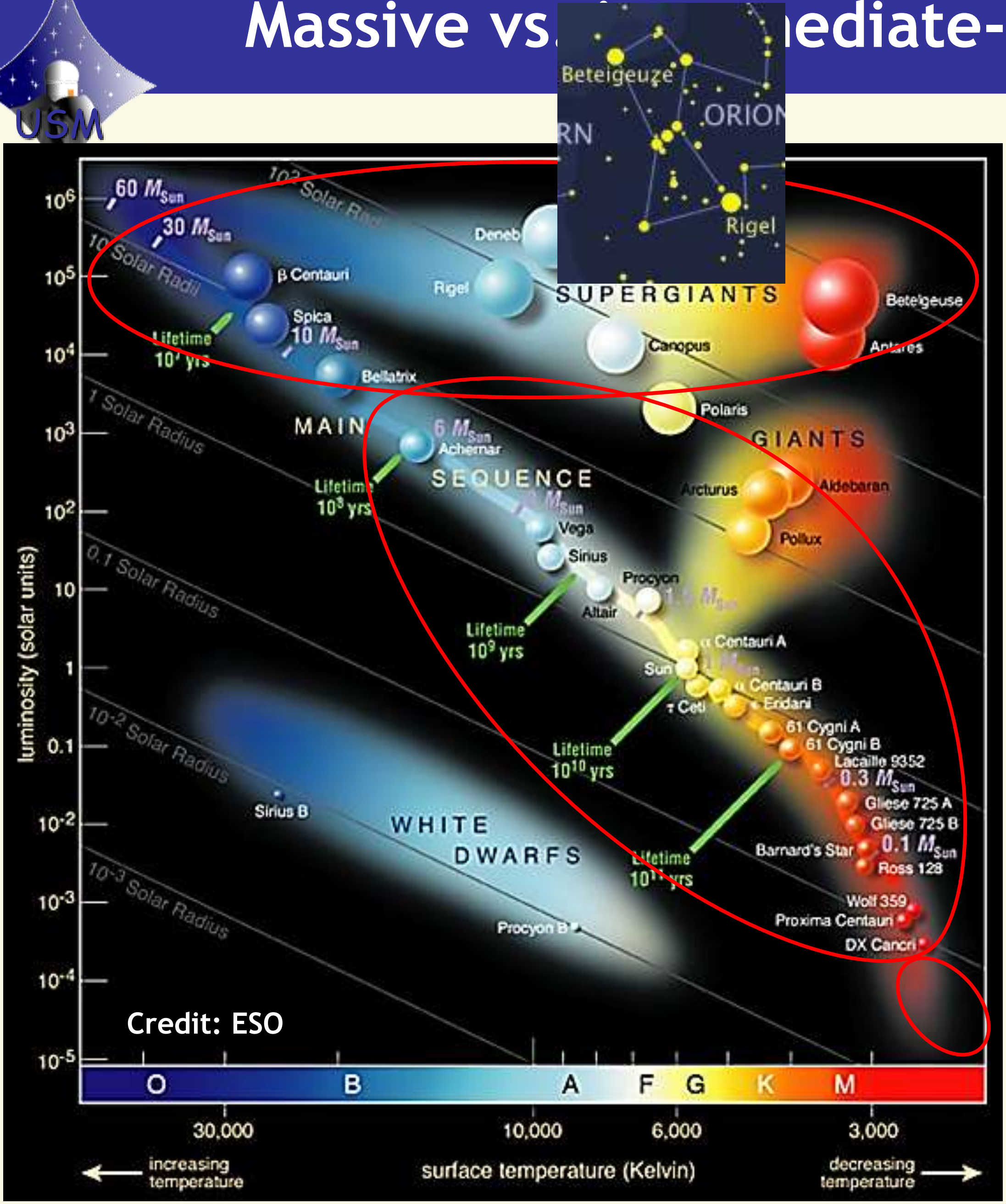

Credit: ESO

- massive stars ($M_{ZAMS} > 8\ M_{sun}$)
  - short life-times (few to 20 million years)
  - end products: core-collapse SNe (sometimes as slow GRBs) → neutron stars, black holes (or even complete disruption in case of pair-instability SNe)
  - Grav. waves from BH mergers!
- intermediate-/low-mass stars ($0.1...0.8\ M_{sun} < M_{ZAMS} < 8\ M_{sun}$)
  - long life-times (0.1 to 100 billion years)
  - end products: White dwarfs, SNIa
- brown dwarfs ($13\ M_{Jupiter} < M < 0.08\ M_{sun}$)
  - 'failed stars', core temperature not sufficient to ignite H-fusion
  - instead, Deuterium and, for higher masses, Lithium fusion

ZAMS: Zero Age Main Sequence
MS: Main sequence, core hydrogen burning

low-mass vs. massive star during the MS

low-mass star (e.g., the sun)

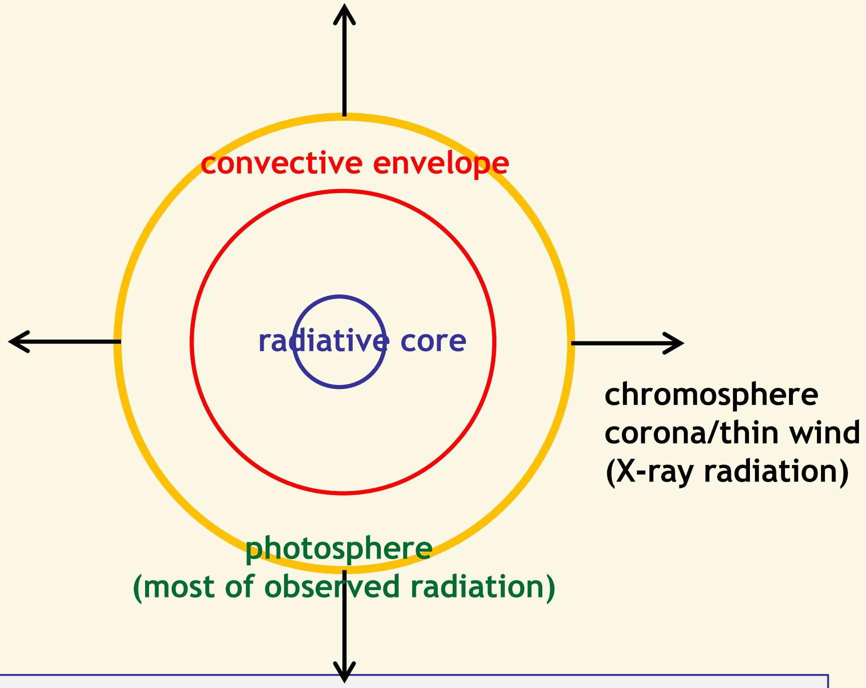

convective envelope

radiative core

chromosphere
corona/thin wind
(X-ray radiation)

photosphere
(most of observed radiation)

- radiative core
- convective envelope
- geometrically thin photosphere
  - level populations collisionally dominated
    →Local thermodynamic equilibrium (LTE):
    Saha-Boltzmann population
- chromosphere (temp. begins to increase outwards)
- hot corona/thin wind (very low mass-loss rate)

massive star
factor 10…20 larger than sun
factor 10^4…10^6 more luminous than sun

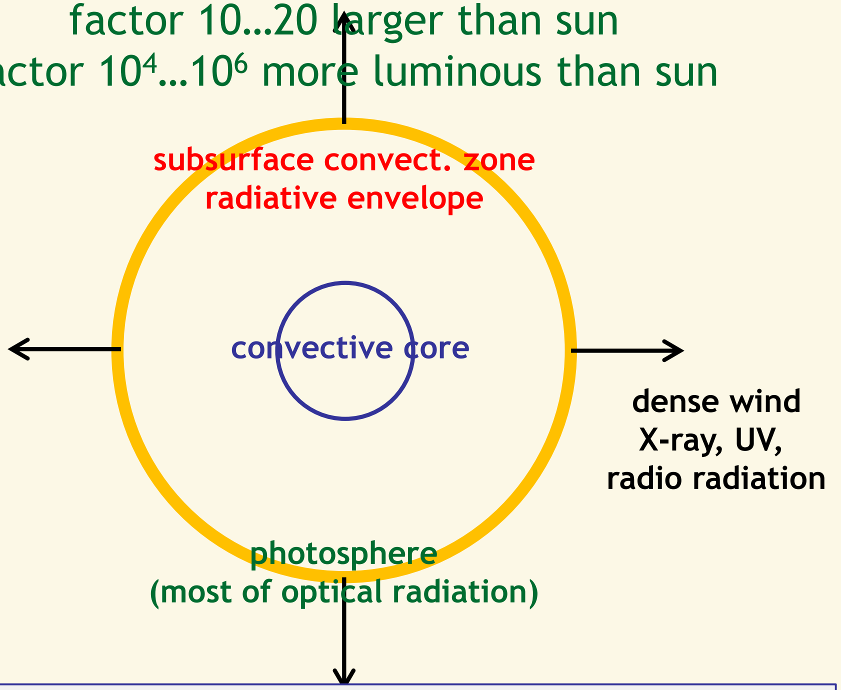

subsurface convect. zone
radiative envelope

convective core

dense wind
X-ray, UV,
radio radiation

photosphere
(most of optical radiation)

- convective core
- radiative envelope with subsurface convection zone
- geometrically thin photosphere + dense wind
  - level populations radiatively dominated
    →non-LTE level population
    (all transition-probabilities need to be
    calculated explicitly)

NOTE: evolved objects (red giants and supergiants) and brown dwarfs are fully convective

Examples for current research:
Observations …

- … in all frequency bands
- both earthbound and via satellites
- Gamma-rays (Integral), X-rays (Chandra, XMM-Newton), (E)UV (IUE, HST), optical (VLT), IR (VLT, JWST, →ELT) , (sub-) mm (ALMA) , radio (VLA, VLBI, →SKAO) …
- photometry, spectroscopy, polarimetry, interferometry, gravitational waves (aLIGO!)
- current telescopes allow for high S/N and high spatial resolution
- because of their high luminosity, massive stars can be spectroscopically observed not only in the Milky Way, but also in many Local Group (and beyond) galaxies (‘record-holder’: blue supergiants in NGC 4258 at a distance of ≈ 7.8 Mpc, Kudritzki+ 2013)

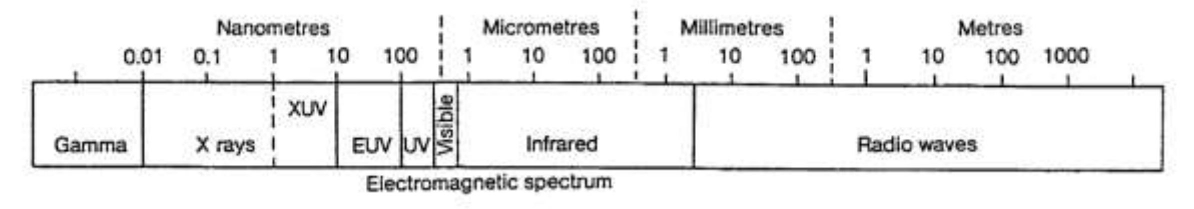

Electromagnetic spectrum

Abbreviations:

IUE – International Ultraviolet Explorer
HST – Hubbble Space Telescope
VLT – Very Large Telescope (Cerro Paranal, Chile)
JWST – James Webb SpaceTelescope
ELT – Extremely Large Telescope (Cerro Armazones, Chile, 20 km away from VLT))
ALMA – Atacama Large Millimeter/Submillimeter Array (Chajnantor-Plateau, Chile, 5000 m altitude)
VLA – Very Large Array (Socorro, New Mexico, USA)
VLBI – Very Large Baseline Interferometer
SKAO – Square Kilometer Array Observatory (South Africa and Australia)

Examples for current research:
Star formation

- **Star formation** – formation of massive stars
  - until 2010, it was not possible to 'make' stars with $M > 40\ M_{sun}$

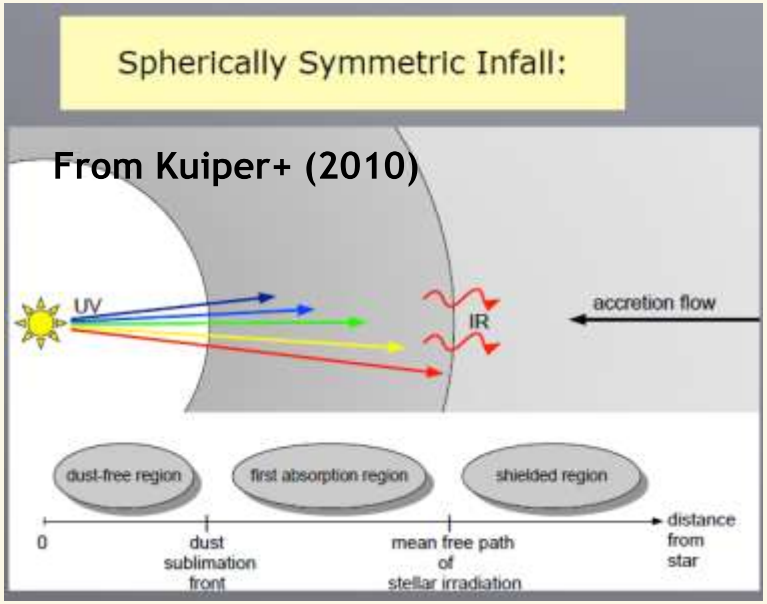

From Kuiper+ (2010)

  - Radiation pressure barrier for spherical infall:
    when core becomes massive, high luminosity heats 'first absorption region',
    radiation pressure due to re-processed IR radiation stops and reverts accretion flow.

Examples for current research:
Star formation

- **Star formation** – formation of massive stars
  - until 2010, it was not possible to ‘make’ stars with M > 40 M_{sun}

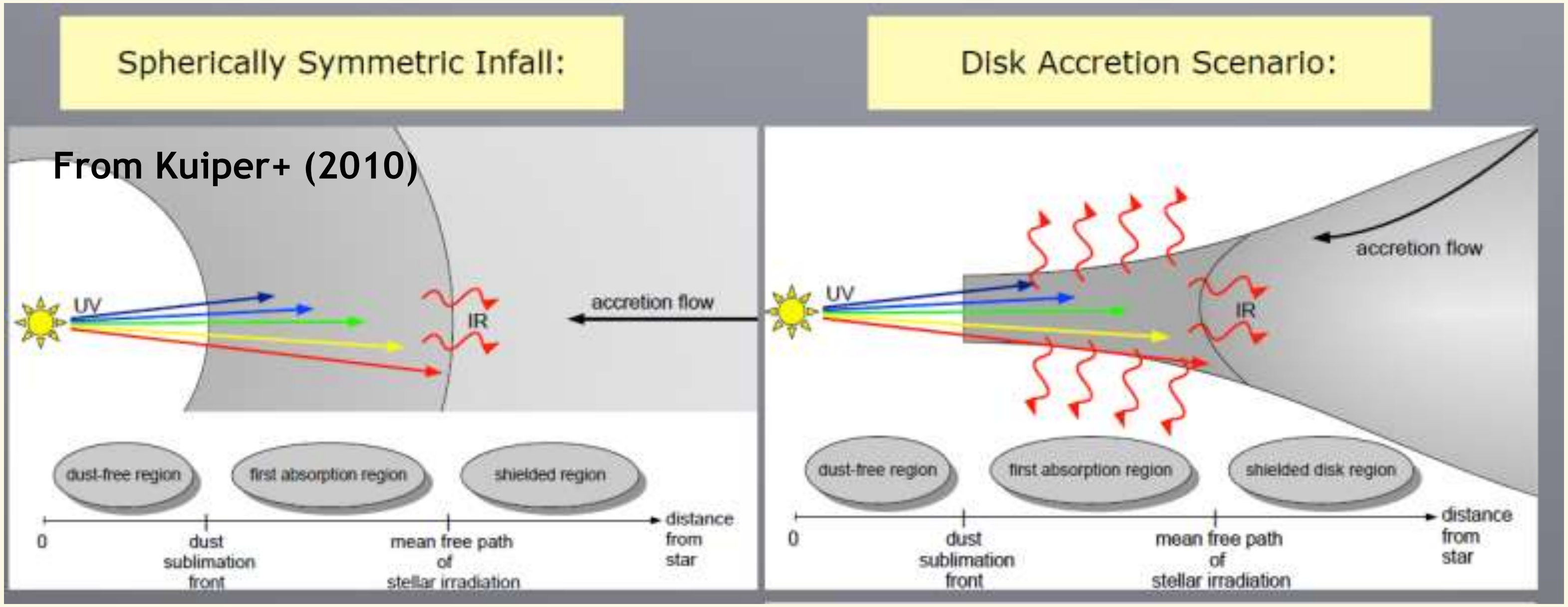

From Kuiper+ (2010)

  - Radiation pressure barrier for spherical infall:
    when core becomes massive, high luminosity heats ‘first absorption region’, radiation pressure due to re-processed IR radiation stops and reverts accretion flow.
  - If accretion via disk, re-processes radiation-field becomes highly anisotropic, the radial component of the radiative acceleration becomes diminished, and further accretion becomes possible. Stars with M > 40 M_{sun} (… 140 M_{sun}) can be formed. (see work by R. Kuiper and collaborators)

Examples for current research: Stellar structure and evolution

- **Stellar structure and evolution**
  - implementation/improved description of various processes, e.g.,
    - impact of mass-loss and rotation (mixing!) in massive stars
    - generation and impact of B-fields
    - convection, mixing processes, core-overshoot etc. still described by simplified approximations in 1-D (e.g., diffusive processes), needs to be studied in 3-D (work in progress)

Examples for current research:
Stellar structure and evolution

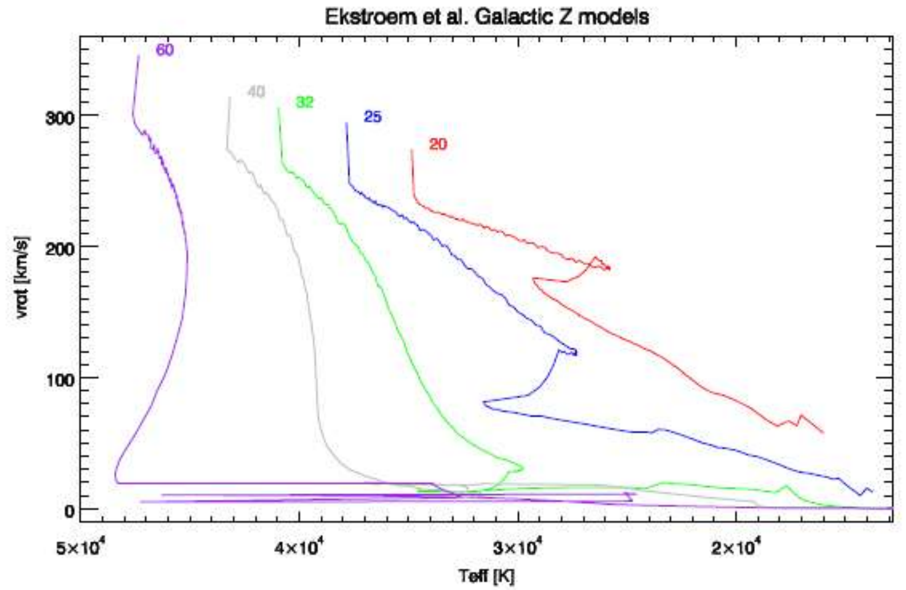
Ekstroem et al. Galactic Z models

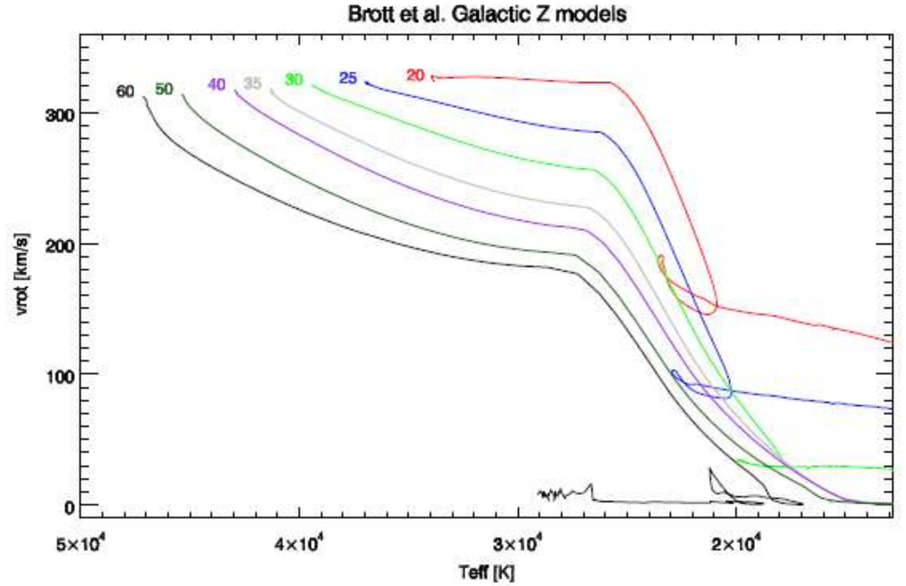
Brott et al. Galactic Z models

- *vrot* vs. *Teff* , for rotating Galactic massive-star models from Ekström+(2012, ‘GENEC’) and Brott+ (2011, ‘STERN’), with *vrot(initial)* ≈ 300km/s
- The main difference on the MS is due to the lack (Ekström) and presence (Brott) of *assumed* internal magnetic fields and the treatment of angular momentum transport.

- NOTE: Even at main sequence, stellar evolution of massive stars unclear in many details!!!!
- Do not believe in statements such as ‘stellar evolution is understood’

Examples for current research:
Stellar structure and evolution

- binarity fraction of Galactic stars
  M-stars: 25%, solar-type: 45%, A-stars: 55% (Duchene & Kraus 2013, review)
  O-stars in Galactic clusters:
    - 70% of all stars will interact with a companion during their lifetime (Sana+ 2012)

- THUS: needs to be included in evolutionary calculations
    - even more approximations regarding tidal effects, mass-transfer, merging …
      (e.g., MESA = Modules for Experiments in Stellar Astrophysics,
      Paxton et al. 2010 and follow-up papers – single stars and binaries,
      ‘binary_c’ by Izzard+ 2004/06/09)

- predictions on pulsations
    - frequency spectrum of excited oscillations
    - period-luminosity relations as a function of metallicity

Asteroseismology: Revealing the internal structure

- non-radial pulsations: examples for different models

following slides adapted
from C. Aerts (Leuven)

Blue: Moving towards Observer   Red: Moving away from Observer

(l,m) = (3,2)
tesseral

(l,m)=(3,0)
axisymmetric

(l,m)=(3,3)
sectoral

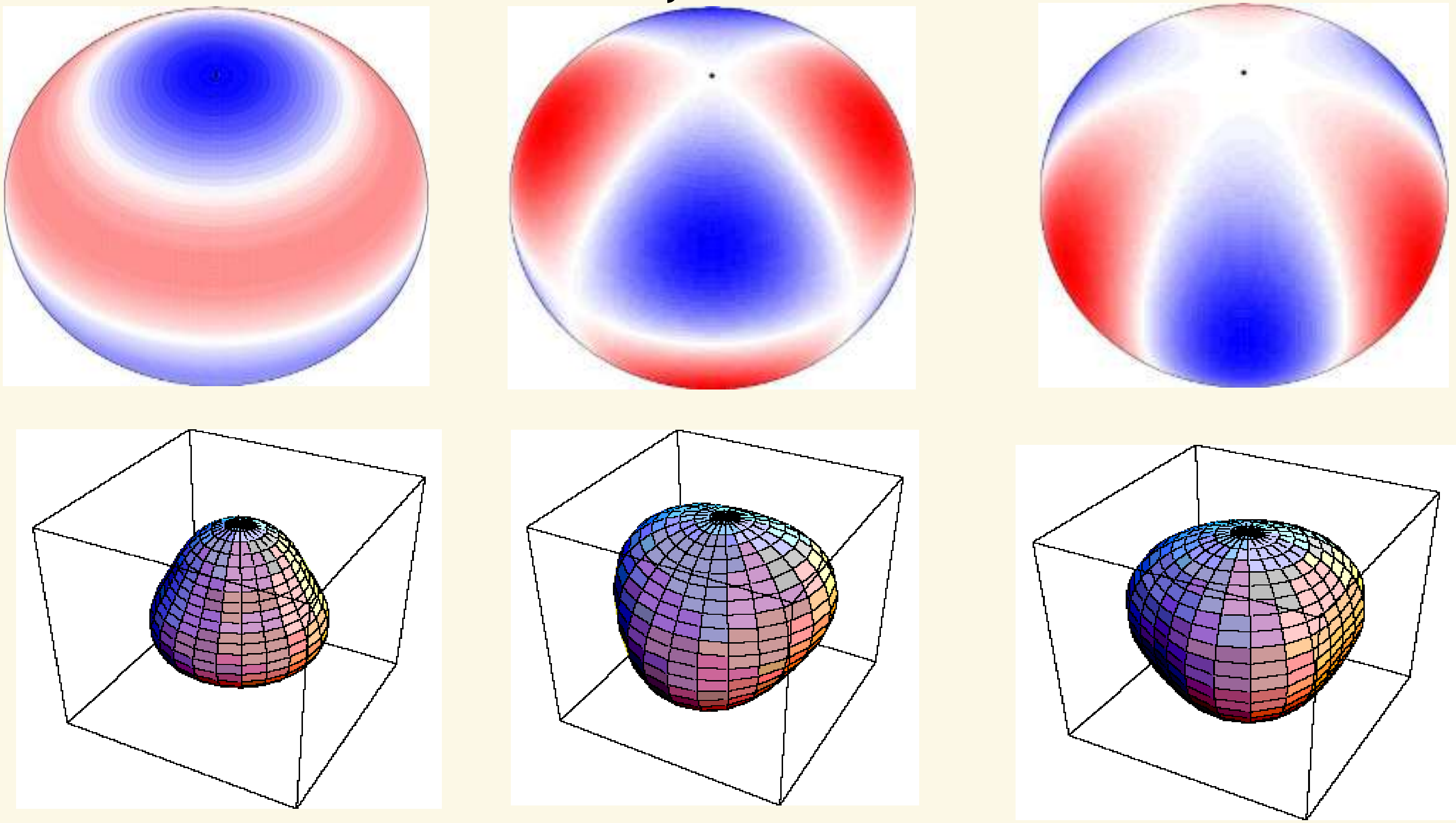

l: nonradial degree, **m**: azimuthal order

Internal behaviour of the oscillations

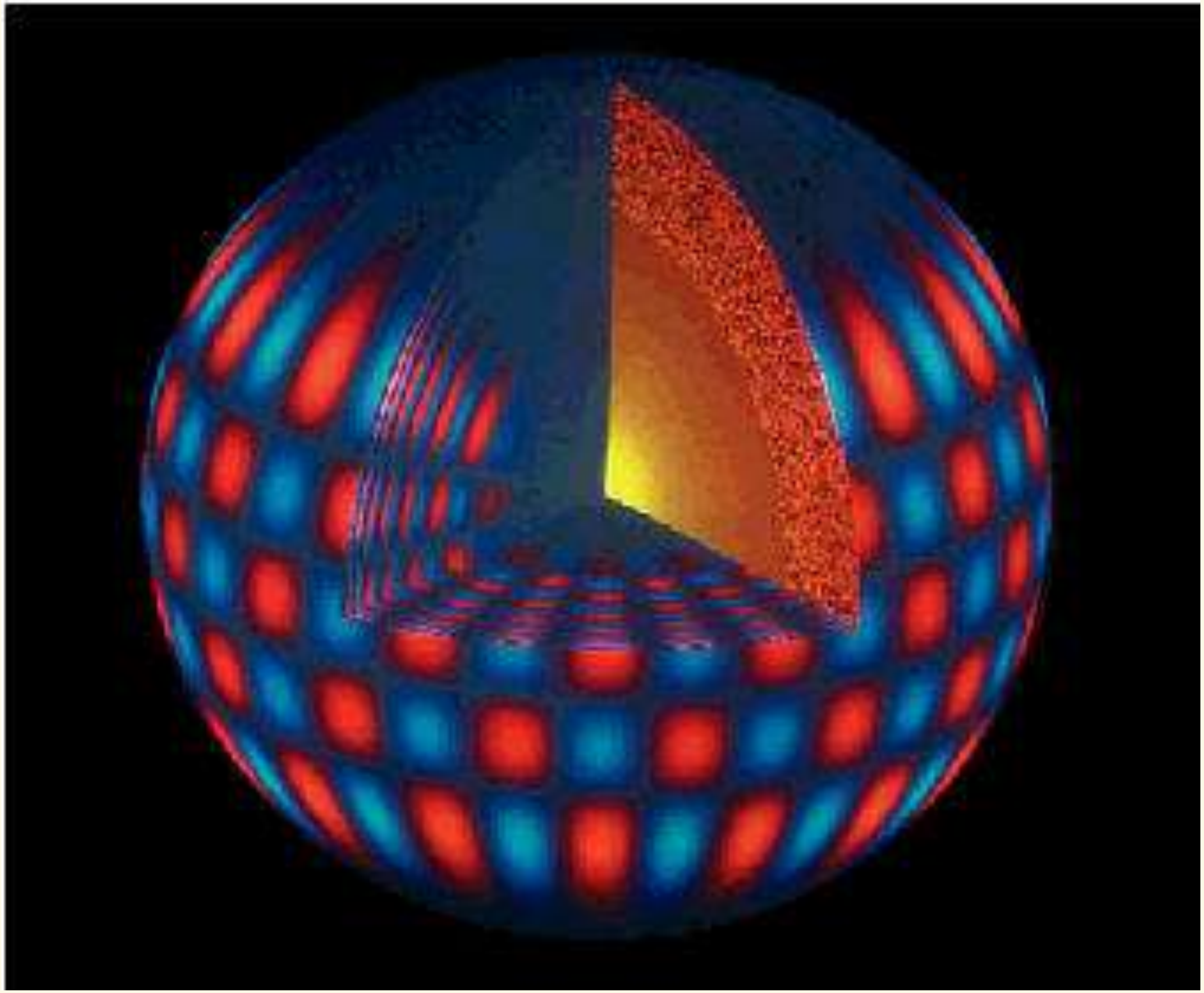

The oscillation pattern at the surface propagates in a continuous way towards the stellar centre.

Study of the surface patterns hence allows to characterize the oscillation throughout the star.

Probing the interior

The oscillations are standing sound waves that are reflected within a cavity

Different oscillations penetrate to different depths and hence probe different layers

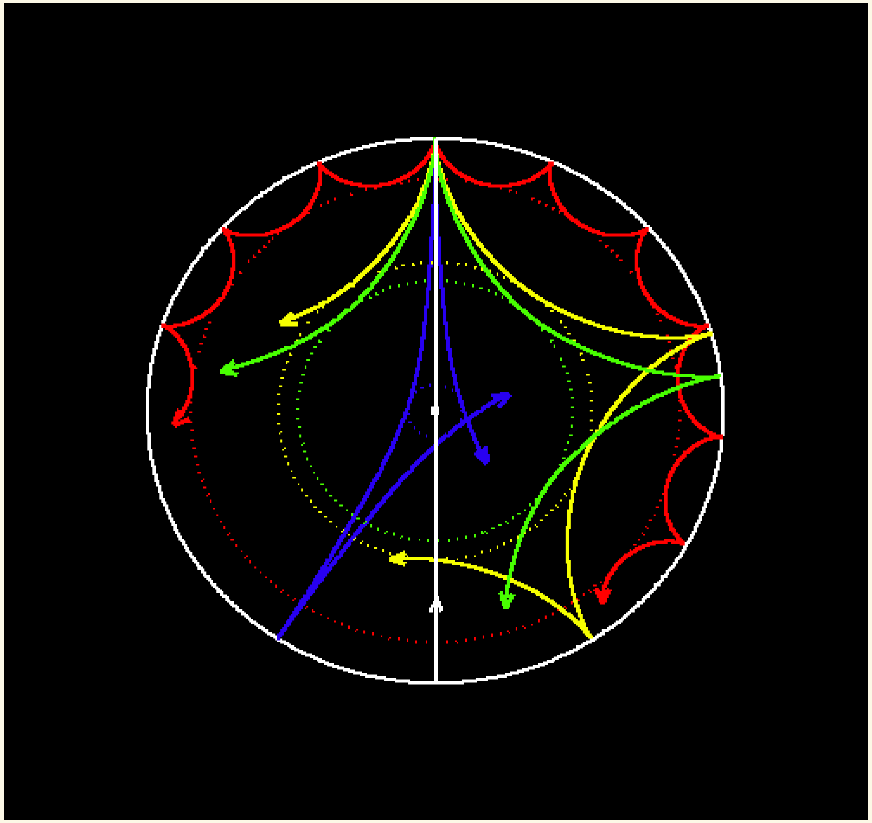

Doppler map of the Sun

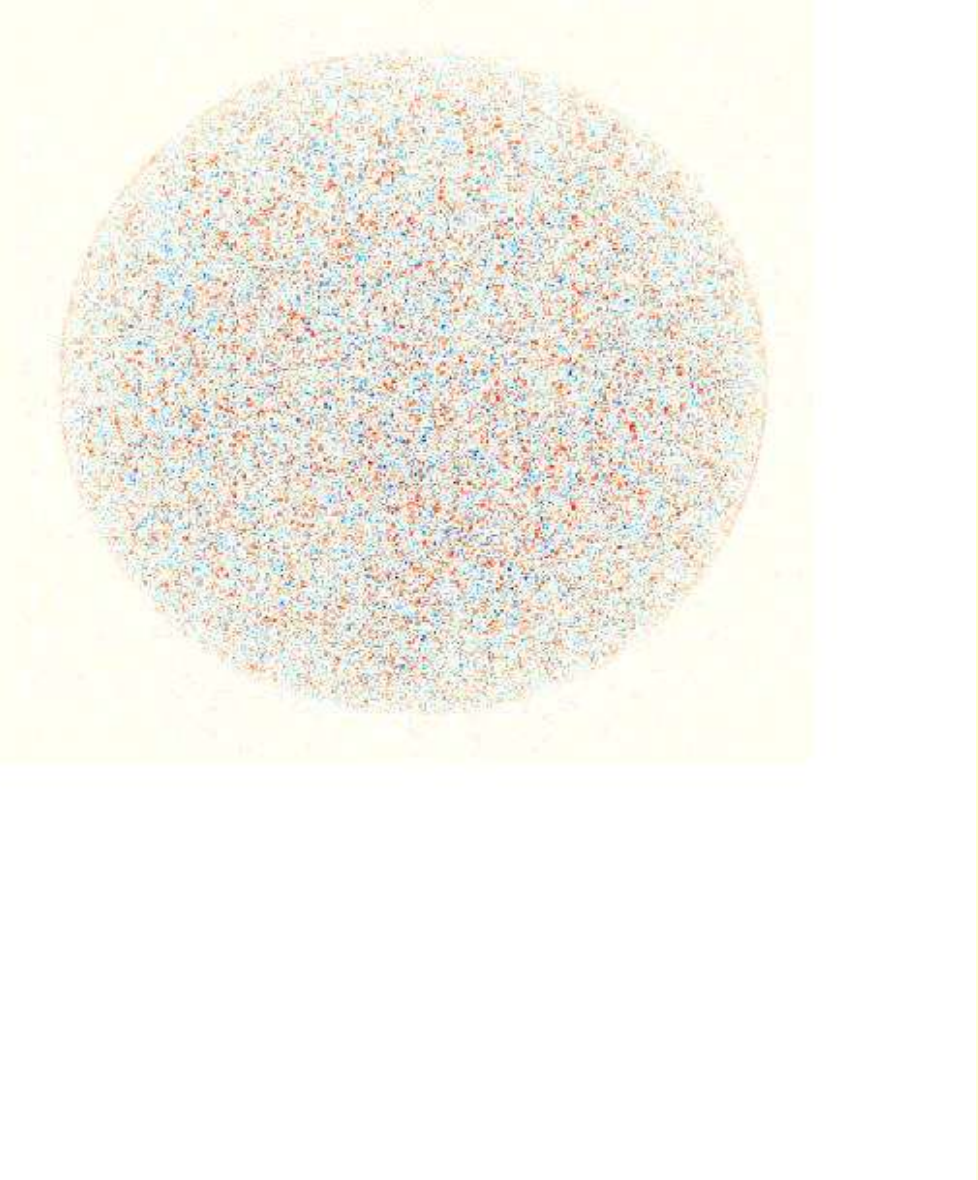

The Sun oscillates in thousands of non-radial modes with periods of ~5 minutes

The Dopplermap shows velocities on the order of some cm/s

Solar frequency spectrum from ESA/NASA satellite SoHO: systematics !

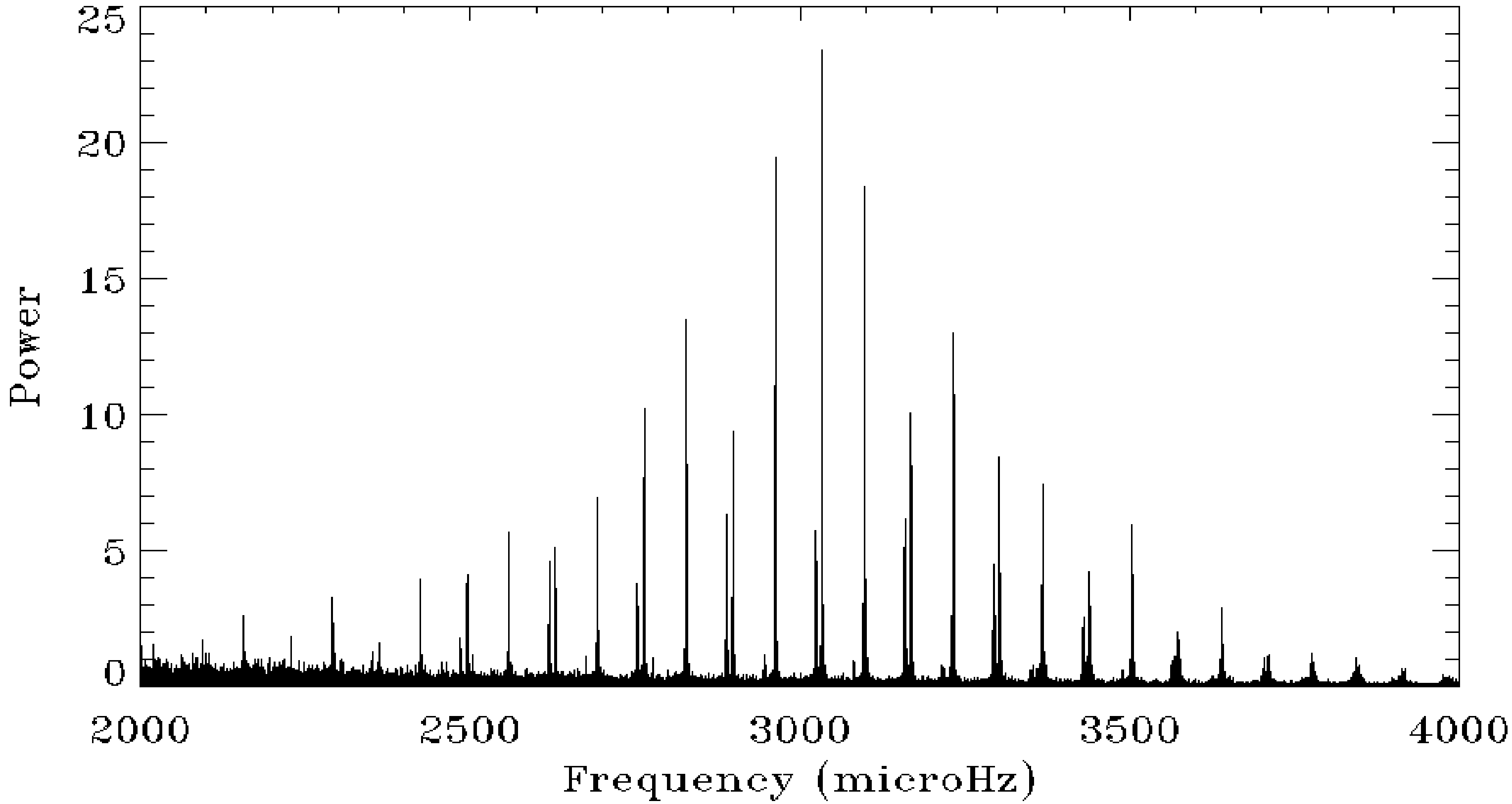

Frequency separations in the Sun

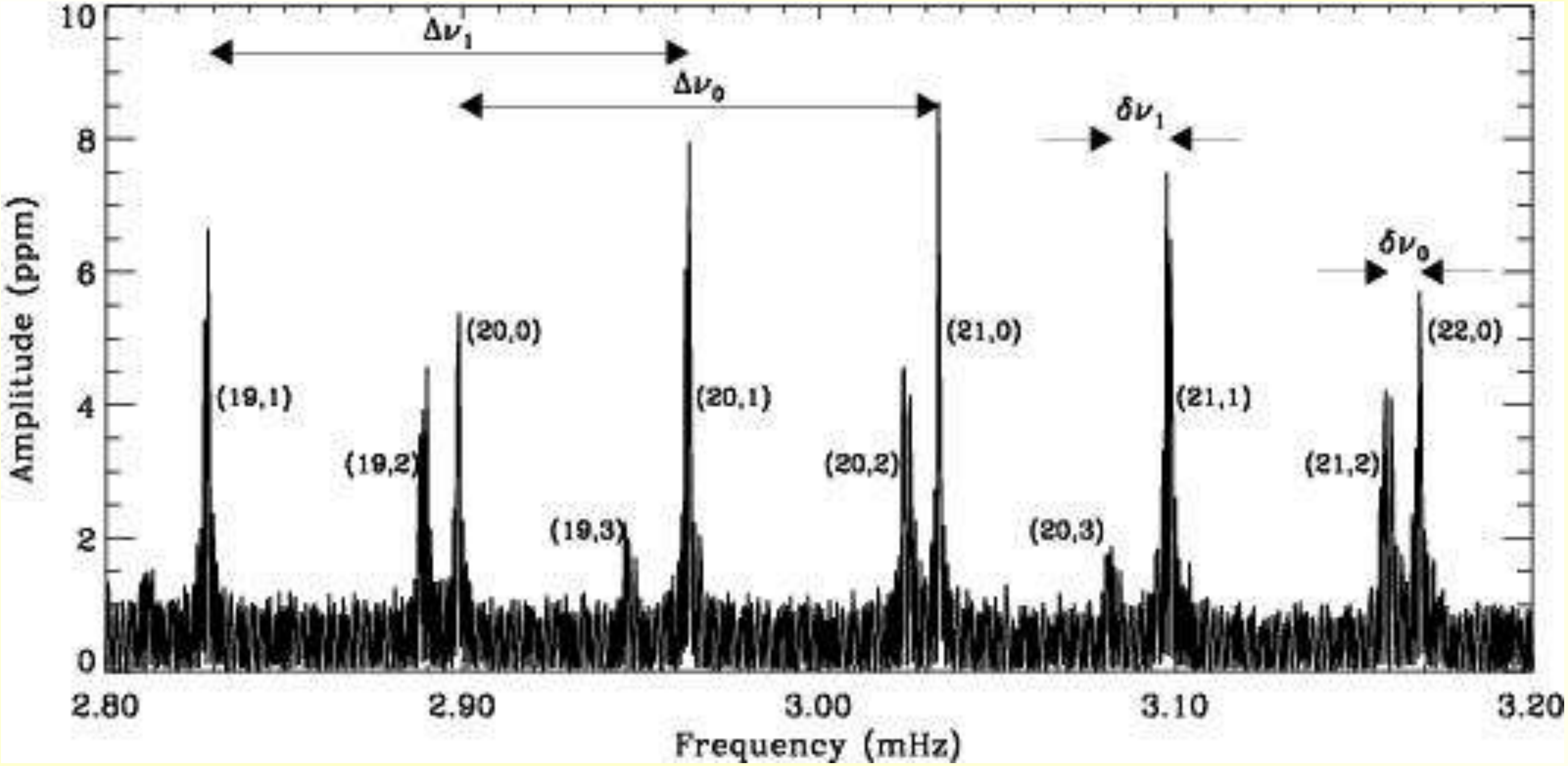

Result: internal sound speed and internal rotation could be determined very accurately by means of helioseismic data from SoHO

Internal rotation of the Sun

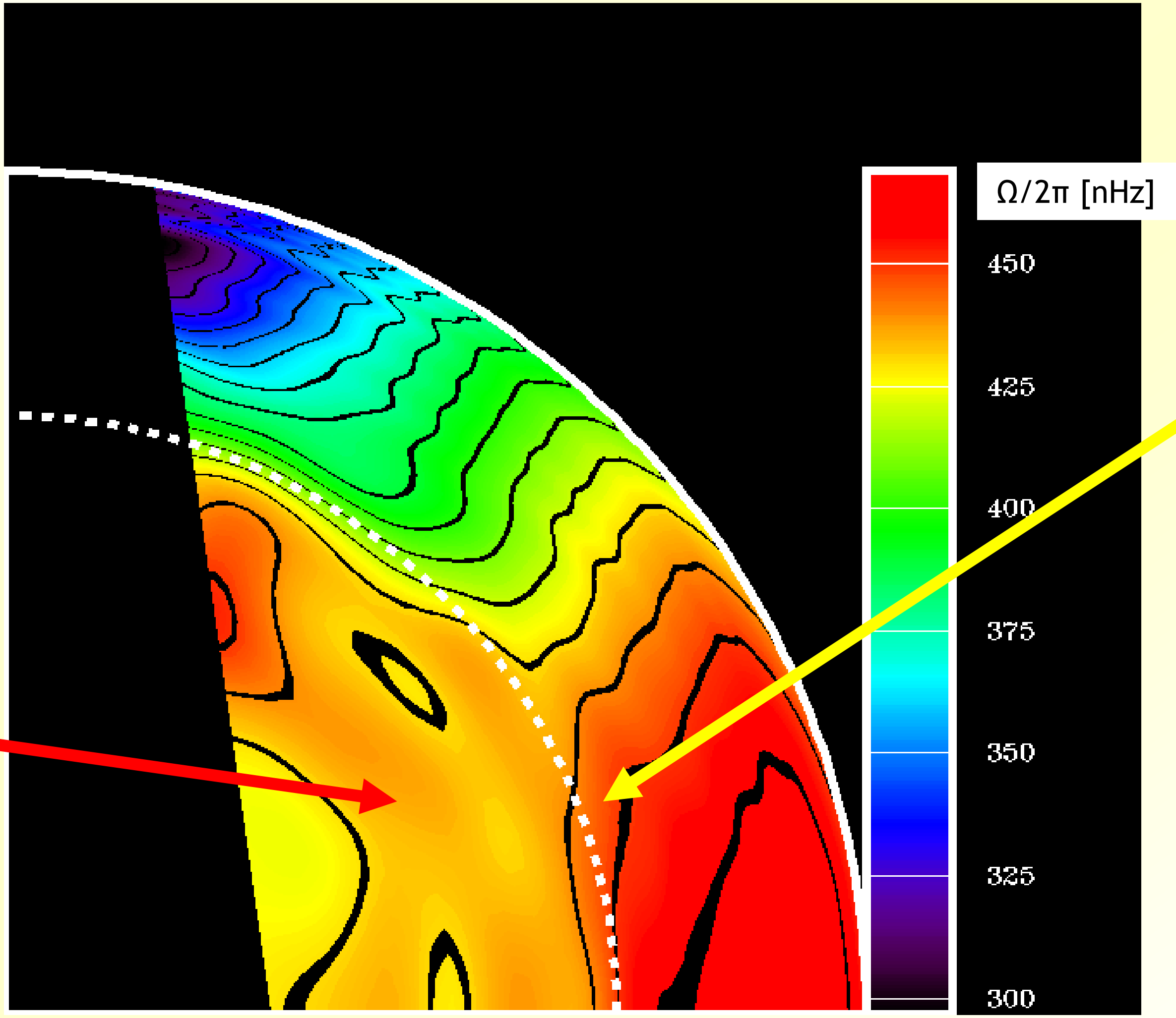

Beginning of outer convection zone

Solar interior has rigid rotation

… towards massive star seismology

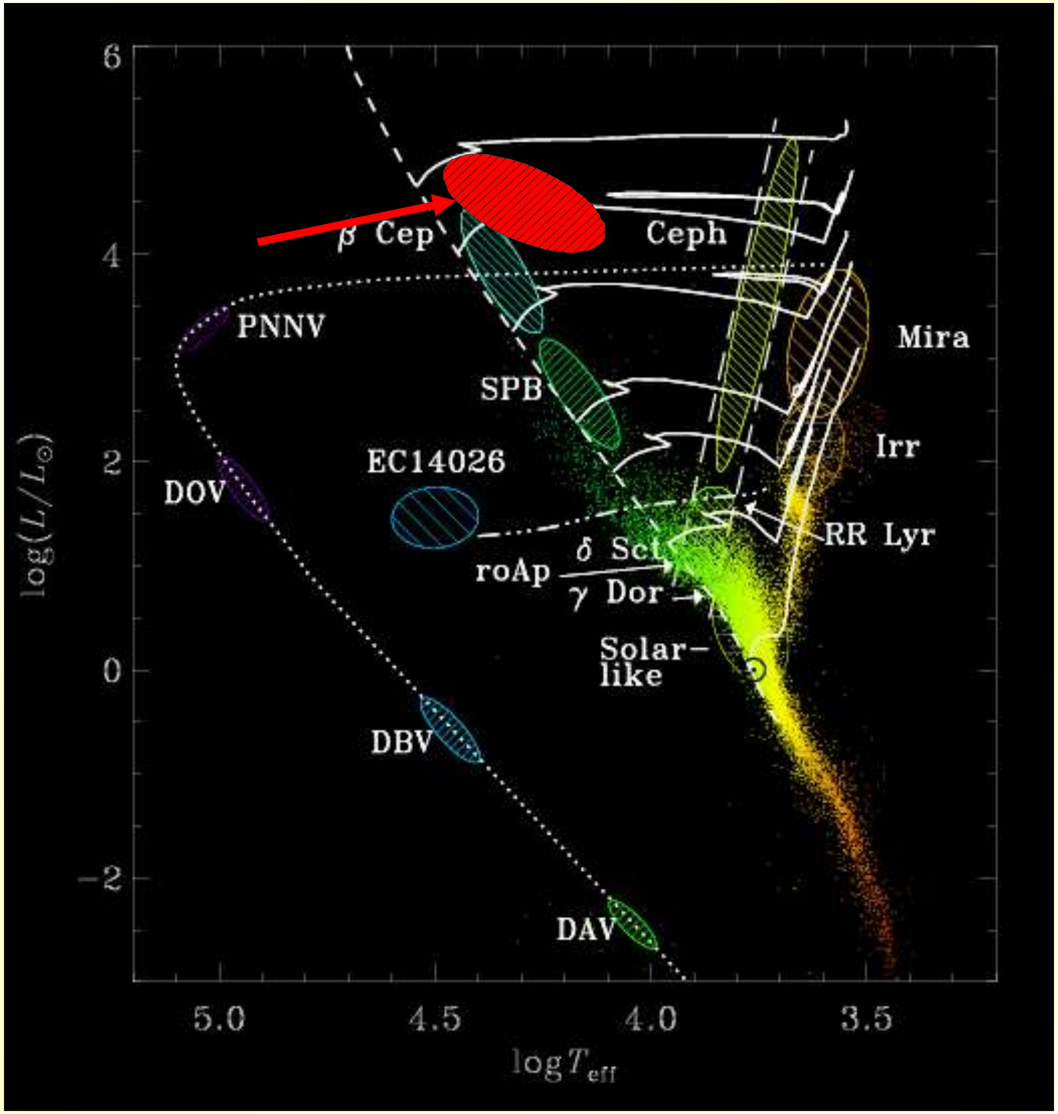

(radial) order: number of nodes between center and surface

- β Cep:
  low order p- and g-modes
- SPB
  slowly pulsating B-stars
  high order g-modes
- Hipparcos:
  29 periodically variable
  B-supergiants
  (Waelkens et al. 1998)
- no instability region
  predicted at that time
- nowdays: additional
  region for high order
  g-mode instability

➔asteroseismology of
evolved massive stars
becomes possible

p-modes: pressure
g-modes: gravity
as restoring force

Space Asteroseismology

COROT: COnvection ROtation and planetary Transits
French-European mission (27 cm mirror)
launched December 2006

Kepler: NASA mission (1.2m mirror),
launched March 2009

TESS = Transiting Exoplanet Survey Satellite,
lense-based mirror 10,5 cm,
launched April 2018 (still in operation)

MOST: Canadian mission
(65 x 65 x 30 cm, 70 kg)
launched in June 2003

BRITE-Constellation:
Canadian-Austrian-Polish mission
(six 20^3 cm nano-satellites, 7kg)
first one launched 2013
asteroseismology of bright (= massive) stars

Examples for current research:
End phases of evolution

- **End phases**
  - evolutionary tracks towards ‘the end’
  - models for SNe and Gamma-ray bursters

Long Gamma Ray Bursts

- long: >2s
- Collapsar: death of a massive star

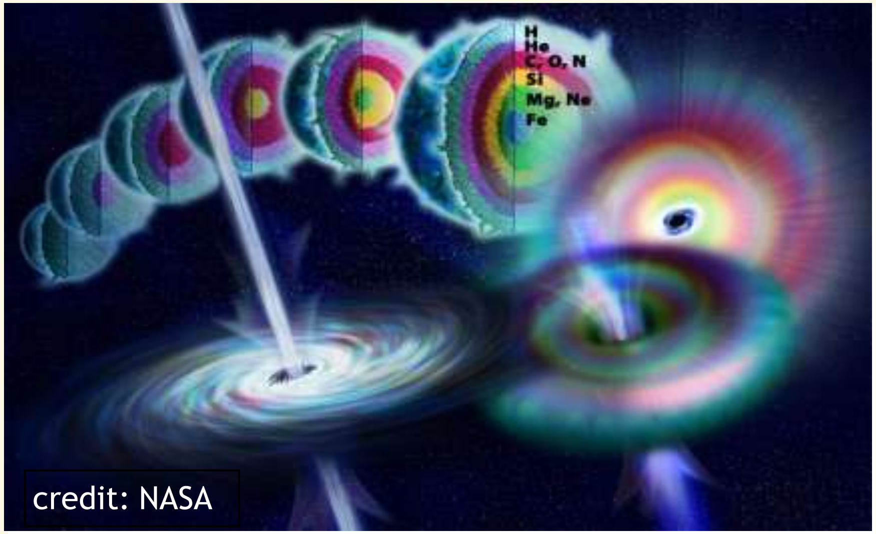

credit: NASA

Collapsar Scenario for Long (slow) GRB (Woosley 1993)

- massive core (enough to produce a BH)
- removal of hydrogen envelope
- rapidly rotating core (enough to produce an accretion disk)

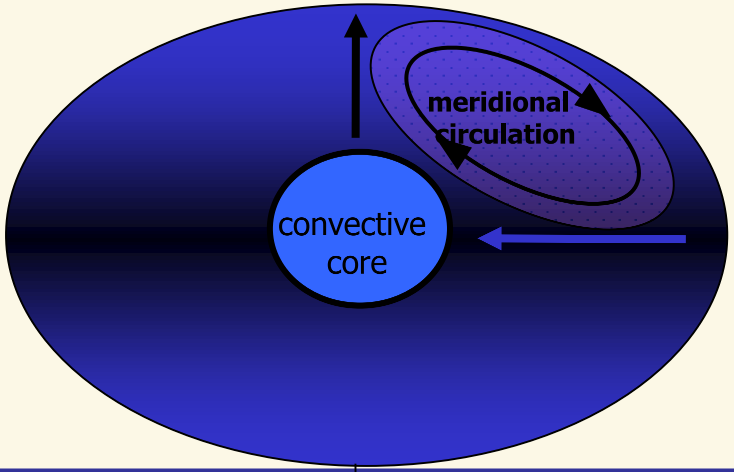

requires **chemically homogeneous evolution** of **rapidly rotating** massive star

- pole hotter than equator (von Zeipel)
- rotational mixing due to meridional circulation (Eddington-Sweet)

Chemically Homogeneous Evolution …

- …if rotational mixing during main sequence *faster than* built-up of chemical gradients due to nuclear fusion (*Maeder 1987*)
- bluewards evolution directly towards Wolf-Rayet phase (no RSG phase).
  Due to meridional circulation, envelope and core are mixed ->
  no hydrogen envelope
- since no RSG phase, higher angular momentum in the core
  (*Yoon & Langer 2005*)

W/W_k: rotational frequency in units of critical one

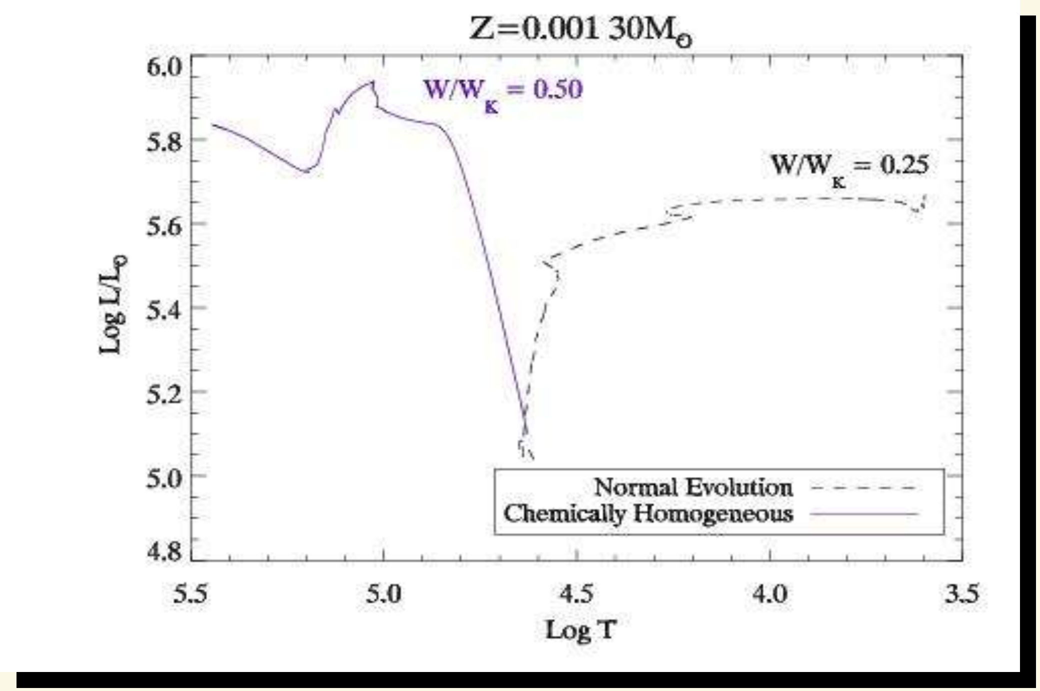

massive stars as progenitors of high redshift GRBs:

✓ early work: Bromm & Loeb 2002, Ciardi & Loeb 2001, Kulkarni et al. 2000, Djorgovski et al. 2001, Lamb & Reichart 2000

✓ At low metallicity stars are expected to be rotating faster because of weaker stellar winds

✓ weaker winds also possible for stars with significant magnetic fields (Petit et al. 2017, Keszthelyi et al. 2019). Roughly 10% of O-stars possess significant B-fields in their outer layers.

Examples for current research:
End phases of evolution

- **End phases**
  - evolutionary tracks towards ‘the end’
  - models for SNe and Gamma-ray bursters
  - models for neutron stars and white dwarfs
  - accretion onto black holes
  - X-ray binaries (‘normal’ star + white dwarf/neutron star/black hole)
  - synthetic spectra of SN-remnants in various phases
  - observations (now including gravitational waves) and comparison with theory
    - first detection of aLIGO was the merger of two black holes with masses around 30 M_{sun} (Abbott et al. 2016)
    - Corresponding theoretical scenario published just before announcement of detection (Marchant+ 2016), predicting one BH merger for 1000 cc-SNe, and a high detection rate with aLIGO

Examples for current research:
Impact on environment

- cosmic re-ionization and chemical enrichment
- chemical yields (due to SNe and winds)
- ionizing fluxes (for HII regions)
- Planetary nebulae (excited by hot central stars)
- impact of winds on ISM (energy/momentum transfer, triggering of star formation)
- stars and their (exo)planets

Feedback

- massive stars determine energy (kinetic and radiation) and momentum budget of surrounding ISM
- kinetic energy and momentum budget via winds (of different strengths, in dependence of evolutionary status)
- massive stars enrich environment with metals, via winds and SNe, determine chemo-dynamical evolution of Galaxies (exclusively before onset of SNe Ia)
  - in particular: first chemical enrichment of Universe by First (VMS) Stars

→"FEEDBACK"

Bubble Nebula
(NGC 7635)
in Cassiopeia

wind-blown
bubble around
BD+602522
(O6.5IIIf)

Chap. 2 – Quantitative spectroscopy

Astrophysics → theory

Astrophysics → experiment

Experiment in astrophysics = Collecting photons from cosmic objects

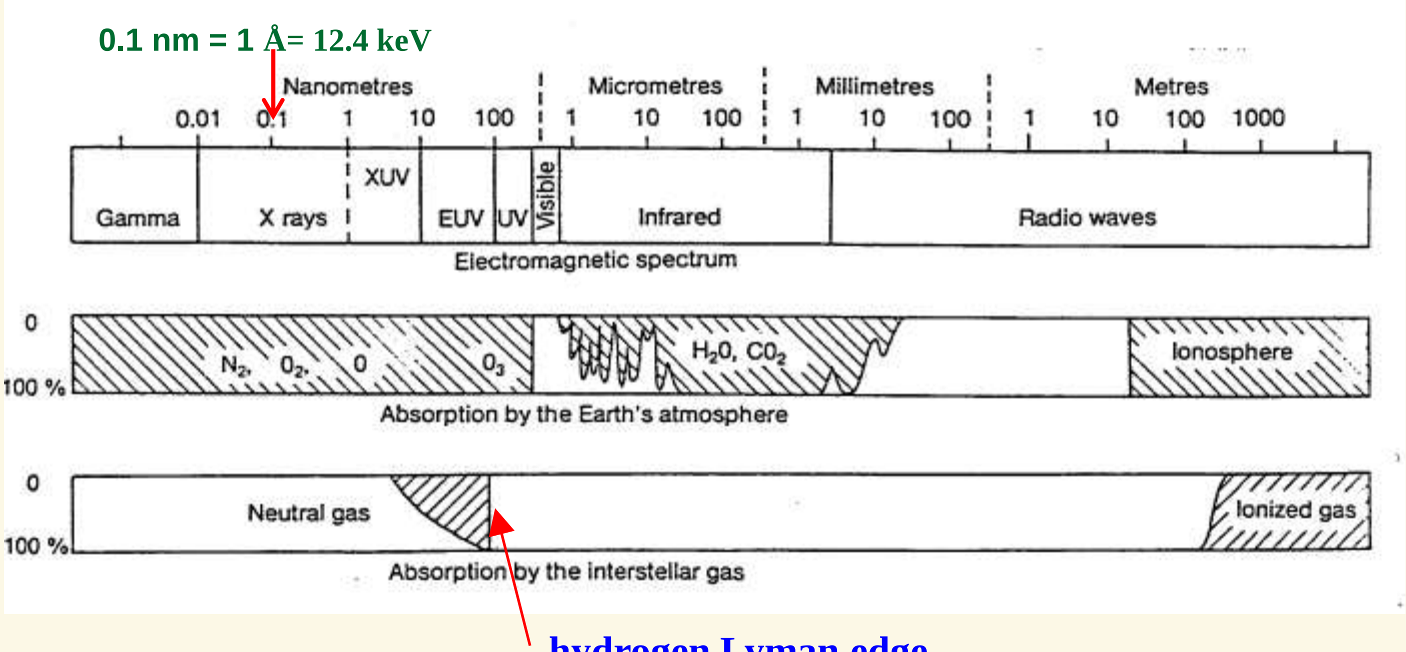

0.1 nm = 1 Å= 12.4 keV

hydrogen Lyman edge

1 Å = 10^{-8} cm = 10^{-4} μm (micron); 1 nm = 10 Å

Collecting: earthbound and via satellites!

Note: Most of these photons originate from the atmospheres of stellar(-like) objects.
Even galaxies consist of stars!

Astrophys. monographs, Univ. Chicago Press (1943)

AN ATLAS OF STELLAR SPECTRA

WITH AN OUTLINE OF SPECTRAL CLASSIFICATION

Morgan, Keenan, Kellman

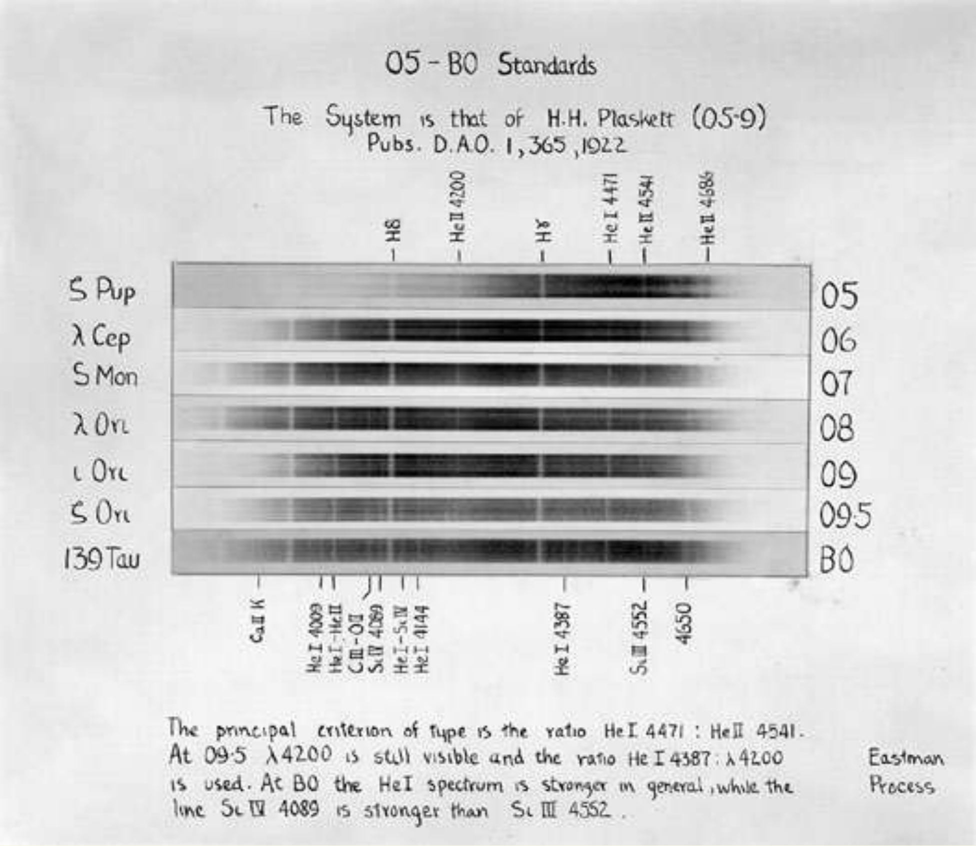

O5 - B0 Standards

The System is that of H.H. Plaskett (O5·9)
Pubs. D.A.O. 1, 365, 1922

The principal criterion of type is the ratio HeI 4471 : HeII 4541. At O9·5 λ4200 is still visible and the ratio HeI 4387 : λ4200 is used. At B0 the HeI spectrum is stronger in general, while the line SiIV 4089 is stronger than SiIII 4552.

Eastman
Process

Empirical system
=>
Physical system

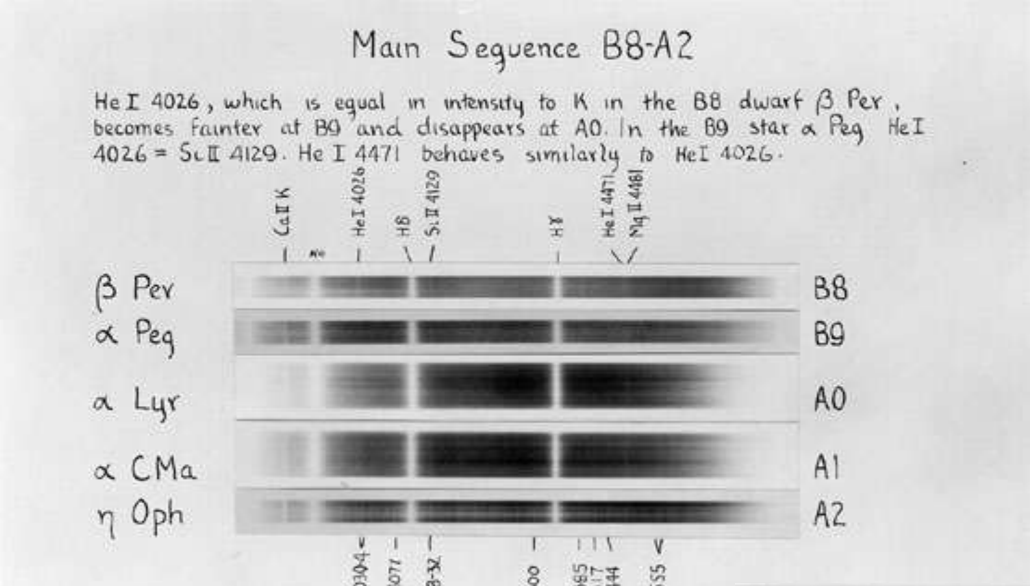

Main Sequence B8-A2

He I 4026, which is equal in intensity to K in the B8 dwarf β Per, becomes fainter at B9 and disappears at A0. In the B9 star α Peg He I 4026 = Si II 4129. He I 4471 behaves similarly to He I 4026.

The singly ionized metallic lines are progressively str and η Oph than in α Lyr. The spectral type is deter ratios: B8, B9: He I 4026 : Ca II K, He I 4026 : Si II 4129, He I 4471 Mg II 4481 : 4385, Si II 4129 : Mn I 4030-4.

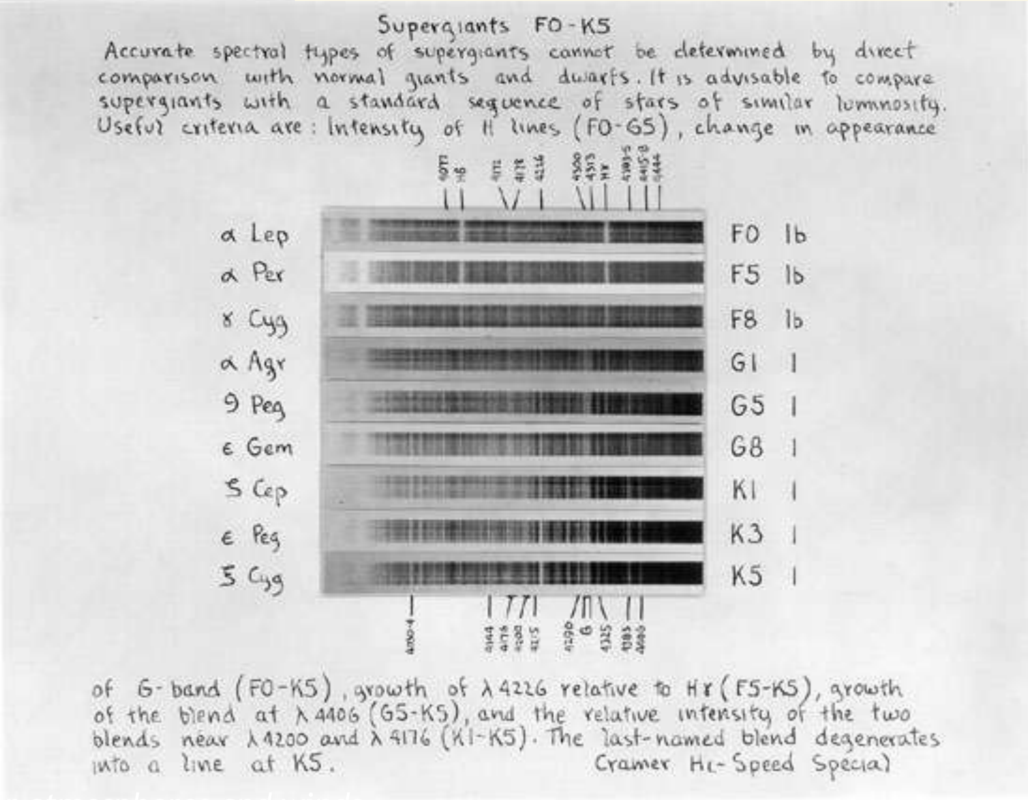

Supergiants F0-K5

Accurate spectral types of supergiants cannot be determined by direct comparison with normal giants and dwarfs. It is advisable to compare supergiants with a standard sequence of stars of similar luminosity. Useful criteria are: Intensity of H lines (F0-G5), change in appearance

of G-band (F0-K5), growth of λ4226 relative to Hγ (F5-K5), growth of the blend at λ4406 (G5-K5), and the relative intensity of the two blends near λ4200 and λ4176 (K1-K5). The last-named blend degenerates into a line at K5.

Cramer Hi-Speed Special

Digitized spectra

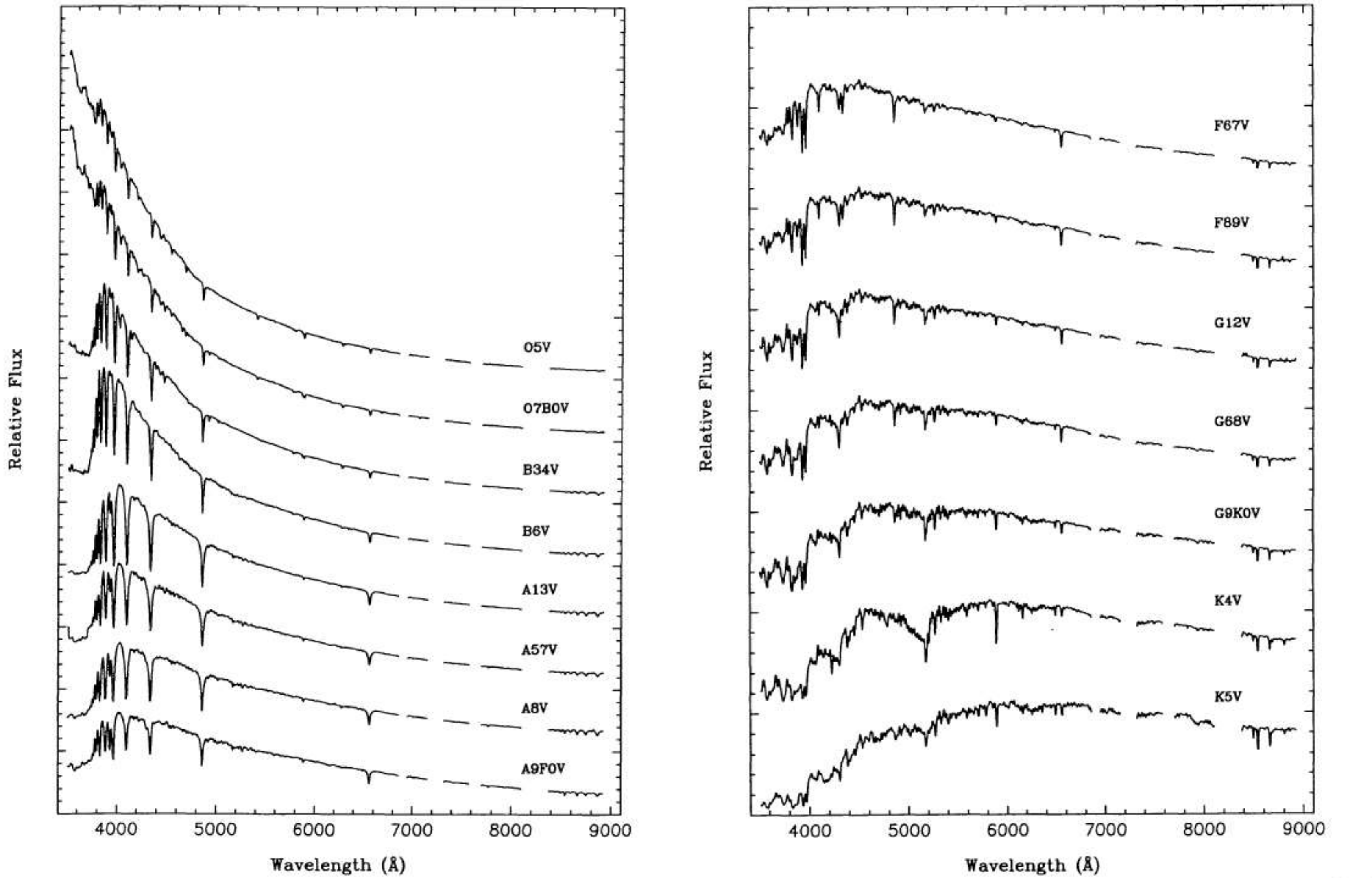

FIG. 1.—Dwarf-type library stars. Near-IR gaps are excised telluric absorption bands. All spectra have been normalized to 100 at 5450 Å. Major tick marks on "Relative Flux" axis are separated by 100 relative units. The M dwarf library stars are displayed with the M giants in Fig. 3.

from Silva & Cornell, 1992

Spectral lines formed in (quasi-)hydrostatic atmospheres

ESO 3.6m
CASPEC

$\Delta\lambda \approx 0.5$Å
S/N 30...70

(Walborn et al.,1995

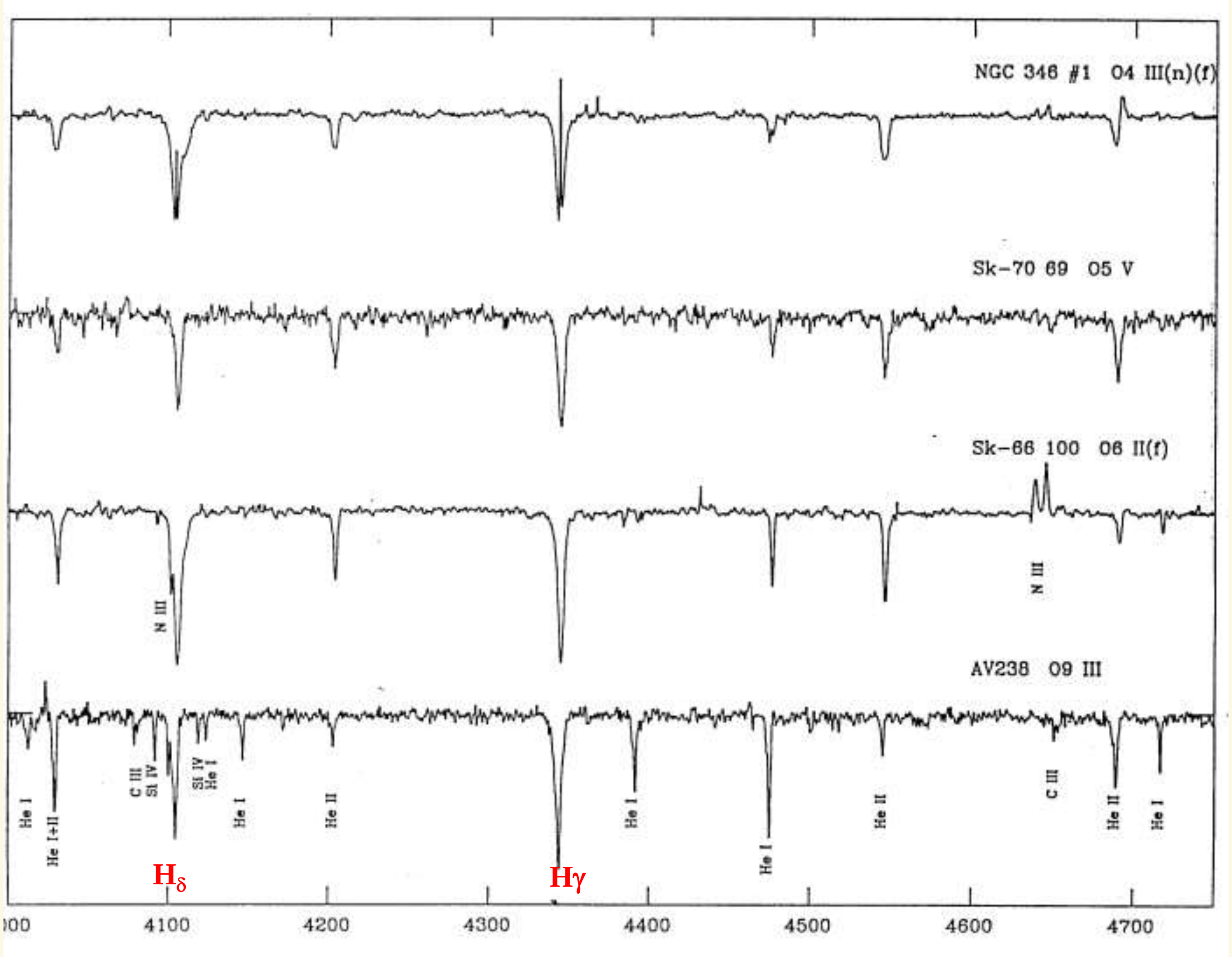

SMC

LMC

LMC

SMC

P-Cygni lines formed in hydrodynamic atmospheres

HST-FOS

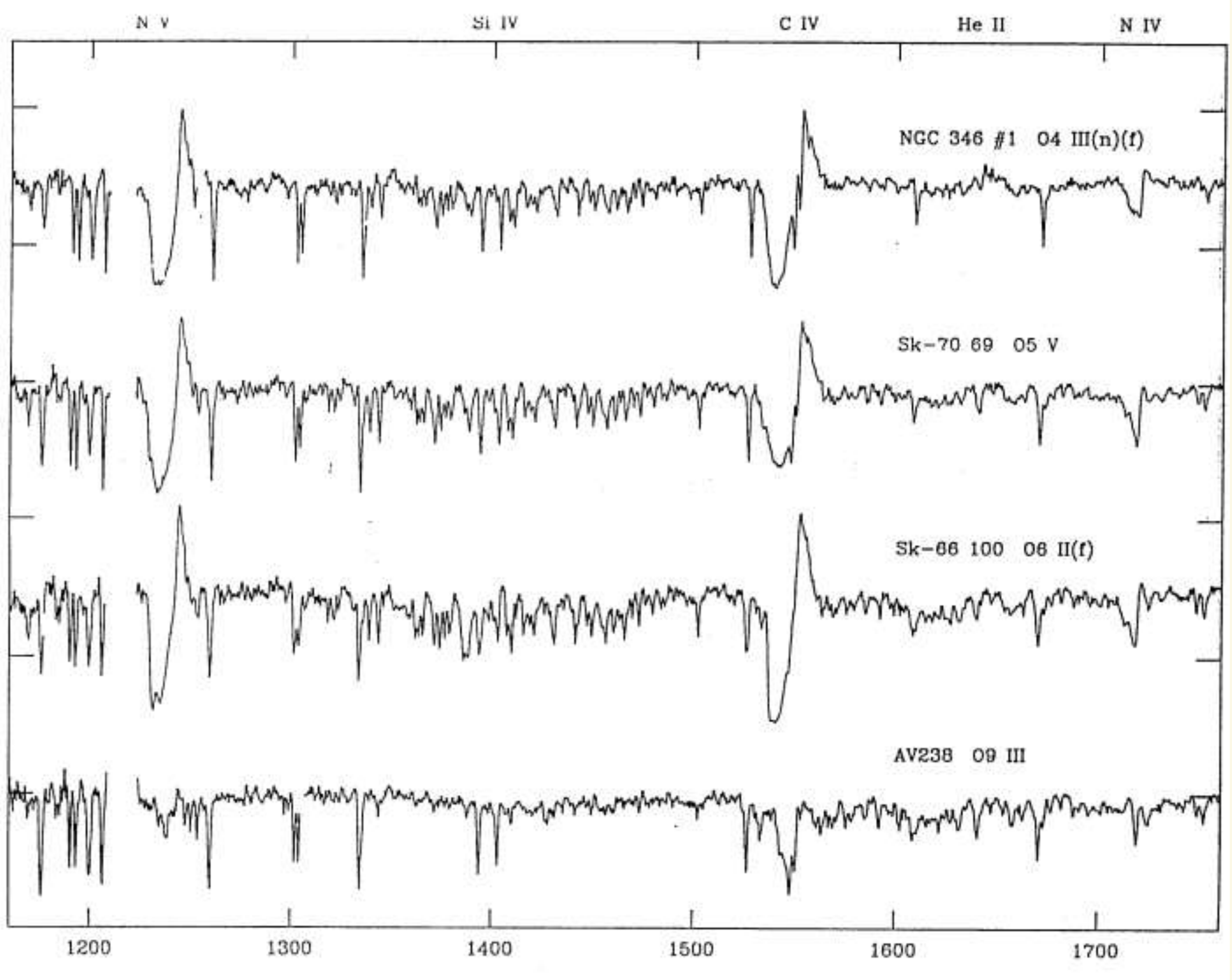

SMC

LMC

LMC

SMC

UV spectrum of the O4I(f) supergiant ζ Pup

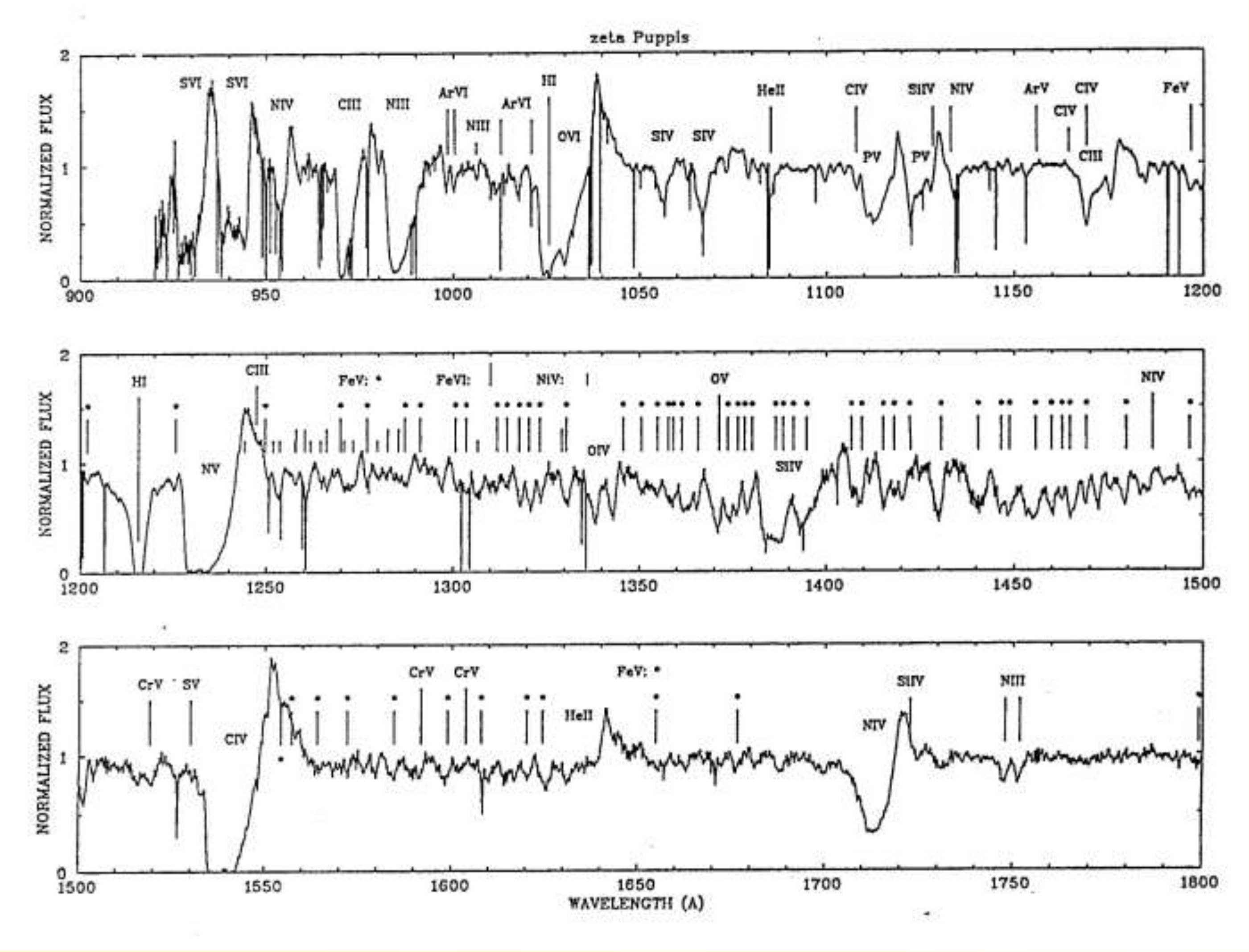

montage of Copernicus (λ < 1500 Å, high res. mode, Δλ ≈ 0.05 Å, Morton & Underhill 1977) and IUE (Δλ ≈ 0.1 Å) observations

Supernova Type II in different phases

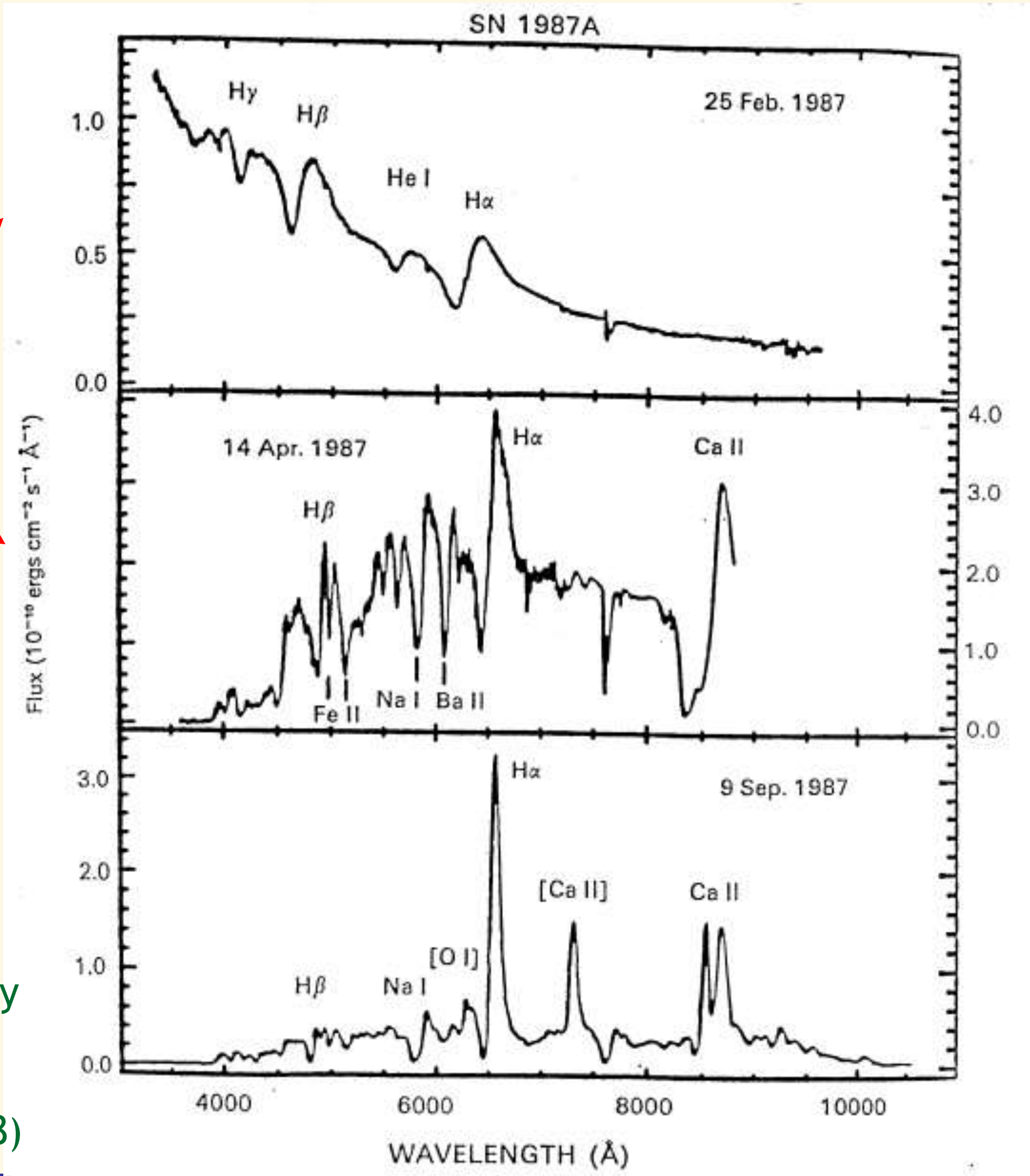

photospheric phase

transition to nebular phase

figure prepared by Mark M. Phillips, reproduced from McCray & Li (1988)

Spectrum of Planetary Nebula

pure emission line spectrum with forbidden lines of O III

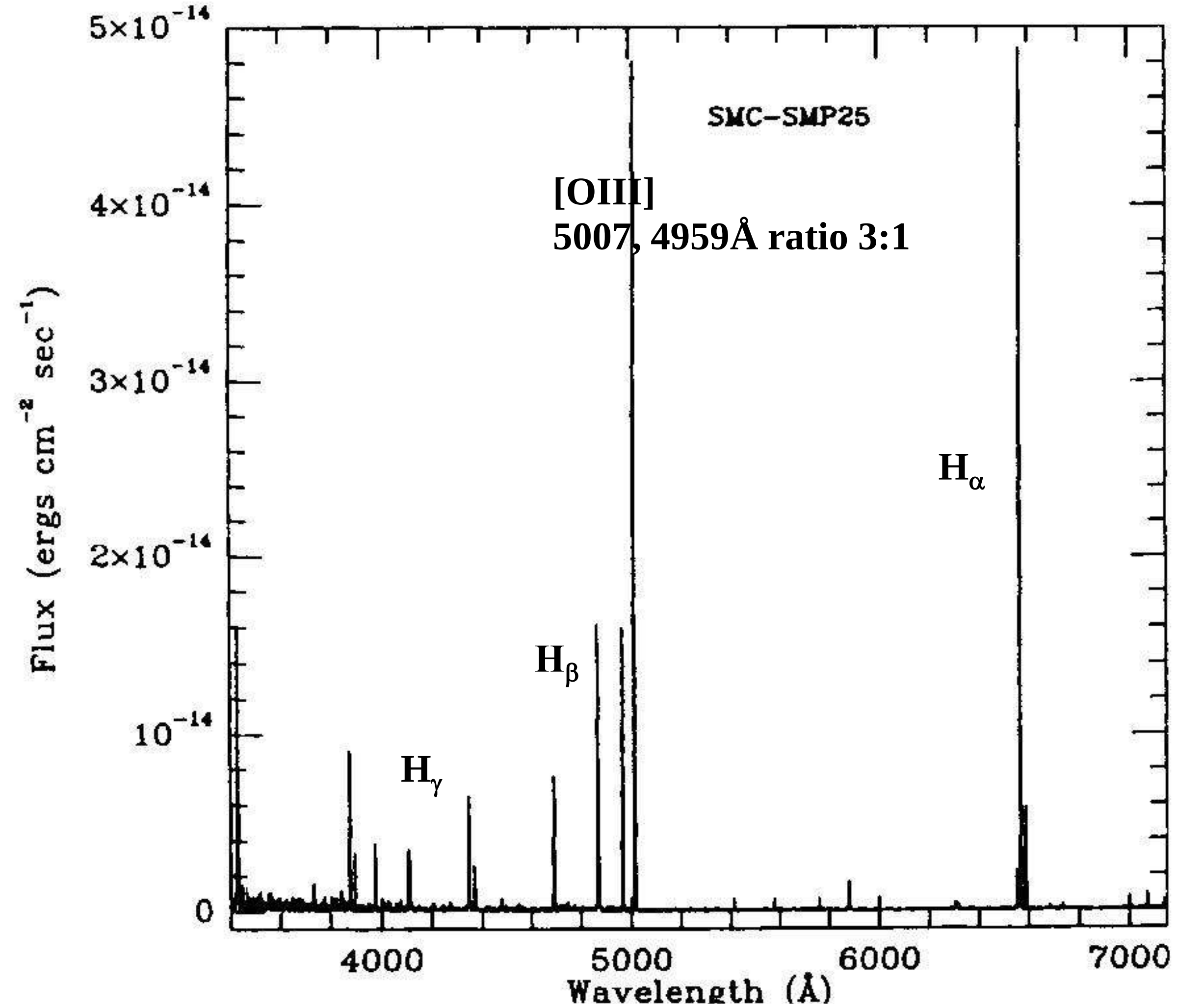

From Meatheringham & Dopita, 1991, ApJS 75

FIG. 1*a*

Quasar spectrum in rest frame of quasar

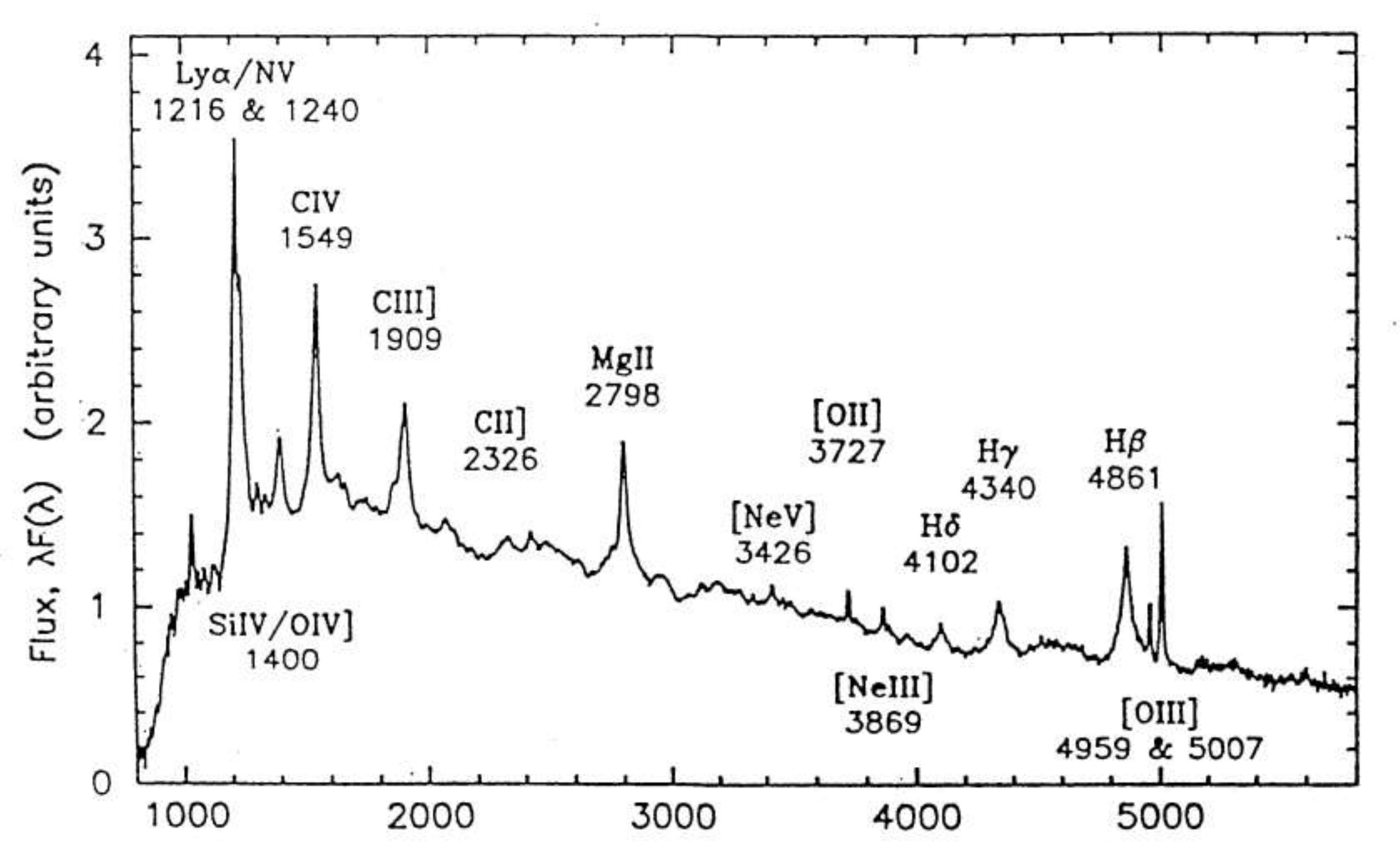

“UV”-spectra of starburst galaxies

galaxy at z = 2.72

local
starburst galaxy,
wavelengths shifted

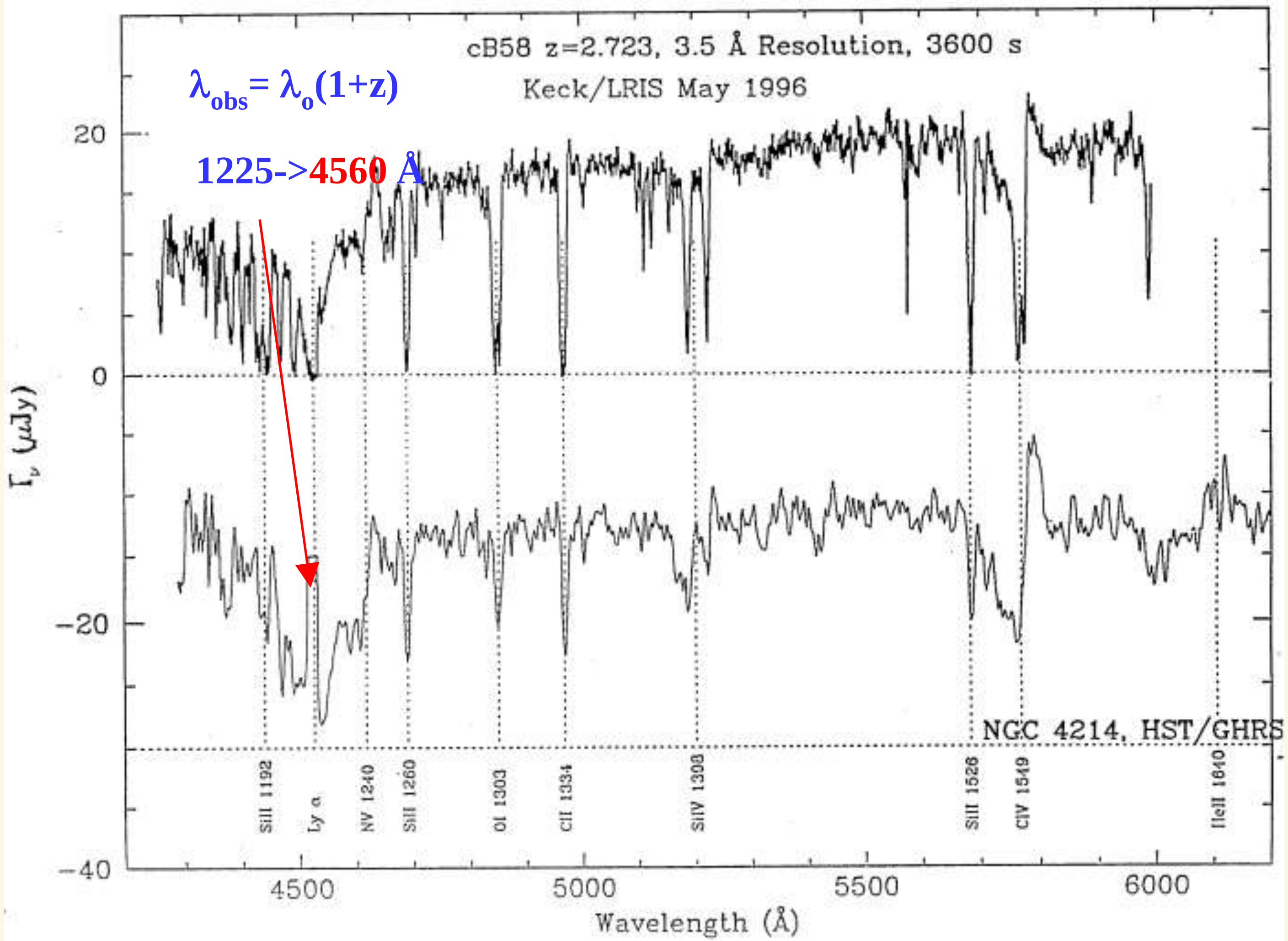

$\lambda_{obs} = \lambda_o(1+z)$

1225->4560 Å

From Steidel et al. (1997)

Atmospheres and nebulae - an overview

Sun

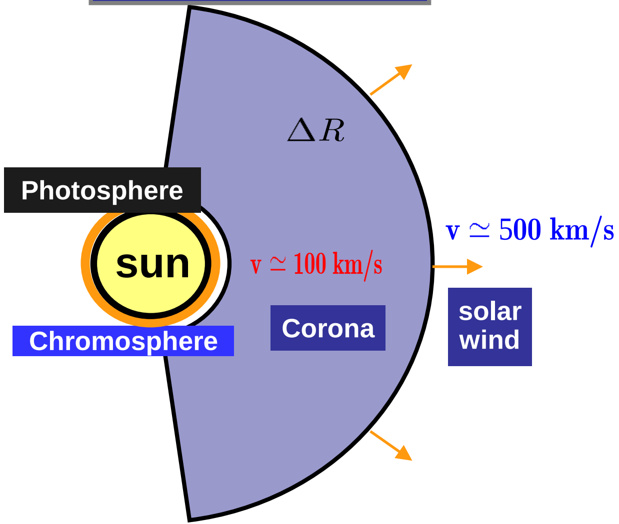

Core:

$M_\odot = 2\ 10^{33}$ g

$R_\odot = 7\ 10^{10}$ cm

$L_\odot = 4\ 10^{33}$ erg s^{-1}

Photosphere:

$\Delta R \sim 200$ km

$T \sim 6000$ K

$n \sim 10^{15}$ cm^{-3}

Chromosphere:

$\Delta R \sim 1000$ km

$T \sim 20000$ K

$n \sim 10^{12}$ cm^{-3}

Corona:

$\Delta R \sim R_\odot$

$T \sim 10^{6}$ K

$n \sim 2 \cdot 10^{6}$ cm^{-3}

hot, massive star

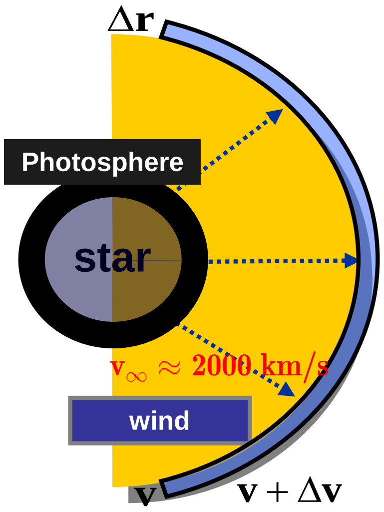

Core:

$M \sim 50\ M_\odot$

$R \sim 20\ R_\odot$

$L \sim 10^5 \mapsto 10^6\ L_\odot$

Photosphere:

$\Delta R / R \sim \Delta R_\odot / R_\odot$

$T \sim 20000 \mapsto 50000$ K

$n \sim 10^{14} \mapsto 10^{12}$ cm^{-3}

Wind:

$\Delta R \sim 100 R_*$

$T \sim 0.9...0.3 \cdot T_{eff}$

$n \sim 10^{12}...10^{8}$ cm^{-3}

Supernova Ia

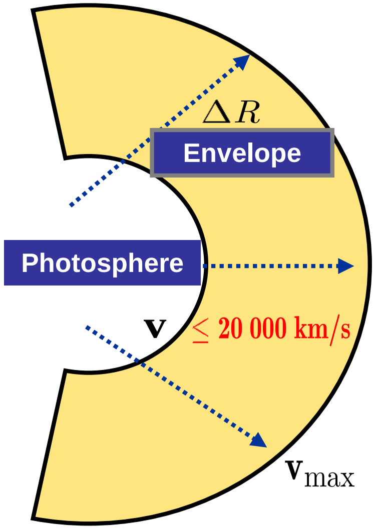

Core:

$M \sim 1.44\ M_\odot$

exploded

$L_{max} \sim 10^{11}\ L_\odot$

Envelope:

$\Delta R \sim 10^5 R_\odot$

$T \sim 12000$ K

$n \sim 10^{6}$ cm^{-3}

Gaseous Nebula

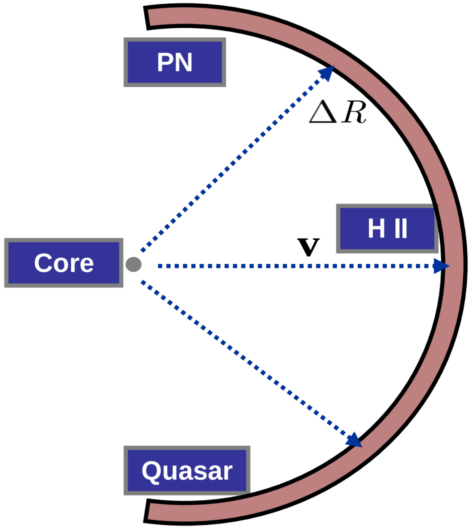

Core:

$M_{PN} \sim 1\ M_\odot$

$M_{HII} \sim 50 \mapsto 10^5\ M_\odot$

$M_Q \sim 10^9 \mapsto 10^{11}\ M_\odot$

$L_{PN} \sim 10^4\ L_\odot$

$L_{HII} \sim 10^6\ L_\odot$

$L_Q \sim 10^{12}\ L_\odot$

Envelope:

$\Delta R \sim 0.1$pc (PN)

$\Delta R \sim 10$ pc (H II)

$\Delta R \sim 10^3$ pc (Quasar)

Stellar atmospheres - an overview

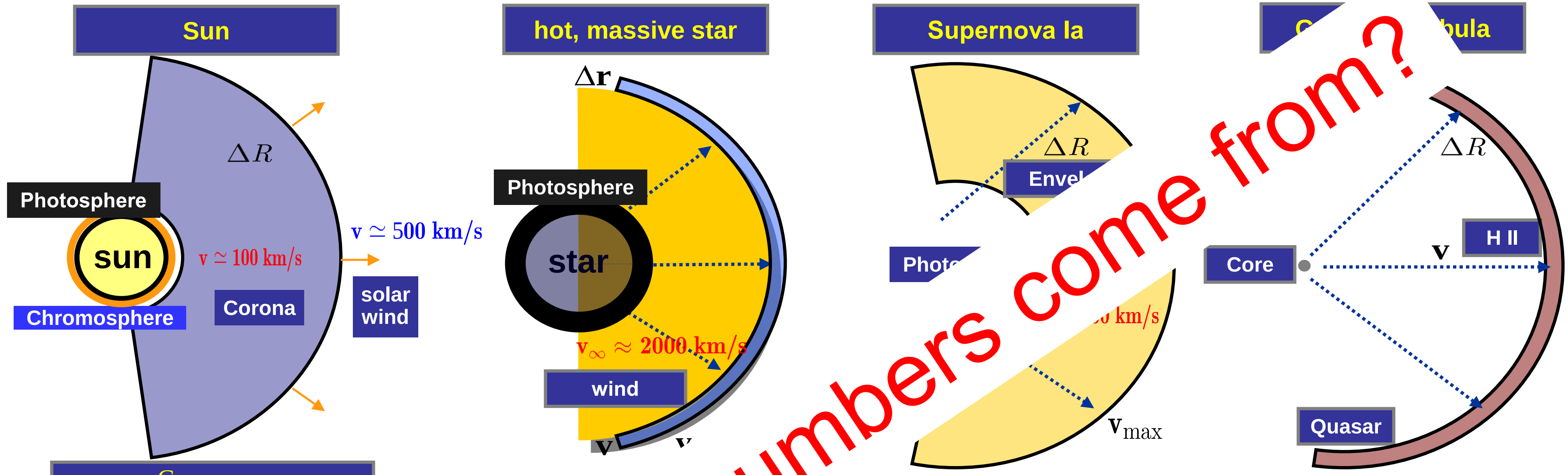

Core:

$M_\odot = 2\ 10^{33}$ g

$R_\odot = 7\ 10^{10}$ cm

$L_\odot = 4\ 10^{33}$ erg s^{-1}

Photosphere:

$\Delta R \sim 200$ km

$T \sim 6000$ K

$n \sim 10^{15}$

Chromosphere:

$\sim R_\odot$

$T \sim 10^6$ K

$n \sim 2 \cdot 10^6$ cm^{-3}

$R_\odot$

$10^5 \mapsto 10^6\ L_\odot$

phere:

$\Delta R / R \sim \Delta R_\odot / R_\odot$

$T \sim 20000 \mapsto 50000$ K

$n \sim 10^{14} \mapsto 10^{12}$ cm^{-3}

Wind:

$\Delta R \sim 100 R_*$

$T \sim 0.9 \ldots 0.3 \cdot T_{eff}$

$n \sim 10^{12} \ldots 10^8$ cm^{-3}

Core:

$M \sim 1.44\ M_\odot$

exploded

$L_{max} \sim 10^{11}\ L_\odot$

Envelope:

$\Delta R \sim 10^5 R_\odot$

$T \sim 12000$ K

$n \sim 10^6$ cm^{-3}

Core:

$M_{PN} \sim 1\ M_\odot$

$M_{HII} \sim 50 \mapsto 10^5\ M_\odot$

$M_Q \sim 10^9 \mapsto 10^{11}\ M_\odot$

$L_{PN} \sim 10^4\ L_\odot$

$L_{HII} \sim 10^6\ L_\odot$

$L_Q \sim 10^{12}\ L_\odot$

Envelope:

$\Delta R \sim 0.1$pc (PN)

$\Delta R \sim 10$ pc (H II)

$\Delta R \sim 10^3$ pc (Quasar)

Where do these numbers come from?

Quantitative spectroscopy...

...gives insight into and understanding of our cosmos

Quantitative spectroscopy = quantitative diagnostics of spectra

- provides
  - stellar properties, mass, radius, luminosity, energy production, chemical composition, properties of outflows
  - properties of (inter) stellar plasmas, temperature, density, excitation, chemical comp., magnetic fields
- INPUT for stellar, galactic and cosmologic evolution and for stellar and galactic structure
- requires
  - plasma physics, plasma is "normal" state of atmospheres and interstellar matter (plasma diagnostics, line broadening, influence of magnetic fields,...)
  - atomic physics/quantum mechanics, interaction light/matter (micro quantities)
  - radiative transfer, interaction light/matter (macroscopic description)
  - thermodynamics, thermodynamic equilibria: TE, LTE (local), NLTE (non-local)
  - hydrodynamics, atmospheric structure, velocity fields, shockwaves,...

one example ...

atomic levels and
allowed transitions
("Grotrian-diagram")
in OIV

gf oscillator strength,
measures "strength"
of transition
(cf. Chap 7)

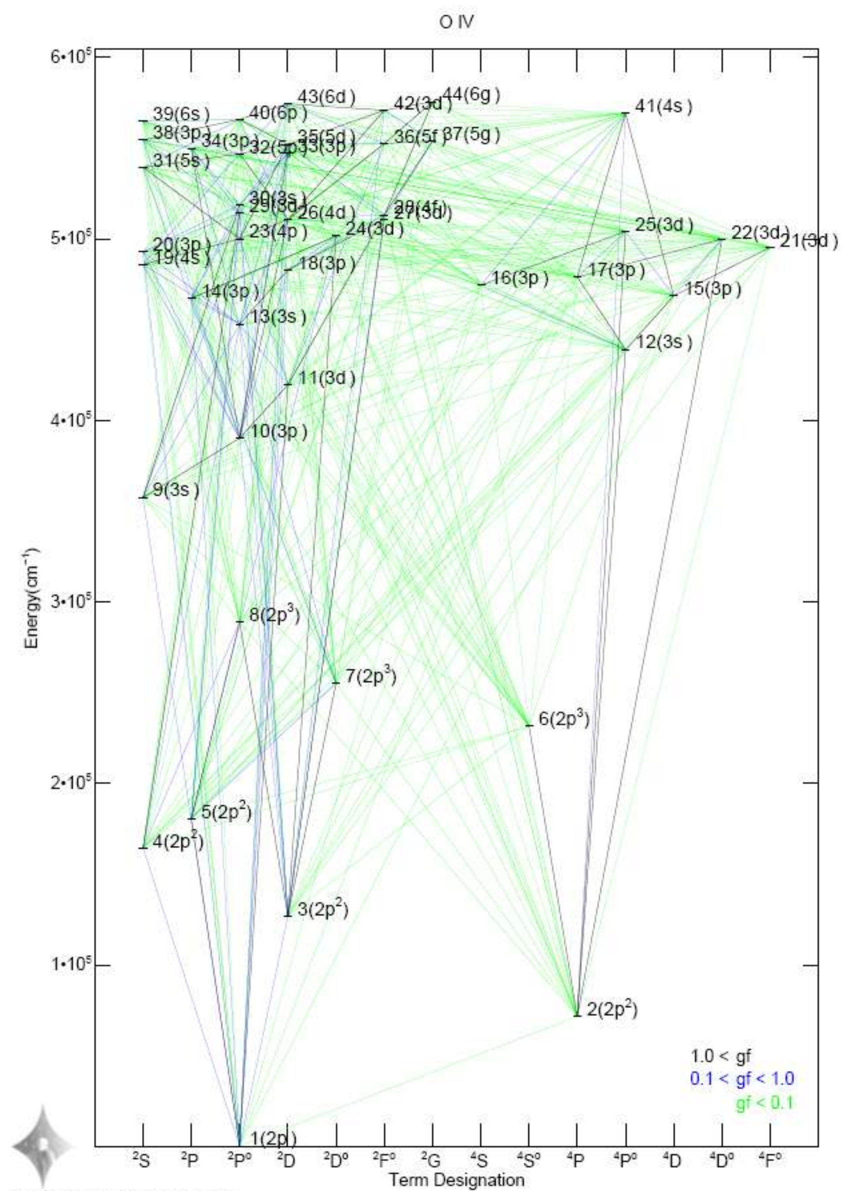

© USM Hot Star Group, 1999-08-30

sites of X-ray emission in
hot stars:

shell collisions

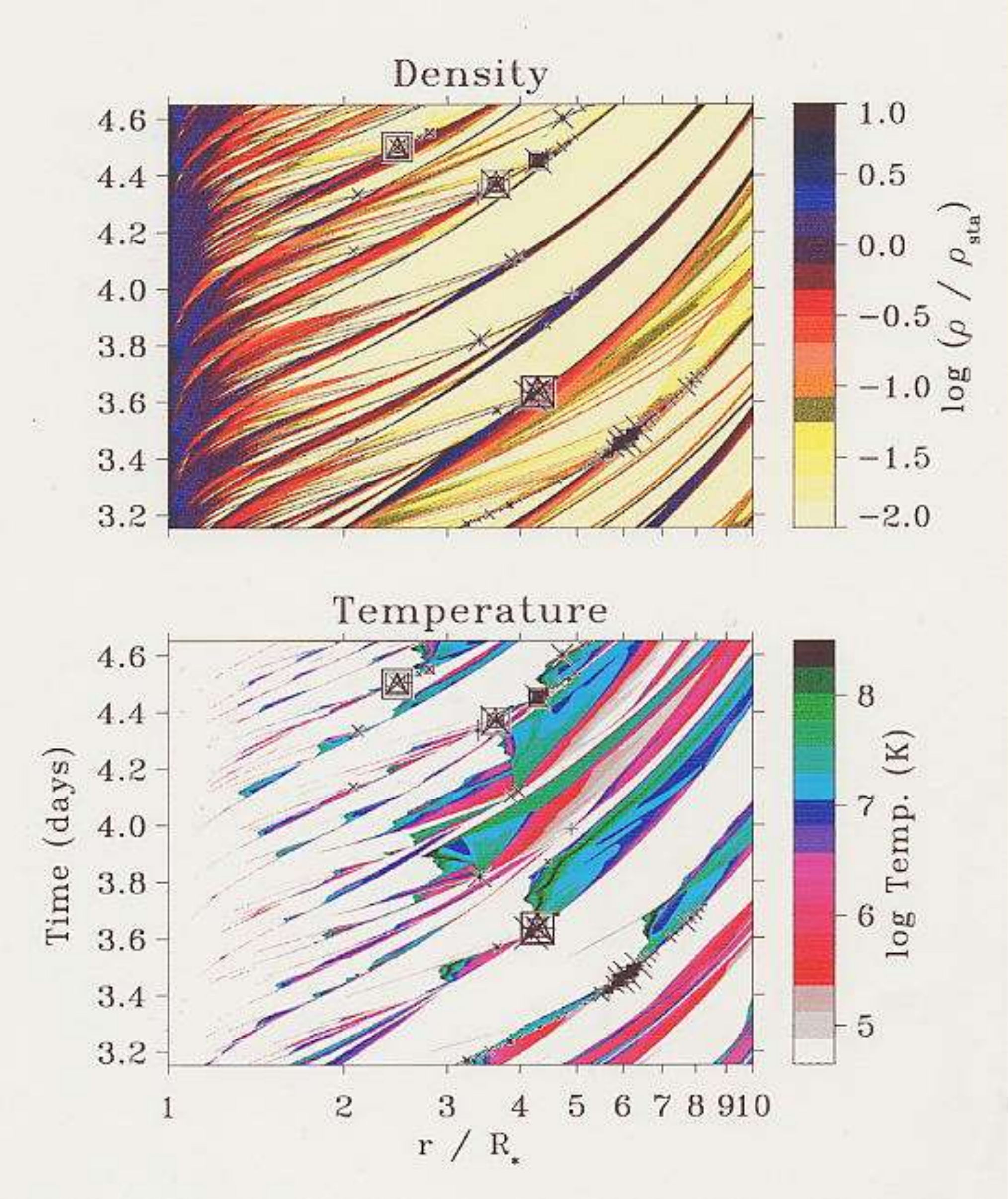

hydrodynamical simulations
of instable hot star winds,
from A. Feldmeier,
by permission

Concept of spectral analysis

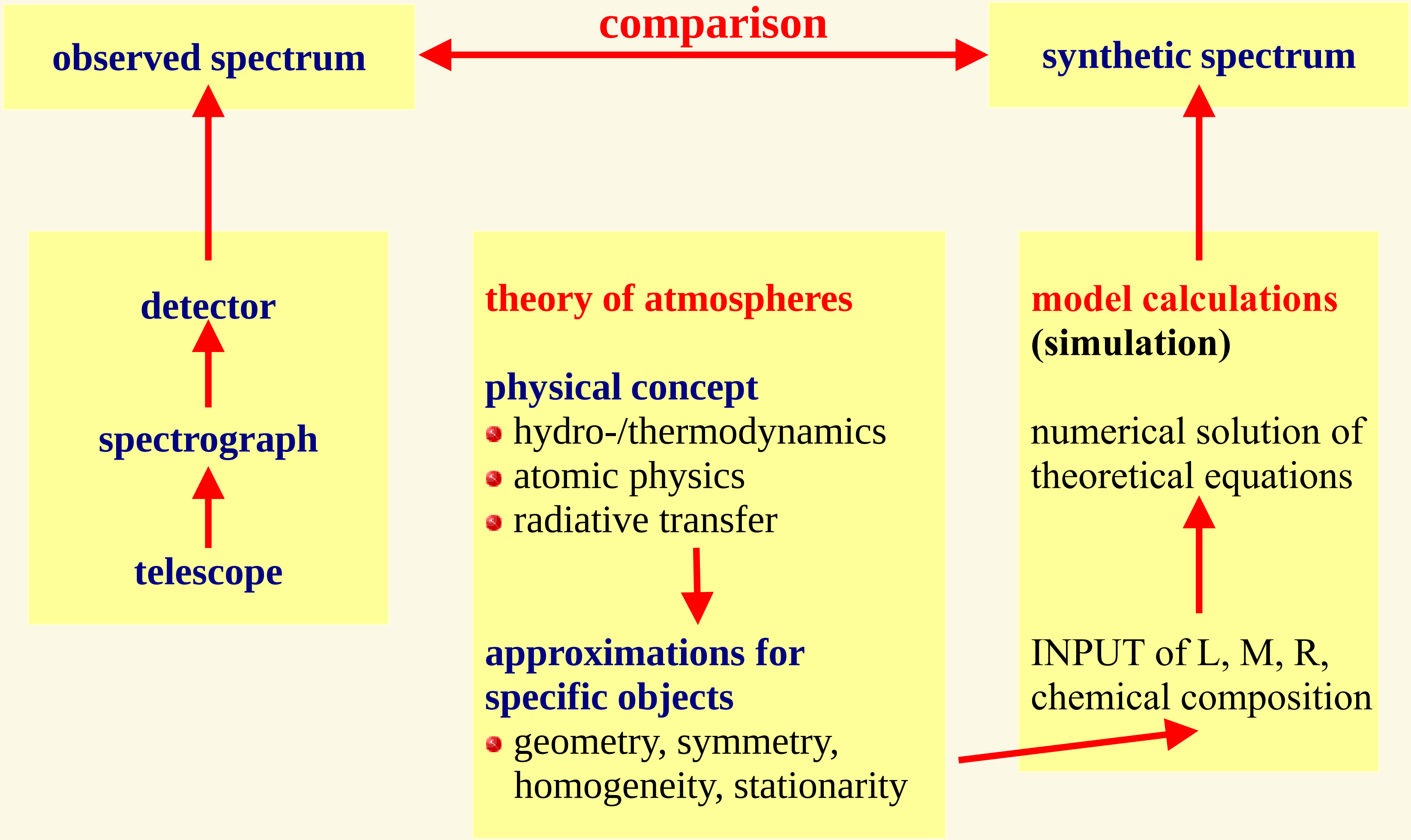

comparison

observed spectrum

synthetic spectrum

detector

spectrograph

telescope

theory of atmospheres

physical concept

- hydro-/thermodynamics
- atomic physics
- radiative transfer

approximations for specific objects

- geometry, symmetry, homogeneity, stationarity

model calculations
(simulation)

numerical solution of theoretical equations

INPUT of L, M, R, chemical composition

advanced reading

The VLT-FLAMES survey of massive stars (‘FLAMES I’)
The VLT-FLAMES Tarantula survey (‘FLAMES II’)

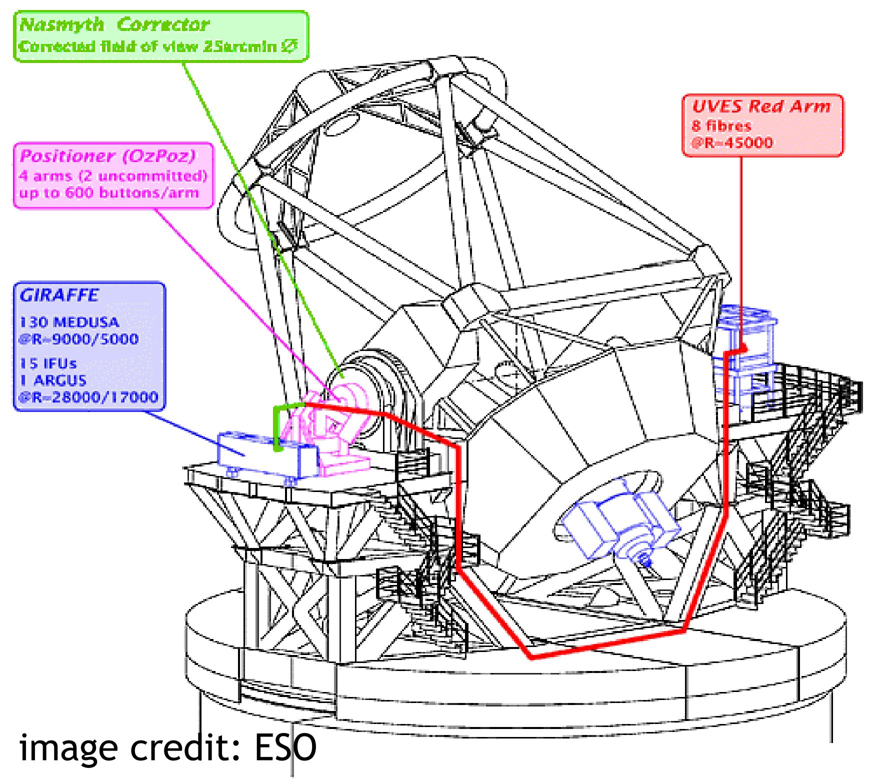

image credit: ESO

FLAMES =
Fibre Large Array Multi Element Spectrograph

image credit: ESO

- **FLAMES I:** high resolution spectroscopy of massive stars in 3 Galactic, 2 LMC and 2 SMC clusters (young and old)
  - total of 86 O- and 615 B-stars
- **FLAMES II**: high resolution spectroscopy of more than 1000 massive stars in Tarantula Nebula (incl. 300 O-type stars)

Major objectives

- rotation and abundances (test rotational mixing)
- stellar mass-loss as a function of metallicity
- binarity/multiplicity (fraction, impact)
- detailed investigation of the closest ‘proto-starburst’

summary of FLAMES I results: Evans et al. (2008),
summary of FLAMES II results: Evans et al. (2019, in prep.)

Optical spectrum of a very hot O-star

Theory vs. observations

- Synthetic spectra from Rivero-Gonzalez et al. (2012)

red: HI
blue: HeI
green: HeII
orange: NIV
magenta: NV

BI237 O2V (f*) (LMC) – vsini = 140 km/s

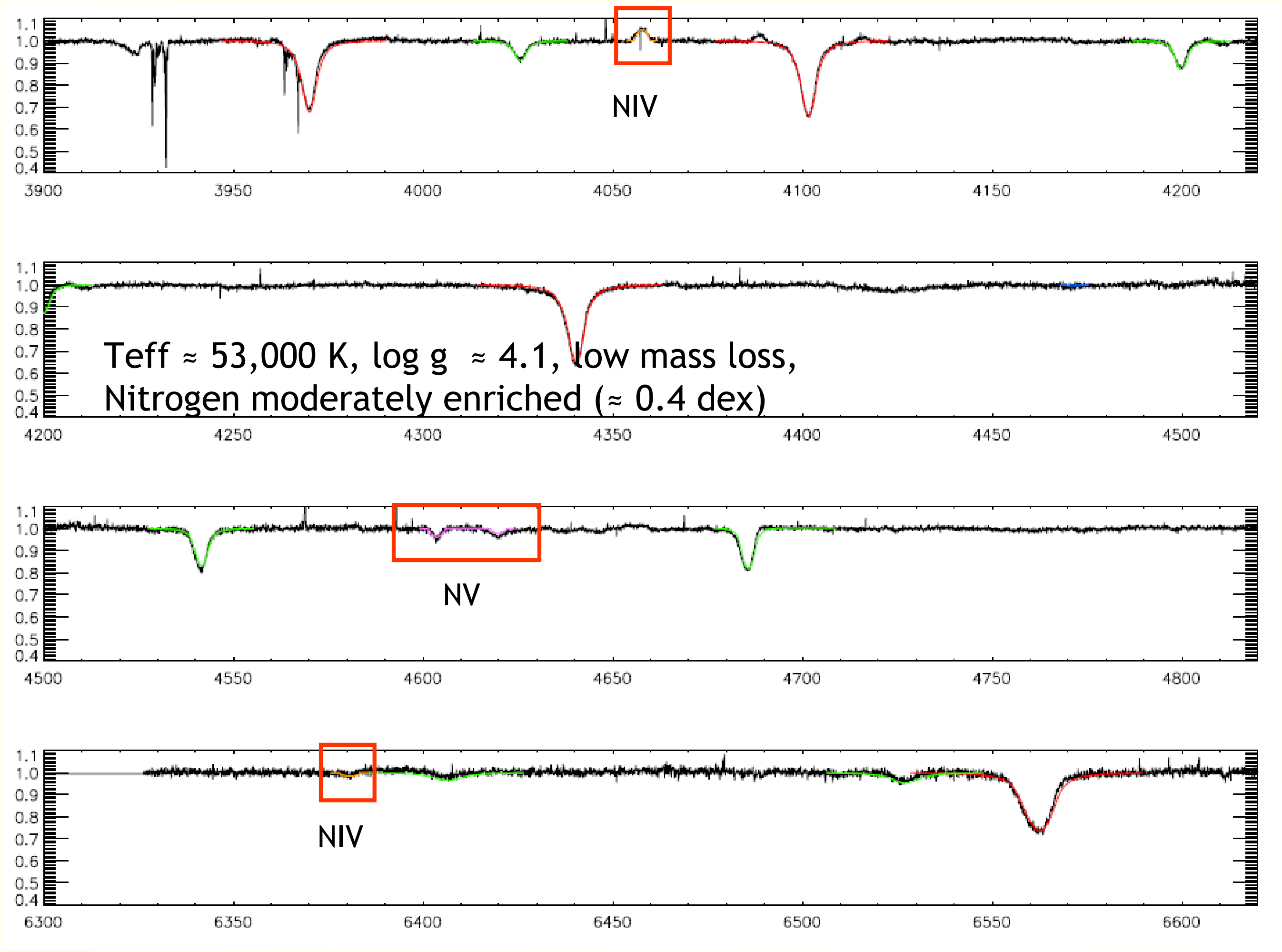
Teff ≈ 53,000 K, log g ≈ 4.1, low mass loss,
Nitrogen moderately enriched (≈ 0.4 dex)

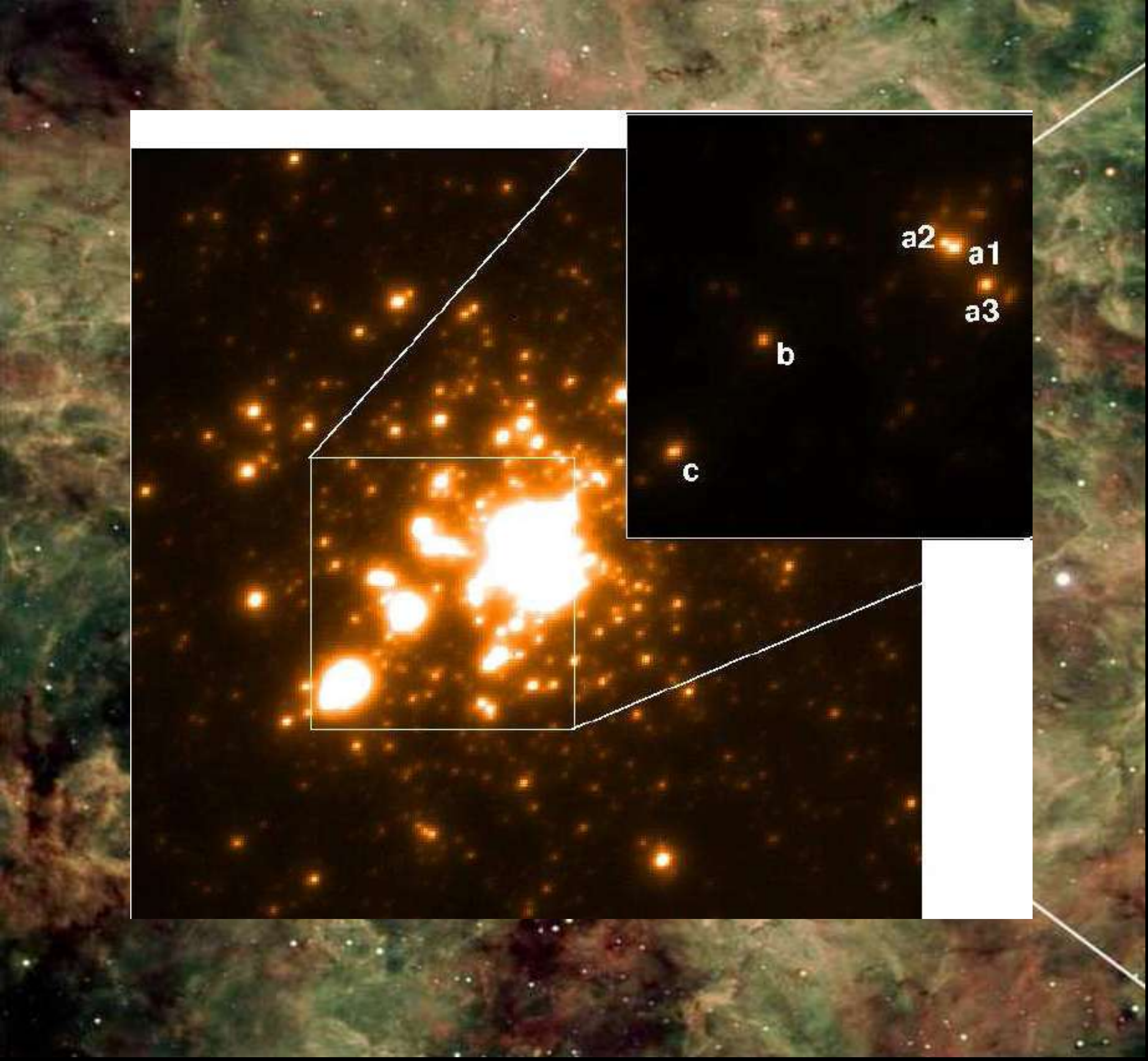

- Tarantula Nebula
  (30 Dor) in the LMC
- Largest starburst region in Local Group
- Target of
  VLT-FLAMES Tarantula survey (‘FLAMES II’,
  PI: Chris Evans)
- Cluster R136 contains some of the *most massive, hottest, and brightest* stars known
- Crowther et al. (2010):
  4 stars with initial masses from 165-320 (!!!) $M_\odot$
- problems with IR-photometry (background-correction), lead to overestimated luminosities → initial masses become reduced: 140 - 195 $M_\odot$ (Rubio-Diez et al., IAUS 329, 2016)

Spectral energy distribution of the most massive stars in our “neighbourhood” - theory vs. observations

from Crowther et al. 2010

lower masses from Rubio-Diez et al 2016

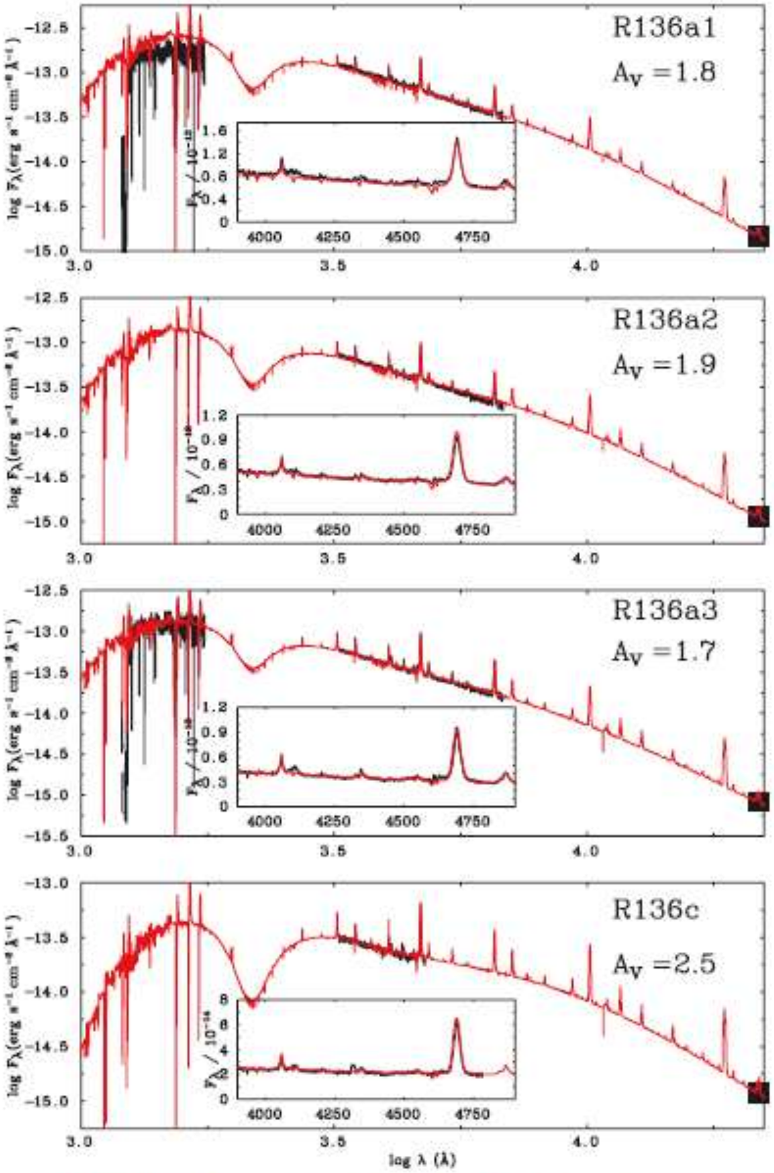

Figure 4. Spectral energy distributions of R136 WN 5h stars from *HST*/FOS together using K_s photometry from VLT/SINFONI calibrated with VLT/MAD imaging. Theoretical spectral energy distributions are shown as red lines.

initial mass (Msun)	current mass (Msun)
320 → <194	265
240 → <140	195
165 → 141	135
220	175
typical uncertainty ± 40 Msun	

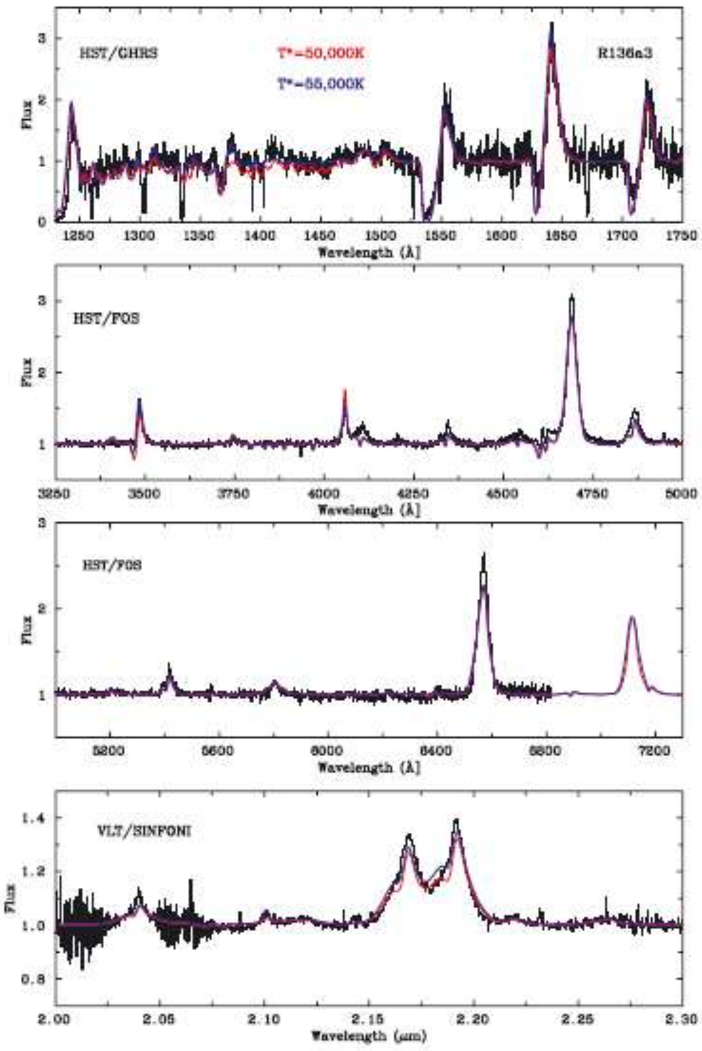

Figure 5. Rectified, ultraviolet (*HST*/GHRS), visual (*HST*/FOS) and near-IR (VLT/SINFONI) spectroscopy of the WN 5h star R136a3 together with synthetic UV, optical and near-IR spectra, for $T_* = 50\,000$ K (red) and $T_* = 55\,000$ K (blue). Instrumental broadening is accounted for, plus an additional rotational broadening of 200 km s^{-1}.

Chap. 3 – The radiation field

Number of particles in $(\mathbf{r}, \mathbf{r} + d\mathbf{r})$ with momenta $(\mathbf{p}, \mathbf{p} + d\mathbf{p})$ at time t

$$\delta N(\mathbf{r},\mathbf{p},t) = f(\mathbf{r},\mathbf{p},t)\; d^3\mathbf{r}\; d^3\mathbf{p}$$

distribution function f

For a detailed derivation and discussion, see, e.g., Cercignani, C., "The Boltzmann Equation and Its Applications", Appl. Math. Sciences 67, Springer, 1987

i) $f(\mathbf{r},\mathbf{p},t)$ is Lorentz-invariant

ii) $\delta N_0 = f(\mathbf{r}_0,\mathbf{p}_0,t_0)\; d^3\mathbf{r}_0\; d^3\mathbf{p}_0$

$$\Big\downarrow \quad \text{evolution}$$

$$\delta N = f(\mathbf{r}_0 + d\mathbf{r}, \mathbf{p}_0 + d\mathbf{p}, t_0 + dt)\; d^3\mathbf{r}\; d^3\mathbf{p}$$

$$(\dot{p} = F) = f(\mathbf{r}_0 + \mathbf{v}dt, \mathbf{p}_0 + \mathbf{F}dt, t_0 + dt)\; d^3\mathbf{r}\; d^3\mathbf{p}$$

Theoretical mechanics: If no collisions, conservation of phase space volume:

$$d^3\mathbf{r}_0\; d^3\mathbf{p}_0 = d^3\mathbf{r}\; d^3\mathbf{p}$$

and

$\delta N_0 = \delta N$ (particles do not "vanish", again no collisions supposed)

$$\Rightarrow \boxed{f(\mathbf{r},\mathbf{p},t) = \text{const}, \quad \text{if no collisions}}$$

$$\Rightarrow \frac{\partial f}{\partial t} + \sum \frac{\partial f}{\partial r_i}\frac{\partial r_i}{\partial t} + \sum \frac{\partial f}{\partial p_i}\frac{\partial p_i}{\partial t} =$$

$$= \underbrace{\frac{\partial f}{\partial t} + (\mathbf{v}\cdot\nabla) f}_{} + (\mathbf{F}\cdot\nabla_p) f = \begin{cases} 0 & \text{Vlasov} \\ \left(\dfrac{\delta \mathrm{f}}{\delta \mathrm{t}}\right)_{\text{coll}} & \text{Boltzmann if collisions} \end{cases}$$

D/Dt f, Lagrangian derivative

total derivative of f measured in fluid frame, at times t, t+Δt and positions **r**, **r** + **v** Δt

- implications for photon gas

$$\mathbf{p} = \frac{h\nu}{c}\mathbf{n}$$

$$d^3\mathbf{p} = p^2 dp d\Omega \qquad \leftarrow \text{ solid angle with respect to } \mathbf{n}$$

absolute value

$$= \left(\frac{h\nu}{c}\right)^2 \frac{h}{c} d\nu d\Omega = \frac{h^3}{c^3}\nu^2 d\nu d\Omega$$

$$\Rightarrow f(\mathbf{r},\mathbf{p},t)\; d^3\mathbf{r}\; d^3\mathbf{p} = \frac{h^3}{c^3}\nu^2 f(\mathbf{r},\mathbf{n},\nu,t)\; d^3\mathbf{r}\; d\nu d\Omega =$$

$$\boxed{= \Psi(\mathbf{r},\mathbf{n},\nu,t)\; d^3\mathbf{r}\; d\nu d\Omega}$$

$$d^3\mathbf{p} = J(\mathbf{p},\mathbf{p}')\, d^3\mathbf{p}', \qquad \mathbf{p}' = (p,\theta,\phi)$$

cartesian Jacobi-det. spherical

$$\mathrm{p_x} = p\sin\theta\cos\phi$$
$$\mathrm{p_y} = p\sin\theta\sin\phi$$
$$\mathrm{p_z} = p\cos\theta$$

$$J = \det\begin{pmatrix} \frac{\partial p_x}{\partial p} & \frac{\partial p_x}{\partial \theta} & \frac{\partial p_x}{\partial \phi} \\ \frac{\partial p_y}{\partial p} & \frac{\partial p_y}{\partial \theta} & \frac{\partial p_y}{\partial \phi} \\ \frac{\partial p_z}{\partial p} & \frac{\partial p_z}{\partial \theta} & \frac{\partial p_z}{\partial \phi} \end{pmatrix} = \det\begin{pmatrix} \sin\theta\cos\phi & \mathrm{p}\cos\theta\cos\phi & \text{-}\mathrm{p}\sin\theta\sin\phi \\ \sin\theta\sin\phi & \mathrm{p}\cos\theta\sin\phi & \mathrm{p}\sin\theta\cos\phi \\ \cos\theta & \text{-}\mathrm{p}\sin\theta & 0 \end{pmatrix}$$

$$= \text{(exercise)} \; \boxed{p^2\sin\theta}$$

$$\Rightarrow d^3\mathbf{p} = dp_x dp_y dp_z = p^2 dp \underbrace{\sin\theta d\theta d\phi}_{d\Omega}$$

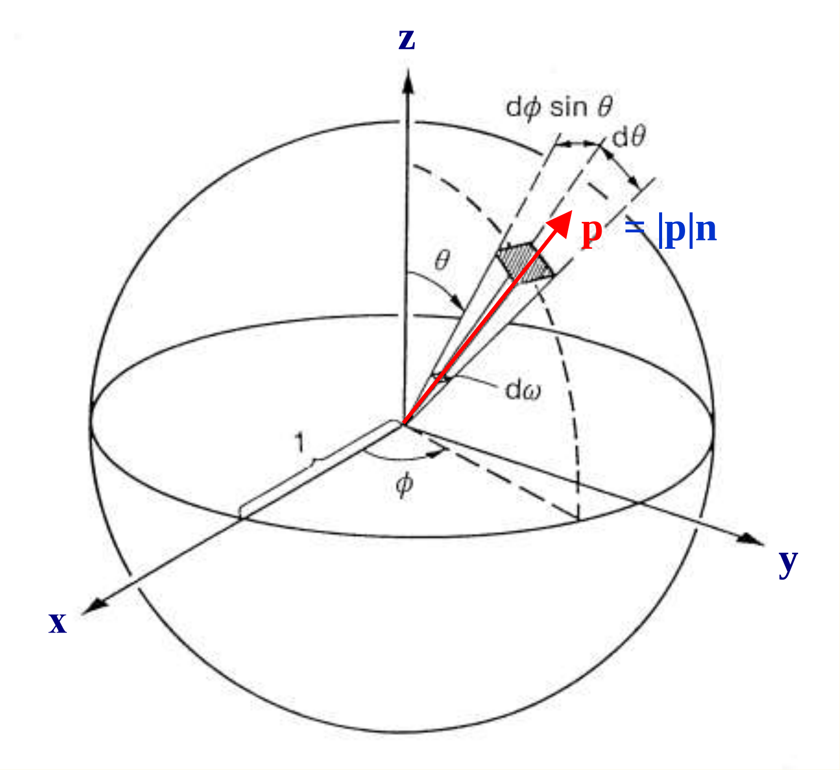

The specific intensity

Number of photons with ν, $\nu+d\nu$ which propagate through surface element $d\mathbf{S}$ into direction $\mathbf{n}$ and solid angle $d\Omega$, at time t and with velocity c:

$$\delta N = \frac{h^3\nu^2}{c^3} f(\mathbf{r},\mathbf{n},\nu,t)\, d^3\mathbf{r}\; d\nu d\Omega$$

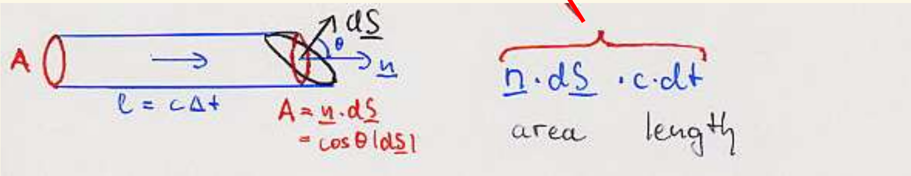

$$= \frac{h^3\nu^2}{c^3} f(\mathbf{r},\mathbf{n},\nu,t) \underset{\uparrow}{\cos\theta}\; cdt\; dS\; d\nu d\Omega$$

$$\sphericalangle(\mathbf{n}, d\mathbf{S})$$

- corresponding energy transport

$$\delta \mathrm{E} = \mathrm{h}\nu\ \delta \mathrm{N} = \underbrace{\frac{h^4\nu^3}{c^2} f(\mathbf{r},\mathbf{n},\nu,t)}_{I(\mathbf{r},\mathbf{n},\nu,t)} \cos\theta\; dS\; d\nu\; dt\; d\Omega$$

specific intensity

[erg cm^{-2} Hz^{-1} s^{-1}sr^{-1}]

summarized

$$\boxed{I = ch\nu\ \Psi = \frac{h^4\nu^3}{c^2} f}$$ function of $\mathbf{r},\mathbf{n},\nu,t$

specific intensity is radiation energy, which is transported into direction $\mathbf{n}$ through surface $d\mathbf{S}$, per frequency, time and solid angle.

specific intensity is a distribution function, and the

basic quantity in theory of radiative transfer

invariance of specific intensity

since $\frac{\mathrm{D}f}{\mathrm{Dt}} = 0$ without collisions (Vlasov equation) and without GR (i.e., $\mathbf{F} \equiv \mathbf{0}$), we have

$I \sim f$

$\Rightarrow$ I = const in fluid frame, as long as no interaction with matter!

If stationary process, i.e. $\partial/\partial t = 0$, then $\underline{\mathrm{n}\nabla}\ I = d/ds\ I = 0$,
where ds is path element, i.e.
I = const also spatially!
(this is the major reason for working with specific intensities)

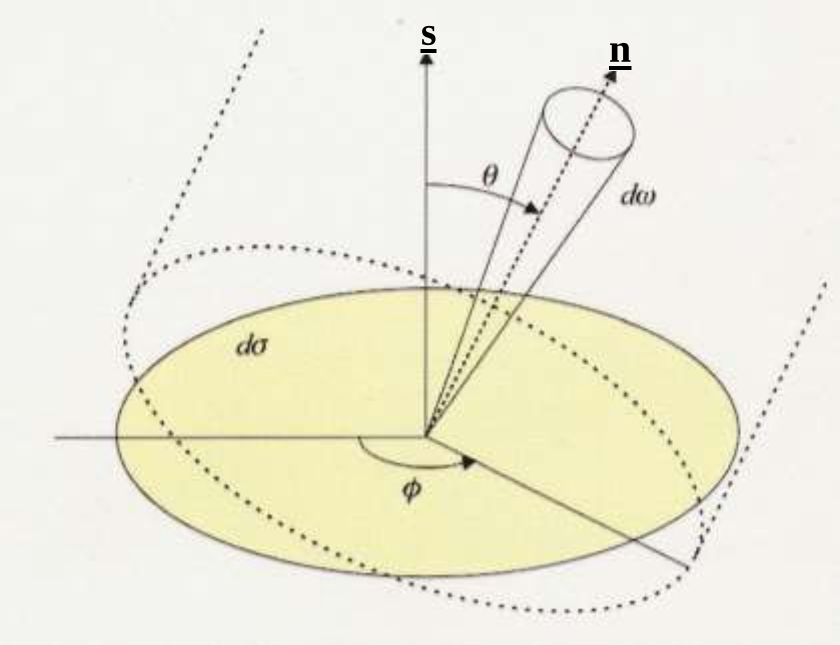

specific intensity is **radiation energy** with frequencies (ν, ν + dν), which is transported through *projected* area element dσcosθ into direction **n**, per time interval dt and solid angle dω.

$$\delta E = I(\vec{r},\vec{n},\nu,t)\cos\theta d\sigma d\nu dt d\omega$$

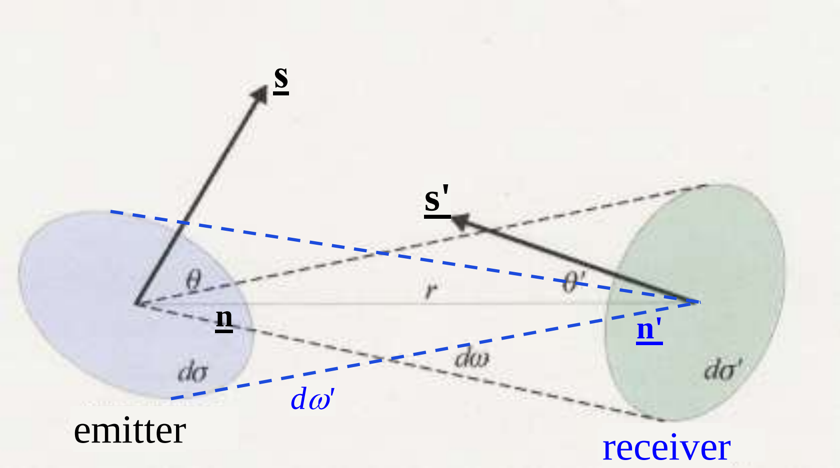

Invariance of specific intensity

Consider pencil of light rays which passes through both area elements δσ (emitter) and δσ' (receiver).

If no energy sinks and sources in between, the amount of energy which passes through both areas is given by

$$\delta E = I_\nu \cos\theta d\sigma dt d\omega =$$

$$\delta E' = I'_\nu \cos\theta' d\sigma' dt d\omega', \text{ and, cf. figure,}$$

$$d\omega = \frac{\text{projected area}}{\text{distance}^2} = \frac{\cos\theta' d\sigma'}{r^2}$$

$$d\omega' = \frac{\cos\theta d\sigma}{r^2}$$

$\Rightarrow I_\nu = I'_\nu$, independent of distance

... but energy/unit area dilutes with r^{-2}!

Plane-parallel and spherical symmetries

stars = gaseous spheres => spherical symmetry

BUT: rapidly rotating stars (e.g., Be-stars, $v_{rot} \approx 300 \dots 400$ km/s) rotationally flattened, only axis-symmetry can be used

AND: atmospheres usually very thin, i.e. $\Delta r / R << 1$

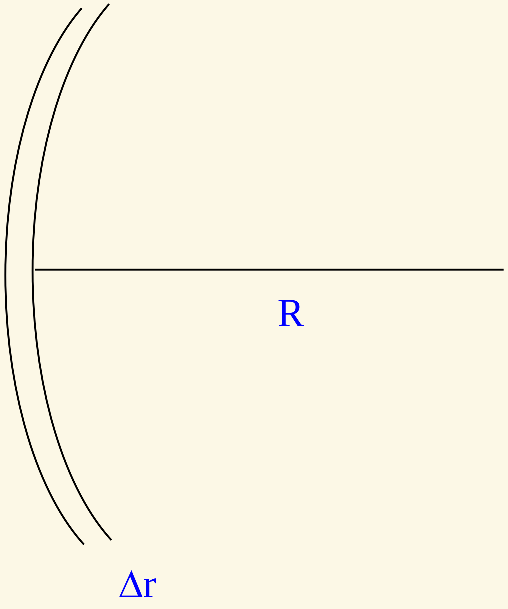

example: the sun

$R_{sun} \approx 700{,}000$ km
Δr (photo) ≈ 300 km

=> $\Delta r / R \approx 4\ 10^{-4}$

BUT corona
$\Delta r / R$ (corona) ≈ 3

as long as $\Delta r / R << 1$ => plane-parallel symmetry

light ray through atmosphere

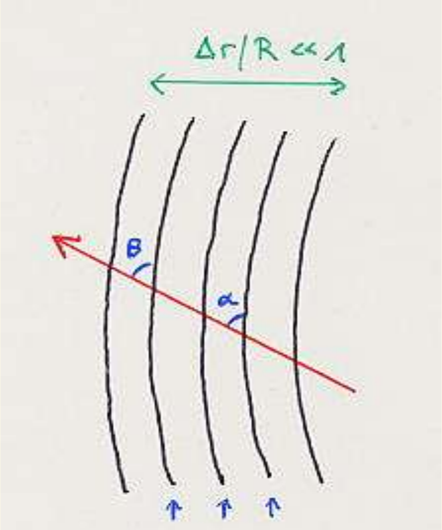

lines of constant temperature
and density (isocontours)

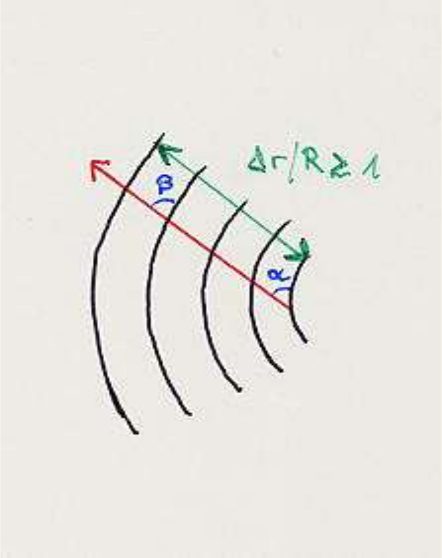

curvature of atmosphere insignificant for photons' path : $\alpha = \beta$

significant curvature : $\alpha \neq \beta$,
spherical symmetry

examples

solar photosphere / cromosphere	solar corona
atmospheres of	atmospheres of
main sequence stars	supergiants
white dwarfs	expanding envelopes (stellar winds)
giants (partly)	of OBA stars, M-giants and supergiants

Co-ordinate systems/symmetries

Cartesian | spherical

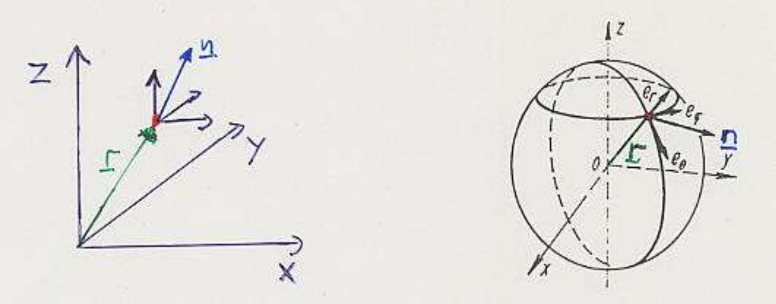

$\mathbf{r} = x\mathbf{e}_\mathrm{x} + y\mathbf{e}_\mathrm{y} + z\mathbf{e}_\mathrm{z}$ $\qquad$ $\mathbf{r} = \Theta\mathbf{e}_\Theta + \Phi\mathbf{e}_\Phi + r\mathbf{e}_\mathrm{r}$

$\mathbf{e}_\mathrm{x}, \mathbf{e}_\mathrm{y}, \mathbf{e}_\mathrm{z}$ right-handed, orthonormal $\mathbf{e}_\Theta, \mathbf{e}_\Phi, \mathbf{e}_\mathrm{r}$

specific intensity:

$I(x,y,z,\mathbf{n},\nu,t)$ $\qquad$ $I(\Theta,\Phi,r,\mathbf{n},\nu,t)$

important symmetries

plane-parallel | spherically symmetric

physical quantities depend | .... depend

only on z, e.g. | only on r, e.g.

$I(\mathbf{r},\mathbf{n},\nu,t) \rightarrow I(z,\mathbf{n},\nu,t)$ $\qquad$ $I(\mathbf{r},\mathbf{n},\nu,t) \rightarrow I(r,\mathbf{n},\nu,t)$

intensity has direction **n** into $d\Omega$

n requires additional angles θ, ϕ with respect to

$\mathbf{e}_\mathrm{x}, \mathbf{e}_\mathrm{y}, \mathbf{e}_\mathrm{z}$ $\qquad$ $\mathbf{e}_\Theta, \mathbf{e}_\Phi, \mathbf{e}_r$

and

$\theta = \sphericalangle(\mathbf{e}_\mathrm{z}, \mathbf{n})$ $\qquad$ $\theta = \sphericalangle(\mathbf{e}_r, \mathbf{n})$

$I_\nu(x,y,z,\theta,\phi,t)$ $\qquad$ $I_\nu(\Theta,\Phi,r,\theta,\phi,t)$

p-p symmetry | spherical symmetry

independent of azimuthal direction, ϕ

$\rightarrow I_\nu(z,\theta,t)$ $\qquad$ $\rightarrow I_\nu(r,\theta,t)$

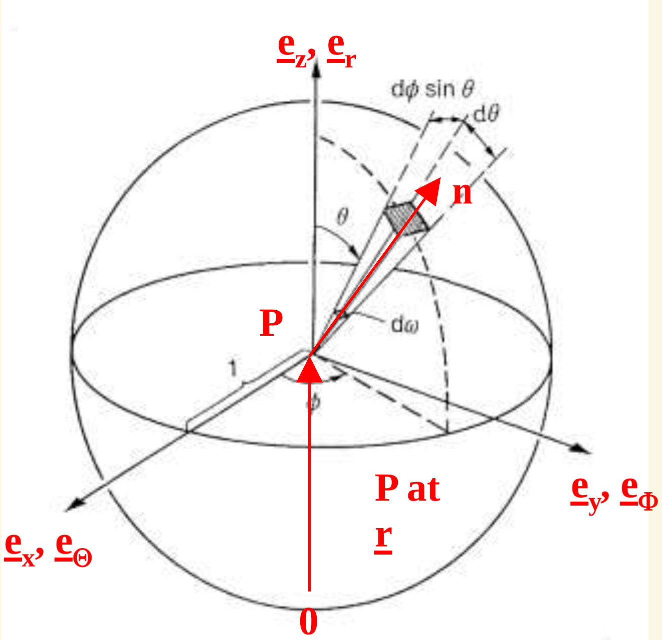

Moments of the specific intensity

1. mean intensity

$$J(\underline{r},\nu,t) = \frac{1}{4\pi} \oint I(\underline{r},\underline{n},\nu,t)\, d\Omega$$

specific intensity, averaged over solid angle

def. of solid angle

solid angle = ratio of area of sphere to radius^2

total solid angle = $\frac{4\pi R^2}{R^2} = 4\pi$

$d\Omega$ with $r=1$ = dA

area = $d\theta \times \sin\theta\, d\phi$

def: $\mu =: \cos\theta$

$d\mu = -\sin\theta\, d\theta \Rightarrow d\Omega = -d\mu\, d\phi$

THUS

$$J(\underline{r},\nu,t) = \frac{1}{4\pi} \int_0^{2\pi} d\phi \int_{0 \to +1}^{\pi \to -1} \underset{\substack{\downarrow \\ \text{usually } f(\theta,\phi)}}{I(\underline{r},\underline{n},\nu,t)}\, \underbrace{\sin\theta\, d\theta}_{-d\mu}$$

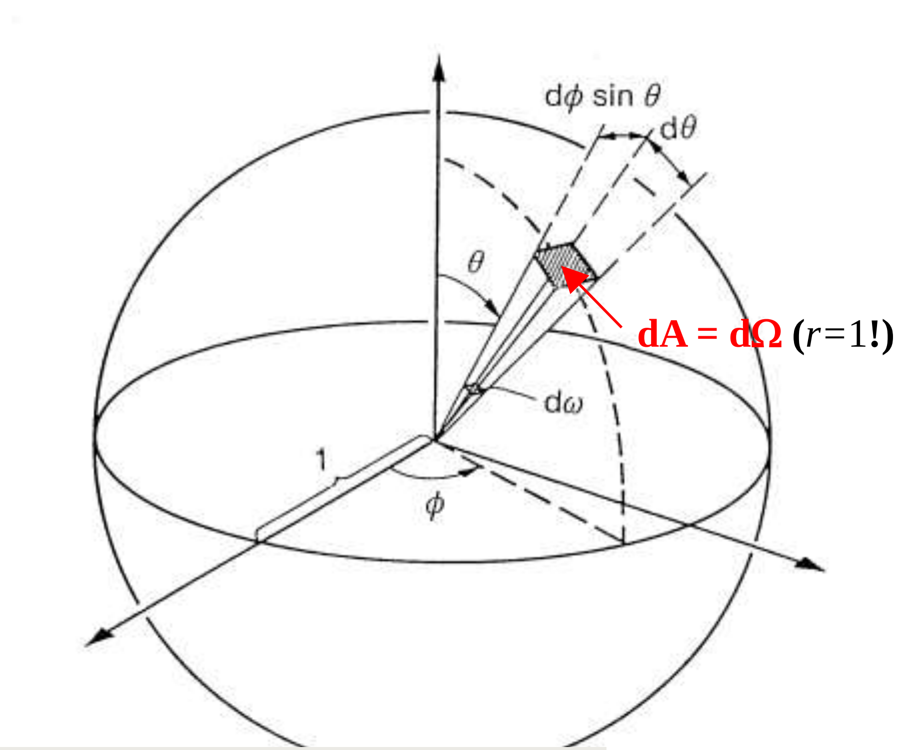

In plane-parallel or spherical symmetry:

$$J_\nu(\underline{r},t) = \frac{1}{4\pi} \int_0^{2\pi} d\phi \int_{-1}^{+1} I_\nu(\underline{r},\mu,t)\, d\mu =$$

$$= \frac{1}{2} \int_{-1}^{+1} I_\nu(\mu)\, d\mu \qquad \text{"0th" moment}$$

The Planck function

... on the other hand

energy density (i.e., per Volume $d^3\underline{r}$) per $d\nu$ (i.e., spectral) = $h\nu \oint$ (distr. function) $d\Omega$

$$u_\nu(\underline{r},t) = h\nu \oint \Psi_\nu(\underline{r},\mu,t)\, d\Omega$$

$$\overset{\text{def.}}{=} \frac{1}{c} \oint I_\nu(\underline{r},\mu,t)\, d\Omega = \frac{4\pi}{c} J_\nu(r,t)$$

$\dim[u_\nu] = \text{erg cm}^{-3}\,\text{Hz}^{-1}$

$\dim[J_\nu] = \text{erg cm}^{-2}\,\text{Hz}^{-1}\,\text{s}^{-1}$

- from thermodynamics, we know spectral energy density of a cavity or black body radiator (in thermodynamic equilibrium, "TE", with isotropic radiation, independent of material)

$$u_\nu(T) = \frac{8\pi h\nu^3}{c^3} \frac{1}{e^{h\nu/kT}-1}$$

$$\Rightarrow J_\nu = \frac{c}{4\pi} u_\nu \quad \text{and} \quad J_\nu = \frac{1}{2}\int_{-1}^{+1} \overset{\text{isotropic}}{I_\nu}\, d\mu = I_\nu$$

specific intensity of a cavity / black body radiator at temperature T

$$\boxed{I_\nu^{*} \overset{\text{T.E.}}{=} B_\nu(T) = \frac{2h\nu^3}{c^2} \frac{1}{e^{h\nu/kT}-1}}$$ "Planck-Function"

properties of Planck function

- $B_\nu(T_1) > B_\nu(T_2) \quad \forall \nu$, if $T_1 > T_2$
  i.e., Planck functions do not cross each other!
- maximum is shifted towards higher wavelengths with decreasing temperature
  $\frac{\nu_{max}}{T}$ = const, Wien's displacement law
- Wien regime $\frac{h\nu}{kT} \gg 1 \Rightarrow B_\nu \approx \frac{2h\nu^3}{c^2} e^{-h\nu/kT}$
- Rayleigh Jeans regime $\frac{h\nu}{kT} \ll 1 \Rightarrow B_\nu \approx \frac{2h\nu^3}{c^2}\frac{kT}{h\nu} = \frac{2\nu^2}{c^2}kT$

NOTE: in a number of cases one finds $B_\lambda \neq B_\nu$ since $B_\lambda d\lambda = B_\nu d\nu$

$$\Rightarrow B_\lambda = B_\nu \left|\frac{d\nu}{d\lambda}\right| = B_\nu \frac{c}{\lambda^2} = \frac{2hc^2}{\lambda^5} \frac{1}{e^{hc/kT\lambda}-1}$$

$\Rightarrow$ Max $(B_\lambda) \neq$ Max (B_ν) !

Planck function $B_\nu(\lambda)$

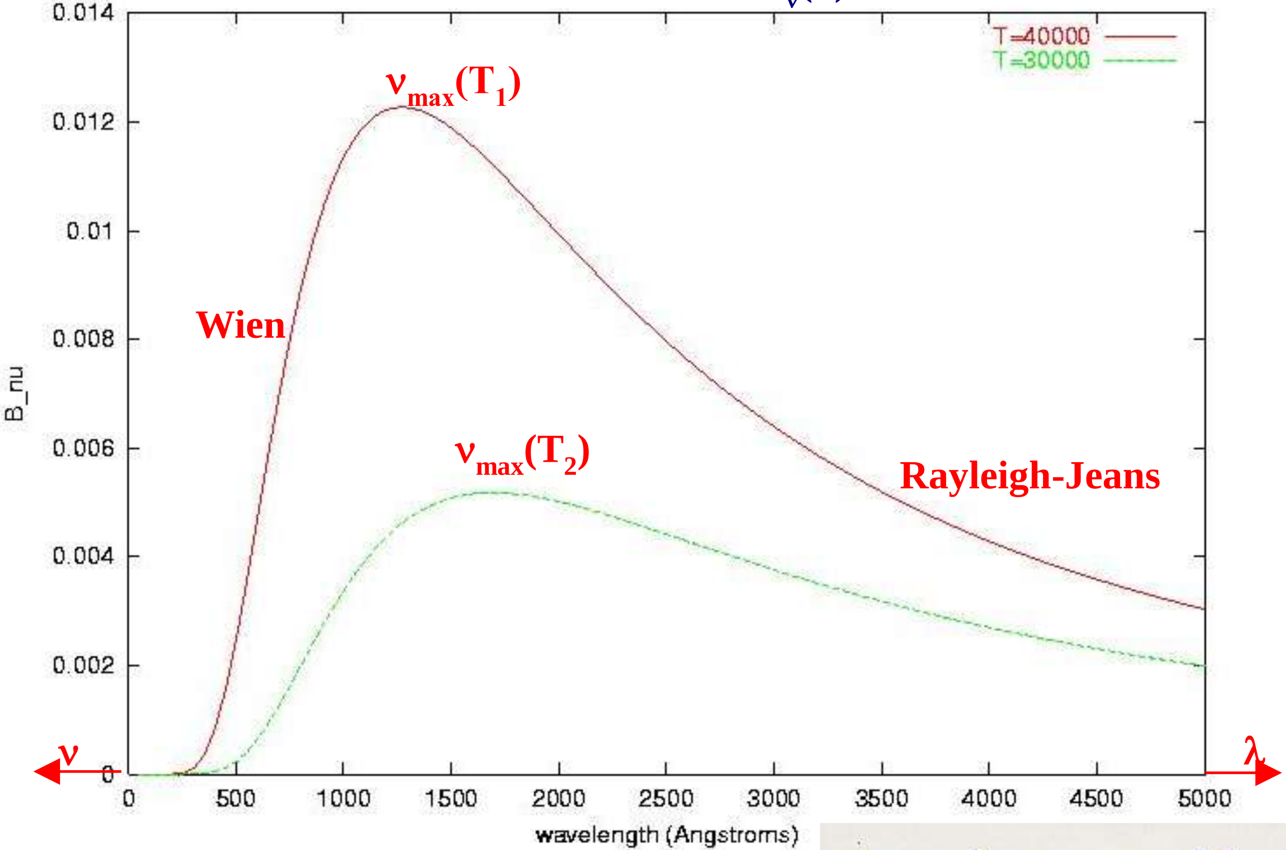

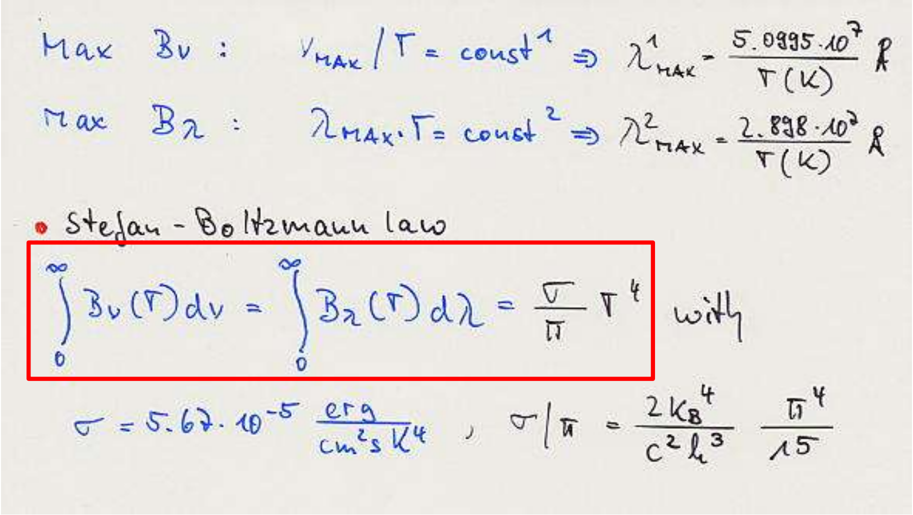

Max $B\nu$: $\nu_{MAX}/T = const^1 \Rightarrow \lambda^1_{MAX} = \frac{5.0995\cdot10^7}{T(K)}$ Å

Max $B\lambda$: $\lambda_{MAX}\cdot T = const^2 \Rightarrow \lambda^2_{MAX} = \frac{2.898\cdot10^7}{T(K)}$ Å

- Stefan-Boltzmann law

$$\boxed{\int_0^\infty B_\nu(T)d\nu = \int_0^\infty B_\lambda(T)d\lambda = \frac{\sigma}{\pi}T^4}$$ with

$\sigma = 5.67\cdot10^{-5}\frac{erg}{cm^2 s K^4}$, $\sigma/\pi = \frac{2k_B^4}{c^2 h^3}\frac{\pi^4}{15}$

1st moment: radiative flux

a) general definition

flux: rate of flow of a quantity across a given surface

flux-density: flux/unit area, also called flux

vector quantity

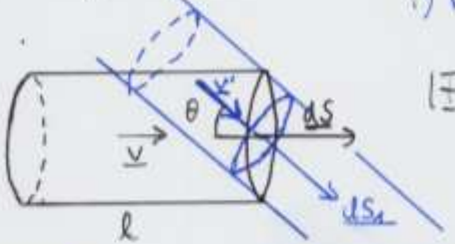

i) mass flux $\underline{v} \parallel d\underline{S}$

$$|\underline{\mathcal{F}}| = \frac{m}{\Delta t\,|d\underline{S}|}$$

$$= \frac{m}{Vol}\,\frac{\ell}{\Delta t} = \rho|v|$$

mass flux = mass density · velocity

ii) $\underline{v}'$ arbitrarily oriented with respect to $d\underline{S}$

$$|\underline{\mathcal{F}}| = \frac{m}{\Delta t\,|dS|} = \frac{m}{\Delta t\,|dS_\perp|}\,\frac{|dS_\perp|}{|dS|} = \frac{m}{Vol}\,|v'|\,\frac{|dS|\cos\theta}{|dS|}$$

$$= \rho|v'|\cos\theta$$

↑ $Vol = |v'|\,\Delta t\,|dS_\perp|$

⇒ mass flux through $d\underline{S}$ = $\underline{\mathcal{F}} \cdot d\underline{S} = \rho\,\underbrace{\underline{v}' \cdot d\underline{S}}_{|v'|\,|dS| \cdot \cos\theta}$

is reduced by factor $\cos\theta$, since less material is transported across smaller effective area ⊥ flow (in same Δt)

iii) mass-loss rate for spherically sym. outflow

$$\dot{M} = \underbrace{(\rho v)(r)}_{\text{mass flux}} \cdot \underbrace{4\pi r^2}_{\text{surface area}}$$

transported mass/unit time across surface with radius r

$\cos\theta = 1$!

b) application to radiation field

- photon flux through surface $d\underline{S}$ into direction $\underline{n}$ and solid angle $d\Omega$ ("radiation pencil")

$$\frac{\delta N}{dt\,d\nu} = \Big(\underbrace{\Psi(\underline{r},\underline{n},\nu,t)\,d\Omega}_{\text{number DENSITY}} \cdot \underbrace{c \cdot \underline{n}}_{\text{velocity}}\Big) \cdot d\underline{S}$$

- net rate of total photon flow across $d\underline{S}$ (i.e., contribution of all pencils)

$$\frac{N}{dt\,d\nu} = \Big(c \oint \Psi(\underline{r},\underline{n},\nu,t)\,\underline{n}\,d\Omega\Big) \cdot d\underline{S}$$

- net rate of radiant energy flow across $d\underline{S}$

$$\frac{E}{dt\,d\nu} = \Big(c h\nu \oint \Psi(\underline{r},\underline{n},\nu,t)\,\underline{n}\,d\Omega\Big)\,d\underline{S} \overset{\text{def.}}{=} \Big(\oint I(\underline{r},\underline{n},\nu,t)\,\underline{n}\,d\Omega\Big)\,d\underline{S}$$

$$= \underline{\mathcal{F}}_\nu(\underline{r},t) \cdot d\underline{S}$$

$$\boxed{\underline{\mathcal{F}}_\nu(\underline{r},t) = \oint I_\nu(\underline{r},\underline{n},t)\,\underline{n}\,d\Omega}$$

radiative flux

$$\dim[\mathcal{F}_\nu] = \frac{\text{erg}}{\text{cm}^2\,\text{s Hz}} = \dim[J_\nu]$$

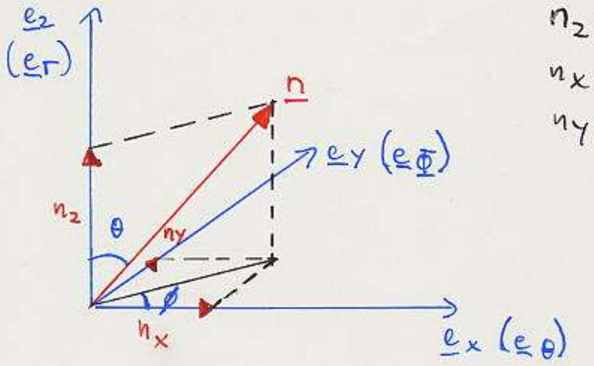

$n_z = \cos\theta = \mu$
$n_x = \sin\theta\cos\phi$
$n_y = \sin\theta\sin\phi$

Note : Carthesian / spherical co-ordinate system

$$\begin{pmatrix}\underline{e}_\theta\\ \underline{e}_\Phi\\ \underline{e}_r\end{pmatrix} \hat{=} (\text{locally}) \begin{pmatrix}\underline{e}_x\\ \underline{e}_y\\ \underline{e}_z\end{pmatrix},$$

θ, ϕ defined similarly

$$\Rightarrow \underline{\mathcal{F}} = \begin{pmatrix}\mathcal{F}_{x,\theta}\\ \mathcal{F}_{y,\Phi}\\ \mathcal{F}_{z,r}\end{pmatrix} = \begin{pmatrix} \oint I n_x d\Omega\\ \oint I n_y d\Omega\\ \oint I n_z d\Omega\end{pmatrix} = \int_0^{2\pi} d\phi \begin{matrix}\cos\phi\\ \sin\phi\\ 1\end{matrix} \int_{-1}^{1} d\mu \begin{matrix} I(1-\mu^2)^{\frac{1}{2}}\\ I(1-\mu^2)^{\frac{1}{2}}\\ I\mu\end{matrix}$$

p.p. / spherical symmetric

$I(\underline{r}, \underline{n}, \nu, t) \Rightarrow I(\begin{smallmatrix}r\\z\end{smallmatrix}, \mu, \nu, t)$ independent of ϕ,

$x(\theta)$, $y(\Phi)$ comp. cancel each other

(math: $\cos\phi$, $\sin\phi$ integrals $=0$)

$$\Rightarrow \underline{\mathcal{F}} = \left(0, 0, 2\pi\int_{-1}^{+1} I(\begin{smallmatrix}r\\z\end{smallmatrix}, \mu, \nu, t)\mu\, d\mu\right)$$

- in analogy to mean intensity $J_\nu = \frac{1}{2}\int_{-1}^{+1} I(\mu)d\mu$

  we define the Eddington flux

$$\boxed{H_\nu(\begin{smallmatrix}r\\z\end{smallmatrix}, t) = \frac{1}{2}\int_{-1}^{+1} I_\nu(\begin{smallmatrix}r\\z\end{smallmatrix}, \mu, t)\mu\, d\mu = \frac{1}{4\pi}\mathcal{F}_\nu(\begin{smallmatrix}r\\z\end{smallmatrix}, t)}$$

"first moment"

- "flux" from a cavity radiator

  small opening

$$\mathcal{F}_\nu = 2\pi\int_{-1}^{+1} I(\mu)\mu\, d\mu = 2\pi\int_0^1 I(\mu)\mu\, d\mu - 2\pi\int_0^1 I(-\mu)\mu\, d\mu$$

$$= \mathcal{F}^+ - \mathcal{F}^-$$

only photons escaping from radiatior

$I(\mu)$, $\mu = 0 \ldots 1$ $= B_\nu(T)$ isotropic radiation
$I(-\mu)$ $= 0$

$$\Rightarrow \mathcal{F} = \int_0^\infty \pi B_\nu(T)d\nu = \pi \cdot \frac{\sigma_B}{\pi} T^4 = \sigma_B T^4$$

REMEMBER Black Body

frequ. integrated	specific and mean intensity	$\frac{\sigma_B}{\pi} T^4$
〃	energy density	$\frac{4\sigma_B}{c} T^4$
〃	flux	$\sigma_B T^4$

Effective temperature

- total radiative energy loss is
  flux (outwards directed) times surface area of star =

  luminosity $L = \mathscr{F}^{+} 4\pi R^2$

  dim[L] = erg/s (units of power), L_{sun}=3.83 10^{33} erg/s

- definition: "effective temperature" is temperature
  of a star with luminosity L at radius R_*,
  if it *were* a black body (semi-open cavity?)

- $T_{\rm eff}$ corresponds roughly to stellar surface temperature
  (more precise → later)

$$\boxed{L =: \sigma_B T_{\rm eff}^{\,4}\, 4\pi R^2 \quad \textit{or} \quad T_{\rm eff} = (L/ \sigma_B 4\pi R^2)^{1/4}}$$

Examples

i) spherical or plane-parallel symmetry, isotropic radiation

$$I_\nu(\mu) = I_0 \quad (\text{e.g., } B_\nu(T))$$

$$\Rightarrow J_\nu = \frac{1}{2}\int_{-1}^{1} I_0 d\mu = I_0$$

$$H_\nu = \frac{1}{2}\int_{-1}^{1} I_0 \mu d\mu = 0$$ [vanishing flux also in radial direction, since same number of photons from above and below surface ⊥ radial direction]

THUS: $I_\nu = I_0 \;\Rightarrow\; J_\nu = I_0,\, H_\nu = 0$

ADVANCED READING: ii) extremely anisotropic radiation

$I_\nu(\mu,\phi) = I_0\delta(\mu-\mu_0)\delta(\phi-\phi_0)$, with Dirac δ-function [planar wave]

$$\Rightarrow J_\nu = \frac{1}{4\pi}\int_0^{2\pi} d\phi \int_{-1}^{1} I_0\delta(\mu-\mu_0)\delta(\phi-\phi_0) d\mu = \frac{I_0}{4\pi}$$

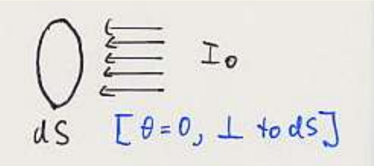

$$\mathbf{H}_\nu = \frac{\mathscr{F}}{4\pi} = \begin{pmatrix} \frac{1}{4\pi}\int_0^{2\pi} \cos\phi d\phi \int_{-1}^{1} I_0\delta(\mu-\mu_0)\delta(\phi-\phi_0)(1-\mu^2)^{1/2} d\mu \\ \frac{1}{4\pi}\int_0^{2\pi} \sin\phi d\phi \int_{-1}^{1} I_0\delta(\mu-\mu_0)\delta(\phi-\phi_0)(1-\mu^2)^{1/2} d\mu \\ \frac{1}{4\pi}\int_0^{2\pi} d\phi \int_{-1}^{1} I_0\delta(\mu-\mu_0)\delta(\phi-\phi_0)\mu d\mu \end{pmatrix} = \frac{1}{4\pi}\begin{pmatrix} I_0 \cos\phi_0 (1-\mu_0^2)^{1/2} \\ I_0 \sin\phi_0 (1-\mu_0^2)^{1/2} \\ I_0 \mu_0 \end{pmatrix} \xrightarrow{\mu_0 \to 1} \begin{pmatrix} 0 \\ 0 \\ I_0/4\pi \end{pmatrix}$$

Generally: $$|\mathbf{H}_\nu| = \frac{I_0}{4\pi}\sqrt{\cos^2\phi_0(1-\mu_0^2) + \sin^2\phi_0(1-\mu_0^2) + \mu_0^2} = \frac{I_0}{4\pi}$$

THUS: uni-directional radiation $\Rightarrow J_\nu = |\mathbf{H}_\nu|$ (independent of co-ordinate system)

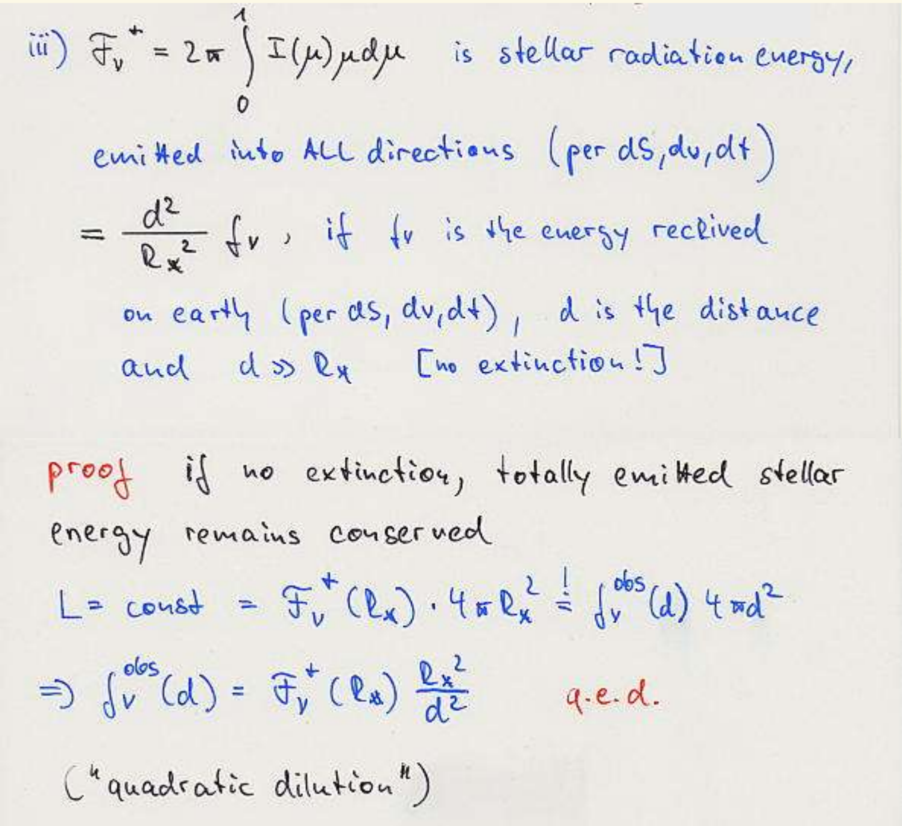

iii) $\mathcal{F}_\nu^+ = 2\pi \int_0^1 I(\mu)\mu d\mu$ is stellar radiation energy, emitted into ALL directions (per dS, dν, dt)

$= \frac{d^2}{R_*^2} f_\nu$, if f_ν is the energy received on earth (per dS, dν, dt), d is the distance and $d \gg R_*$ [no extinction!]

proof if no extinction, totally emitted stellar energy remains conserved

$$L = \text{const} = \mathcal{F}_\nu^+(R_*) \cdot 4\pi R_*^2 \overset{!}{=} f_\nu^{obs}(d)\, 4\pi d^2$$

$$\Rightarrow f_\nu^{obs}(d) = \mathcal{F}_\nu^+(R_*) \frac{R_*^2}{d^2}$$ q.e.d.

("quadratic dilution")

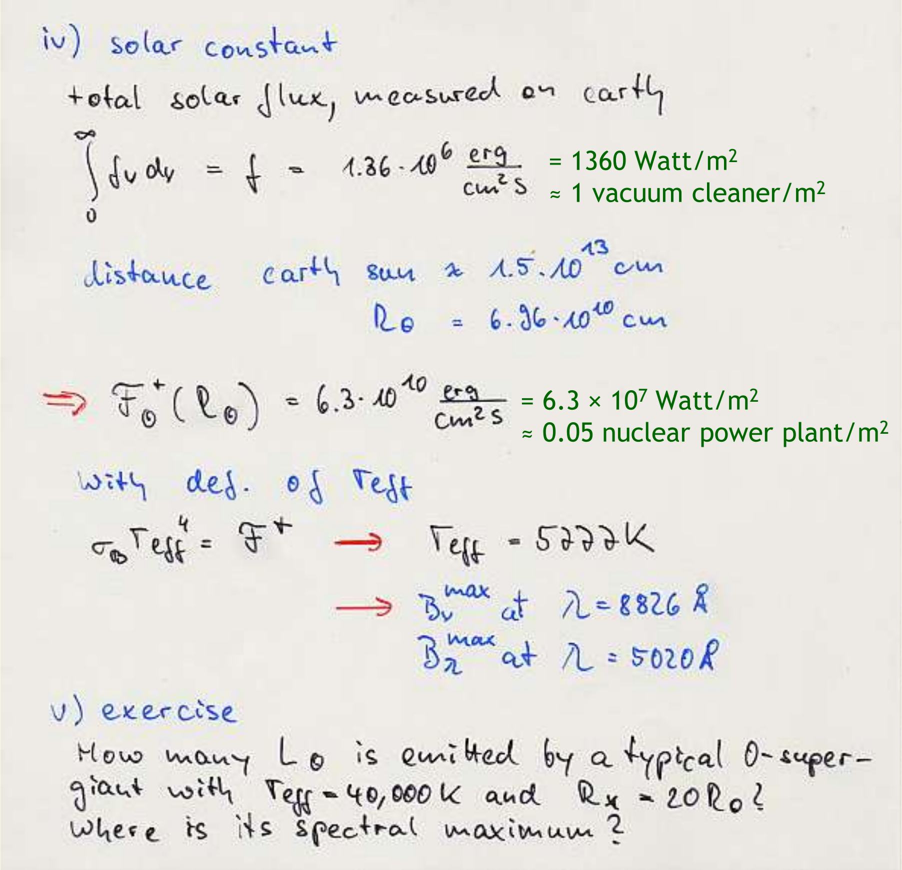

iv) solar constant

total solar flux, measured on earth

$$\int_0^\infty f_\nu d\nu = f = 1.36 \cdot 10^6 \frac{erg}{cm^2 s}$$ = 1360 Watt/m^2 ≈ 1 vacuum cleaner/m^2

distance earth sun $\approx 1.5 \cdot 10^{13}$ cm

$R_\odot = 6.96 \cdot 10^{10}$ cm

$$\Rightarrow \mathcal{F}_\odot^+(R_\odot) = 6.3 \cdot 10^{10} \frac{erg}{cm^2 s}$$ = 6.3 × 10^7 Watt/m^2 ≈ 0.05 nuclear power plant/m^2

with def. of T_{eff}

$\sigma_B T_{eff}^4 = \mathcal{F}^+ \longrightarrow T_{eff} = 5777K$

$\longrightarrow B_\nu^{max}$ at $\lambda = 8826$ Å

B_λ^{max} at $\lambda = 5020$ Å

v) exercise

How many $L_\odot$ is emitted by a typical O-supergiant with $T_{eff} = 40{,}000$ K and $R_* = 20 R_\odot$? Where is its spectral maximum?

2nd moment: radiation pressure (stress) tensor

P_{ij} is net flux of momentum, in the j-th direction, through a unit area oriented perpendicular to the ith direction (per unit time and frequency)

- this is just the general definition of "pressure" in any fluid

$$P_{ij}(\underline{r},\nu,t) = \oint \underbrace{\psi(\underline{r},\underline{n},\nu,t)\left(\frac{h\nu}{c}n_j\right)}_{\substack{\text{transported quantity}\\ = \text{distrib. function} \cdot \text{momentum}}}\underbrace{(c\cdot n_i)}_{\text{velocity}}d\Omega$$

$$\overset{\text{def}}{=} \frac{1}{c}\oint I(\underline{r},\underline{n},\nu,t)\, n_i n_j\, d\Omega$$

- $P_{ij} = P_{ji}$ generally
- NOW p-p/sph. symmetry

  from def. of n_i, $i=1,3$ $\qquad P_{ij}=0$ for $i \neq j$

$$P = \begin{pmatrix} p_R & 0 & 0 \\ 0 & p_R & 0 \\ 0 & 0 & p_R \end{pmatrix} - \frac{1}{2}\begin{pmatrix} 3p_R-u & 0 & 0 \\ 0 & 3p_R-u & 0 \\ 0 & 0 & 0 \end{pmatrix}$$

with respect to

$(\underline{e}_x, \underline{e}_y, \underline{e}_z)$ or $(\underline{e}_\Theta, \underline{e}_\Phi, \underline{e}_r)$

$p_R = \frac{4\pi}{c}K$ radiation pressure scalar

$u = \frac{4\pi}{c}J$ radiation energy density

$K_\nu = \frac{1}{2}\int_{-1}^{+1} I_\nu(r,\mu,t)\,\mu^2 d\mu$ "2nd moment"

Note In p-p/spherical symmetry the radiation pressure tensor is described by only two scalar quantities!

isotropic radiation (→ stellar interior) cavity radiation

$I_\nu(r,\mu,t) \rightarrow I_\nu(r,t)$

$$\left.\begin{aligned} K &= \frac{I}{2}\int_{-1}^{+1}\mu^2 d\mu \\ J &= \frac{I}{2}\int_{-1}^{+1} d\mu \end{aligned}\right\} \quad K = \frac{1}{3}J \quad \text{or} \quad p_R = \frac{1}{3}u$$

$$\Rightarrow P_\nu = \begin{pmatrix} p_R & 0 & 0 \\ 0 & p_R & 0 \\ 0 & & p_R \end{pmatrix}$$

ONE quantity sufficient

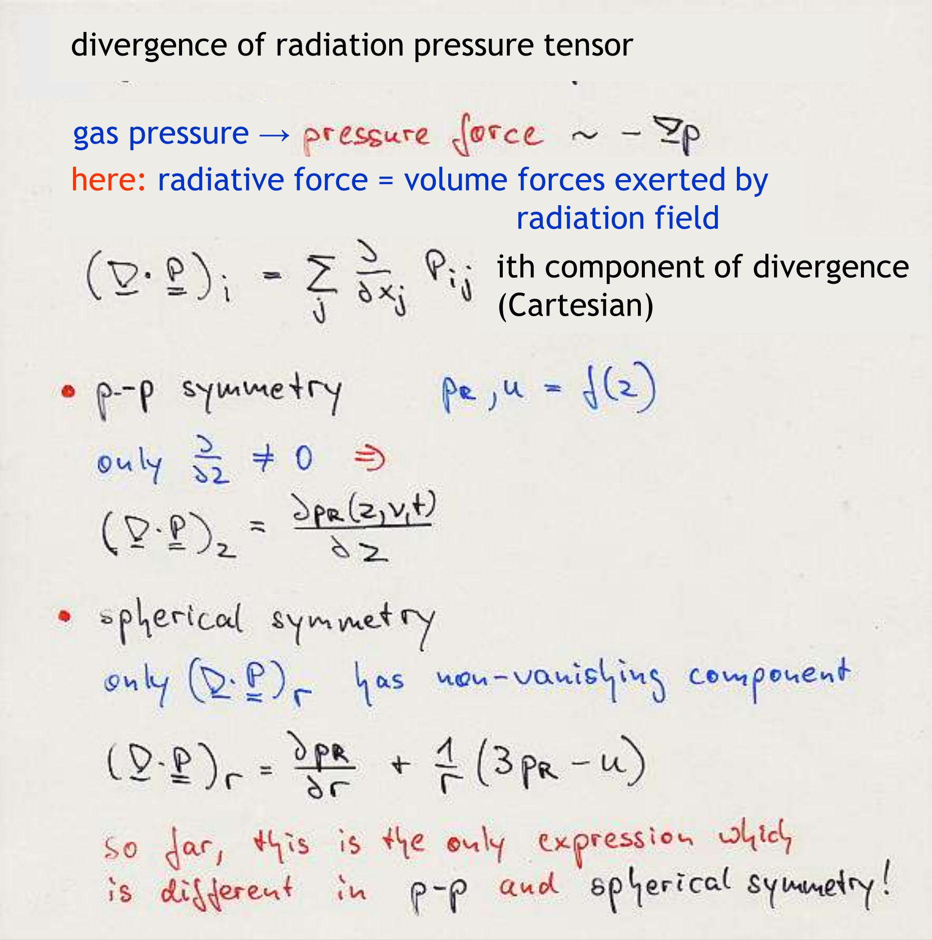

divergence of radiation pressure tensor

gas pressure → pressure force $\sim -\underline{\nabla} p$

here: radiative force = volume forces exerted by radiation field

$$(\underline{\nabla}\cdot\underline{\underline{P}})_i = \sum_j \frac{\partial}{\partial x_j} P_{ij}$$

ith component of divergence (Cartesian)

- p-p symmetry $\quad p_R, u = f(z)$

  only $\frac{\partial}{\partial z} \neq 0 \Rightarrow$

  $$(\underline{\nabla}\cdot\underline{\underline{P}})_z = \frac{\partial p_R(z,\nu,t)}{\partial z}$$

- spherical symmetry

  only $(\underline{\nabla}\cdot\underline{\underline{P}})_r$ has non-vanishing component

  $$(\underline{\nabla}\cdot\underline{\underline{P}})_r = \frac{\partial p_R}{\partial r} + \frac{1}{r}(3p_R - u)$$

  so far, this is the only expression which is different in p-p and spherical symmetry!

advanced reading

Divergence of radiation pressure tensor

For symmetric tensors T^{ij} $(i, j = \Theta, \Phi, r)$ one can prove the following relations

(e.g., Mihalas & Weibel Mihalas, "Foundations of Radiation Hydrodynamics", Appendix)

$$(\nabla \cdot T)_r = \frac{1}{r^2}\frac{\partial(r^2 T^{rr})}{\partial r} + f(T^{r\Theta}) + f(T^{r\Phi}) - \frac{1}{r}(T^{\Theta\Theta} + T^{\Phi\Phi})$$

$$(\nabla \cdot T)_\Theta = \frac{1}{r}\left\{ f(T^{r\Theta}) + \frac{1}{r\sin\theta}\frac{\partial(\sin\theta T^{\Theta\Theta})}{\partial\theta} + f(T^{\Theta\Phi}) + \frac{1}{r}(T^{r\Theta} - \cot\theta T^{\Phi\Phi}) \right\}$$

$$(\nabla \cdot T)_\Phi = \frac{1}{r\sin\theta}\left\{ f(T^{r\Phi}) + f(T^{\Theta\Phi}) + \frac{1}{r\sin\theta}\frac{\partial T^{\Phi\Phi}}{\partial\phi} + f(\cot\theta T^{\Theta\Phi}) \right\}$$

where f are (different) functions of the tensor-elements which are not relevant here.

Since in spherical symmetry the radiation pressure tensor P is diagonal (i.e., symmetric), and since p_R and u are functions of r alone, we have

$$(\nabla \cdot P)_r = \frac{1}{r^2}\left(2rP^{rr} + r^2\frac{\partial P^{rr}}{\partial r}\right) - \frac{1}{r}(P^{\Theta\Theta} + P^{\Phi\Phi}) = \frac{\partial P^{rr}}{\partial r} + \frac{1}{r}(2P^{rr} - P^{\Theta\Theta} - P^{\Phi\Phi})$$

(which in the isotropic case would yield $(\nabla \cdot P)_r = \frac{\partial P^{rr}}{\partial r} = \frac{\partial p_R}{\partial r}$)

$$(\nabla \cdot P)_\Theta = \frac{1}{r^2\sin\theta}\left(\cos\theta P^{\Theta\Theta} + \sin\theta\frac{\partial T^{\Theta\Theta}}{\partial\theta}\right) - \frac{1}{r^2}\cot\theta P^{\Phi\Phi} \rightarrow 0 \text{ (in spherical symmetry)}$$

$(\nabla \cdot P)_\Phi \rightarrow 0$ (in spherical symmetry).

Finally, we obtain

$$(\nabla \cdot P) \rightarrow (\nabla \cdot P)_r = \mathbf{e_r} \cdot \left\{ \frac{\partial p_R}{\partial r} + \frac{1}{r}\left(2p_R - 2\left(p_R - \frac{1}{2}(3p_R - u)\right)\right)\right\} =$$

$$= \mathbf{e_r} \cdot \left(\frac{\partial p_R}{\partial r} + \frac{1}{r}(3p_R - u)\right), \text{ q.e.d.}$$

Summarizing comparison: from p-p to spherical symmetry

specific intensity and moments similarly defined if $z \rightarrow r$

$I(z,\mu) \rightarrow I(r,\mu)$ with $\mu = \cos\theta$ and $\theta = \sphericalangle(\mathbf{e}_\mathbf{r}, \mathbf{n})$ [in the following, ν- and t-dependence suppressed]

from symmetry about azimuthal direction:

$$\text{n}^{\text{th}} \text{ moment} = \frac{1}{2}\int_{-1}^{+1} I(r,\mu)\mu^n \mathrm{d}\mu,$$ as in p-p case when $z \rightarrow r$; n=0,1,2 $\rightarrow J(r), H(r), K(r)$

flux(-density) $\mathscr{F} = \begin{pmatrix} 0 \\ 0 \\ 4\pi\mathrm{H} \end{pmatrix}$: only z- or r-component different from zero, prop. to Eddington-flux

radiation stress tensor **P**: only diagonal elements different from zero

only difference refers to divergence of radiation stress tensor, $\nabla \cdot \mathbf{P}$

in pp-symmetry, only z-component different from zero, and

$$\left(\nabla \cdot \mathbf{P}\right)_z = \frac{\partial p_\mathrm{R}}{\partial z}$$ with p_R (radiation pressure scalar) $= \frac{4\pi}{c} K(z)$

in spherical symmetry, only r-component different from zero, and

$$\left(\nabla \cdot \mathbf{P}\right)_r = \frac{\partial p_\mathrm{R}}{\partial r} + \frac{3p_\mathrm{R} - u}{r}$$ with u (radiation energy density) $= \frac{4\pi}{c} J(r)$

Chap. 4 – Coupling with matter

The equation of radiative transfer

- had Boltzmann eq. for particle distrib. function f

$$\left(\frac{\partial}{\partial t} + \underline{v}\cdot\underline{\nabla} + \underline{F}\cdot\underline{\nabla}_p\right) f = \left(\frac{\delta f}{\delta t}\right)_{\text{coll}}$$

for photons $v = c\cdot\underline{n}$, $\underline{F} \equiv 0$ without GR

$$\Rightarrow \left(\frac{\partial}{\partial t} + c\,\underline{n}\cdot\underline{\nabla}\right)\Psi_\nu = \left(\frac{\delta \Psi_\nu}{\delta t}\right)_{\text{coll}} \leftarrow$$

photon creation/destr. along path in phase space

with

$$\Psi_\nu(\underline{r},\underline{n},t)\, d^3\underline{r}\, d\nu\, d\Omega = f(\underline{r},\underline{p},t)\, d^3\underline{r}\, d^3\underline{p}$$

and

$$\left(\frac{\partial}{\partial t} + c\cdot\underline{n}\cdot\underline{\nabla}\right)\frac{I_\nu}{ch\nu} = \frac{1}{ch\nu}\left(\frac{\delta I_\nu}{\delta t}\right)_{\text{"coll"}}$$

$$\Rightarrow \left(\frac{1}{c}\frac{\partial}{\partial t} + \underline{n}\cdot\underline{\nabla}\right) I_\nu = \left(\frac{\delta I_\nu}{ds}\right)_{\text{"coll"}} = \frac{\delta I_\nu^{em} - \delta I_\nu^{abs}}{ds}$$

$\Uparrow$ gain/loss by interaction with matter

with

$$I_\nu = ch\nu\,\Psi_\nu, \quad ds = c\cdot\delta t$$

Equation of radiative transfer for specific intensity

Emissivity and opacity

a) vacuum

$\rightarrow$ no "collisions" $\rightarrow$ Vlasov equation

$$\Rightarrow \left[\frac{1}{c}\frac{\partial}{\partial t} + \underline{n}\cdot\underline{\nabla}\right] I = 0$$

stationary

$$\underset{\uparrow}{(\underline{n}\cdot\underline{\nabla})} I = \frac{d}{ds} I = 0 \Rightarrow I = \text{const} \quad (\text{cf. Chap 3})$$

directional derivative

b) energy gain by emission

add energy to ray (matter in dV radiates) by emission / photon creation

$$\delta E_\nu^{+} = \delta E_\nu^{em} \overset{\text{def}}{=} \eta_\nu(\underline{r},\underline{n},t)\, dV\, d\Omega\, d\nu\, dt$$

$$= \eta_\nu(\underline{r},\underline{n},t)\, \underbrace{\underbrace{\underline{n}\cdot d\underline{S}}_{\cos\theta\, dS} \cdot ds}_{dV}\, d\Omega\, d\nu\, dt$$

compare with def. of specific energy

$$\delta E_\nu = I_\nu(\underline{r},\underline{n},t) \cos\theta\, dS\, d\Omega\, d\nu\, dt$$

$$\Rightarrow \delta I_\nu^{em} = \eta_\nu\, ds$$

macroscopic emission coefficient

$$\dim[\eta_\nu] = \text{erg}\ \text{cm}^{-3}\ \text{sr}^{-1}\ \text{Hz}^{-1}\ \text{s}^{-1}$$

c) energy loss by absorption

remove energy from ray (matter in dV absorbs) by absorption / photon distruction

NOTE i) energy gain/emission property of interacting matter

ii) BUT: energy loss must depend on properties of matter and radiation, since

no radiation field ⇒ no loss

no matter ⇒ no loss

THUS following definition

$$\delta E_\nu^- = \delta E_\nu^{abs} = (\chi_\nu I_\nu)(\underline{r},\underline{n},t)\cos\theta\, dS\, ds\, d\Omega\, d\nu\, dt$$

$$\delta I_\nu^{abs} = \chi_\nu I_\nu ds$$

χ_ν absorption coefficient or opacity

$\dim[\chi_\nu] = \mathrm{cm}^{-1}$

d) optical depth

define $d\tau_\nu = \chi_\nu ds \rightarrow \tau_\nu(s) = \int_0^s \chi_\nu(s) ds$

$\delta I_\nu^{abs} = I_\nu d\tau_\nu$ the higher τ, the more is absorbed

$\dim[\tau_\nu]$ dimensionless

interpretation later

e) emission and absorption in parallel

$$\left(\frac{\delta I_\nu}{ds}\right)_{cou} = \frac{\delta I_\nu^{em} - \delta I_\nu^{abs}}{ds} = \eta_\nu - \chi_\nu I_\nu$$

⇒ finally

$$\boxed{\left(\frac{1}{c}\frac{\partial}{\partial t} + \underline{n}\cdot\underline{\nabla}\right) I_\nu = \eta_\nu - \chi_\nu I_\nu}$$

η_ν, χ_ν depend on microphysics of interacting matter

NOTE
- in static media η_ν, χ_ν (mostly) isotropic
- in moving media: Dopplereffect
  matter "sees" light at frequencies different than the observer ⇒ dependency on angle

The equation of transfer for specific geometries

a) plane-parallel symmetry

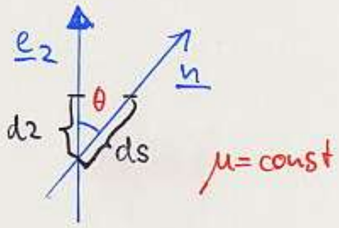

$$dz = \mu\, ds$$

$$\rightarrow (\underline{n}\cdot\underline{\nabla}) = \frac{d}{ds} = \mu \frac{d}{dz}$$

$$\boxed{\left(\frac{1}{c}\frac{\partial}{\partial t} + \mu \frac{\partial}{\partial z}\right) I_\nu(z,\mu,t) = \eta_\nu - \chi_\nu I_\nu}$$

b) spherical symmetry

along ds, $\mu \neq \mathrm{const}$

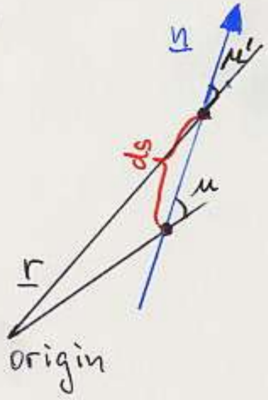

without proof

$$(\underline{n}\cdot\underline{\nabla}) = \frac{d}{ds} = \mu\frac{\partial}{\partial r} + \frac{1-\mu^2}{r}\frac{\partial}{\partial \mu}$$

$$\boxed{\left(\frac{1}{c}\frac{\partial}{\partial t} + \mu \frac{\partial}{\partial r} + \frac{1-\mu^2}{r}\frac{\partial}{\partial \mu}\right) I_\nu(r,\mu,t) = \eta_\nu - \chi_\nu I_\nu}$$

c) in general

$$\left[\frac{\partial}{\partial t}, \frac{\partial}{\partial r}, \frac{\partial}{\partial \theta}, \frac{\partial}{\partial \Phi}, \frac{\partial}{\partial \mu}, \frac{\partial}{\partial \phi}\right] I_\nu(\theta,\Phi,r,\mu,\phi,t)$$

The equation of transfer (cont'd)

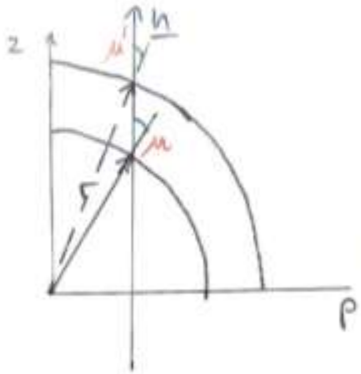

so-called p-z geometry

$$\frac{d}{ds} = \frac{d}{dz}\Big|_p$$

mit $r^2 = z^2 + p^2$

$\mu = \frac{z}{r}$

$$\Rightarrow \frac{d}{ds} = \frac{d}{dz}\Big|_p = \frac{\partial r}{\partial z}\Big|_p \frac{\partial}{\partial r} + \frac{\partial \mu}{\partial z}\Big|_p \frac{\partial}{\partial \mu}$$

$$r^2 = z^2 + p^2 \quad \Rightarrow \quad \frac{\partial r}{\partial z}\Big|_p = \frac{z}{r} = \mu$$

$$\mu = \frac{z}{(z^2+p^2)^{\frac{1}{2}}} \quad \Rightarrow \quad \frac{\partial \mu}{\partial z}\Big|_p = \frac{1}{r} - \frac{z^2}{r^3} = \frac{1}{r}(1-\mu^2)$$

$$\Rightarrow \underline{n}\cdot\underline{\nabla} = \frac{d}{ds} = \mu\frac{\partial}{\partial r} + \frac{1-\mu^2}{r}\frac{\partial}{\partial \mu}$$

$$\left\| \left(\frac{1}{c}\frac{\partial}{\partial t} + \mu\frac{\partial}{\partial r} + \frac{1-\mu^2}{r}\frac{\partial}{\partial \mu}\right) I_\nu(r,\mu,t) = \eta_\nu - \chi_\nu I_\nu \right\|$$

General (without proof) for θ, Φ, r

$$\left(\frac{1}{c}\frac{\partial}{\partial t} + \mu\frac{\partial}{\partial r} + \frac{\gamma}{r}\frac{\partial}{\partial \theta} + \frac{\sigma}{r\sin\theta}\frac{\partial}{\partial \Phi} + \frac{1-\mu^2}{r}\frac{\partial}{\partial \mu} - \frac{\sigma\cot\theta}{r}\frac{\partial}{\partial \phi}\right) I_\nu(\theta,\Phi,r,\mu,\phi,\nu,t) = \eta_\nu - \chi_\nu I_\nu$$

mit $\gamma = \cos\phi\sin\theta$
$\sigma = \sin\phi\sin\theta$

Source function and Kirchhoff-Planck law

Source function

transfer equation

$$\left(\frac{1}{c}\frac{\partial}{\partial t} + \underline{n}\cdot\underline{\nabla}\right) I_\nu = \eta_\nu - \chi_\nu I_\nu \quad \Big| \frac{1}{\chi_\nu}$$

now: stationary, $d\tau_\nu = \chi_\nu ds$, $\frac{\partial}{\partial s} = \underline{n}\cdot\underline{\nabla}$

$$\Rightarrow \frac{d}{\chi_\nu ds} I_\nu = \frac{d}{d\tau_\nu} I_\nu = \frac{\eta_\nu}{\chi_\nu} - I_\nu \overset{\text{def}}{=} S_\nu - I_\nu$$

compact form of transfer equation

$\frac{dI_\nu}{d\tau_\nu} = S_\nu - I_\nu$ with source function S_ν

- valid in any geometry, if stationary + $\frac{d}{d\tau_\nu} = \frac{\underline{n}\cdot\underline{\nabla}}{\chi_\nu}$

physical interpretation

- later we will show that mean free path of photons corresponds to $\tau_\nu = 1$

$\Rightarrow 1 \approx \chi_\nu \Delta s$, $\Delta s = \frac{1}{\chi_\nu}$

$\Rightarrow S_\nu = \frac{\eta_\nu}{\chi_\nu} = \eta_\nu \Delta s$

source function corresponds to emitted intensity δI_ν^{em} over mean free path

Kirchhoff-Planck law

- assume thermodynamic equilibrium (TE)

→ radiation field homogeneous
stationary

$\rightarrow \left(\frac{1}{c}\frac{\partial}{\partial t} + \underline{n}\,\underline{\nabla}\right) =: 0$

intensity Planck-function

$\rightarrow 0 = I_\nu - S_\nu = B_\nu - S_\nu$

TE: $\boxed{S_\nu^* = \frac{\eta_\nu^*}{\chi_\nu^*} = B_\nu(T)}$ ← Kirchhoff-Planck law

or other way round

TE: $\eta_\nu^* = \chi_\nu^* B_\nu(T)$ [only one quantity to be specified]

True absorption and scattering

"true" absorption processes:

radiation energy => thermal pool
if not TE, temperature T(r) is changed
examples: photo-ionization
bound-bound absorption with subsequent collisional de-excitation

scattering:

no interaction with thermal pool
absorbed photon energy is directly reemitted (as photon)
no influence on T(r)
But direction $\underline{\mathbf{n}}$ -> $\underline{\mathbf{n}}'$ is changed (change in frequency mostly small)

examples: Thomson scattering at free electrons
Rayleigh scattering at atoms and molecules
resonance line scattering

ESSENTIAL POINT

true processes:

localized interaction with thermal pool,
drive physical conditions into local equilibrium
often (e.g., in LTE – page 133/136): $\eta_\nu(\mathrm{true}) = \kappa_\nu B_\nu(T)$

scattering processes:

(almost) no influence on local thermodynamic properties of plasma
propagate information of radiation field (sometimes over large distances)
η_ν (Thomson) = $\sigma_{\mathrm{TH}}\, J_\nu$ (-> next page)

Thomson scattering

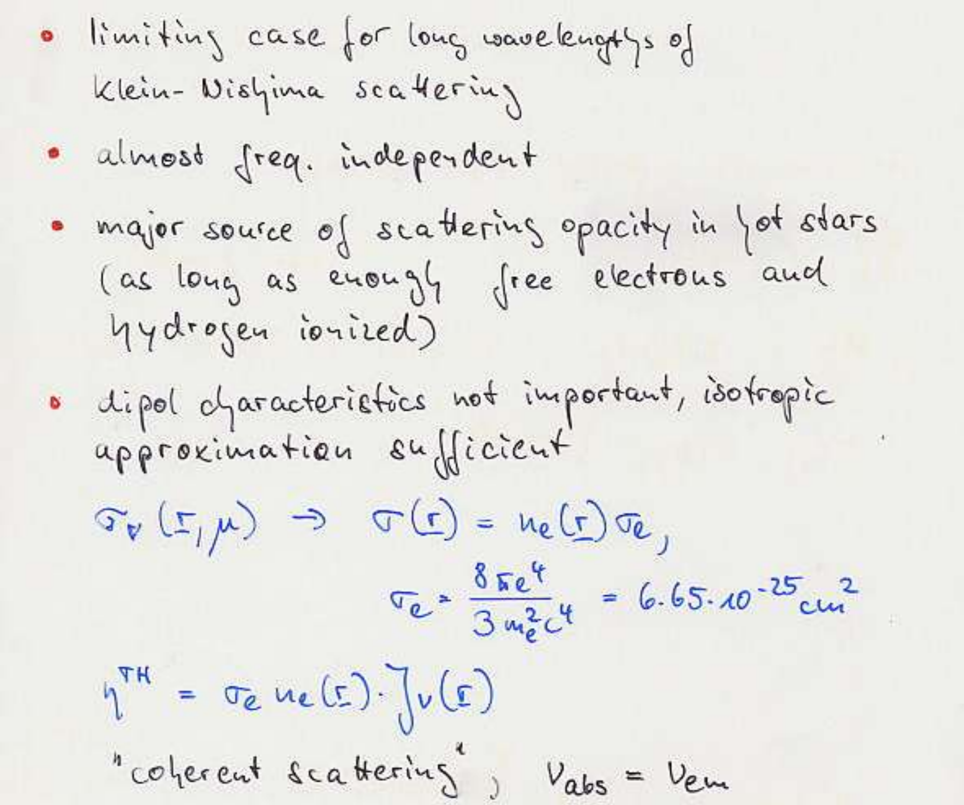

- limiting case for long wavelengths of Klein-Nishima scattering
- almost freq. independent
- major source of scattering opacity in hot stars (as long as enough free electrons and hydrogen ionized)
- dipol characteristics not important, isotropic approximation sufficient

$$\sigma_\nu(\underline{r},\mu) \rightarrow \sigma(\underline{r}) = n_e(\underline{r})\sigma_e,$$

$$\sigma_e = \frac{8\pi e^4}{3 m_e^2 c^4} = 6.65 \cdot 10^{-25} \mathrm{cm}^2$$

$$\eta^{TH} = \sigma_e n_e(\underline{r}) \cdot J_\nu(\underline{r})$$

"coherent scattering", $\nu_{abs} = \nu_{em}$

ADVANCED READING:

Motivation - energy conservation of scattering, with $\chi_\nu = \sigma_\nu$, and assuming isotropic scattering

absorbed energy/area element $\propto \int \sigma_\nu I_\nu d\Omega = \sigma_\nu 4\pi J_\nu$

=

emitted energy/area element $\propto \int \eta_\nu d\Omega = \eta_\nu 4\pi$

$\Rightarrow \boxed{\eta_\nu = \sigma_\nu J_\nu}$

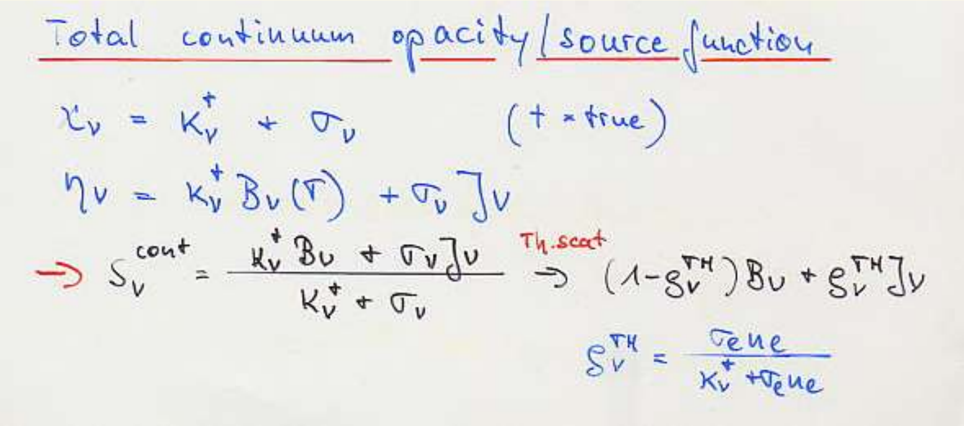

Total continuum opacity/source function

$$\chi_\nu = \kappa_\nu^t + \sigma_\nu \qquad (t = \text{true})$$

$$\eta_\nu = \kappa_\nu^t B_\nu(T) + \sigma_\nu J_\nu$$

$$\Rightarrow S_\nu^{cont} = \frac{\kappa_\nu^t B_\nu + \sigma_\nu J_\nu}{\kappa_\nu^t + \sigma_\nu} \xrightarrow{\text{Th.scat}} (1-s_\nu^{TH}) B_\nu + s_\nu^{TH} J_\nu$$

$$s_\nu^{TH} = \frac{\sigma_e n_e}{\kappa_\nu^t + \sigma_e n_e}$$

Moments of the transfer equation

transfer equation (≘ Boltzmann equation with $\underline{F} \equiv 0$)

$$\left(\frac{1}{c}\frac{\partial}{\partial t} + \underline{n}\cdot\underline{\nabla}\right) I_\nu = \eta_\nu - \chi_\nu I_\nu$$

0th moment: $\oint d\Omega$

note: $\underline{n}$ commutes with $\frac{\partial}{\partial t}$, $\underline{\nabla}$, since (t, $\underline{r}$, $\underline{n}$ independent variables here)

- integrate transfer equation over $d\Omega$

$$\frac{4\pi}{c}\frac{\partial}{\partial t} J_\nu + \underline{\nabla}\cdot\underline{\mathcal{F}}_\nu = \oint(\eta_\nu - \chi_\nu I_\nu)\,d\Omega$$

- if χ_ν, η_ν isotropic, i.e., no velocity fields $\rightarrow \; = 4\pi(\eta_\nu - \chi_\nu J_\nu)$

- Now frequency integration

$$\frac{4\pi}{c}\frac{\partial}{\partial t} J(\underline{r},t) + \underline{\nabla}\cdot\underline{\mathcal{F}}(\underline{r},t) = \int_0^\infty d\nu \oint(\eta_\nu - \chi_\nu I_\nu)\,d\Omega$$

total rad. energy added and removed

- IF energy transported by radiation alone (i.e., no convection) and no energy is created (which is true for stellar atmospheres)

$\Rightarrow$

$$\int_0^\infty d\nu \oint(\eta_\nu - \chi_\nu I_\nu)\,d\Omega = 0$$

"radiative equilibrium"

static atm. $\longrightarrow$

$$\boxed{\int_0^\infty d\nu\,(\eta_\nu - \chi_\nu J_\nu) = \int_0^\infty d\nu\,\chi_\nu(S_\nu - J_\nu) = 0}$$

- if radiation field time independent

"flux conservation"

$$\begin{tikzcd} & \boxed{\underline{\nabla}\cdot\underline{\mathcal{F}} = 0} \arrow[dl, "pp"'] \arrow[dr, "spherical"] & \\ \frac{L}{4\pi R_*^2} = \mathcal{F}(z) = \text{const} & & r^2\mathcal{F}(r) = \text{const} = \frac{L}{4\pi} \end{tikzcd}$$

- radiative equilibrium and flux conservation equivalent formulations, are used to calculate $T(r)$

0th moment: frequency-dependent, stationary and static

$$\boxed{\nabla\cdot\mathcal{F}_\nu = 4\pi(\eta_\nu - \chi_\nu J_\nu)}$$

static: $v=0$ (or $v \ll v_{sound}$)
stationary: time-independent, $\partial/\partial t=0$

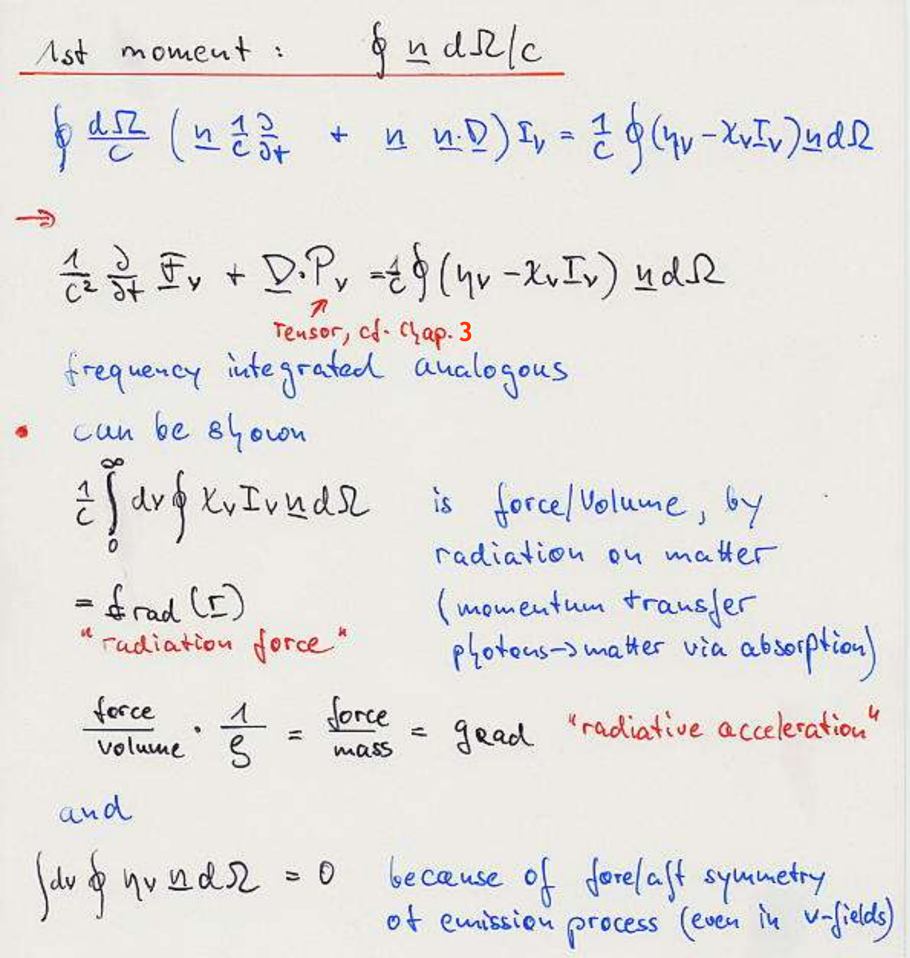

1st moment : $\oint \underline{n}\, d\Omega / c$

$$\oint \frac{d\Omega}{c} \left(\underline{n} \frac{1}{c} \frac{\partial}{\partial t} + \underline{n}\ \underline{n} \cdot \underline{\nabla} \right) I_\nu = \frac{1}{c} \oint (\eta_\nu - \chi_\nu I_\nu)\, \underline{n}\, d\Omega$$

$\Rightarrow$

$$\frac{1}{c^2} \frac{\partial}{\partial t} \underline{\mathcal{F}}_\nu + \underline{\nabla} \cdot \underset{\substack{\nearrow \\ \text{Tensor, cf. Chap. 3}}}{P_\nu} = \frac{1}{c} \oint (\eta_\nu - \chi_\nu I_\nu)\, \underline{n}\, d\Omega$$

frequency integrated analogous

- can be shown

$$\frac{1}{c} \int_0^\infty d\nu \oint \chi_\nu I_\nu \underline{n}\, d\Omega$$

is force/Volume, by radiation on matter (momentum transfer photons→matter via absorption)

$$= \underline{f}_{\text{rad}}(\underline{r})$$

"radiation force"

$$\frac{\text{force}}{\text{volume}} \cdot \frac{1}{\rho} = \frac{\text{force}}{\text{mass}} = g_{\text{rad}}$$

"radiative acceleration"

and

$$\int d\nu \oint \eta_\nu \underline{n}\, d\Omega = 0$$

because of fore/aft symmetry of emission process (even in v-fields)

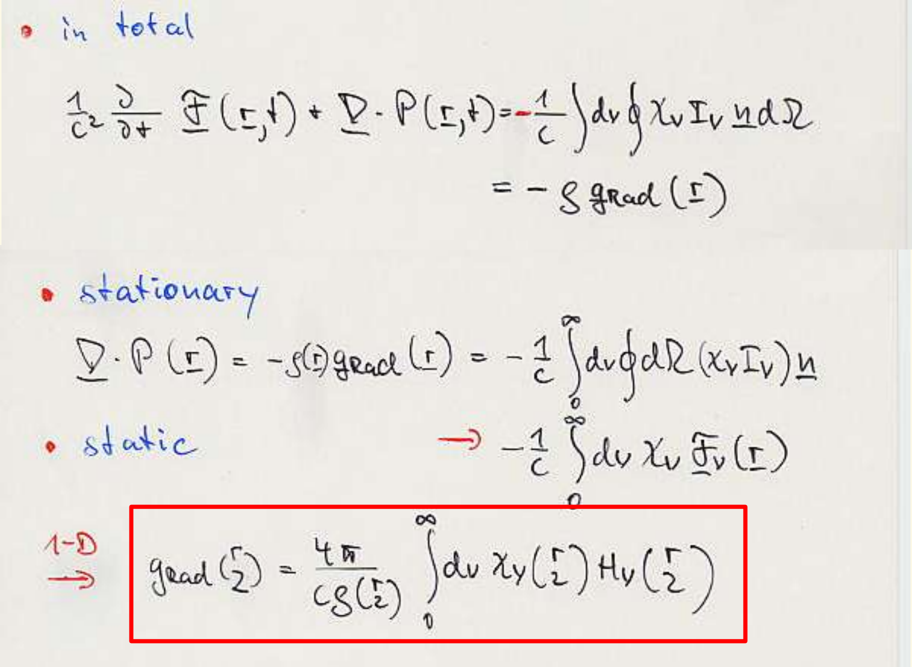

- in total

$$\frac{1}{c^2} \frac{\partial}{\partial t} \underline{\mathcal{F}}(\underline{r},t) + \underline{\nabla} \cdot P(\underline{r},t) = -\frac{1}{c} \int d\nu \oint \chi_\nu I_\nu \underline{n}\, d\Omega$$

$$= -\rho\, \underline{g}_{\text{rad}}(\underline{r})$$

- stationary

$$\underline{\nabla} \cdot P(\underline{r}) = -\rho(\underline{r})\, \underline{g}_{\text{rad}}(\underline{r}) = -\frac{1}{c} \int_0^\infty d\nu \oint d\Omega\, (\chi_\nu I_\nu)\, \underline{n}$$

- static

$$\Rightarrow -\frac{1}{c} \int_0^\infty d\nu\, \chi_\nu \underline{\mathcal{F}}_\nu(\underline{r})$$

1-D $\Rightarrow$

$$\boxed{g_{\text{rad}}\binom{r}{2} = \frac{4\pi}{c\rho\binom{r}{2}} \int_0^\infty d\nu\, \chi_\nu\binom{r}{2} H_\nu\binom{r}{2}}$$

1st moment: frequency-dependent, stationary and static

$$\boxed{\nabla \cdot P_\nu = -\frac{1}{c} \chi_\nu \mathscr{F}_\nu}$$

The change in radiative pressure drives the flux!

static: v=0 (or v << v_{sound})

stationary: time-independent, $\partial/\partial t=0$

Summary: moments of the RTE ...

... expressed also in terms of $J_\nu,\ H_\nu,\ K_\nu$

general case, 0^{th} moment

$$\frac{4\pi}{\mathrm{c}}\frac{\partial}{\partial t}J_\nu + \nabla\cdot\mathscr{F}_\nu = \oint(\eta_\nu - \chi_\nu I_\nu)\,\mathrm{d}\Omega$$

general case, 1^{st} moment

$$\frac{1}{\mathrm{c}^2}\frac{\partial}{\partial t}\mathscr{F} + \nabla\cdot\mathbf{P}_\nu = \frac{1}{c}\oint(\eta_\nu - \chi_\nu I_\nu)\,\mathbf{n}\mathrm{d}\Omega$$

plane-parallel, stationary $(\partial/\partial t = 0)$ and static $(\mathrm{v}\approx 0)$

$$\frac{\mathrm{d}H_\nu}{\mathrm{dz}} = \eta_\nu - \chi_\nu J_\nu$$

$$\frac{\mathrm{d}K_\nu}{\mathrm{dz}} = -\chi_\nu H_\nu$$

spherically symmetric, stationary and (quasi-)static

[no/negligible Dopplershifts $\Rightarrow$ no winds or continuum problems (except for edges)

Otherwise, opacities become angle-dependent (Doppler-shifts), and cannot be put in front of the integrals]

$$\frac{1}{r^2}\frac{\partial(r^2 H_\nu)}{\partial r} = \eta_\nu - \chi_\nu J_\nu$$

$$\frac{\partial K_\nu}{\partial r} + \frac{3K_\nu - J_\nu}{r} = -\chi_\nu H_\nu$$

when frequency integrated, = 0, if ONLY radiation energy transported: radiative equilibrium
→ (for stationary conditions) flux conservation

when frequency integrated, = $-\boldsymbol{f}_{\text{rad}}$

Chap. 5 – Radiative transfer: simple solutions

Pure absorption and optical depth

- from here on, stationary description
  (→ stellar atmospheres)
- radiative transfer without emission

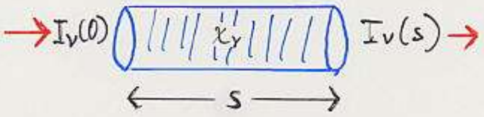

$$\frac{dI_\nu}{ds} = -\chi_\nu I_\nu$$

$$\frac{dI_\nu}{I_\nu} = -\chi_\nu(s)\,ds$$

$$\ln I_\nu(s) - \ln I_\nu(0) = -\int_0^s \chi_\nu(s')\,ds'$$

$$I_\nu(s) = I_\nu(0)\,e^{-\int_0^s \chi_\nu(s')ds'} = I_\nu(0)\,e^{-\tau_\nu(s)}$$

optical depth, central quantity
(more precisely: optical thickness)

or

$$I_\nu(\tau_\nu) = I_\nu(0)\,e^{-\tau_\nu}$$

- since $I_\nu \sim e^{-\tau_\nu}$, we look only until $\tau_\nu = 1$
  (freq. dep.!)
- Question: What is the average distance over which photons travel?

Answer: $\langle\tau_\nu\rangle = \int_0^\infty \tau_\nu\, p(\tau_\nu)\, d\tau_\nu$

expectation value

probability density function

$p(\tau_\nu)\,d\tau$ gives probability, that photon is absorbed in interval $\tau_\nu, \tau_\nu + d\tau_\nu$

- is probability, that photon is NOT absorbed between $0, \tau_\nu$ and then absorbed between $\tau_\nu, \tau_\nu + d\tau_\nu$

a) prob., that photon is absorbed

$$P(0,\tau_\nu) = \frac{\Delta I(\tau)}{I_0} = \frac{I_0 - I(\tau_\nu)}{I_0} = 1 - \frac{I(\tau_\nu)}{I_0}$$

b) prob, that photon is not absorbed

$$1 - P(0,\tau_\nu) = \frac{I(\tau_\nu)}{I_0} = e^{-\tau_\nu}$$

c) prob., that photon is absorbed in $\tau_\nu, \tau_\nu + d\tau_\nu$

$$P(\tau_\nu, \tau_\nu + d\tau_\nu) = \left|\frac{dI(\tau_\nu)}{I(\tau_\nu)}\right| = d\tau_\nu$$

d) total probability is $e^{-\tau_\nu} d\tau_\nu$

THUS

$$\langle\tau_\nu\rangle = \int_0^\infty \tau_\nu e^{-\tau_\nu} d\tau_\nu = \underline{1}$$

mean free path $\bar{s}$ corresponds to $\langle\tau_\nu\rangle = 1$

$$\Delta\tau_\nu = \chi_\nu \Delta s \rightarrow \underbrace{\Delta s}_{=\bar{s}} = \frac{1}{\chi_\nu}, \quad \text{q.e.d.}$$

USUAL convention

- Since we "measure" from outside to inside, $\tau_\nu = 0$ is defined at outer "edge" of atmosphere

$$\Rightarrow ds = -\,dz \;(\text{or } -dr)$$

$$\Rightarrow \underbrace{d\tau_\nu}_{>0!} = -\chi_\nu \underbrace{\begin{pmatrix} dz \\ dr \end{pmatrix}}_{<0!}$$

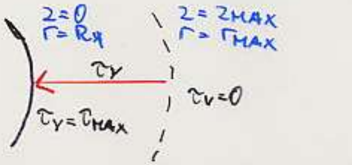

Formation of spectral lines: the principle

- look always down to $\tau_\nu \approx 1$
- BUT line: χ_ν large $\rightarrow \bar{s}$ small
  cont.: χ_ν small $\rightarrow \bar{s}$ large

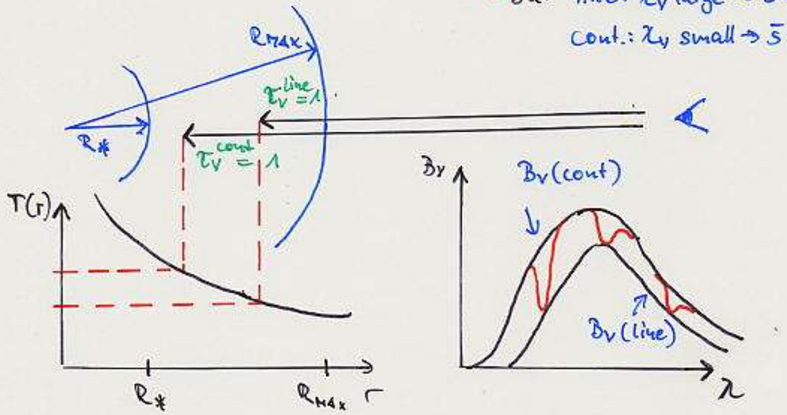

$$T(r_{cont}) > T(r_{line})\ !$$

"Formal solution"

solve eq. of RT with known source function

- pp geometry

$$\mu \frac{dI_\nu}{dz} = \eta_\nu - \chi_\nu I_\nu$$

$$\rightarrow \mu \frac{dI_\nu}{d\tau_\nu} = I_\nu - S_\nu \qquad (\tau_\nu = 0 \text{ outside!})$$

- solution with integrating factor $e^{-\tau_\nu/\mu}$

multiply equation, integrate between τ_1 and τ_2
τ_2 (inside) > τ_1 (outside)

$\Rightarrow$

$$I_\nu(\tau_1,\mu) = \underbrace{I_\nu(\tau_2,\mu)\,e^{-(\tau_2-\tau_1)/\mu}}_{\uparrow\ >0\ \checkmark} + \underbrace{\int_{\tau_1}^{\tau_2} S_\nu(t_\nu)\,e^{-(t_\nu-\tau_1)/\mu}\,\frac{dt_\nu}{\mu}}_{\uparrow\ >0\ \checkmark}$$

intensity "emitted" at τ_2, loss (abs) by factor $e^{-\Delta\tau}$
$\hat{=}$ pure absorption case

gain by emission with subsequent absorption
$e^{-(t_\nu-\tau_1)/\mu}$

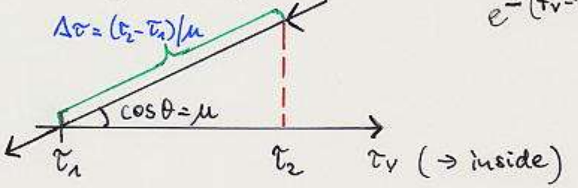

Boundary conditions

a) incident intensity from inside
$\mu > 0$ at $\tau_2 = \tau_{max}$

- either $I_\nu(\tau_2 = \tau_{max}, \mu) = I_\nu^+(\mu)$ (e.g., from diffusion approx)
- or "semi-infinite" atmosphere

$\tau_2 = \tau_{max} \rightarrow \infty$ with $\lim_{\tau_\nu \to \infty} I_\nu(\tau_\nu,\mu)\,e^{-\tau_\nu/\mu} = 0$

($I_\nu(\tau_\nu,\mu)$ increases slower than exp.)

$$\Rightarrow I_\nu(\tau_\nu,\mu) = \int_{\tau_\nu}^{\infty} S_\nu(t)\,e^{-(t-\tau_\nu)/\mu}\,\frac{dt}{\mu} \qquad \mu > 0$$

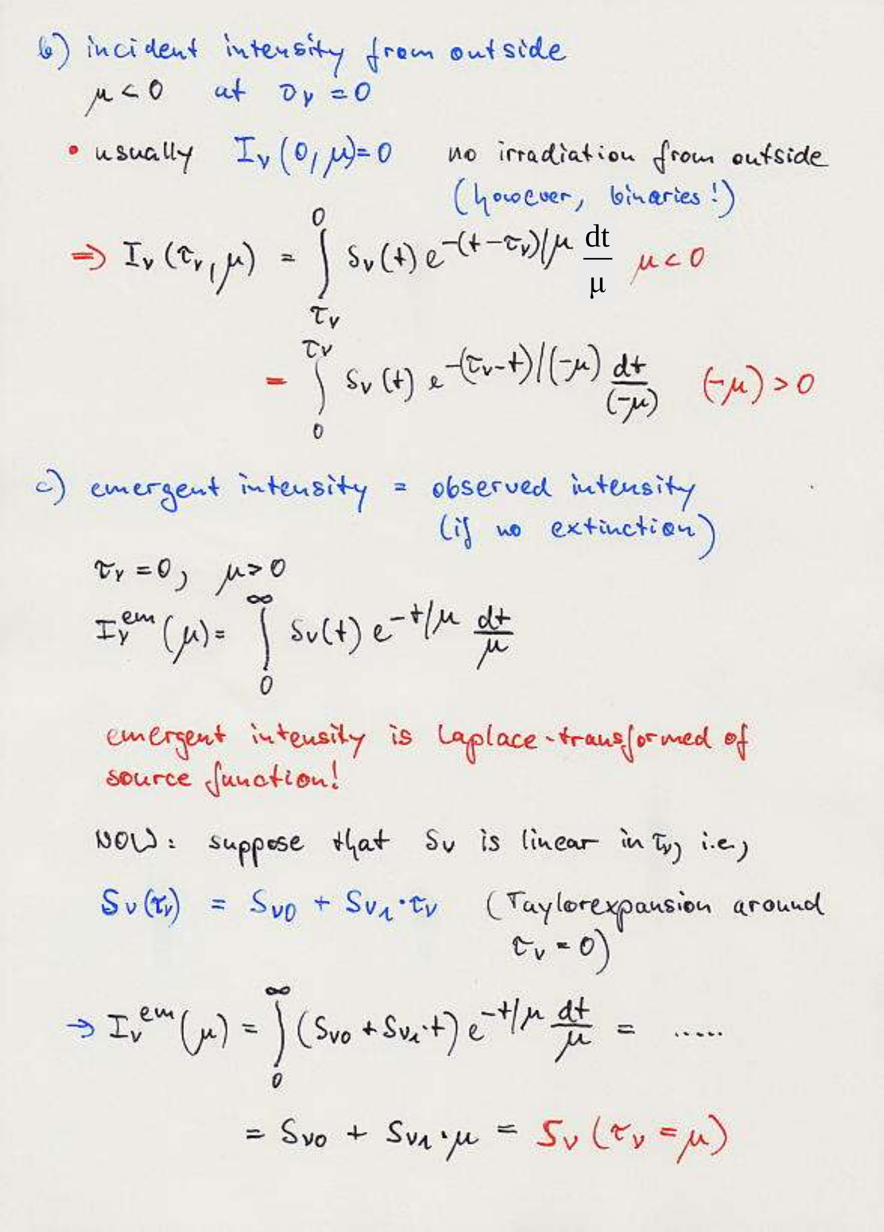

b) incident intensity from outside

$\mu < 0$ at $\tau_\nu = 0$

- usually $I_\nu(0,\mu) = 0$ no irradiation from outside (however, binaries!)

$$\Rightarrow I_\nu(\tau_\nu,\mu) = \int_{\tau_\nu}^{0} S_\nu(t)\, e^{-(t-\tau_\nu)/\mu} \frac{dt}{\mu} \qquad \mu < 0$$

$$= \int_{0}^{\tau_\nu} S_\nu(t)\, e^{-(\tau_\nu - t)/(-\mu)} \frac{dt}{(-\mu)} \qquad (-\mu) > 0$$

c) emergent intensity = observed intensity (if no extinction)

$\tau_\nu = 0, \quad \mu > 0$

$$I_\nu^{em}(\mu) = \int_0^\infty S_\nu(t)\, e^{-t/\mu} \frac{dt}{\mu}$$

emergent intensity is Laplace-transformed of source function!

NOW: suppose that S_ν is linear in τ_ν, i.e.,

$S_\nu(\tau_\nu) = S_{\nu 0} + S_{\nu 1} \cdot \tau_\nu$ (Taylorexpansion around $\tau_\nu = 0$)

$$\rightarrow I_\nu^{em}(\mu) = \int_0^\infty (S_{\nu 0} + S_{\nu 1} \cdot t)\, e^{-t/\mu} \frac{dt}{\mu} = \;.....$$

$$= S_{\nu 0} + S_{\nu 1} \cdot \mu = S_\nu(\tau_\nu = \mu)$$

Eddington-Barbier-relation

$$\boxed{I_\nu^{em}(\mu) \approx S_\nu(\tau_\nu = \mu)}$$

We "see" source function at location $\tau_\nu = \mu$ (remember: τ_ν radial quantity)
(corresponds to optical depth along path $\tau_\nu / \mu = 1!$)

Generalization of principle that we can see only until $\Delta\tau_\nu = 1$

i) spectral lines (as before)

for fixed μ, $\tau_\nu / \mu = 1$ is reached further out in lines (compared to continuum)
=> $S_\nu^{line}(\tau_\nu^{line}/\mu = 1) < S_\nu^{cont}(\tau_\nu^{cont}/\mu = 1)$ => "dip" is created

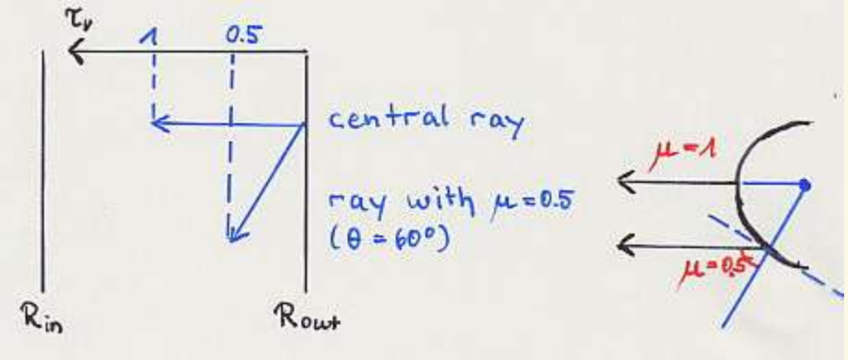

ii) limb darkening

for $\mu = 1$ (central ray), we reach maximum in depth (geometrical)
temperature / source function rises with τ
=> central ray: largest source function, limb darkening

iii) "observable" information only from layers with $\tau_\nu \leq 1$
deepest atmospheric layers can be analyzed only indirectly

Solar limb-darkening
Empirical temperature stratification

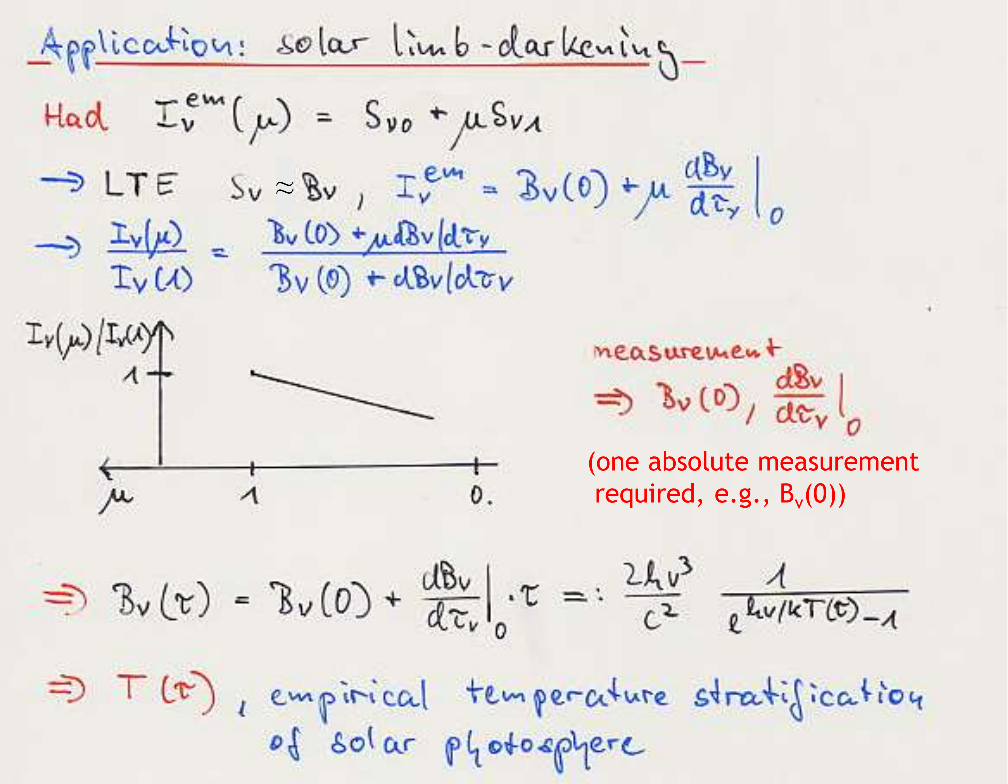

Application: solar limb-darkening

Had $I_\nu^{em}(\mu) = S_{\nu 0} + \mu S_{\nu 1}$

→ LTE $S_\nu \approx B_\nu$, $I_\nu^{em} = B_\nu(0) + \mu \frac{dB_\nu}{d\tau_\nu}\Big|_0$

→ $\frac{I_\nu(\mu)}{I_\nu(1)} = \frac{B_\nu(0) + \mu dB_\nu/d\tau_\nu}{B_\nu(0) + dB_\nu/d\tau_\nu}$

measurement

⇒ $B_\nu(0), \frac{dB_\nu}{d\tau_\nu}\Big|_0$

(one absolute measurement required, e.g., $B_\nu(0)$)

⇒ $B_\nu(\tau) = B_\nu(0) + \frac{dB_\nu}{d\tau_\nu}\Big|_0 \cdot \tau =: \frac{2h\nu^3}{c^2} \frac{1}{e^{h\nu/kT(\tau)}-1}$

⇒ $T(\tau)$, empirical temperature stratification of solar photosphere

empirical temperature structure of solar photosphere by Holweger & Müller (1974)

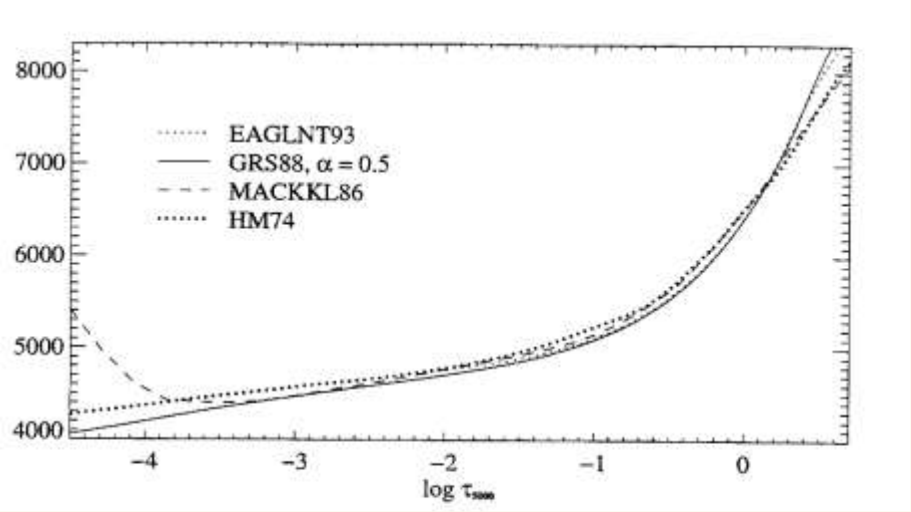

Lambda operator

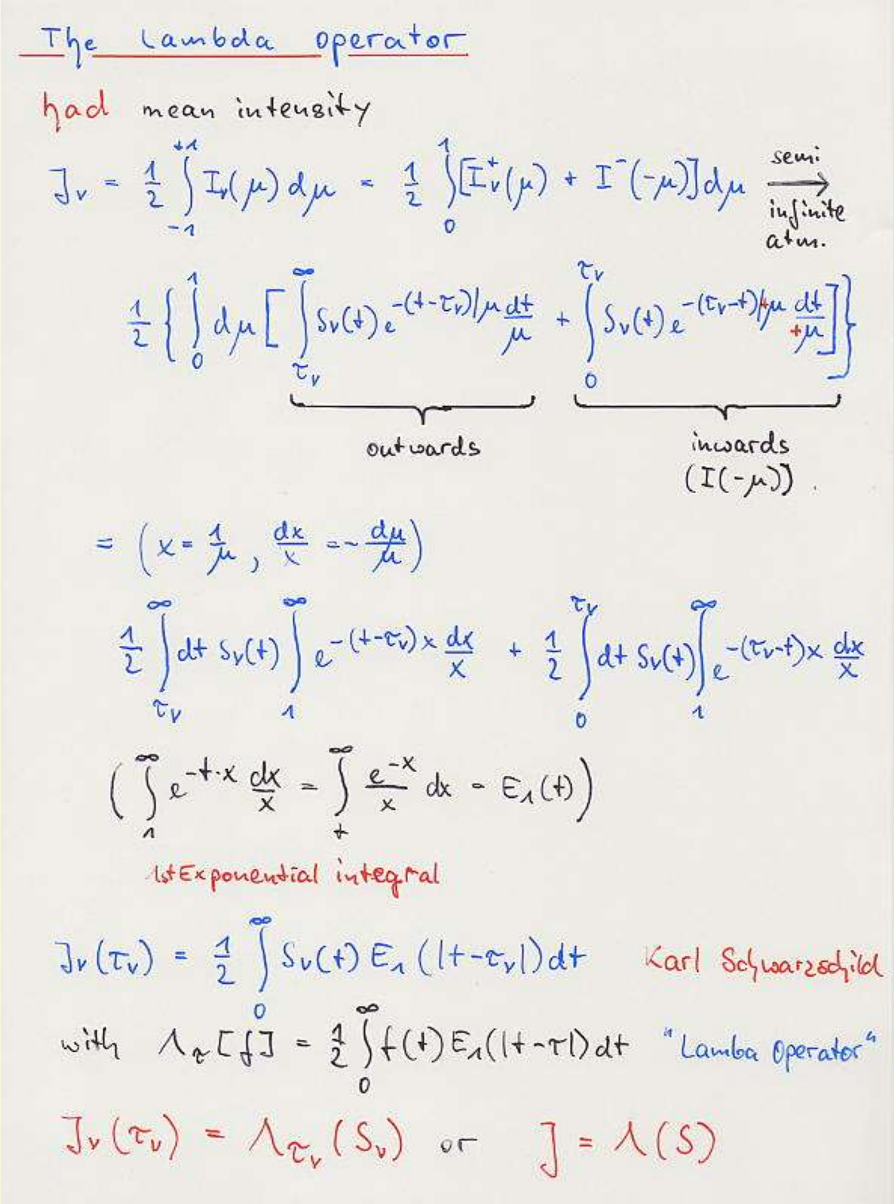

The Lambda operator

had mean intensity

$$J_\nu = \frac{1}{2}\int_{-1}^{+1} I_\nu(\mu)\,d\mu = \frac{1}{2}\int_0^1 [I_\nu^+(\mu) + I^-(-\mu)]\,d\mu \xrightarrow[\text{infinite atm.}]{\text{semi}}$$

$$\frac{1}{2}\left\{\int_0^1 d\mu\left[\underbrace{\int_{\tau_\nu}^{\infty} S_\nu(t)\,e^{-(t-\tau_\nu)/\mu}\frac{dt}{\mu}}_{\text{outwards}} + \underbrace{\int_0^{\tau_\nu} S_\nu(t)\,e^{-(\tau_\nu-t)/+\mu}\frac{dt}{+\mu}}_{\substack{\text{inwards}\\ (I(-\mu))}}\right]\right\}$$

$$= \left(x = \frac{1}{\mu},\ \frac{dx}{x} = -\frac{d\mu}{\mu}\right)$$

$$\frac{1}{2}\int_{\tau_\nu}^{\infty} dt\, S_\nu(t)\int_1^{\infty} e^{-(t-\tau_\nu)x}\frac{dx}{x} + \frac{1}{2}\int_0^{\tau_\nu} dt\, S_\nu(t)\int_1^{\infty} e^{-(\tau_\nu-t)x}\frac{dx}{x}$$

$$\left(\int_1^{\infty} e^{-t\cdot x}\frac{dx}{x} = \int_t^{\infty}\frac{e^{-x}}{x}\,dx = E_1(t)\right)$$

1st Exponential integral

$$J_\nu(\tau_\nu) = \frac{1}{2}\int_0^{\infty} S_\nu(t)\,E_1(|t-\tau_\nu|)\,dt$$ Karl Schwarzschild

with $\Lambda_\tau[f] = \frac{1}{2}\int_0^{\infty} f(t)\,E_1(|t-\tau|)\,dt$ "Lamba Operator"

$$J_\nu(\tau_\nu) = \Lambda_{\tau_\nu}(S_\nu) \quad \text{or} \quad J = \Lambda(S)$$

Diffusion approximation

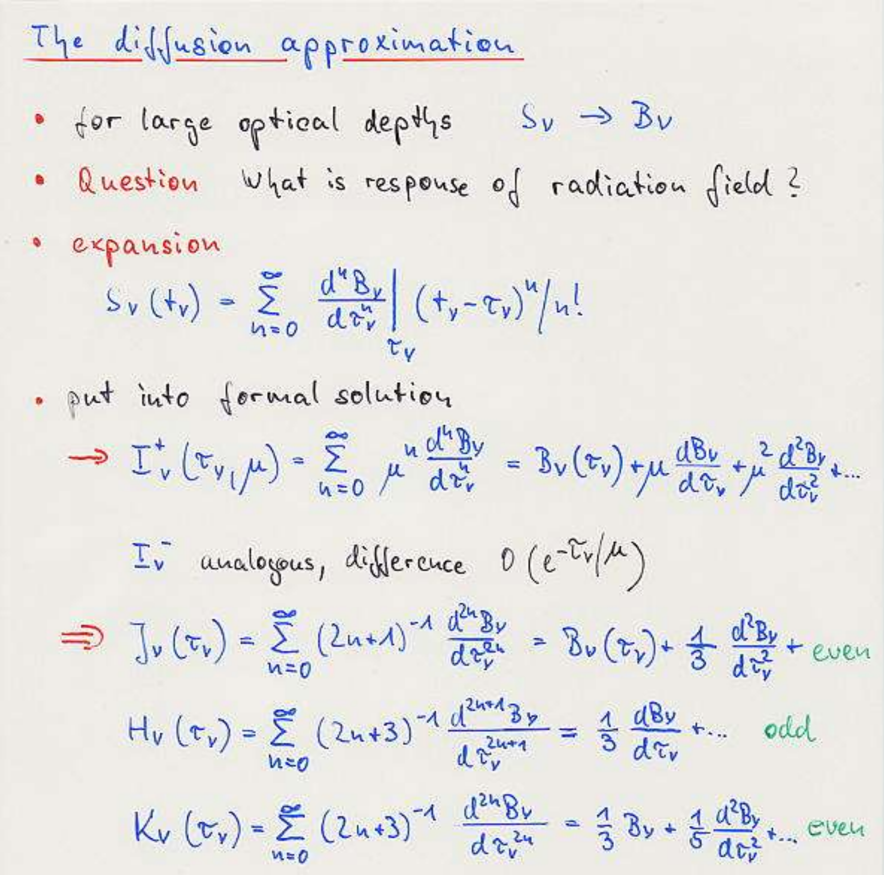

The diffusion approximation

- for large optical depths $S_\nu \rightarrow B_\nu$
- Question: what is response of radiation field?
- expansion

$$S_\nu(t_\nu) = \sum_{n=0}^{\infty} \left.\frac{d^n B_\nu}{d\tau_\nu^n}\right|_{\tau_\nu} (t_\nu - \tau_\nu)^n / n!$$

- put into formal solution

$$\rightarrow I_\nu^+(\tau_\nu, \mu) = \sum_{n=0}^{\infty} \mu^n \frac{d^n B_\nu}{d\tau_\nu^n} = B_\nu(\tau_\nu) + \mu \frac{dB_\nu}{d\tau_\nu} + \mu^2 \frac{d^2 B_\nu}{d\tau_\nu^2} + \ldots$$

I_ν^- analogous, difference $O(e^{-\tau_\nu/\mu})$

$$\Rightarrow J_\nu(\tau_\nu) = \sum_{n=0}^{\infty} (2n+1)^{-1} \frac{d^{2n} B_\nu}{d\tau_\nu^{2n}} = B_\nu(\tau_\nu) + \frac{1}{3} \frac{d^2 B_\nu}{d\tau_\nu^2} + \text{even}$$

$$H_\nu(\tau_\nu) = \sum_{n=0}^{\infty} (2n+3)^{-1} \frac{d^{2n+1} B_\nu}{d\tau_\nu^{2n+1}} = \frac{1}{3} \frac{dB_\nu}{d\tau_\nu} + \ldots \quad \text{odd}$$

$$K_\nu(\tau_\nu) = \sum_{n=0}^{\infty} (2n+3)^{-1} \frac{d^{2n} B_\nu}{d\tau_\nu^{2n}} = \frac{1}{3} B_\nu + \frac{1}{5} \frac{d^2 B_\nu}{d\tau_\nu^2} + \ldots \quad \text{even}$$

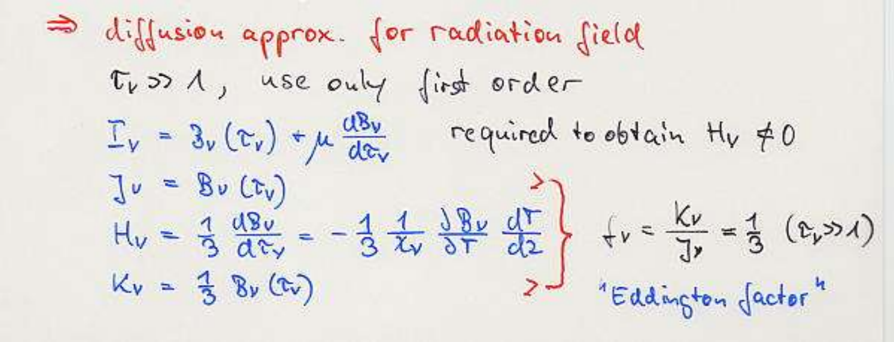

⇒ diffusion approx. for radiation field

$\tau_\nu \gg 1$, use only first order

$I_\nu = B_\nu(\tau_\nu) + \mu \frac{dB_\nu}{d\tau_\nu}$ required to obtain $H_\nu \neq 0$

$$\left.\begin{aligned} J_\nu &= B_\nu(\tau_\nu) \\ H_\nu &= \frac{1}{3} \frac{dB_\nu}{d\tau_\nu} = -\frac{1}{3} \frac{1}{\chi_\nu} \frac{\partial B_\nu}{\partial T} \frac{dT}{dz} \\ K_\nu &= \frac{1}{3} B_\nu(\tau_\nu) \end{aligned}\right\} \quad f_\nu = \frac{K_\nu}{J_\nu} = \frac{1}{3} \quad (\tau_\nu \gg 1)$$

"Eddington factor"

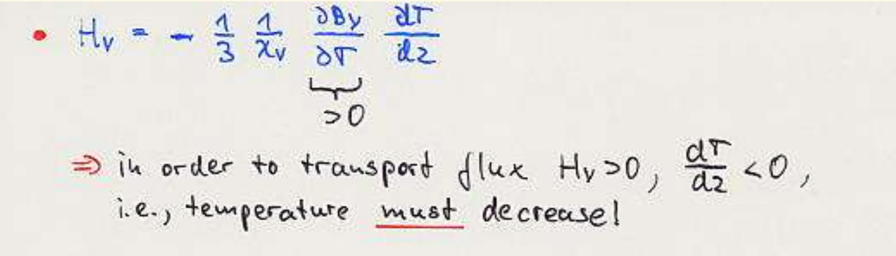

- $$H_\nu = -\frac{1}{3} \frac{1}{\chi_\nu} \underbrace{\frac{\partial B_\nu}{\partial T}}_{>0} \frac{dT}{dz}$$

⇒ in order to transport flux $H_\nu > 0$, $\frac{dT}{dz} < 0$, i.e., temperature must decrease!

Thermalization

From approximate solution of moments equations accounting for true plus scattering continuum opacity (Milne-Eddington model → advanced reading), it turns out that the difference between mean intensity and Planck-function (as a function of optical depth) can be written as

$$J_\nu - B_\nu \approx f(\varepsilon_\nu)\exp\left[-(3\varepsilon_\nu)^{1/2}\tau_\nu\right],$$

with *thermalization parameter*

$$\varepsilon_\nu = \frac{\kappa_\nu^{\mathrm{t}}}{\kappa_\nu^{\mathrm{t}} + \sigma_\nu}$$

given by the ratio of true and total opacity.

Thus, only for large arguments of the exponent we achieve $J_\nu \to B_\nu$, namely if

$$\tau_\nu \geq \frac{1}{\sqrt{\varepsilon_\nu}}$$

with $\frac{1}{\sqrt{\varepsilon_\nu}}$ the so-called thermalization depth [$\sqrt{3}$ in denominator neglected]

a) for $\sigma_\nu \ll \kappa_\nu^{\mathrm{t}}$ (negligible scattering) $\to J_\nu(\tau_\nu \geq 4...5) \to B_\nu$

b) SN remnants: scattering dominated, very large thermalization depth

The Milne-Eddington model

The Milne-Eddington model for continua with scattering

- allows understanding of emergent (continuum) fluxes from stellar atmospheres
- can be extended to include lines
- required for curve of growth method (➔ Chap. 7)

assume source function (→ page 78)

$$S_\nu = (1-\rho_\nu)B_\nu + \rho_\nu J_\nu \quad \text{with} \quad \rho_\nu = \frac{\sigma_e n_e}{\overset{+}{\kappa}_\nu + \sigma_e n_e}$$

$$=: \varepsilon_\nu B_\nu + (1-\varepsilon_\nu) J_\nu, \quad \varepsilon_\nu = 1-\rho_\nu$$

and

$$B_\nu = a_\nu + b_\nu \cdot \tau_\nu \quad + \quad \text{plane-parallel symmetry}$$

- 0th moment

$$\frac{\partial H_\nu}{\partial \tau_\nu} = J_\nu - S_\nu \quad , \quad d\tau_\nu = -(\overset{+}{\kappa}_\nu + n_e\sigma_e)dz$$

$$= J_\nu - (\varepsilon_\nu B_\nu + (1-\varepsilon_\nu)J_\nu) = \varepsilon_\nu (J_\nu - B_\nu)$$

- 1st moment

$$\frac{\partial K_\nu}{\partial \tau_\nu} = H_\nu$$

in diffusion approximation, we had

$$K_\nu = \frac{1}{3} J_\nu \quad (\tau_\nu \rightarrow \infty)$$

- Eddington's approximation (1929, 'The formation of absorption lines')

use $K_\nu / J_\nu = \frac{1}{3}$ everywhere ... not so wrong

$$\Rightarrow \frac{\partial K_\nu}{\partial \tau_\nu} = H_\nu \rightarrow \frac{1}{3}\left(\frac{\partial J_\nu}{\partial \tau_\nu}\right) = H_\nu$$

⇒ (with 0th moment)

$$\frac{1}{3}\frac{\partial^2 J_\nu}{\partial \tau_\nu^2} = \varepsilon_\nu (J_\nu - B_\nu) = \frac{1}{3}\frac{\partial^2 (J_\nu - B_\nu)}{\partial \tau_\nu^2},$$

since B_ν linear in τ_ν!

assume $\varepsilon_\nu = \text{const}$ (otherwise similar solution)

$$J_\nu - B_\nu = \text{const}' \cdot \exp(-(3\varepsilon_\nu)^{\frac{1}{2}}\tau_\nu) \quad \left[\begin{matrix}\text{with lower b.c.} \\ J_\nu \rightarrow B_\nu \text{ for } \tau \rightarrow \infty\end{matrix}\right]$$

- Eddington's approximation implies also

a) $J_\nu(0) = \sqrt{3}\, H_\nu(0)$ (without proof)

b) $\frac{\partial K_\nu}{\partial \tau_\nu} = H_\nu \rightarrow \frac{1}{3}\frac{\partial J_\nu}{\partial \tau_\nu}\Big|_0 = H_\nu(0)$

Thus $\frac{1}{\sqrt{3}}\frac{\partial J_\nu}{\partial \tau_\nu}\Big|_0 = J_\nu(0)$

⇒ insert in above equation

$$\text{const}' = \frac{b_\nu/\sqrt{3} - a_\nu}{(1+\varepsilon_\nu^{\frac{1}{2}})}$$

$$\Rightarrow J_\nu = a_\nu + b_\nu\tau_\nu + \frac{b_\nu/\sqrt{3} - a_\nu}{1+\varepsilon_\nu^{\frac{1}{2}}}\, e^{-(3\varepsilon_\nu)^{\frac{1}{2}}\tau_\nu}$$

advanced reading

$$J_\nu = a_\nu + b\,\tau_\nu + \frac{b_\nu/\sqrt{3} - a_\nu}{1 + \varepsilon_\nu^{\frac{1}{2}}}\, e^{-(3\varepsilon_\nu)^{\frac{1}{2}}\tau_\nu}$$

$$J_\nu(0) = a_\nu + \frac{b_\nu/\sqrt{3} - a_\nu}{1 + \varepsilon_\nu^{\frac{1}{2}}}$$

$$H_\nu(0) = \frac{1}{\sqrt{3}} J_\nu(0)$$

- assume isothermal atmosphere, $b_\nu = 0$ (possible, if gradient not too strong)

$$\Rightarrow J_\nu(0) = \frac{\varepsilon_\nu^{\frac{1}{2}}}{1 + \varepsilon_\nu^{\frac{1}{2}}}\, a_\nu \quad \begin{cases} \nearrow B_\nu/2 \text{ for } \varepsilon_\nu = 1, \text{ i.e. } \sigma = 0 \\ \searrow \varepsilon_\nu^{\frac{1}{2}} B_\nu \ll B_\nu \text{ for } \varepsilon_\nu \ll 1 \end{cases}$$

→ $J_\nu(0) < B_\nu(0)$!!!

- Thermalization

  only for large arguments of the exponent, we have $J_\nu \approx B_\nu$

  $\Rightarrow \tau_\nu \gtrsim \frac{1}{\varepsilon_\nu^{\frac{1}{2}}}$ thermalisation depth

  a) $\sigma \ll k^+ \Rightarrow J_\nu(\tau_\nu \gtrsim 1) \to B_\nu$

  b) SN remnants : scattering dominated, very large thermalization depth

- pure scattering (test case)

  $\frac{\partial H_\nu}{\partial \tau_\nu} = J_\nu - S_\nu = 0$ for $\varepsilon_\nu = 0$ Flux conservation

  $+ \; H_\nu \approx \frac{1}{3}\frac{\partial B_\nu}{\partial \tau_\nu}$ from diffusion limit

in Milne Eddington model

$$H_\nu(0) = \frac{1}{\sqrt{3}}\left(a_\nu + \frac{b_\nu/\sqrt{3} - a_\nu}{1 + e_\nu^{\frac{1}{3}}}\right) \overset{\varepsilon_\nu \to 0}{\Rightarrow} \frac{b_\nu}{3} \mathrel{\hat{=}} \frac{1}{3}\frac{\partial B_\nu}{\partial \tau_\nu}$$

consistent result

- Question : why $J_\nu(0) \ll B_\nu(0)$?
  - remember: $J_\nu(0)$ determined by $S_\nu(\tau_\nu = 1)$
  - $J_\nu(1)$ might fall significantly below $B_\nu(1)$, since many photons can escape from photosphere (into interstellar medium)
  - minimum value is given by incident flux, if no thermal emission
- interesting possibility

  if ε_ν small, $H_\nu(0)$ can become larger than $H_\nu(0)$ $(\varepsilon_\nu = 1)$, if

$$\underbrace{a_\nu + \frac{b_\nu/\sqrt{3} - a_\nu}{2}}_{J_\nu(0,\,\varepsilon_\nu = 1)} < \underbrace{\frac{b_\nu}{\sqrt{3}}}_{J_\nu(0,\,\varepsilon_\nu \ll 1)}, \quad \text{i.e. } \frac{b_\nu}{a_\nu} > \sqrt{3}$$

  i.e. for large temperature gradients

  (information is transported from hotter regions to outer boundary by scattering dominated stratifications)
- further consequences later

Basic assumptions

1. Geometry
plane-parallel or spherically symmetric (→ Chap. 3)

2. Homogeneity
atmospheres assumed to be homogenous (both vertical and horizontal)

BUT: **sun** with spots, granulation, non-radial pulsations ...
white dwarfs with depth dependent abundances (diffusion)
stellar winds of hot stars (partly) with clumping **($<\rho^2> \neq <\rho>^2$)**
complete atmospheres of hot massive stars maybe strongly turbulent (Debnath+ 2024)

HOPE: "mean" = homogenous model describes non-resolvable phenomena in a reasonable way
[attention for (magnetic) Ap-stars: ***very*** strong inhomogeneities!]

3. Stationarity
vast majority of spectra time-independent => **$\partial/\partial t = 0$**

BUT: explosive phenomena (supernovae)
pulsations
close binaries with mass transfer ...

Density stratification

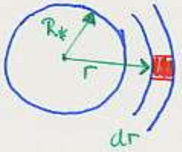

$dm = \rho A dr$

mass element dm
in (spherically sym.) atmosphere

assume (at first) no velocity-fields, i.e. hydrostatic stratification

$\sum_i df_i = 0$, if f_i are forces acting on dm

- $df_{grav} = -G \frac{M_r\, dm}{r^2} = -g(r)\, dm$ with grav. accel.

  $g(r) = \frac{G M_r}{r^2}$ and M_r mass within r

- df_p pressure forces

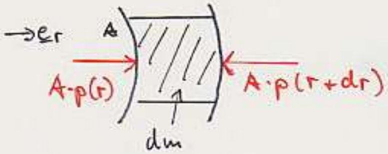

gaspressure causes forces on surfaces $\perp \underline{e}_r$. Forces on surfaces $\parallel \underline{e}_r$ compensate each other in spherical (or p-p) symmetry

$$df_p = A \cdot p(r) - A\, p(r+dr) = -A \frac{dp}{dr} dr$$

- df_{Rad} (radiation force) $= g_{rad}(r)\, dm$

$$\sum dk_i = -g(r)\, dm + g_{rad}(r)\, dm - A \frac{dp}{dr} dr = 0$$

$$dm = A \cdot \rho(r)\, dr$$

$$\Rightarrow \boxed{\frac{1}{\rho} \frac{dp}{dr} = -g(r) + g_{rad}(r)}$$ or

$$\frac{dp}{dr} = -\rho(r) \left[g(r) - g_{rad}(r) \right]$$

Hydrostatic equilibrium

Approximation $\left\| g(r) = \frac{G M_r}{r^2} \rightarrow \frac{G M_*}{r^2} \right\|$

since mass within atmosph: $M(r) - M(R_*) \ll M(R_*)$

example: The sun

$$\Delta M_{phot} = \bar{\rho} \frac{4\pi}{3} \left((R+\Delta r)^3 - R^3 \right) \approx \bar{\rho}\, 4\pi R^2 \Delta r$$

$R \approx 7 \cdot 10^{10}$ cm, $\Delta r \approx 3 \cdot 10^7$ cm (later), $\bar{\rho} \approx m_H \bar{N}$,
with $\bar{N} = 10^{15}\,\text{cm}^{-3}$ and $m_H \approx 1.7 \cdot 10^{-24}$ g

$\Rightarrow \Delta M_{phot} \approx 3 \cdot 10^{21}\,\text{g} \ll M_\odot \approx 2 \cdot 10^{33}\,\text{g}$

(same argument holds also if atmosphere is extended)

in plane-parallel geometry, we have additionally
$\Delta r \ll R_*$, thus $\left\| g(r) = g_* = \frac{G M_*}{R_*^2} \right\|$

examples	main seq. stars		log g [cgs] ≈ 4
	supergiants	(O → A)	3.5 … 0.8
	white dwarfs		8 !
	sun		4.44
	earth		3.0

- if stellar wind present, hydrodynamic description

  $\dot{M} = 4\pi r^2 \rho(r)\, v(r)$ equation of continuity

  $\rightarrow v(r) = \frac{\dot{M}}{4\pi} \frac{1}{r^2 \rho(r)} \neq 0$ (everywhere)

Question When are velocity fields important, i.e. induce significant deviations from hydrostatic equilibrium?

Hydrodynamic description

Hydrodynamic description: inclusion of velocity fields

Equation of continuity:

$$\frac{\partial \rho}{\partial t} + \nabla \cdot (\rho \mathbf{v}) = 0$$

Equation of momentum

("Euler equation")

$$\frac{\partial \rho \mathbf{v}}{\partial t} + \underbrace{\nabla \cdot (\rho \mathbf{v} \otimes \mathbf{v})}_{\mathbf{v}[\nabla \cdot (\rho \mathbf{v})]+[\rho \mathbf{v} \cdot \nabla]\mathbf{v}} = -\nabla p + \rho \mathbf{g}^{\text{ext}}$$

$$\underbrace{\Rightarrow}$$

stationarity, i.e., $\frac{\partial}{\partial t}=0$
and spherical symmetry,
i.e.,$\nabla \cdot \mathbf{u} \rightarrow \frac{1}{r^2}\frac{\partial}{\partial r}(r^2 u_r)$

$$r^2 \rho \mathrm{v} = \text{const} = \frac{\dot{M}}{4\pi} \quad \text{(I)}$$

with $\nabla \cdot (\rho \mathbf{v}) = 0$

$$\underbrace{\rho \mathrm{v} \frac{\partial \mathrm{v}}{\partial r}}_{\text{"advection term", (from inertia)}} = -\frac{\partial p}{\partial r} + \rho g_r^{\text{ext}} \quad \text{(II)}$$

I: Conservation of mass-flux

II: "Equation of motion"

with gravity and radiative acceleration

$$\Rightarrow \quad \rho(r)\mathrm{v}(r)\frac{\partial \mathrm{v}}{\partial r} = -\frac{\partial p}{\partial r} + \rho(r)\left(-\frac{GM_*}{r^2} + g_{\text{Rad}}(r)\right)$$

or, to be compared with hydrostatic equilibrium

$$\frac{\partial p}{\partial r} = \rho(r)\left(-\frac{GM_*}{r^2} + g_{\text{Rad}}(r)\right) - \rho(r)\mathrm{v}(r)\frac{\partial \mathrm{v}}{\partial r}$$

$$\left.\begin{array}{l}\text{hydrostatic equilibrium} \\ \text{in p-p symmetry:}\end{array}\right\} \frac{\partial p}{\partial z} = \rho(z)\left(-\frac{GM_*}{R_*^2} + g_{\text{Rad}}(z)\right)$$

Exercise:
Show, by using the cont. eq.,
that the Euler eq. can
be alternatively written as

$$\frac{\partial \mathbf{v}}{\partial t} + (\mathbf{v} \cdot \nabla)\mathbf{v} = -\frac{\nabla p}{\rho} + \mathbf{g}^{\text{ext}}$$

When is (quasi-)hydrostatic approach justified?

By using $p = \frac{k_B T}{\mu m_H}\rho = v_{\rm sound}^2 \rho$ (equation of state, with μ mean molecular weight, and $v_{\rm sound}$ the isothermal sound speed) ,

and $\dot{M} = 4\pi r^2 \rho v = \text{const}$ (for the hydrodynamic case)

the equations of motion and of hydrostatic equilibrium can be rewritten:

$$\left(v_{\rm sound}^2 - v^2(r)\right)\frac{\partial\rho}{\partial r} = -\rho(r)\left(g_{\rm grav}(r) - g_{\rm Rad}(r) + \frac{{\rm d}v_{\rm sound}^2}{{\rm d}r} - \frac{2v^2(r)}{r}\right) \quad \text{[hydrodynamic]}$$

$$v_{\rm sound}^2 \frac{\partial\rho}{\partial z} = -\rho(z)\left(g_{\rm grav}(R_*) - g_{\rm Rad}(z) + \frac{{\rm d}v_{\rm sound}^2}{{\rm d}z}\right) \quad \text{[hydrostatic, p-p]}$$

Conclusion:

- ☐ for v << $v_{\rm sound}$, hydrodynamic density stratification becomes (“quasi”-) hydrostatic
- ☐ this is reached in deeper photospheric layers, well below the sonic point, defined by $v(r_s)=v_{\rm sound}$
  example: $v_{\rm sound}$ (sun) $\approx$ 6 km/s, $v_{\rm sound}$ (O-star) $\approx$ 20 km/s

Thus: p-p atmospheres using hydrostatic equilibrium give reasonable results *even in the presence of winds* as long as investigated features (continua, lines) are formed below the sonic point.

Barometric formula

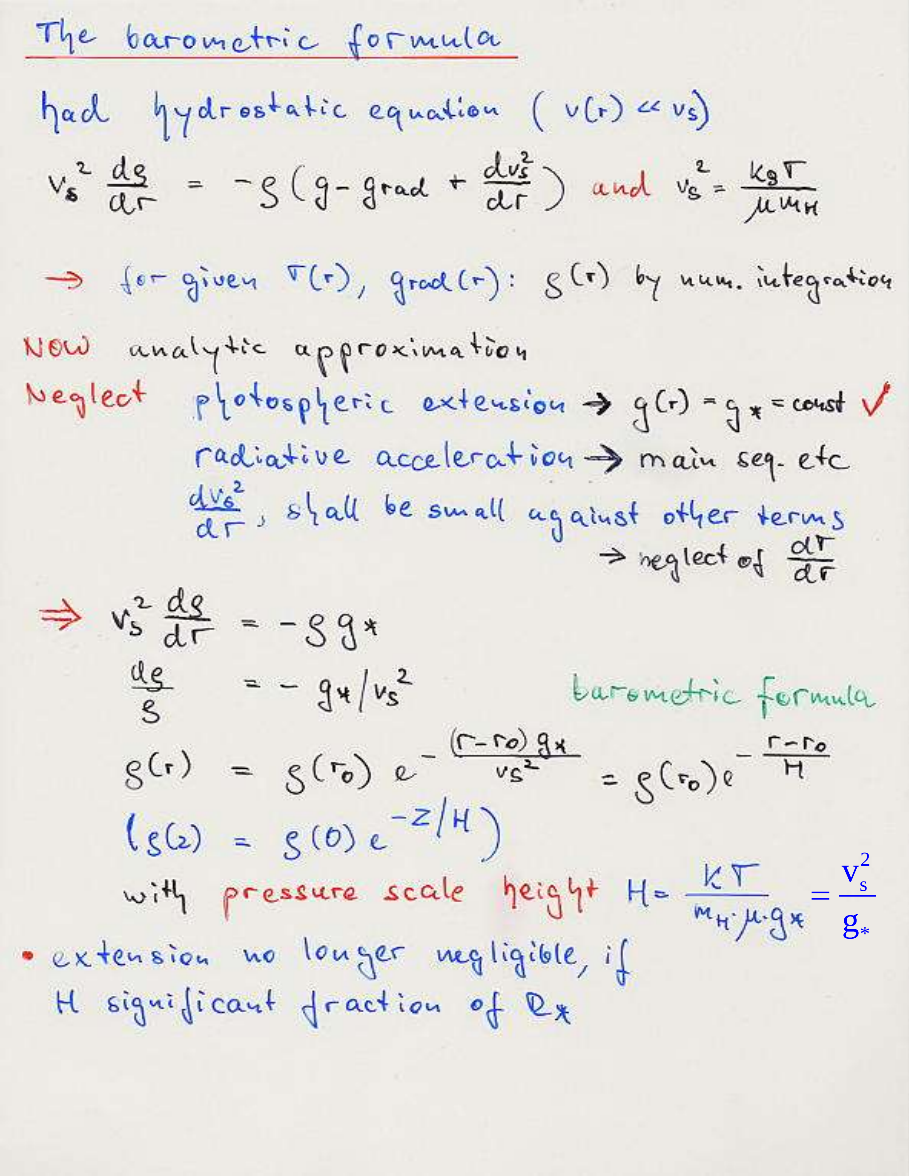

The barometric formula

had hydrostatic equation $(v(r) \ll v_s)$

$$v_s^2 \frac{d\rho}{dr} = -\rho\left(g - g_{rad} + \frac{dv_s^2}{dr}\right) \text{ and } v_s^2 = \frac{k_B T}{\mu m_H}$$

$\rightarrow$ for given $T(r)$, $g_{rad}(r)$: $\rho(r)$ by num. integration

NOW analytic approximation

Neglect photospheric extension $\rightarrow g(r) = g_* = \text{const}$ ✓

radiative acceleration $\rightarrow$ main seq. etc

$\frac{dv_s^2}{dr}$, shall be small against other terms

$\rightarrow$ neglect of $\frac{dT}{dr}$

$$\Rightarrow v_s^2 \frac{d\rho}{dr} = -\rho g_*$$

$$\frac{d\rho}{\rho} = -g_*/v_s^2$$

barometric formula

$$\rho(r) = \rho(r_0)\, e^{-\frac{(r-r_0)g_*}{v_s^2}} = \rho(r_0)\, e^{-\frac{r-r_0}{H}}$$

$$(\rho(z) = \rho(0)\, e^{-z/H})$$

with pressure scale height $H = \frac{kT}{m_H \cdot \mu \cdot g_*} = \frac{v_s^2}{g_*}$

- extension no longer negligible, if H significant fraction of R_*

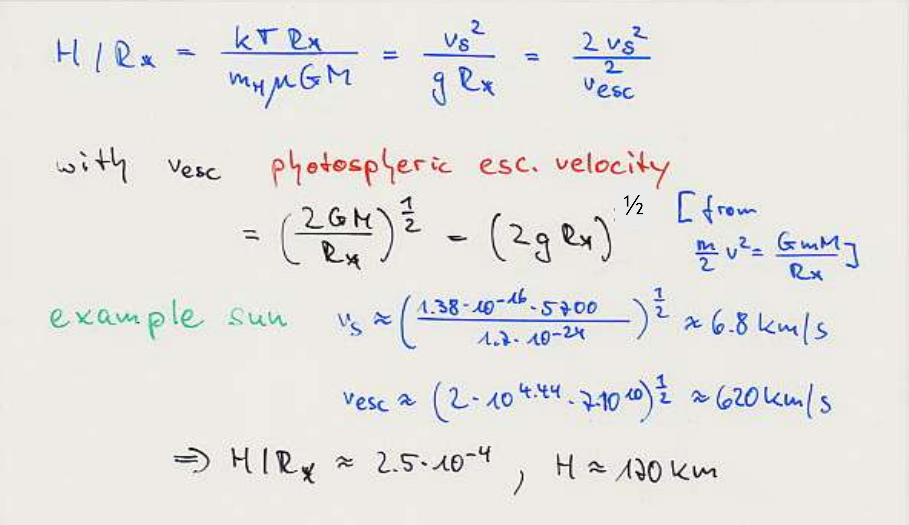

$$H/R_* = \frac{kTR_*}{m_H \mu G M} = \frac{v_s^2}{g R_*} = \frac{2 v_s^2}{v_{esc}^2}$$

with v_{esc} photospheric esc. velocity

$$= \left(\frac{2GM}{R_*}\right)^{\frac{1}{2}} = (2gR_*)^{1/2} \quad \left[\text{from } \frac{m}{2}v^2 = \frac{GmM}{R_*}\right]$$

example sun $v_s \approx \left(\frac{1.38 \cdot 10^{-16} \cdot 5700}{1.7 \cdot 10^{-24}}\right)^{\frac{1}{2}} \approx 6.8 \text{ km/s}$

$$v_{esc} \approx (2 \cdot 10^{4.44} \cdot 7 \cdot 10^{10})^{\frac{1}{2}} \approx 620 \text{ km/s}$$

$$\Rightarrow H/R_* \approx 2.5 \cdot 10^{-4}, \quad H \approx 170 \text{ km}$$

advanced reading

Total pressure

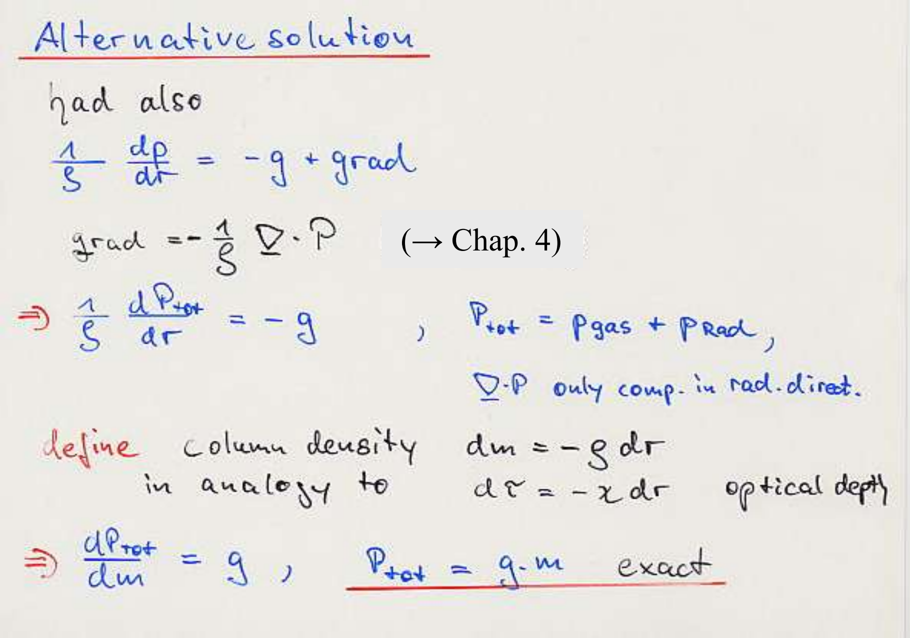

Alternative solution

had also

$$\frac{1}{\rho}\frac{dp}{dr} = -g + g_{rad}$$

$$g_{rad} = -\frac{1}{\rho}\nabla\cdot P$$ (→ Chap. 4)

⇒ $\frac{1}{\rho}\frac{dP_{tot}}{dr} = -g$, $P_{tot} = p_{gas} + p_{Rad}$,

$\nabla\cdot P$ only comp. in rad. direct.

define column density $dm = -\rho\, dr$

in analogy to $d\tau = -\chi\, dr$ optical depth

⇒ $\frac{dP_{tot}}{dm} = g$, $P_{tot} = g\cdot m$ exact

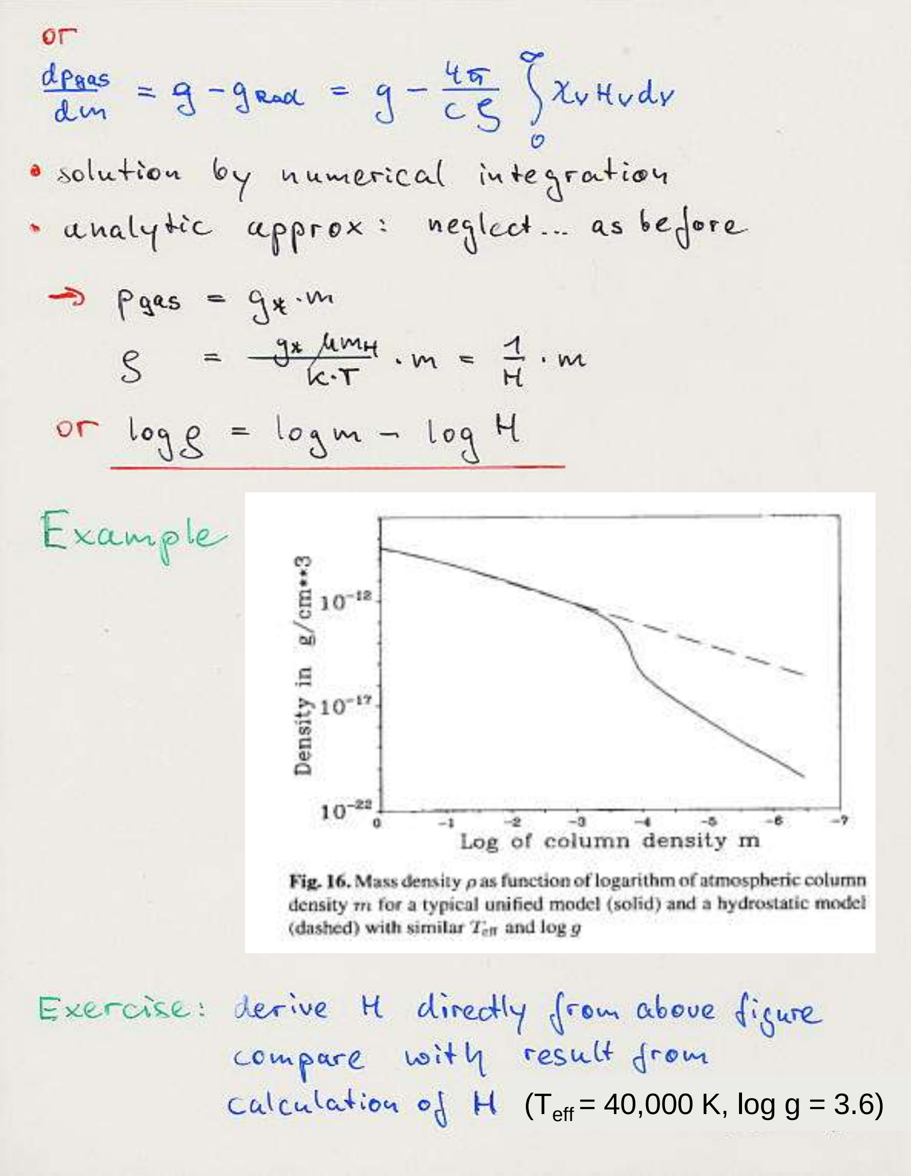

or

$$\frac{dp_{gas}}{dm} = g - g_{Rad} = g - \frac{4\pi}{c\rho}\int_0^\infty \chi_\nu H_\nu d\nu$$

- solution by numerical integration
- analytic approx: neglect... as before

→ $p_{gas} = g_*\cdot m$

$\rho = \frac{g_*\, \mu m_H}{k\cdot T}\cdot m = \frac{1}{H}\cdot m$

or $\log\rho = \log m - \log H$

Example

Fig. 16. Mass density ρ as function of logarithm of atmospheric column density m for a typical unified model (solid) and a hydrostatic model (dashed) with similar $T_{\rm eff}$ and $\log g$

Exercise: derive H directly from above figure
compare with result from
calculation of H ($T_{\rm eff}$ = 40,000 K, log g = 3.6)

Unified atmospheres – density/velocity stratification for stars with winds

photosphere + wind = unified atmosphere (Gabler et al. 1989)

Two possibilities:

a) stratification from theoretical wind models [Castor et al. 1975, Pauldrach et al. 1986, WM-Basic (Pauldrach et al. 2001), see ‘intermezzo’]
   Disadvantage: difficult to manipulate if theory not applicable or too simplified

b) combine quasi-hydrostatic photosphere and empirical wind structure [PHOENIX (Hauschildt 1992), CMFGEN (Hillier & Miller 1998), PoWR (Gräfener et al. 2002), FASTWIND (Puls et al. 2005), see ‘intermezzo’]
   Disadvantage: transition regime ill-defined

deep layers: at first $\rho(\mathrm{r})$ calculated (quasi-hydrostatic, with $\mathrm{g}_{\mathrm{grav}}(r)$ and $\mathrm{g}_{\mathrm{rad}}(\mathrm{r})$)

$$\rightarrow \mathrm{v}(r) = \frac{\dot{M}}{4\pi r^2 \rho(r)} \quad \text{for } \mathrm{v} \ll \mathrm{v}_{\mathrm{sound}} \text{ (roughly: } \mathrm{v} < 0.1\ \mathrm{v}_{\mathrm{sound}})$$

outer layers: at first $\mathrm{v(r)} = \mathrm{v}_\infty (1 - \frac{bR_*}{r})^\beta$, "beta-velocity-law", from observations/theory (b from transition velocity)

$$\rightarrow \rho(r) = \frac{\dot{M}}{4\pi r^2 \mathrm{v}(r)}$$

transition zone: smooth transition from deeper to outer stratification

Input/fit parameters: $\dot{M}$, v_∞, β, location of transition zone

advanced reading

Unified atmospheres – density/velocity stratification for stars with winds

abscissa: $\tau_{\rm Ross}$ Rosseland optical depth (frequency averaged opacity, see page 110)

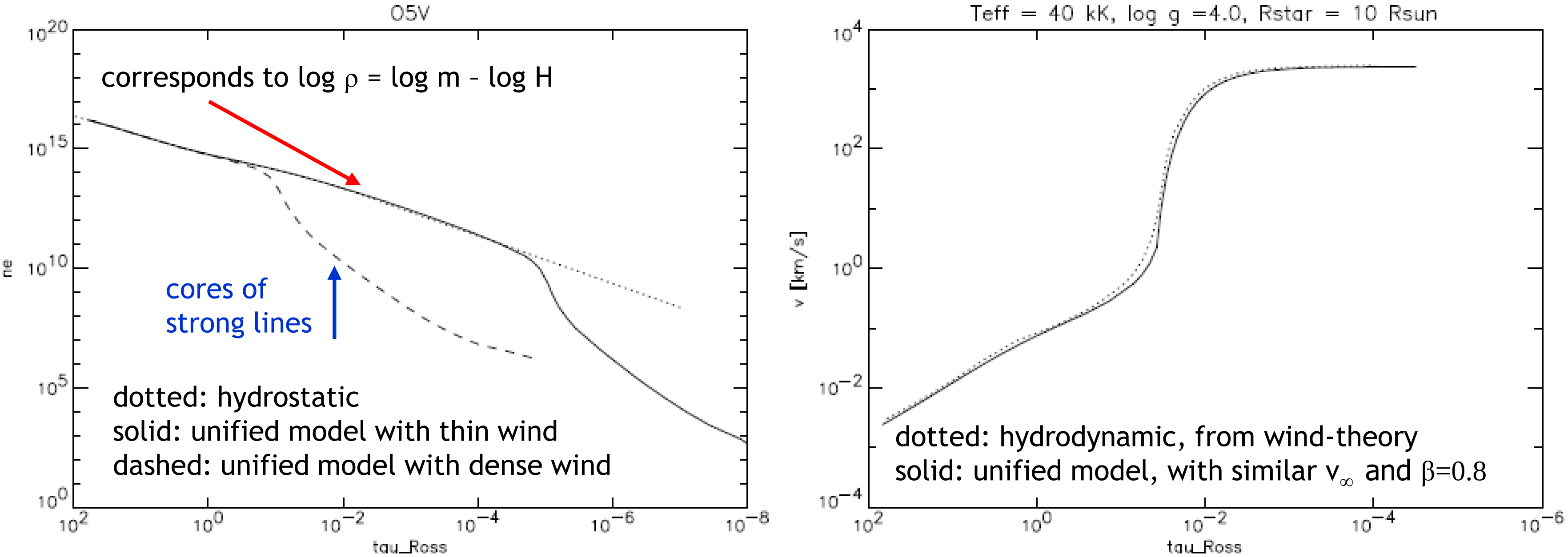

corresponds to log ρ = log m – log H

cores of strong lines

dotted: hydrostatic
solid: unified model with thin wind
dashed: unified model with dense wind

dotted: hydrodynamic, from wind-theory
solid: unified model, with similar v_∞ and β=0.8

Figure : (Left) Electron-density as a function of the Rosseland optical depth, $\tau_{\rm Ross}$, for different atmospheric models of an O5-dwarf. Dotted: hydrostatic model atmosphere; solid, dashed: unified model with a thin and a moderately dense wind, respectively. In case of the denser wind, the cores of optical lines ($\tau_{\rm Ross} \approx 10^{-1} - 10^{-2}$) are formed at significantly different densities than in the hydrostatic model, whereas the unified, thin-wind model and the hydrostatic one would lead to similar results.

Figure : (Right) Velocity fields in unified models of an O-star with a thin wind. Dotted: hydrodynamic solution; solid: analytical velocity law with similar terminal velocity and $\beta = 0.8$ (see text).

NOTE: at same τ or m, wind-density (for $v \geq v_{\rm sound}$) lower than if in hydrostatic equilibrium

Plane-parallel or unified model atmospheres?

- Unified models required if $\tau_{\mathrm{Ross}} \geq 10^{-2}$ at transition between photosphere and wind (roughly at $0.1{*}\mathrm{v}_{\mathrm{sound}}$)
- rule of thumb using a typical velocity law (β=1)

$$\dot{M}_{\max} = \dot{M}(\tau_{\mathrm{Ross}} = 10^{-2} \text{ at } 0.1 \text{ v}_{\mathrm{sound}}) \approx 6 \cdot 10^{-8} M_{\odot} yr^{-1} \cdot \frac{R_{*}}{10 R_{\odot}} \cdot \frac{\mathrm{v}_{\infty}}{1000 kms^{-1}}$$

- if $\dot{M}(\text{actual}) < \dot{M}_{\max}$ for considered object,

  then (most) diagnostic features formed in quasi-hydrostatic part of atmosphere

→ plane-parallel, hydrostatic models possible for **optical** spectroscopy of late O-dwarfs and B-stars up to luminosity classes II (early subtypes) or Ib (mid/late subtypes)

- **check required!**

Eddington limit

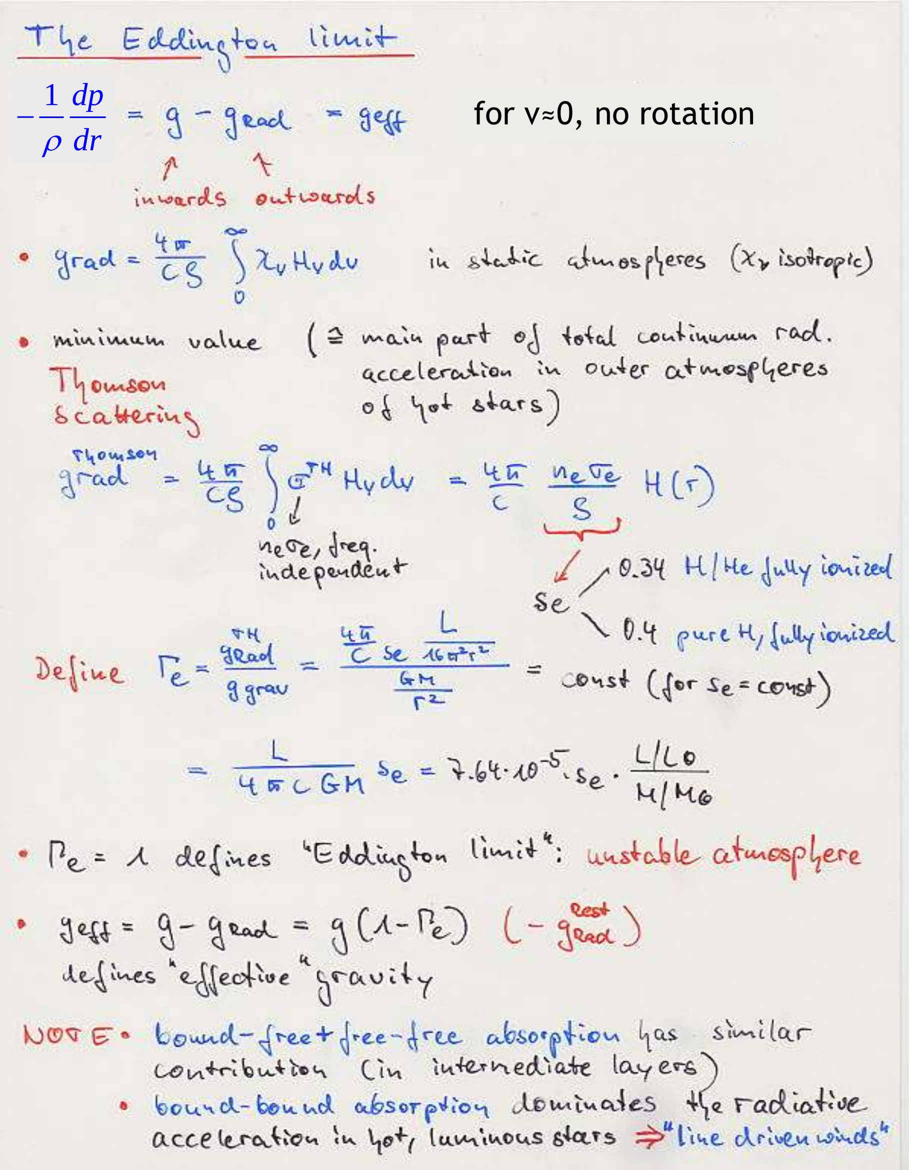

The Eddington limit

$$-\frac{1}{\rho}\frac{dp}{dr} = \underset{\text{inwards}}{\underset{\uparrow}{g}} - \underset{\text{outwards}}{\underset{\uparrow}{g_{rad}}} = g_{eff}$$

for v≈0, no rotation

- $g_{rad} = \frac{4\pi}{c\rho}\int_0^\infty \chi_\nu H_\nu d\nu$ in static atmospheres (χ_ν isotropic)
- minimum value (≙ main part of total continuum rad. acceleration in outer atmospheres of hot stars)

Thomson scattering

$$g_{rad}^{\text{Thomson}} = \frac{4\pi}{c\rho}\int_0^\infty \underset{\substack{\downarrow \\ n_e\sigma_e,\ \text{freq.} \\ \text{independent}}}{\sigma^{TH}} H_\nu d\nu = \frac{4\pi}{c}\underbrace{\frac{n_e\sigma_e}{\rho}}_{s_e} H(r)$$

s_e ↗ 0.34 H/He fully ionized, ↘ 0.4 pure H, fully ionized

Define $\Gamma_e = \frac{g_{rad}^{TH}}{g_{grav}} = \frac{\frac{4\pi}{c}s_e\frac{L}{16\pi^2r^2}}{\frac{GM}{r^2}}$ = const (for s_e = const)

$$= \frac{L}{4\pi c GM}s_e = 7.64\cdot10^{-5}\cdot s_e\cdot\frac{L/L_\odot}{M/M_\odot}$$

- $\Gamma_e = 1$ defines "Eddington limit": unstable atmosphere
- $g_{eff} = g - g_{rad} = g(1-\Gamma_e)\ (-g_{rad}^{rest})$ defines "effective" gravity

NOTE
- bound-free + free-free absorption has similar contribution (in intermediate layers)
- bound-bound absorption dominates the radiative acceleration in hot, luminous stars ⇒ "line driven winds"

Summary: stellar atmospheres – the solution principle

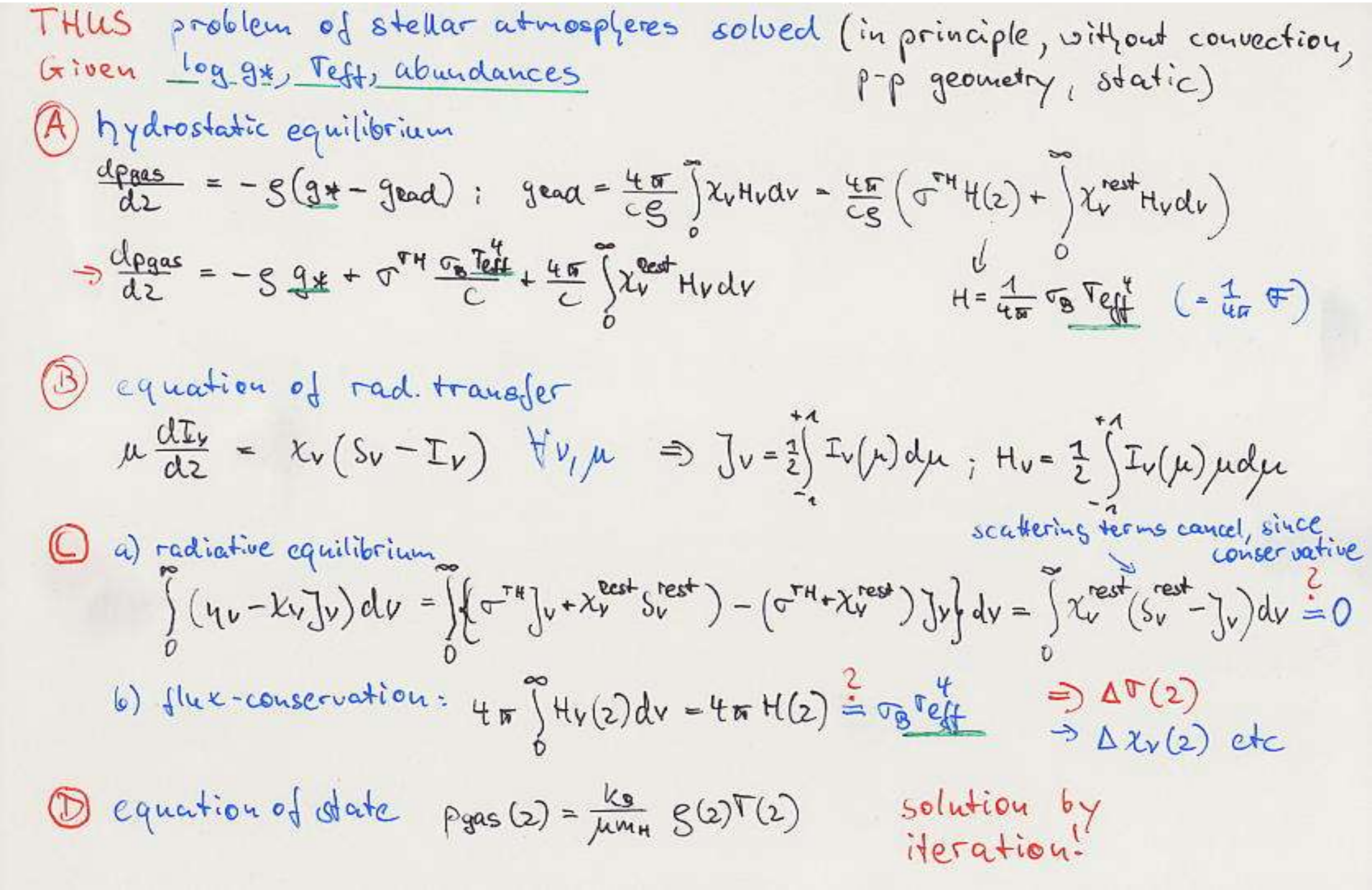

THUS problem of stellar atmospheres solved (in principle, without convection, p-p geometry, static)

Given _log g_*, $T_{\rm eff}$, abundances_

Ⓐ hydrostatic equilibrium

$$\frac{dp_{\rm gas}}{dz} = -\rho(\underline{g_*} - g_{\rm rad})\ ; \quad g_{\rm rad} = \frac{4\pi}{c\rho}\int_0^\infty \chi_\nu H_\nu d\nu = \frac{4\pi}{c\rho}\Big(\sigma^{\rm TH} H(z) + \int_0^\infty \chi_\nu^{\rm rest} H_\nu d\nu\Big)$$

$$\Rightarrow \frac{dp_{\rm gas}}{dz} = -\rho\, \underline{g_*} + \sigma^{\rm TH}\frac{\sigma_B T_{\rm eff}^4}{c} + \frac{4\pi}{c}\int_0^\infty \chi_\nu^{\rm rest} H_\nu d\nu$$

$$\downarrow \quad H = \frac{1}{4\pi}\sigma_B \underline{T_{\rm eff}^4} \quad \Big(= \frac{1}{4\pi}\mathcal{F}\Big)$$

Ⓑ equation of rad. transfer

$$\mu\frac{dI_\nu}{dz} = \chi_\nu(S_\nu - I_\nu) \quad \forall \nu, \mu \quad \Rightarrow J_\nu = \frac{1}{2}\int_{-1}^{+1} I_\nu(\mu) d\mu\ ; \quad H_\nu = \frac{1}{2}\int_{-1}^{+1} I_\nu(\mu)\mu d\mu$$

Ⓒ a) radiative equilibrium

scattering terms cancel, since conservative

$$\int_0^\infty (\eta_\nu - \chi_\nu J_\nu) d\nu = \int_0^\infty \{(\sigma^{\rm TH} J_\nu + \chi_\nu^{\rm rest} S_\nu^{\rm rest}) - (\sigma^{\rm TH} + \chi_\nu^{\rm rest}) J_\nu\} d\nu = \int_0^\infty \chi_\nu^{\rm rest}(S_\nu^{\rm rest} - J_\nu) d\nu \overset{?}{=} 0$$

b) flux-conservation:

$$4\pi\int_0^\infty H_\nu(z) d\nu = 4\pi H(z) \overset{?}{=} \underline{\sigma_B T_{\rm eff}^4}$$

$\Rightarrow \Delta T(z)$

$\rightarrow \Delta\chi_\nu(z)$ etc

Ⓓ equation of state

$$p_{\rm gas}(z) = \frac{k_B}{\mu m_H}\rho(z) T(z)$$

solution by iteration!

Solution of differential equations A and B by discretization
differential operators => finite differences
all quantities have to be evaluated on suitable grid

Eq. of radiative transfer (B)
usually solved by the so-called
Feautrier and/or Rybicki scheme

advanced reading

Ray-by-ray solution – p-z geometry for spherically symmetric problems

NOTE: the following method (based on Hummer & Rybicki 1971) works ONLY for spherically symmetric problems and no Doppler-shifts!

a) define p-rays (impact-parameter) tangential to each discrete radial shell

b) augment those by a bunch of (equidistant) p-rays resolving the core

c) use only the forward hemisphere, i.e.,

$$z_{di} = \sqrt{r_d^2 - p_i^2} \quad \text{and } z_{di} > 0$$

$\Rightarrow$ all points $z_{di}, i = 1, \mathrm{NP}$, are located on the same r_d-shell, i.e., have the same physical parameters such as emissivities, opacities, velocities, ... (due to spherical symmetry, and neglect of Doppler-shifts)

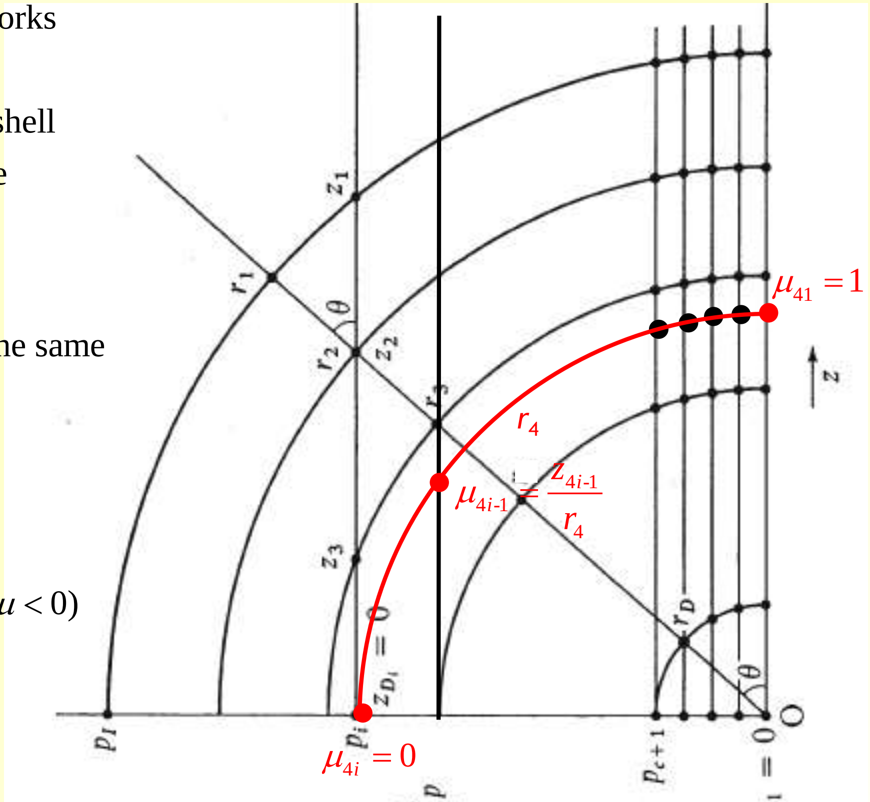

Now one solves the RTE along each p-ray: from first principles,

$$\pm \frac{\mathrm{d}I_\nu^\pm(z, p_i)}{\mathrm{dz}} = \eta_\nu(r) - \chi_\nu(r) I_\nu^\pm(z, p_i) \quad \text{(with '+' for } \mu > 0 \text{ and '} - \text{' for } \mu < 0)$$

using appropriate boundary conditions (core vs. non-core rays), and standard methods (finite differences etc.)

After being calculated, $I_\nu^\pm(z_{di}(r_d), p_i), \ i = 1, \mathrm{NP}$, samples the specific intensity at the same radius, r_d, but at different angles,

$\pm\mu_{\mathrm{di}} = \frac{z_{di}}{r_d}$, starting at $|\mu_{\mathrm{di}}| = 1$ for $i = 1$ and $d = 1, \mathrm{NZ}$ (central ray, p_i=0) to $\mu_{\mathrm{di}} = 0$ (tangent ray, where $p_i = r_d$ and thus $z_{di} = 0$).

In other words, along individual r_d-shells, the specific intensities $I_\nu^\pm(r_d, \mu) = I_\nu^\pm(z_d, \mu)$ are sampled for all relevant μ, and corresponding moments can be calculated by integration.

Feautrier-variables

In fact, the RTE is not solved for $I_\nu^\pm$ seperately, but for a linear combination of I_ν^+ and I_ν^-, using the so-called Feautrier-variables u_ν and v_ν, which allows to construct a 2nd order scheme as in the plane-parallel case: higher accuracy, diffusion limit can be easily represented

$$u_\nu(z,p) = \frac{1}{2}(I_\nu^+(z,p) + I_\nu^-(z,p)) \qquad \text{mean intensity like}$$

$$\mathrm{v}_\nu(z,p) = \frac{1}{2}(I_\nu^+(z,p) - I_\nu^-(z,p)) \qquad \text{flux like}$$

$$\Rightarrow \frac{\partial \mathrm{v}_\nu}{\partial z} = \chi_\nu(S_\nu - u_\nu), \quad \frac{\partial u_\nu}{dz} = -\chi_\nu \mathrm{v}_\nu$$

$$\Rightarrow \frac{\partial^2 u_\nu}{\partial \tau_\nu^2} = u_\nu - S_\nu \quad (\text{2nd order, with } d\tau_\nu = -\chi_\nu dz)$$

... and corresponding boundary conditions

inner boundary: for core rays, first order, using the diffusion approximation; for non-core rays, 2nd order, using symmetry arguments

outer boundary: either $I_\nu^-(z_{\max}, p) = 0$, or higher order for optically thick conditions (e.g., shortward of HeII Lyman edge)

Formal solution for $I_\nu(\mu)$ (or $u_\nu(\mu)$ and $\mathrm{v}_\nu(\mu)$) and corresponding angle-averaged quantities (moments) affected by inaccuracies, due to specific way of discretization, but ratios of moments much more precise (errors cancel to a large part)

Continuum transfer in extended atmospheres

Thus: variable Eddington-factor method

solve the moments equations (only radius-dependent), and use Eddington-factors from formal solution to close the relations. Ensures high accuracy (since direct solution for angle-averaged quantities, and 2nd order scheme), whilst Eddington-factors (from the formal solution) quickly stablilize in the course of global iterations.

Using the 0th and 1st moment of the RTE and $f_\nu = K_\nu / J_\nu$, we obtain

$$\frac{\partial(r^2 H_\nu)}{\partial \tau_\nu} = r^2 (J_\nu - S_\nu)$$

$$\frac{\partial(f_\nu J_\nu)}{\partial \tau_\nu} - \frac{(3 f_\nu - 1) J_\nu}{\chi_\nu r} = H_\nu$$

Introducing a "sphericality factor" q_ν via $\ln(r^2 q_\nu) = \int\limits_{r_\mathrm{core}}^{r} \left[(3 f_\nu - 1)/(r' f_\nu)\right] \mathrm{d}r' + \ln(r^2_\mathrm{core})$, the 2nd equation becomes

$\dfrac{\partial(f_\nu q_\nu r^2 J_\nu)}{\partial \tau_\nu} = q_\nu r^2 H_\nu$, and can be combined with the first one to yield a 2nd order scheme for $r^2 J_\nu$

$\dfrac{\partial^2(f_\nu q_\nu r^2 J_\nu)}{\partial X_\nu^2} = \dfrac{1}{q_\nu} r^2 (J_\nu - S_\nu)$ with $\mathrm{d}X_\nu = q_\nu \mathrm{d}\tau_\nu$ [for comp.: in p-p, $\dfrac{\partial^2(f_\nu J_\nu)}{\partial \tau_\nu^2} = (J_\nu - S_\nu)$, limit for $q_\nu \rightarrow 1$ and $r^2 \rightarrow R_*^2$]

Grey temperature stratification

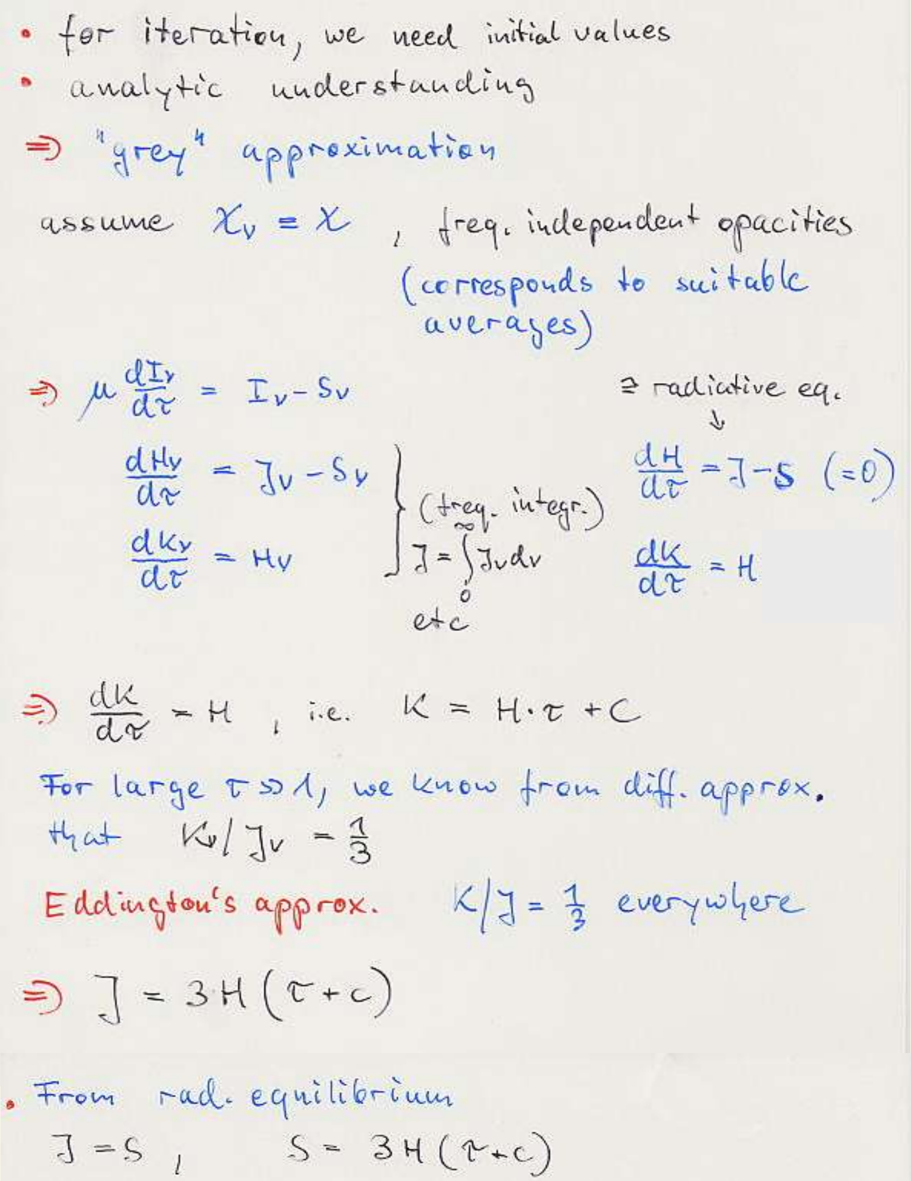

- for iteration, we need initial values
- analytic understanding

⇒ "grey" approximation

assume $\chi_\nu = \chi$, freq. independent opacities (corresponds to suitable averages)

⇒ $\mu \frac{dI_\nu}{d\tau} = I_\nu - S_\nu$

$$\left.\begin{aligned} \frac{dH_\nu}{d\tau} &= J_\nu - S_\nu \\ \frac{dK_\nu}{d\tau} &= H_\nu \end{aligned}\right\} \text{(freq. integr.)}$$

$J = \int_0^\infty J_\nu d\nu$ etc

⇒ radiative eq. ↓

$\frac{dH}{d\tau} = J - S \quad (=0)$

$\frac{dK}{d\tau} = H$

⇒ $\frac{dK}{d\tau} = H$, i.e. $K = H \cdot \tau + C$

For large $\tau \gg 1$, we know from diff. approx. that $K_\nu / J_\nu = \frac{1}{3}$

Eddington's approx. $K/J = \frac{1}{3}$ everywhere

⇒ $J = 3H(\tau + c)$

- From rad. equilibrium

$J = S$, $\quad S = 3H(\tau + c)$

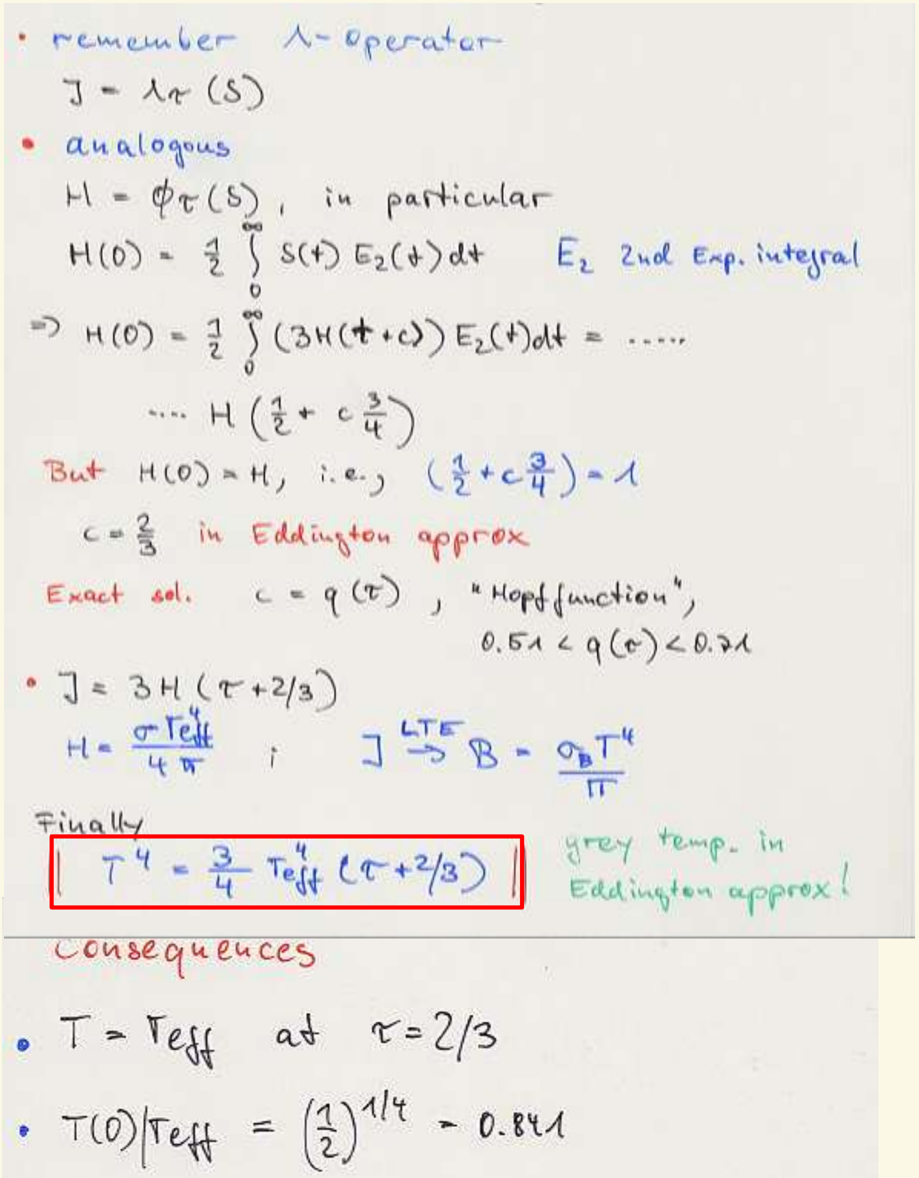

- remember Λ-operator

$J = \Lambda_\tau(S)$

- analogous

$H = \phi_\tau(S)$, in particular

$H(0) = \frac{1}{2}\int_0^\infty S(t)\,E_2(t)\,dt \qquad E_2$ 2nd Exp. integral

⇒ $H(0) = \frac{1}{2}\int_0^\infty (3H(t+c))\,E_2(t)\,dt = \ldots\ldots$

$\ldots\ldots H\left(\frac{1}{2} + c\frac{3}{4}\right)$

But $H(0) = H$, i.e., $\left(\frac{1}{2} + c\frac{3}{4}\right) = 1$

$c = \frac{2}{3}$ in Eddington approx

Exact sol. $c = q(\tau)$, "Hopf function",

$0.51 < q(\tau) < 0.71$

- $J = 3H(\tau + 2/3)$

$H = \frac{\sigma T_{\rm eff}^4}{4\pi}$; $\quad J \overset{\rm LTE}{\rightarrow} B = \frac{\sigma_B T^4}{\pi}$

Finally

$$\boxed{T^4 = \frac{3}{4} T_{\rm eff}^4 (\tau + 2/3)}$$

grey temp. in Eddington approx!

Consequences

- $T = T_{\rm eff}$ at $\tau = 2/3$
- $T(0)/T_{\rm eff} = \left(\frac{1}{2}\right)^{1/4} = 0.841$

advanced reading

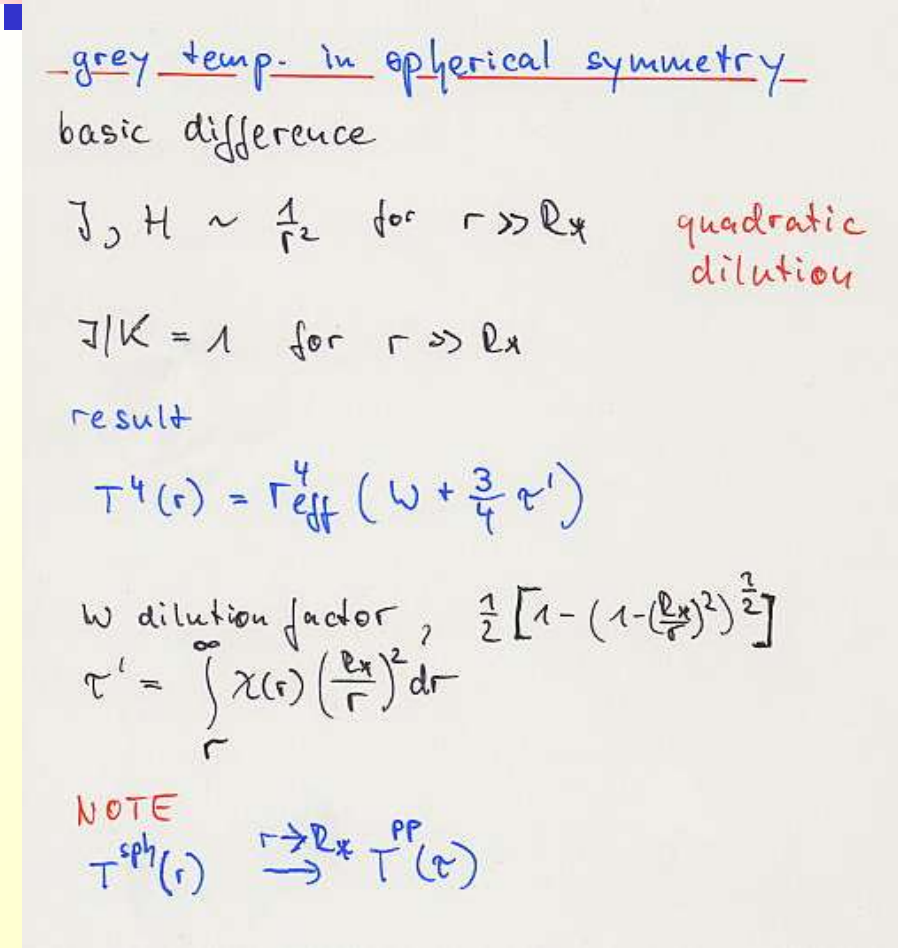

grey temp. in spherical symmetry

basic difference

$J, H \sim \frac{1}{r^2}$ for $r \gg R_*$ quadratic dilution

$J/K = 1$ for $r \gg R_*$

result

$$T^4(r) = T_{\text{eff}}^4\left(W + \frac{3}{4}\tau'\right)$$

W dilution factor , $\frac{1}{2}\left[1-\left(1-\left(\frac{R_*}{r}\right)^2\right)^{\frac{1}{2}}\right]$

$$\tau' = \int_r^\infty \chi(r)\left(\frac{R_*}{r}\right)^2 dr$$

NOTE

$$T^{\text{sph}}(r) \xrightarrow{r \to R_*} T^{\text{PP}}(\tau)$$

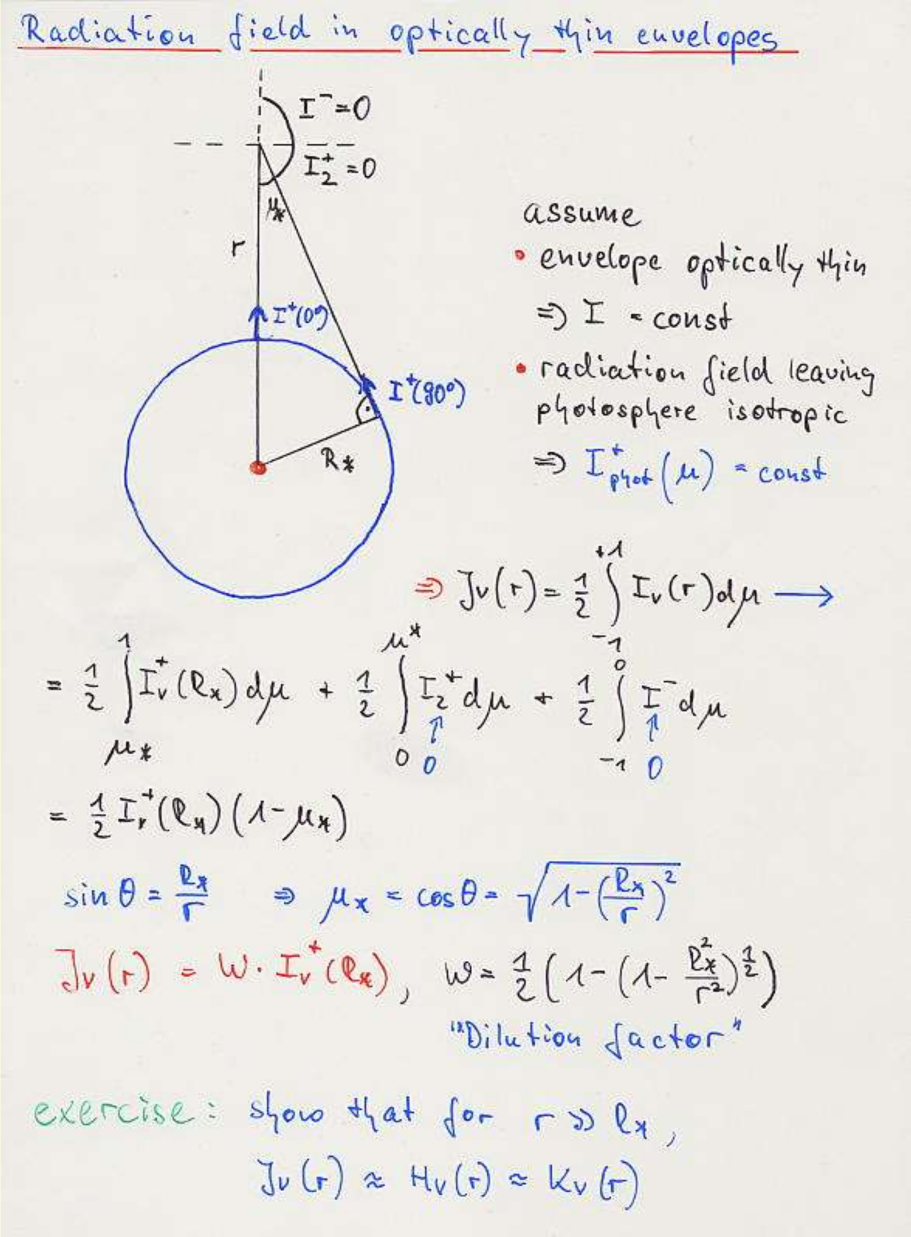

Radiation field in optically thin envelopes

assume

- envelope optically thin

  $\Rightarrow I = \text{const}$
- radiation field leaving photosphere isotropic

  $\Rightarrow I^+_{\text{phot}}(\mu) = \text{const}$

$$\Rightarrow J_\nu(r) = \frac{1}{2}\int_{-1}^{+1} I_\nu(r)\,d\mu \longrightarrow$$

$$= \frac{1}{2}\int_{\mu_*}^{1} I_\nu^+(R_*)\,d\mu + \frac{1}{2}\int_0^{\mu^*} \underset{\overset{\uparrow}{0}}{I_2^+}\,d\mu + \frac{1}{2}\int_{-1}^{0} \underset{\overset{\uparrow}{0}}{I^-}\,d\mu$$

$$= \frac{1}{2} I_\nu^+(R_*)(1-\mu_*)$$

$$\sin\theta = \frac{R_*}{r} \quad \Rightarrow \mu_* = \cos\theta = \sqrt{1-\left(\frac{R_*}{r}\right)^2}$$

$$J_\nu(r) = W \cdot I_\nu^+(R_*), \quad W = \frac{1}{2}\left(1-\left(1-\frac{R_*^2}{r^2}\right)^{\frac{1}{2}}\right)$$

"Dilution factor"

exercise: show that for $r \gg R_*$,

$$J_\nu(r) \approx H_\nu(r) \approx K_\nu(r)$$

Rosseland opacities

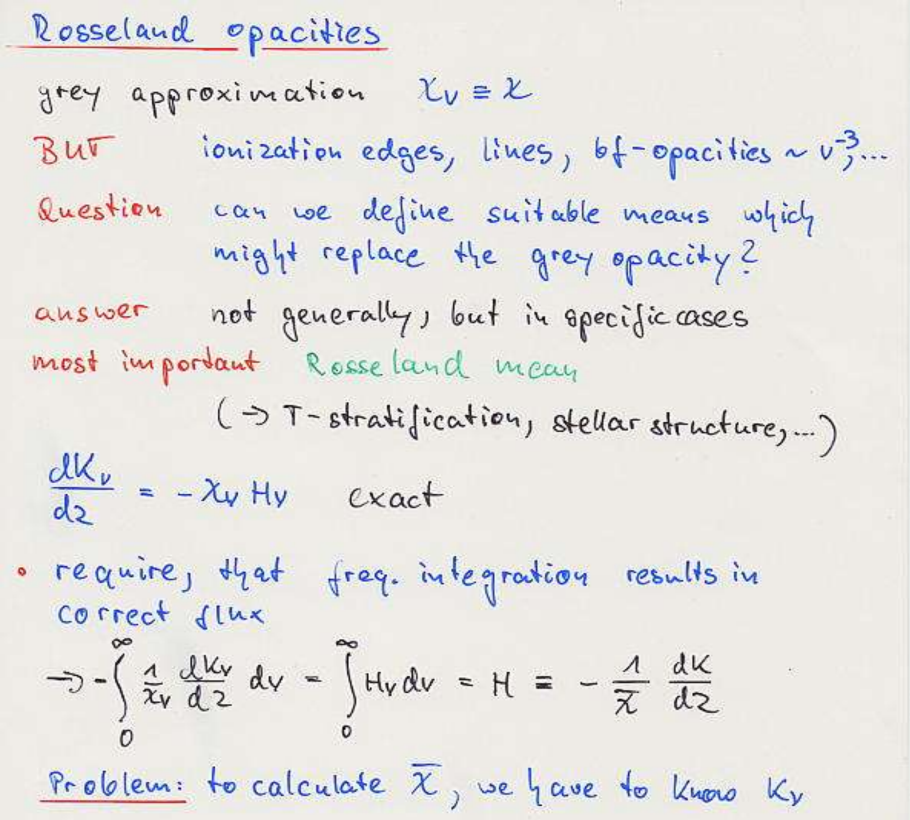

Rosseland opacities

grey approximation $\chi_\nu \equiv \chi$

BUT ionization edges, lines, bf-opacities $\sim \nu^{-3}$, ...

Question can we define suitable means which might replace the grey opacity?

answer not generally, but in specific cases

most important Rosseland mean

(→ T-stratification, stellar structure, ...)

$$\frac{dK_\nu}{dz} = -\chi_\nu H_\nu \quad \text{exact}$$

- require, that freq. integration results in correct flux

$$\to -\int_0^\infty \frac{1}{\chi_\nu}\frac{dK_\nu}{dz}\,d\nu = \int_0^\infty H_\nu\,d\nu = H \equiv -\frac{1}{\bar{\chi}}\frac{dK}{dz}$$

Problem: to calculate $\bar{\chi}$, we have to know K_ν

- thus, use additionally diffusion approximation

$$K_\nu = \frac{1}{3}B_\nu \quad \text{and} \quad H_\nu = \frac{1}{3}\frac{dB_\nu}{d\tau_\nu}$$

$$\Rightarrow \frac{1}{\bar{\chi}_\mathrm{R}} = -\frac{H}{dK/dz} \to \frac{\int_0^\infty \frac{1}{3}\frac{1}{\chi_\nu}\frac{\partial B_\nu}{\partial T}\frac{dT}{dz}\,d\nu}{\int_0^\infty \frac{1}{3}\frac{\partial B_\nu}{\partial T}\frac{dT}{dz}\,d\nu} = \frac{\int_0^\infty \frac{1}{\chi_\nu}\frac{\partial B_\nu}{\partial T}\,d\nu}{\int_0^\infty \frac{\partial B_\nu}{\partial T}\,d\nu} = \frac{\int_0^\infty \frac{1}{\chi_\nu}\frac{\partial B_\nu}{\partial T}\,d\nu}{\frac{4\sigma_\mathrm{B}}{\pi}T^3}$$

$$\left[\text{since} \int B_\nu\,d\nu = \frac{\sigma_\mathrm{B}}{\pi}T^4 \to \frac{\partial}{\partial T} = \frac{4\sigma_\mathrm{B}}{\pi}T^3\right]$$

⇒ Rosseland opacity

$$\boxed{\bar{\chi}_\mathrm{R} = \frac{\frac{4\sigma_\mathrm{B}}{\pi}T^3}{\int_0^\infty \frac{1}{\chi_\nu}\frac{\partial B_\nu}{\partial T}\,d\nu}}$$

- can be calculated without radiative transfer
- harmonic weighting: maximum flux transport where χ_ν is small!

- alternatively, from construction (for $\tau_\nu \gg 1$)

$$\frac{1}{\bar{\chi}_\mathrm{R}} = -\frac{H}{dK/dz} \rightarrow -\frac{H}{\int_0^\infty \frac{1}{3}\frac{\partial B_\nu}{\partial z} d\nu} = -\frac{H}{\frac{1}{3}\frac{dT}{dz}\int_0^\infty \frac{\partial B_\nu}{\partial T} d\nu} = -\frac{H}{\frac{1}{3}\frac{4\sigma_\mathrm{B}}{\pi}T^3\frac{dT}{dz}}$$

$\Rightarrow$

i) $F = 4\pi H = \frac{16\sigma_\mathrm{B}}{3} T^3 \frac{dT}{d\tau_\mathrm{R}}$

ii) in spherical geometry

$$\frac{L(r)}{4\pi r^2} = -\frac{16\sigma_\mathrm{B}}{3\bar{\chi}_\mathrm{R}} T^3 \frac{dT}{dr}$$ (used for stellar structure)

iii) integrate i), + $\mathscr{F} = \sigma_\mathrm{B} T_\mathrm{eff}^4$

$\rightarrow T^4 = T_\mathrm{eff}^4 \frac{3}{4}(\tau_\mathrm{Ross} + const),$ as in grey case, but now with τ_Ross

THUS possibility to obtain initial (or approx.) values for temperature stratification ($\approx$ exact for large optical depths)

$$\left.\begin{array}{l} \text{calculate (LTE) opacities } \chi_\nu \\ \text{calculate } \bar{\chi}_\mathrm{R},\ \tau_\mathrm{R} \\ \text{calculate } T(\tau_\mathrm{R}) \end{array}\right\} \text{again, iteration required}$$

Now we define the stellar radius via

$$\boxed{R_* = R(\tau_\mathrm{Ross} = 2/3)}$$

as the average layer ("'stellar surface") where the observed UV/optical radiation is created.

Furthermore, if we approximate $const = 2/3$ as in the (approx.) grey case, i.e.,

$$\boxed{T^4(\tau_\mathrm{Ross}) \approx T_\mathrm{eff}^4 \frac{3}{4}(\tau_\mathrm{Ross} + 2/3)}$$

then we obtain $T(\tau_\mathrm{Ross} = 2/3) = T(R_*) = T_\mathrm{eff}$ and the definition $L = 4\pi R_*^2 \sigma_\mathrm{B} T_\mathrm{eff}^4$ has also a physical meaning (at least for LTE conditions): "the effective temperature is the atmospheric temperature of a star at its surface".

Note: in reality, $T(\tau_\mathrm{Ross} = 2/3)$ deviates (slightly) from T_eff, since $const \neq 2/3$, and because of deviations from LTE

... back to Milne Eddington Model (page 92)

had $B_\nu(\tau_\nu) = a_\nu + b_\nu \tau_\nu$ linear approx

and $J_\nu(0) = \frac{b_\nu}{\sqrt{3}}$ for $\varepsilon_\nu = 0$ pure scattering

$= a_\nu + \frac{b_\nu/\sqrt{3} - a_\nu}{2}$ for $\varepsilon_\nu = 1$ purely thermal

$$\varepsilon_\nu = \frac{\kappa_\nu^+}{\kappa_\nu^+ + \sigma_e n_e}$$

- since temperature stratification known by now, can perform some estimates concerning continuum fluxes

$$\left.\begin{aligned} &\text{had } T^4 \approx T_{\rm eff}^4 \tfrac{3}{4}\left(\tau_R + 2/3\right) \\ &T(0)^4 = T_{\rm eff}^4 \tfrac{3}{4} \cdot 2/3 \end{aligned}\right\} T^4 = T^4(0)\left(1 + \tfrac{3}{2}\tau_R\right)$$

$$B_\nu(\tau_R) \approx B_\nu(T_0) + \left(\frac{\partial B_\nu}{\partial \tau_R}\right)_0 \tau_R = B_0 + B_1 \tau_R$$

$$\Rightarrow B_1 = \frac{\partial B_\nu}{\partial T}\Big|_{T_0} \cdot \frac{\partial T}{\partial \tau_R}\Big|_{T_0} = B_\nu \frac{h\nu/kT \cdot \frac{1}{T} e^{h\nu/kT}}{(e^{h\nu/kT} - 1}\Big|_{T_0} \frac{\partial T}{\partial \tau_R}\Big|_{T_0}$$

$$= B_\nu \frac{u_0}{1 - e^{-u_0}} \frac{1}{T_0} \frac{\partial T}{\partial \tau_R}\Big|_0 \quad \text{with } u_0 = \frac{h\nu}{kT_0}$$

$$4T^3 \frac{\partial T}{\partial \tau_R} = T^4(0)\frac{3}{2}, \quad \frac{\partial T}{\partial \tau_R}\Big|_{T_0} = \frac{3}{8} T_0$$

Thus $B_1 = B_0 \frac{u_0}{1 - e^{-u_0}} \frac{3}{8}$ → (Rayleigh-Jeans) $B_1 = \frac{3}{8} B_0$
→ (Wien) $B_1 = \frac{3}{8} u_0 B_0$

example $T_{\rm eff} = 40{,}000$ K, $\lambda = 500, 912$ Å
[Hydrogen $\overset{\text{Balmer}}{\text{Lyman}}$ continuum, $\varepsilon_\nu \ll 1$)

$T_0 = 33{,}600$ K

$u_0 = \substack{8.56 \\ 4.70} \rightarrow B_1 \approx \substack{3.21 \\ 1.76} B_0$

→ if $(\kappa_\nu^+ + \sigma_\nu) \approx \bar{\chi}_R$ $\quad J_\nu(0, \varepsilon_\nu = 1) \approx \substack{1.42 \\ 1.0} B_0$

$H_\nu(0) = \frac{1}{\sqrt{3}} J_\nu(0)$ $\quad J_\nu(0, \varepsilon_\nu \to 0) \approx \substack{1.85 \\ 1.01} B_0$

can look down deeper into atm.

- additional effect 1

T-stratification with respect to $\tau_R(\bar{\chi}_R)$, but radiation transfer with respect to freq. τ_ν

$$J_\nu = B_\nu + \ldots = a_\nu + b_\nu \tau_\nu + \ldots$$

$$B_\nu = B_{\nu 0} + B_1 \tau_R = B_{\nu 0} + B_1 \tau_\nu \frac{\tau_R}{\tau_\nu} \approx B_{\nu 0} + \underbrace{B_1 \frac{\bar{\chi}_R}{\chi_\nu}}_{b_\nu} \cdot \tau_\nu$$

effective gradient increased, if κ_ν small compared to $\bar{\chi}_R$

- additional effect 2

far away from ionization edges (where ε_ν is small, anyway), also χ_ν small ($\kappa_\nu^+ \sim \left(\frac{\nu_0}{\nu}\right)^3$, cf Chapter 5) → additional enhancement

advanced reading

H/He continuum of a hot star around 1000 Å

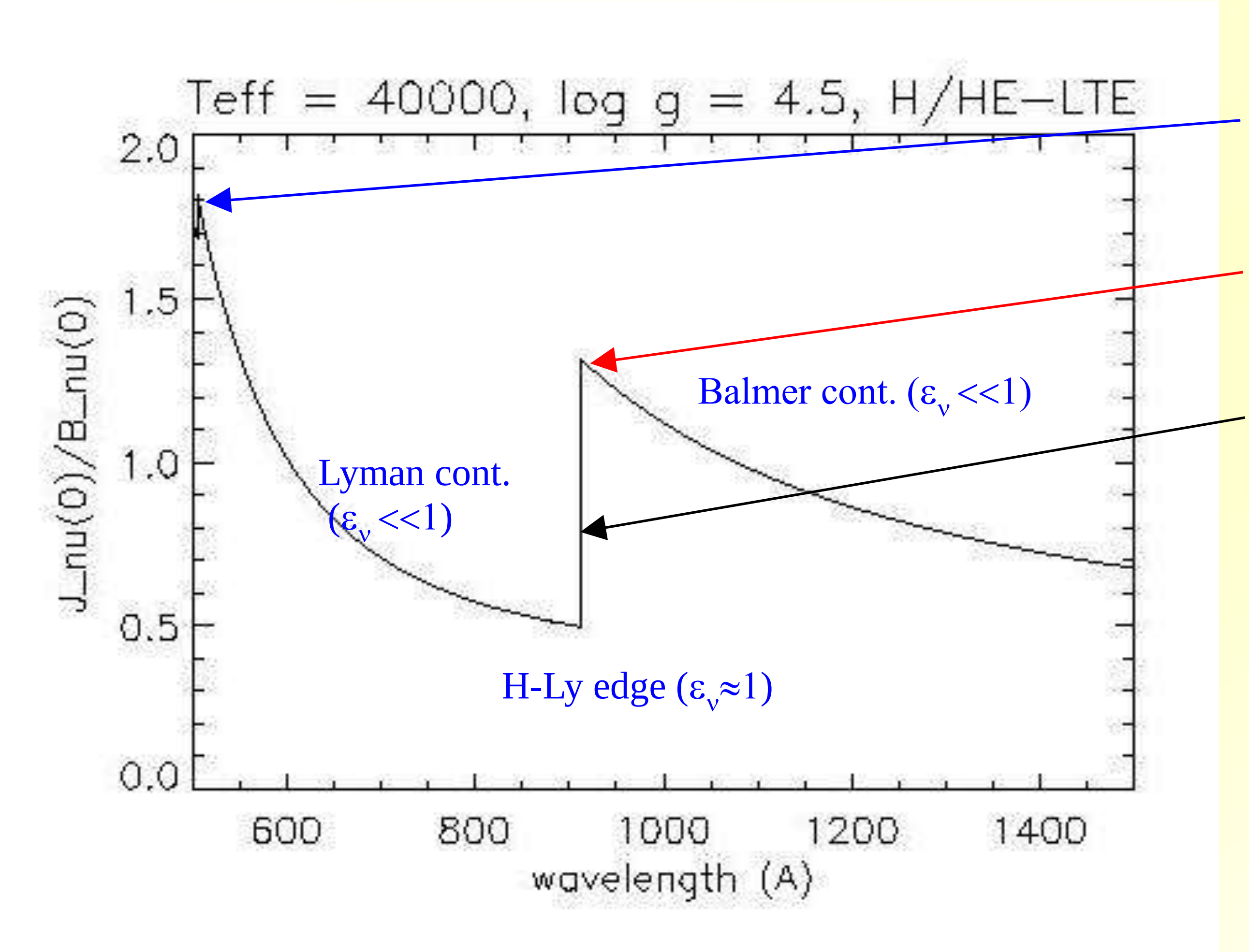

Predictions

Lyman cont: $J_\nu / B_\nu \geq 1.85$, OK
(at 500 Å) $(\chi_\nu \approx \chi_R)$

Balmer cont: $J_\nu / B_\nu \geq 1.01$, OK
(at 912 Å) $(\chi_\nu < \chi_R)$

Lyman edge: $J_\nu / B_\nu \leq 1.0$, OK
(911 Å) $(\chi_\nu > \chi_R)$

note: large opacity leads to very small effective T-gradient, minimum value $J_\nu / B_\nu = 0.5$, (cf. page 93)

Convection (simplified)

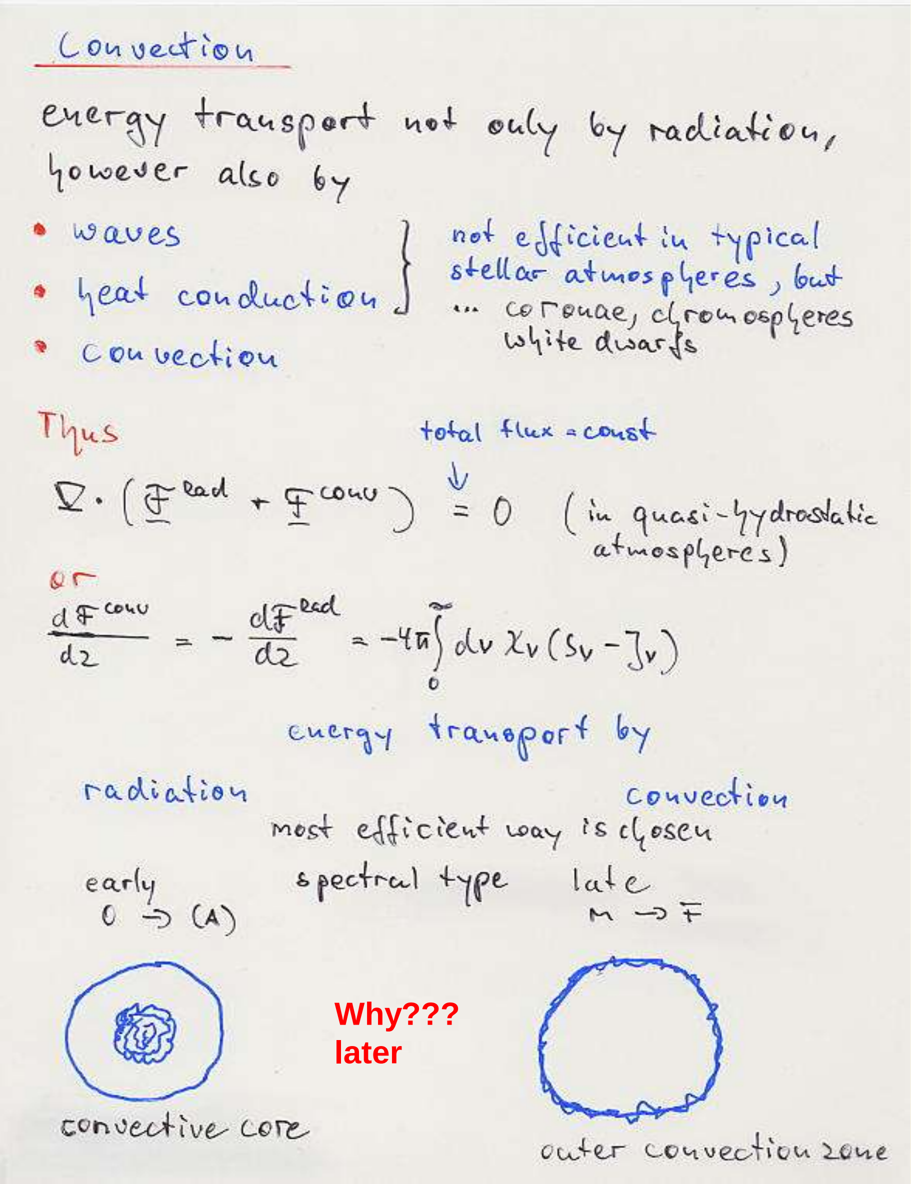

Convection

energy transport not only by radiation, however also by

- waves
- heat conduction
- convection

} not efficient in typical stellar atmospheres, but ... coronae, chromospheres white dwarfs

Thus

total flux = const

$$\nabla \cdot \left(\underline{F}^{rad} + \underline{F}^{conv} \right) \overset{\downarrow}{=} 0$$

(in quasi-hydrostatic atmospheres)

or

$$\frac{dF^{conv}}{dz} = - \frac{dF^{rad}}{dz} = -4\pi \int_0^\infty d\nu\, \chi_\nu (S_\nu - J_\nu)$$

energy transport by

radiation   convection

most efficient way is chosen

early   spectral type   late

O → (A)   M → F

convective core

outer convection zone

Why???
later

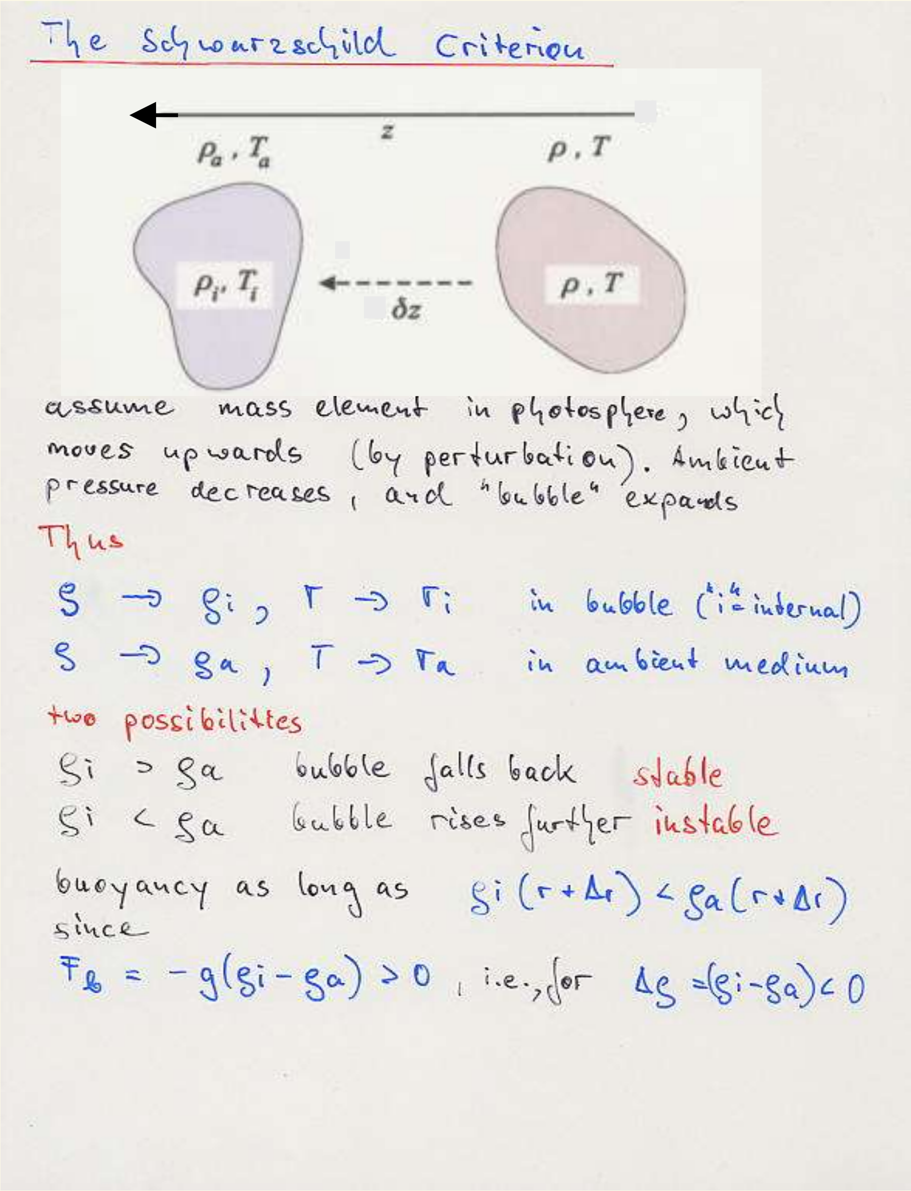

The Schwarzschild Criterion

assume mass element in photosphere, which moves upwards (by perturbation). Ambient pressure decreases, and "bubble" expands

Thus

$\rho \rightarrow \rho_i$, $T \rightarrow T_i$ in bubble ("i" = internal)

$\rho \rightarrow \rho_a$, $T \rightarrow T_a$ in ambient medium

two possibilittes

$\rho_i > \rho_a$ bubble falls back stable

$\rho_i < \rho_a$ bubble rises further instable

buoyancy as long as $\rho_i(r+\Delta r) < \rho_a(r+\Delta r)$

since

$F_b = -g(\rho_i - \rho_a) > 0$, i.e., for $\Delta\rho = (\rho_i - \rho_a) < 0$

The Schwarzschild criterion

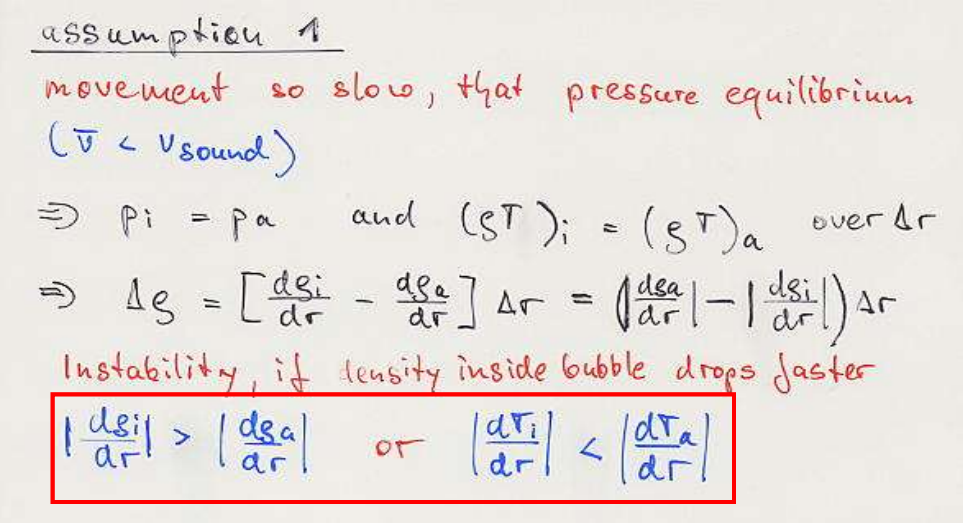

assumption 1

movement so slow, that pressure equilibrium ($\bar{v} < v_{sound}$)

$\Rightarrow$ $p_i = p_a$ and $(\rho T)_i = (\rho T)_a$ over Δr

$$\Rightarrow \Delta\rho = \left[\frac{d\rho_i}{dr} - \frac{d\rho_a}{dr}\right]\Delta r = \left(\left|\frac{d\rho_a}{dr}\right| - \left|\frac{d\rho_i}{dr}\right|\right)\Delta r$$

Instability, if density inside bubble drops faster

$$\boxed{\left|\frac{d\rho_i}{dr}\right| > \left|\frac{d\rho_a}{dr}\right| \quad \text{or} \quad \left|\frac{dT_i}{dr}\right| < \left|\frac{dT_a}{dr}\right|}$$

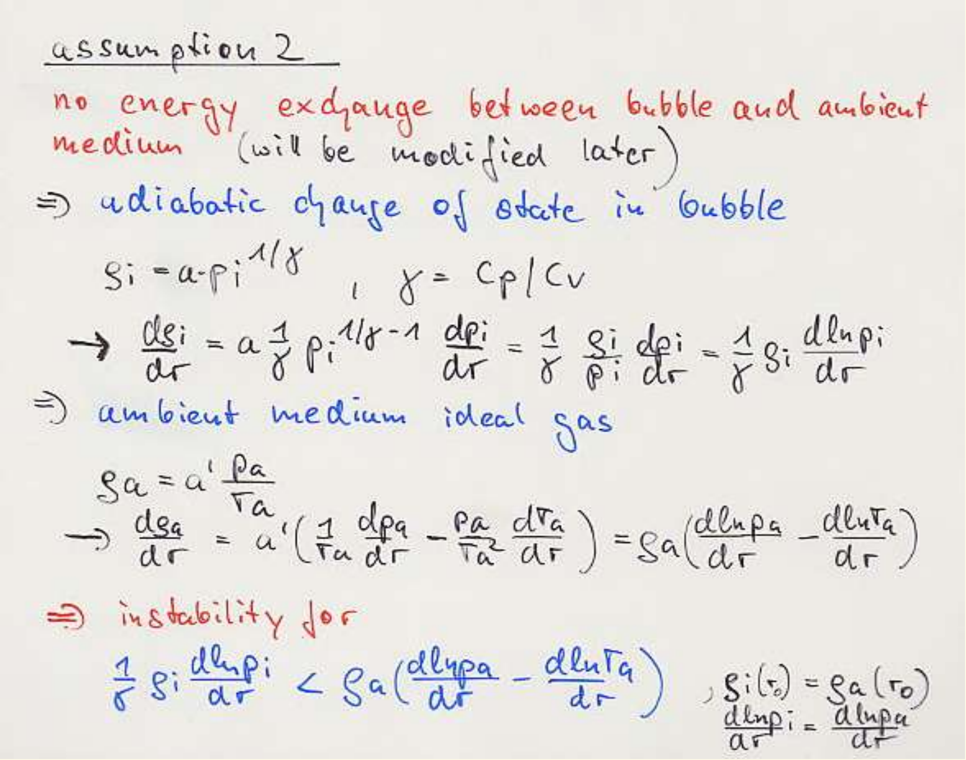

assumption 2

no energy exchange between bubble and ambient medium (will be modified later)

$\Rightarrow$ adiabatic change of state in bubble

$$\rho_i = a \cdot p_i^{1/\gamma} \,, \quad \gamma = c_p / c_v$$

$$\rightarrow \frac{d\rho_i}{dr} = a \frac{1}{\gamma} p_i^{1/\gamma - 1} \frac{dp_i}{dr} = \frac{1}{\gamma} \frac{\rho_i}{p_i} \frac{dp_i}{dr} = \frac{1}{\gamma} \rho_i \frac{d\ln p_i}{dr}$$

$\Rightarrow$ ambient medium ideal gas

$$\rho_a = a' \frac{p_a}{T_a}$$

$$\rightarrow \frac{d\rho_a}{dr} = a'\left(\frac{1}{T_a}\frac{dp_a}{dr} - \frac{p_a}{T_a^2}\frac{dT_a}{dr}\right) = \rho_a\left(\frac{d\ln p_a}{dr} - \frac{d\ln T_a}{dr}\right)$$

$\Rightarrow$ instability for

$$\frac{1}{\gamma}\rho_i \frac{d\ln p_i}{dr} < \rho_a\left(\frac{d\ln p_a}{dr} - \frac{d\ln T_a}{dr}\right) \,, \quad \rho_i(r_0) = \rho_a(r_0) \,, \quad \frac{d\ln p_i}{dr} = \frac{d\ln p_a}{dr}$$

$$\frac{1}{\gamma}\frac{d\ln p}{dr} < \left(\frac{d\ln p}{dr} - \frac{d\ln T}{dr}\right)$$

$$\Rightarrow \left(\frac{d\ln p}{dr} < 0\right) \quad \frac{1}{\gamma} > 1 - \frac{d\ln T}{d\ln p}$$

$$\boxed{\nabla_a = \frac{d\ln T_a}{d\ln p} > 1 - \frac{1}{\gamma} = \nabla_{ad} \quad \text{"Schwarzschild criterion"}}$$

convection, if $\nabla_a > \nabla_{ad}$

- ∇_a : if no convection, radiative stratification

$$\nabla_a = \nabla_{rad} = \frac{d\ln T/dr}{d\ln p/dr} = \frac{3}{16}\frac{\bar{\chi}\,\mathcal{F}_{rad}}{\sigma_B T^4} \Big/ \frac{g_{eff}\,\mu m_H}{kT}$$

↖ 1/H

large opacity
favours convection

$$= \frac{3}{16}\left(\frac{T_{eff}}{T}\right)^4 \cdot \underbrace{(\bar{\chi}\,H)} \lesssim \frac{3}{16}\left(\frac{T_{eff}}{T}\right)^4$$

≤ 1 in photosphere

- $\nabla_{ad} = \left(\frac{d\ln T}{d\ln P}\right)_{ad} = \frac{\gamma - 1}{\gamma}$

mono-atomic gas: $\nabla_{ad} = 0.4,$ and $\frac{3}{16} \approx 0.19$

- must include ionization effects (number of particles!) and radiation pressure (weak influence in atmosph.)
- pure hydrogen, fully ionized
  $\nabla_{ad} = 0.4 \gg \nabla_{rad}$
  $\Rightarrow$ hot star atmospheres (convectively) stable!

- pure hydrogen: minimum for 50% ionization
  $\nabla_{ad} \approx 0.07 < \nabla_{rad}$ solar convection zone, T = 9000 K!

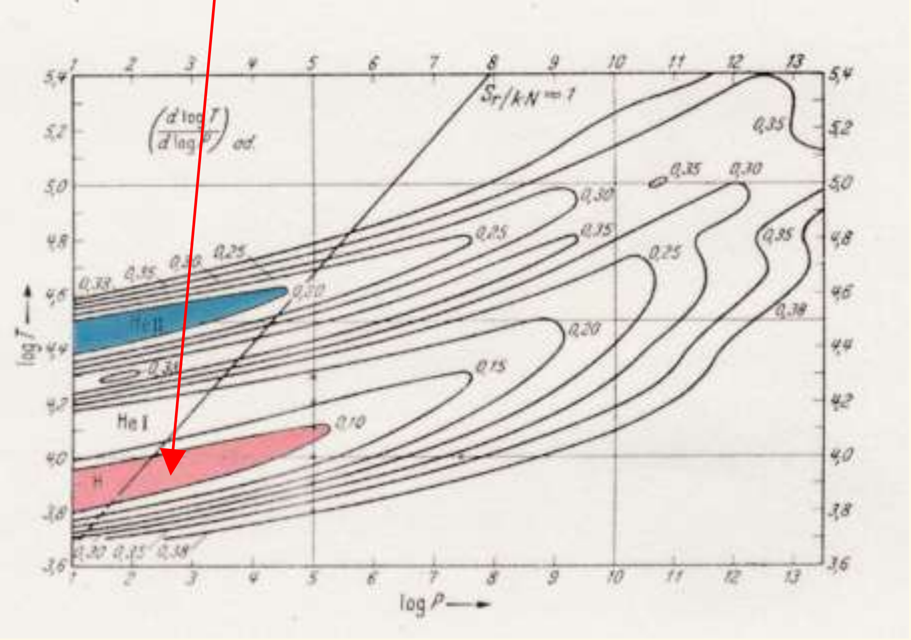

∇_{ad} as function of T and p

Mixing length theory

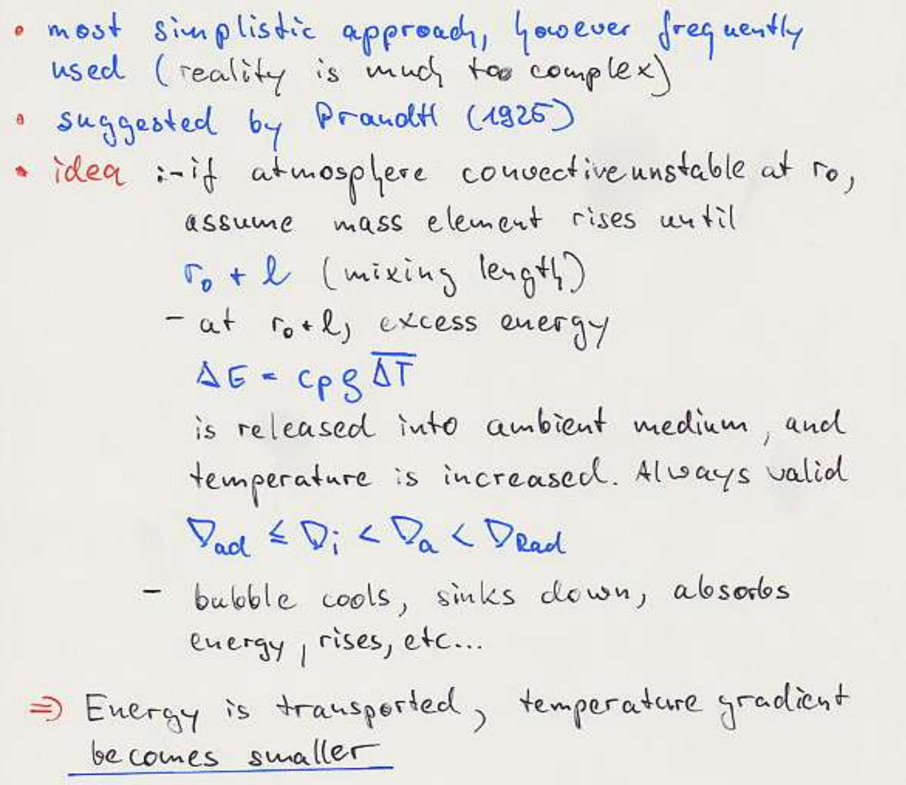

- most simplistic approach, however frequently used (reality is much too complex)
- suggested by Prandtl (1925)
- idea :- if atmosphere convective unstable at r_0, assume mass element rises until $r_0 + \ell$ (mixing length)
  - at $r_0+\ell$, excess energy
    $\Delta E = c_p \rho \overline{\Delta T}$
    is released into ambient medium, and temperature is increased. Always valid
    $\nabla_{ad} \le \nabla_i < \nabla_a < \nabla_{rad}$
  - bubble cools, sinks down, absorbs energy, rises, etc...

⇒ Energy is transported, temperature gradient becomes smaller

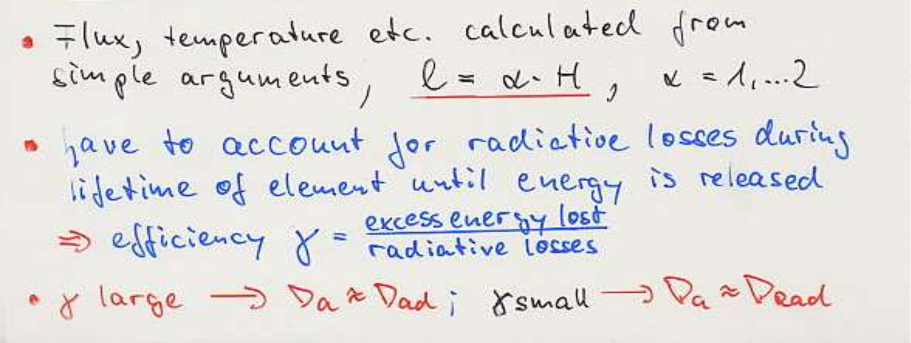

- Flux, temperature etc. calculated from simple arguments, $\ell = \alpha \cdot H$, $\alpha = 1, \ldots 2$
- have to account for radiative losses during lifetime of element until energy is released
  ⇒ efficiency $\gamma = \dfrac{\text{excess energy lost}}{\text{radiative losses}}$
- γ large ⟶ $\nabla_a \approx \nabla_{ad}$; γ small ⟶ $\nabla_a \approx \nabla_{rad}$

Note:
- mixing length theory only 0th order approach
- modern approach: calculate consistent hydrodynamic solution (e.g., solar convective layer+photosphere, Asplund+, see 'Intermezzo')

radiative vs. adiabatic T-stratification

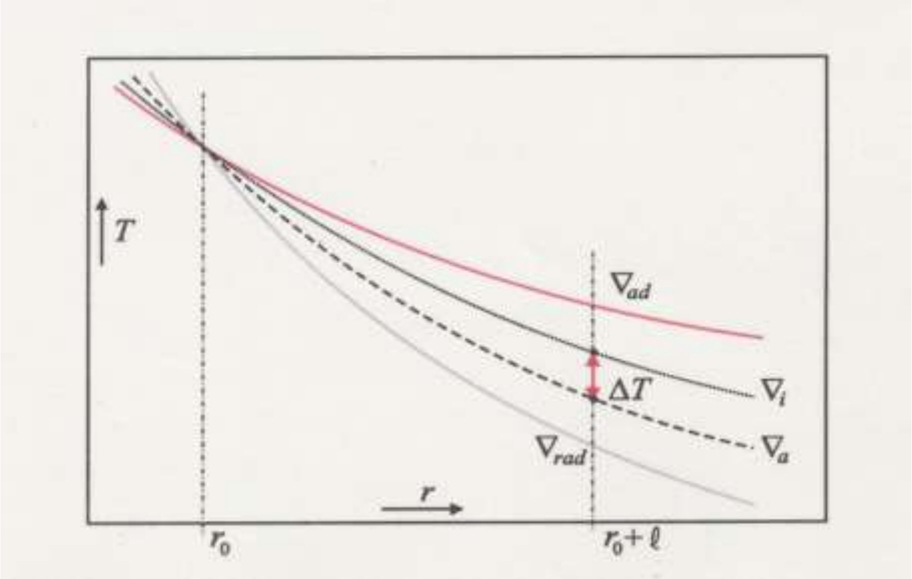

Model for solar photosphere

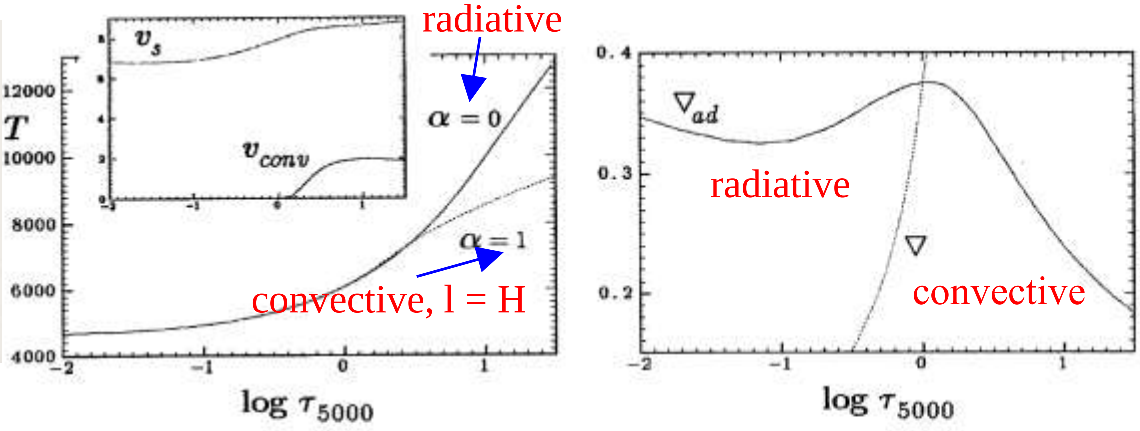

Mixing length theory – some details

$\Delta E = \rho C_p \delta T$ is excess energy density delivered to ambient medium when bubble merges with surroundings. C_p is specific heat per mass.

$\Rightarrow F_{conv} = \Delta E \bar{v} = C_p \delta T \rho \bar{v}$ is convective flux (transported energy) with $\bar{v}$ average velocity of rising bubble over distance Δr ($\rho \bar{v}$ mass flux).

δT is temperature difference between bubble and ambient medium.

$$\delta T = \left[\left(-\frac{dT}{dr}\bigg|_a\right) - \left(-\frac{dT}{dr}\bigg|_i\right)\right]\Delta r > 0$$ when convective instable,

since then $\left[(-\Delta T)_a - (-\Delta T)_i\right] > 0$

From the definiton of ∇,

$$-\frac{dT}{dr} = -\frac{T}{p}\frac{dp}{dr}\nabla = \frac{T}{H}\nabla,$$ with pressure scale height H, since

$$p = \frac{k\rho T}{\mu m_H}, \quad \frac{dp}{dr} = -g\rho \text{ and } \frac{1}{p}\frac{dp}{dr} = -\frac{\mu m_H g}{kT} = -\frac{1}{H}$$

(assuming hydrostatic equilibrium and neglecting radiation pressure; inclusion of p_{rad} possible, of course)

Defining l as the **mixing length** after which element dissolves, and averaging over all elements (distributed randomly over their paths), we may write $\Delta r = \frac{l}{2}$.

$$\Rightarrow F_{conv} = C_p \rho \bar{v} (\nabla_a - \nabla_i) \frac{T}{H}\frac{l}{2} = \boxed{\frac{1}{2} C_p \rho \bar{v} T (\nabla_a - \nabla_i)\alpha},$$ with

mixing length parameter $\alpha = \frac{l}{H}$ (from fits to observations, α=O(1))

The average velocity is calculated by assuming that the work done by the buoyant force is (partly) converted to kinetic energy, where the average of this work might be calculated via

$$\bar{w} = \int_0^{l/2} F_b(\Delta r) d(\Delta r),$$

and the upper limit results from averaging over elements passing the point under consideration. The buoyant force is given by (see page 109)

$$F_b = -g\delta\rho = -g(\rho_i - \rho_a) > 0$$

Using the equation of state, and accounting for pressure equilibrium ($p_i = p_a$), we find $\frac{\delta\rho}{\rho} = -Q\frac{\delta T}{T}$ with $Q = \left(1 - \frac{\partial \ln \mu}{\partial \ln T}\bigg|_p\right)$, to account for ionization effects.

$$\Rightarrow F_b = -g\delta\rho = gQ\frac{\rho}{T}\delta T = gQ\frac{\rho}{T}\left[\left(-\frac{dT}{dr}\bigg|_a\right) - \left(-\frac{dT}{dr}\bigg|_i\right)\right]\Delta r =$$

$$gQ\frac{\rho}{H}(\nabla_a - \nabla_i)\Delta r := A\Delta r.$$ Thus, F_b is linear in Δr, and

$$\bar{w} = \int_0^{l/2} A\Delta r d(\Delta r) = A\frac{l^2}{8} = gQ\rho\frac{H}{8}(\nabla_a - \nabla_i)\left(\frac{l}{H}\right)^2$$

Mixing length theory – some details

Let's assume now that 50% of the work is lost to friction (pushing aside the turbulent elements), and 50% is converted into kinetic energy of the bubbles, i.e.,

$$\frac{1}{2}\overline{w} = \frac{1}{2}\rho\overline{v}^2 \quad \Rightarrow \boxed{\overline{v} = \left(\frac{\overline{w}}{\rho}\right)^{1/2} = \left(\frac{gQH}{8}\right)^{1/2} (\nabla_a - \nabla_i)^{1/2}\alpha,}$$

and the convective flux is finally given by

$$\boxed{F_{conv} = \left(\frac{gQH}{32}\right)^{1/2} (\rho C_p T)(\nabla_a - \nabla_i)^{3/2}\alpha^2.}$$

NOTE : different averaging factors possible and actually found in different versions!

Remember that still $\nabla_{ad} \le \nabla_i < \nabla_a < \nabla_{rad}$.

The gradients ∇_i and ∇_a are calculated from the efficiency γ and the condition that the *total* flux remains conserved (outside the nuclear energy creating core), i.e.,

$$r^2(F_{conv} + F_{rad}) = r^2 F_{tot} = R_*^2 F_{rad}(R_*) = R_*^2 \sigma_B T_{eff}^4 = \frac{L}{4\pi}$$

or from the condition that

$(F_{conv} + F_{rad}) = \frac{L_r}{4\pi r^2}$ with L_r the luminosity at r.

Usually, a tricky iteration cycle is necessary.

Convective vs. radiative energy transport

- major difference in internal structure at MS – convective vs. radiative energy transport:
  - if T-stratification shallow (compared to adiabatic gradient) → radiative energy transport;
  - else convective energy transport
- cool (low-mass stars) during MS:
  - interior: p-p chain, shallow dT/dr → radiative core
  - outer layers: H/He recombines → large opacities → steep dT/dr, low adiabatic gradient → convective envelope
- hot (massive) stars during MS:
  - interior: CNO cycle, steep dT/dr → convective core
  - outer layers: H/He ionized → low opacities → shallow dT/dr, large adiabatic gradient → radiative envelope

Note: (i) transition from p-p chain to CNO cycle around 1.3 to 1.4 M_{sun} at ZAMS

(ii) most massive stars have a sub-surface convection zone due to iron opacity peak

(iii) evolved objects (red giants and supergiants) and brown dwarfs **are fully convective**

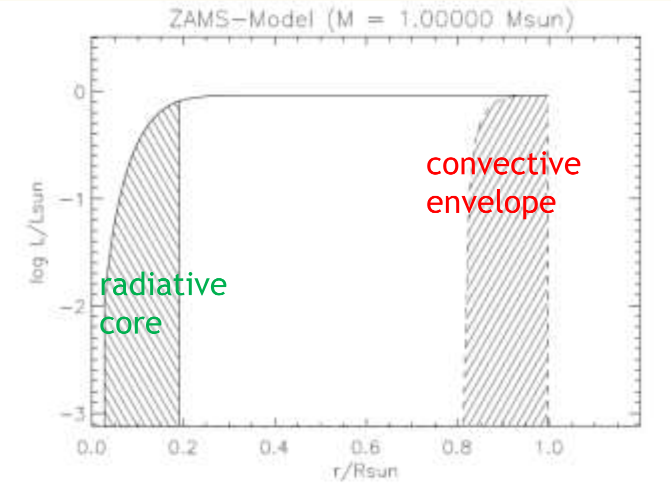

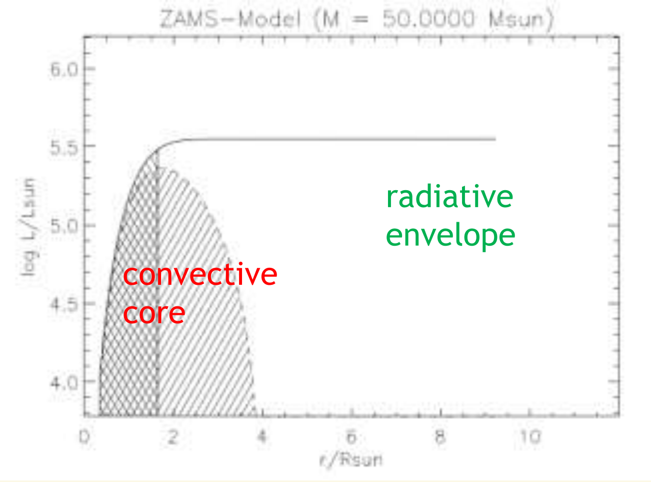

Chap. 7 Microscopic theory

Absorption- and emission coefficients

- can calculate now a lot, if absorption- and emission-coefficients given, e.g.

$$\chi_\nu \sim \sigma_{lu} \bullet \phi(\nu) \bullet n_l(r)$$

cross-section (quantum mech.)

profile function (normalized)

occupation numbers

- LTE: Saha-Boltzmann
- NLTE: detailed calculation

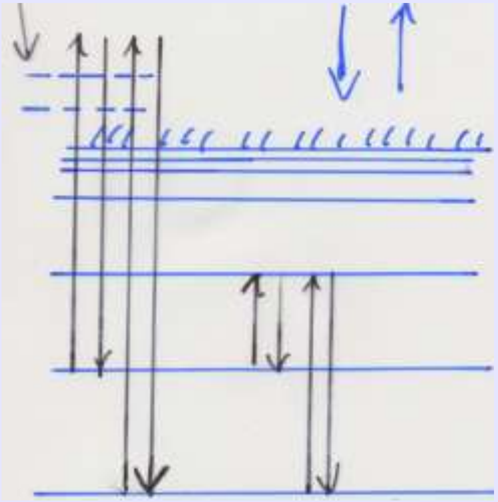

if necessary, next higher ion

"free-free" (Bremsstrahlung)

ionization edge

u excited level

l excited level

ground level

"bound-free" (ionization/ recombination)

"bound-bound" (line transition)

absorption

$h\nu + E_l \rightarrow E_u$

emission

- spontaneous ← isotropic

  $E_u \rightarrow E_l + h\nu$

- stimulated

  $h\nu + E_u \rightarrow E_l + 2\,h\nu$

  same angular distribution

Line transitions

- Einstein coefficients

probability, that photon with energy ~[ν, ν+dν] is absorbed by atom in state E_l with resulting transition $l \rightarrow u$, per second

$$dW^{abs}(\nu,\Omega,l,u) = \underbrace{\underset{\substack{\swarrow \\ \text{atomic} \\ \text{property}}}{B_{lu}} \cdot \underset{\substack{\downarrow \\ \text{prop. to} \\ \text{number of} \\ \text{incident} \\ \text{photons}}}{I_\nu(\Omega)}}_{\text{prob. for } l\rightarrow u} \; \underset{\substack{\downarrow \\ \text{probability,} \\ \text{that } \nu \in \\ [\nu,\nu+d\nu]}}{\varphi(\nu)d\nu} \; \frac{d\Omega}{4\pi} \leftarrow \substack{\text{prob.,} \\ \text{that} \\ \Omega \in \\ [\Omega,\Omega+d\Omega]}$$

B_{lu} Einstein coefficient for absorption

analogously $\qquad \psi_\nu \neq \varphi_\nu$ without further assumpt.

$$dW^{sp}(\nu,\Omega,u,l) = A_{ul}\,\psi(\nu)\,d\nu\,\frac{d\Omega}{4\pi}$$

$$dW^{stim}(\nu,\Omega,u,l) = B_{ul}\,I_\nu(\Omega)\,\psi(\nu)\,d\nu\,\frac{d\Omega}{4\pi}$$

(q.m.)

compare absorbed energy

$$dE_\nu^{abs} = n_l\,dW^{abs}\cdot h\nu\,dV - \underbrace{n_u\,dW^{stim}\,h\nu\,dV}_{\substack{\text{stimulated emission} \\ \text{delivers back part of absorbed} \\ \text{energy, with same angular} \\ \text{distrib. as } I_\nu(\Omega)}}$$

and emitted energy

$$dE_\nu^{em} = n_u\,dW^{sp}\,h\nu\,dV$$

with definition of opacity and emissivity

$$\Rightarrow \chi_\nu^{line} = \frac{h\nu}{4\pi}\varphi(\nu)\left[n_l B_{lu} - n_u B_{ul}\underset{\substack{\uparrow \\ =1 \text{ for} \\ \text{"complete redistribution"}}}{\frac{\psi(\nu)}{\varphi(\nu)}}\right]$$

$$\eta_\nu^{line} = \frac{h\nu}{4\pi}\psi(\nu)\,n_u A_{ul}$$

- Einstein coefficients are atomic properties, must NOT depend on thermodynamic state of matter

Thus assume thermodynamic equilibrium

- from chap 4, we know $S_\nu^* = \frac{\eta_\nu^*}{\chi_\nu^*} = B_\nu(T)$

(and $\psi_\nu^* = \varphi_\nu$)

$$\Rightarrow S_\nu^* = \frac{n_u A_{ul}}{n_l B_{lu} - n_u B_{ul}}$$

freq. independent (also valid in (N)LTE, if "complete redistribution")

$$= \frac{A_{ul}}{B_{ul}} \frac{1}{\left(\frac{n_l}{n_u}\right)^* \frac{B_{lu}}{B_{ul}} - 1}$$

- TE : Boltzmann excitation, $\left(\frac{n_u}{n_l}\right)^* = \underset{\substack{\uparrow \\ \text{stat. weights}}}{\frac{g_u}{g_l}} e^{-h\nu_{ul}/kT}$

- $B_\nu = \frac{2h\nu^3}{c^2}\frac{1}{e^{h\nu/kT}-1} = S_\nu^* = \frac{A_{ul}}{B_{ul}}\frac{1}{\left(\frac{g_l B_{lu}}{g_u B_{ul}}\right)e^{h\nu/kT}-1}$

$$\Rightarrow \boxed{\underset{\uparrow}{g_l}\,\underset{\uparrow}{B_{lu}} = \underset{\uparrow}{g_u}\,\underset{\uparrow}{B_{ul}}, \qquad A_{ul} = \frac{2h\nu^3}{c^2}B_{ul}}$$

ONLY ONE EINSTEIN COEFF. HAS TO BE CACULATED!

- has to be calculated from quantum mechanics (from "dipoloperator")
- result

$$\boxed{\frac{h\nu}{4\pi} B_{lu} = \frac{\pi e^2}{m_e c} f_{lu}}$$

f "oscillator strength", dimensionless

↑ classical result, from electrodynamics

"strong" transitions have $f \approx 0.1 \dots 10$

and "selection rules", e.g. $\Delta l = \pm 1$

"forbidden transitions": magnetic dipole, electr. quadrupol: f very low, 10^{-5} and lower

- THUS

$$\chi_\nu = \frac{\pi e^2}{m_e c} f_{lu}\left(n_l - \frac{g_l}{g_u} \cdot n_u\right) \cdot \varphi_\nu$$

$$= \frac{\pi e^2}{m_e c} (gf)_{lu} \cdot \left(\frac{n_l}{g_l} - \frac{n_u}{g_u}\right) \cdot \varphi_\nu$$

↑ "gf-value" $= g_l \cdot f_{lu}$

with $\int_{-\infty}^{\infty} \varphi(\nu) d\nu = 1$

$$\frac{\pi e^2}{m_e c} \approx 0.02654 \frac{cm^2}{s}$$

Profile function?

Line broadening

1. Radiation damping ("natural" line broadening)

- QED effect
- heuristic finite life time with respect to spontaneous emission

$\tau = \frac{1}{A_{ul}}$ (e.g., 10^{-8}s for H $2 \rightarrow 1$)

and uncertainty principle

$\Delta E \cdot \tau \gtrsim \hbar$

$\Rightarrow$ broadening (classical theory: damping by radiation)

→ dispersion (Lorentzian) profile

$$\boxed{\phi(\nu) = \frac{\Gamma/4\pi^2}{(\nu-\nu_0)^2 + (\Gamma/4\pi)^2}}$$

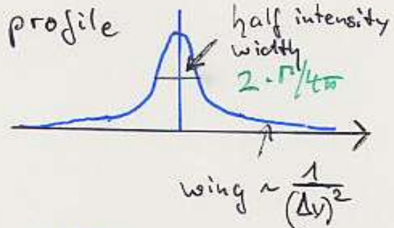

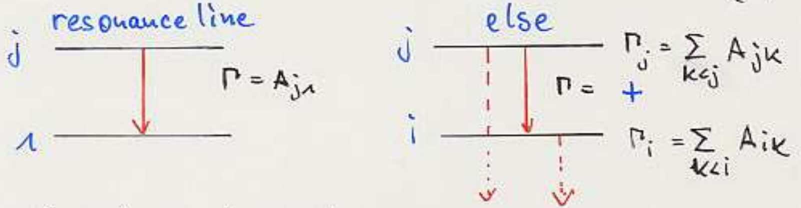

- of primary importance for strong lines (res. lines) in low density environment (no other broadening mechanisms), e.g. L_α in interstellar medium

2. Collisional broadening

- radiating atoms perturbed by passing particles
- brief perturbation, close perturbers

"impact theory"

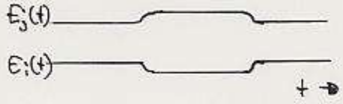

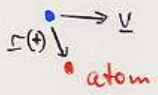

$\Delta E(t) \sim \frac{1}{r^n(t)}$

n=2 linear Stark effect

for levels with degenerate angular momentum, e.g., H I, He II

$\Delta E \sim F = \frac{q}{r^2}$

↑ field strength

very important, if many electrons: photospheres of hot stars, $n_e \gtrsim 10^{12}\,\mathrm{cm}^{-3}$

n=3 resonance broadening

atom A is perturbed by atom A' of same species in "cool" stars, e.g. Balmer lines in sun

n=4 quadratic Stark effect

metal ions in photospheres of hot stars

$\Delta E \sim F^2$

n=6 van der Vaals broadening

atom A perturbed by atom B in cool stars, e.g. Na perturbed by H in sun

resulting profiles are dispersion profiles!

- impact theory fails for (far) wings

⇒ statistical description (mean field of ensemble of perturbers)

+ q.m.

approximate behaviour for linear Stark broadening

$\varphi(\Delta\nu \to \infty) \sim \frac{1}{(\Delta\nu)^{5/2}}$ (instead of $\frac{1}{(\Delta\nu)^2}$)

3. Thermal velocities : Doppler broadening

- radiating atoms have thermal velocity (so far assumed as zero)

Maxwellian distribution

$$P(v_x, v_y, v_z)\, dv_x\, dv_y\, dv_z = \left(\frac{m}{2\pi kT}\right)^{3/2} e^{-\frac{m}{2kT}(v_x^2+v_y^2+v_z^2)} dv_x dv_y dv_z$$

+ Doppler effect

$$\underset{\substack{\uparrow \\ \text{observer's}}}{\nu} = \underset{\substack{\uparrow \\ \text{atomic frame}}}{\nu'} + \nu_0 \frac{\mathbf{n}\cdot\mathbf{v}}{c}$$

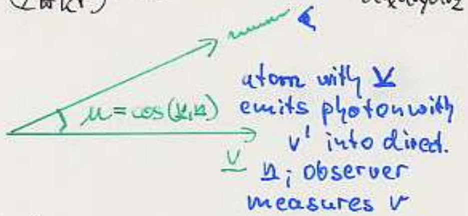

atom with $\underline{v}$ emits photon with ν' into direct. $\underline{n}$; observer measures ν

⇒ convolution; as long as isotropic emission:

$$\phi(\nu) = \frac{1}{\pi^{1/2}} \int_{-\infty}^{+\infty} e^{-v^2} \varphi(\nu - \nu_0 - \Delta\nu_D v)\, dv$$

φ ↙ profile function in atomic frame

$\Delta\nu_D$ ↓ $\frac{\nu_0 v_{th}}{c}$ "Doppler width"

$v_{th} = \left(\frac{2kT}{m_A}\right)^{\frac{1}{2}}$ therm. velocity

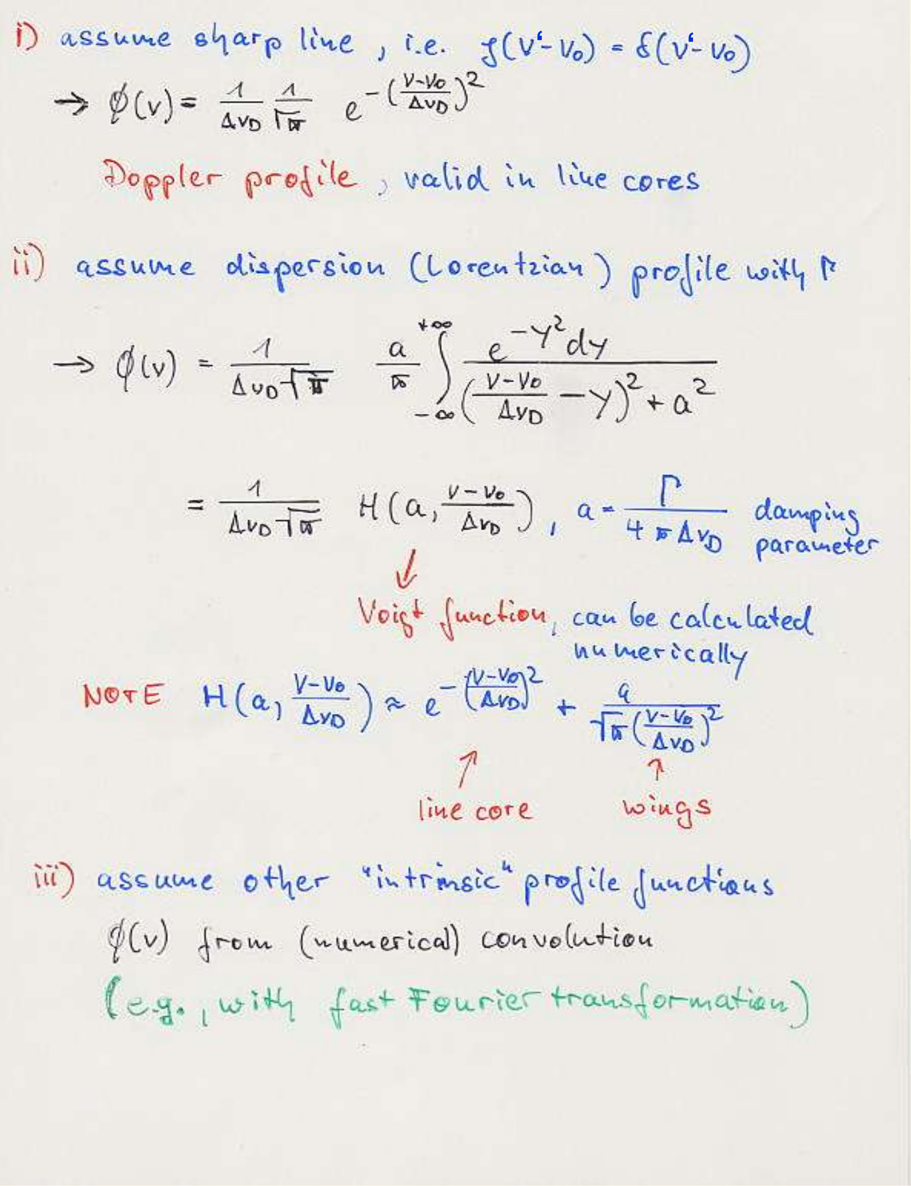

i) assume sharp line, i.e. $g(\nu'-\nu_0) = \delta(\nu'-\nu_0)$

$$\rightarrow \phi(\nu) = \frac{1}{\Delta\nu_D}\frac{1}{\sqrt{\pi}}\, e^{-\left(\frac{\nu-\nu_0}{\Delta\nu_D}\right)^2}$$

Doppler profile, valid in line cores

ii) assume dispersion (Lorentzian) profile with Γ

$$\rightarrow \phi(\nu) = \frac{1}{\Delta\nu_D\sqrt{\pi}}\; \frac{a}{\pi}\int_{-\infty}^{+\infty} \frac{e^{-y^2}dy}{\left(\frac{\nu-\nu_0}{\Delta\nu_D}-y\right)^2+a^2}$$

$$= \frac{1}{\Delta\nu_D\sqrt{\pi}}\; H\left(a,\frac{\nu-\nu_0}{\Delta\nu_D}\right), \quad a = \frac{\Gamma}{4\pi\Delta\nu_D}$$ damping parameter

↓

Voigt function, can be calculated numerically

NOTE $H\left(a,\frac{\nu-\nu_0}{\Delta\nu_D}\right) \approx e^{-\left(\frac{\nu-\nu_0}{\Delta\nu_D}\right)^2} + \frac{a}{\sqrt{\pi}\left(\frac{\nu-\nu_0}{\Delta\nu_D}\right)^2}$

↑ line core ↑ wings

iii) assume other "intrinsic" profile functions

$\phi(\nu)$ from (numerical) convolution

(e.g., with fast Fourier transformation)

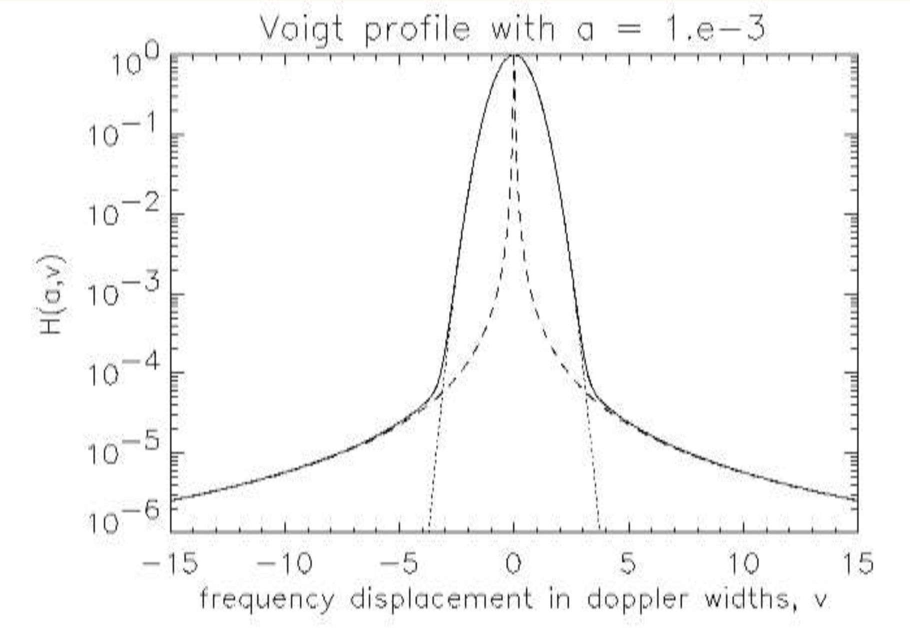

fully drawn: Voigt profile H(a,v)
dotted : exp($-v^2$), Doppler profile (core)
dashed: a / ($\sqrt{\pi}\, v^2$), dispersion profile (wings)

Curve of growth method

Theoretical curve of growth

- standard diagnostic tool to determine metal abundances in cool stars in a simple way
- assumptions
  pure absorption line
  Milne Eddington model, LTE, $\varepsilon_\nu = 1$ (no scattering)

$$\chi_\nu = \chi_c + \underbrace{\bar{\chi}_L \phi_\nu}_{\chi_\nu^{\text{Line}}} = \chi_c (1 + \beta_\nu), \quad \beta_\nu = \underset{\substack{\uparrow \\ \text{depth independent}}}{\frac{\bar{\chi}_L}{\chi_c}} \phi_\nu$$

$$B_\nu(\tau) = a + b\,\tau_c \quad \text{defined on continuum scale}$$

$$= a + b \frac{\chi_c}{\chi_\nu} \tau_\nu = a + \underbrace{b \frac{1}{1+\beta_\nu}}_{\hat{=}\, b_\nu \text{ in Milne-Edd. model}} \tau_\nu$$

- From Milne Edd. model we have (page 92/93)

$$H_\nu^{\text{Line}}(0),\ \varepsilon_\nu = 1 = \frac{1}{\sqrt{3}} J_\nu(0) = \frac{1}{\sqrt{3}} \left(a + \frac{\frac{1}{1+\beta_\nu} \frac{b}{\sqrt{3}} - a}{2} \right)$$

$$H_\nu^{\text{cont}}(0),\ \varepsilon_\nu = 1 = (\beta_\nu = 0) = \frac{1}{\sqrt{3}} \left(a + \frac{b/\sqrt{3} - a}{2} \right)$$

⇒ residual intensity ("line profile"

$$R_\nu = \frac{H_\nu^{\text{Line}}}{H_\nu^{\text{cont}}} = \frac{b \frac{1}{1+\beta_\nu} + \sqrt{3}\,a}{b + \sqrt{3}\,a}$$

$$\beta_\nu = \frac{\pi e^2}{m_e c} f_{lu} \frac{n_e}{\chi_c} \left(1 - e^{-h\nu/kT}\right) \phi(\nu) = \beta_0 \phi(\nu)$$

↙ Voigt profile!

line depth

$$A_\nu = 1 - R_\nu = \frac{\beta_0 \phi_\nu}{1 + \beta_0 \phi_\nu} \underbrace{\left(\frac{b}{b + \sqrt{3}\,a} \right)}_{A_0 \text{ central depth of line with } \beta_0 \to \infty}$$

$$A_\nu = A_0 \beta_0 \frac{\phi_\nu}{1 + \beta_0 \phi_\nu}$$

equivalent width $W_\nu = \int_0^\infty A_\nu \, d\nu$ area below continuum (see also p. 8.3)

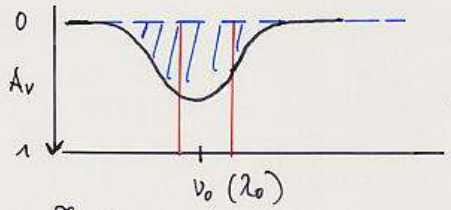

W_λ width of line in Å, if line would have depth "1"

$$\Rightarrow W_\nu = A_0 \beta_0 \int_0^\infty \frac{\phi_\nu}{1 + \beta_0 \phi_\nu} \, d\nu$$

$$W_\lambda = \int_0^\infty A(\lambda)\, d\lambda \approx \left(\int_0^\infty A_\nu \, d\nu \right) \frac{\lambda_0^2}{c} \qquad W_\lambda = \frac{\lambda_0^2}{c} \cdot W_\nu$$

with Voigt profile H (Doppler core + Lorentz wings)

$$W_\nu = A_0 \beta_0 \frac{1}{\sqrt{\pi}\,\Delta\nu_D} \int_0^\infty \frac{H\left(\frac{\nu-\nu_0}{\Delta\nu_D}\right) d\nu}{1 + \frac{\beta_0}{\sqrt{\pi}\,\Delta\nu_D} H\left(\frac{\nu-\nu_0}{\Delta\nu_D}\right)} \qquad v = \frac{\nu - \nu_0}{\Delta\nu_D}, \quad d\nu = dv\, \Delta\nu_D$$

$= \ldots$

$$W_\nu = \frac{A_0\beta_0}{\sqrt{\pi}} \int_{-\infty}^{+\infty} \frac{H(v)\,dv}{1+\frac{\beta_0}{\sqrt{\pi}\Delta\nu_D} H(v)}$$

3 regimes

a) linear regime: Doppler core not saturated, $H(a,v) = e^{-v^2}$

$$\Rightarrow W_\nu \approx \frac{A_0\beta_0}{\sqrt{\pi}} \int_{-\infty}^{+\infty} \frac{e^{-v^2}dv}{1+\frac{\beta_0}{\sqrt{\pi}\Delta\nu_D} e^{-v^2}}$$

$$\rightarrow (\beta_0/\Delta\nu_D < 1) \quad \frac{A_0\beta_0}{\sqrt{\pi}} \int_{-\infty}^{+\infty} e^{-v^2}\left(1-\frac{\beta_0}{\Delta\nu_D\sqrt{\pi}} e^{-v^2}+\dots\right)dv$$

$\approx A_0\beta_0 \sim \beta_0$, independent on $\Delta\nu_D$

b) saturation part: line reaches maximum depth ($\approx A_0$), however wings still unimportant

as above, i.e. $\phi_\nu \sim e^{-v^2}$, however $\beta_0/\Delta\nu_D > 1$

$\Rightarrow$ (integration tricky)

$$W_\nu = 2A_0\Delta\nu_D\sqrt{\ln\beta^*}\left(1-(\pi^2/24(\ln\beta^*)^2-\dots\right)$$

with $\beta^* = \beta_0/\sqrt{\pi}\Delta\nu_D$

flat growth with $\sqrt{\ln\beta^*}$, $W_\nu \sim \Delta\nu_D$

c) damping (square-root) part

line wings dominate equivalent width

$$\Rightarrow W_\nu \approx \frac{A_0\beta_0}{\sqrt{\pi}} \int_{-\infty}^{+\infty} \frac{a/(\sqrt{\pi}v^2)\,dv}{1+\frac{\beta_0}{\sqrt{\pi}\Delta\nu_D}\frac{a}{\sqrt{\pi}v^2}} \qquad a \text{ damping parameter}$$

$$= \frac{A_0\beta_0}{\pi} a \int_{-\infty}^{+\infty} \frac{dv}{v^2+\frac{\beta_0 a}{\pi\Delta\nu_D}}$$

$$= A_0\left(a\pi\Delta\nu_D\beta_0\right)^{\frac{1}{2}}$$ (attention: typo in Mihalas)

growth with $\beta_0^{\frac{1}{2}}$

in total, we have $W_\nu = f(\beta_0)$ or $f\left(\frac{\beta_0}{\Delta\nu_D\sqrt{\pi}}\right) = f(\beta^*)$

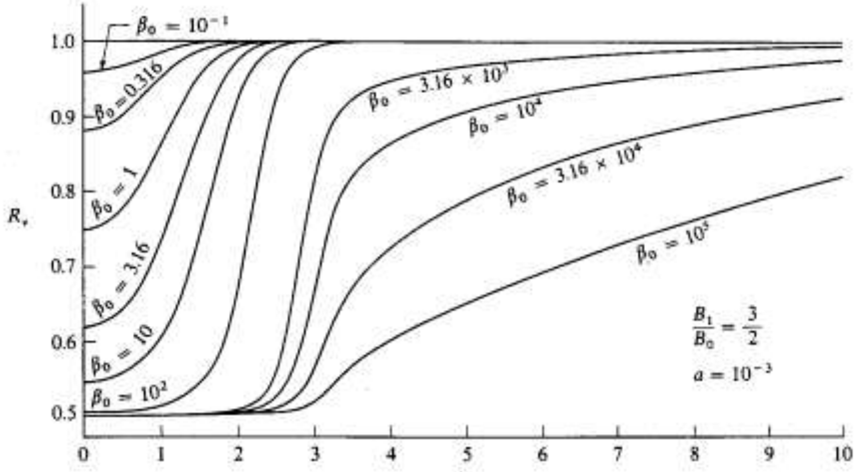

Voigt profile with $A_O = 0.5$, $\beta_o =: \beta^*$

Development of a spectrum line with increasing number of atoms along the line of sight. The line is assumed to be formed in pure absorption. For $\beta_0 \lesssim 1$, the line strength is directly proportional to the number of absorbers. For $30 \lesssim \beta_0 \lesssim 10^3$ the line is saturated, but the wings have not yet begun to develop. For $\beta_0 \gtrsim 10^4$ the line wings are strong and contribute most of the equivalent width.

Now:

$$\beta^* = \frac{\pi e^2}{m_e c} f_{lu} \frac{n_l}{\chi_c} \left(1 - e^{-h\nu/kT_e}\right) \frac{1}{\Delta\nu_D \sqrt{\pi}}$$

$$\chi_c = \chi_c^0 \left(1 - e^{-h\nu/kT_e}\right)$$ LTE, next section

$$n_l = n_1 \frac{g_l}{g_1} e^{-h\nu_{l1}/kT_e}$$ Boltzmann excitation, next section

$$\Delta\nu_D = \frac{\nu_0 v_{th}}{c} = \sqrt{\frac{2kT}{m}} \frac{1}{\lambda}$$

$$\Rightarrow \log \beta^* = \log\left(g_l f_{lu} \cdot \lambda\right) + \log\left(e^{-E_{1l}/kT_e}\right) + \log\left(\frac{n_1}{g_1 \chi_c^0} \frac{\sqrt{\pi} e^2}{m_e c} \sqrt{\frac{m}{2kT_e}}\right)$$

$$= \log\left(g_l f_{lu} \cdot \lambda\right) - \frac{5040 \cdot E_{1l}}{T_e} + \log C$$

in one ionization stage and if E in eV

- in one ionization stage, $C \approx$ const

→ lines belonging to one ionization stage should form curve of growth, since β^* varies as function of considered transition

→ if T_e and χ_c^0 known

→ shift "observed" $W_\nu(\beta^*_{lu})$ horizontally until curve matches theoretical curve

→ n_1 ⇒ (using Saha-Boltzmann equation for ionization, next section)

abundances

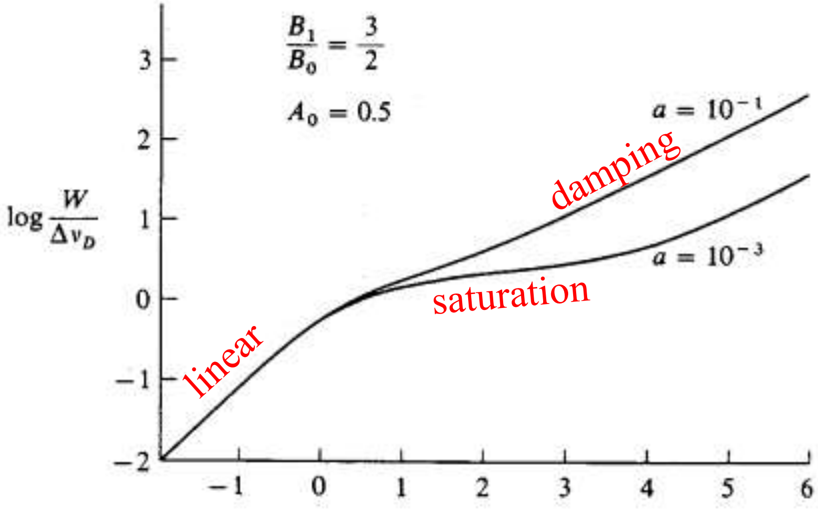

$$\log \beta^* = \log \beta_o / (\sqrt{\pi} \Delta\nu_D)$$

FIGURE 10-2
Curves of growth for pure absorption lines. Note that the larger the value of *a*, the sooner the square-root part of the curve rises away from the flat part.

measure W(λ) for different lines (with different strengths) of one ionization stage

plot as function of $\log(g_l f_{lu}\lambda) - \frac{5040 E_{1l}}{T_e} + \log C$, with "C" fit-quantity

shift horizontally until *theoretical curve of growth* W(β^*) is matched => log C => $\frac{n_1}{\chi_c^0}$ => n_1

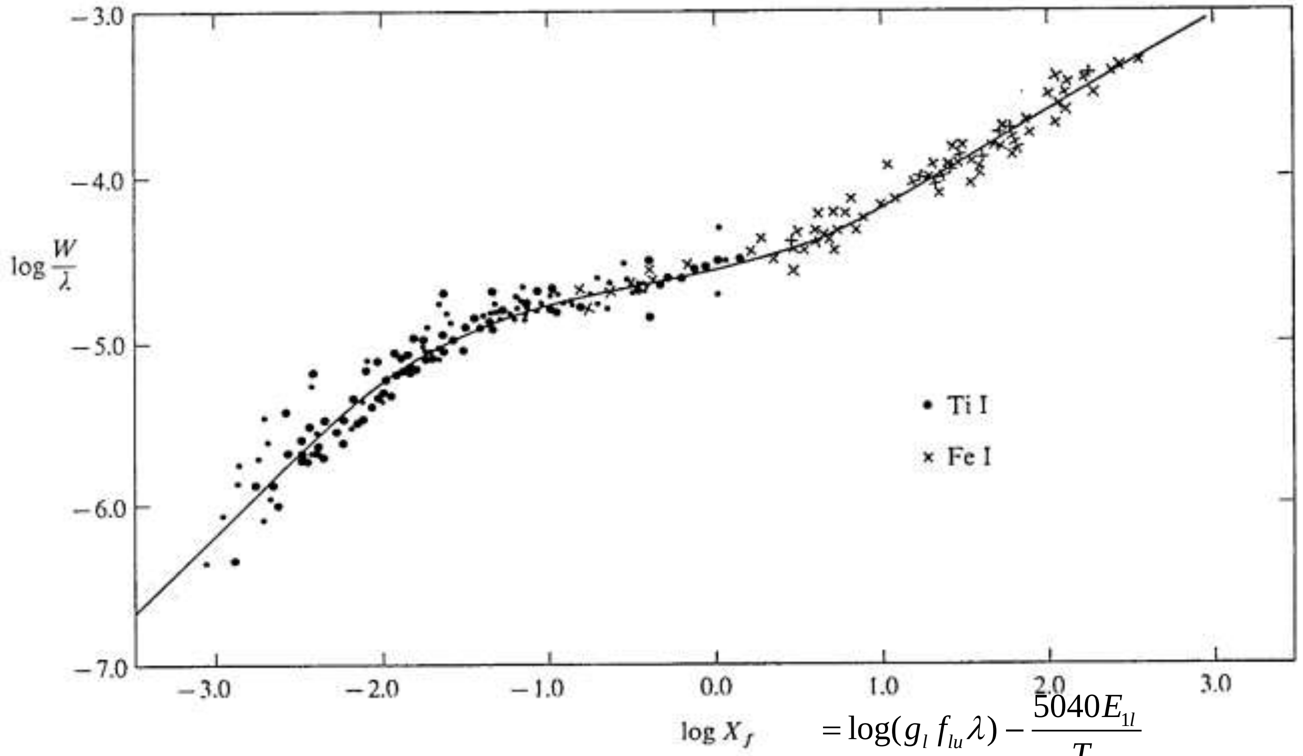

$$= \log(g_l f_{lu}\lambda) - \frac{5040 E_{1l}}{T_e}$$

Empirical curve of growth for solar Fe I and Ti I lines. Abscissa is based on laboratory *f*-values. From **(686)**.

Ti I lines shifted horizontally to define a unique relation

Continous processes

Continous absorption/emission and scattering

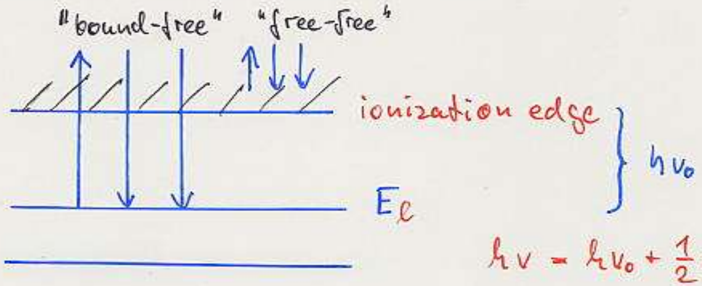

$h\nu = h\nu_0 + \frac{1}{2} m_e v^2$

- bound free processes

"one" transition : $\chi_\nu^{bf} = n_\ell \sigma_{\ell k}(\nu)$, $\nu > \nu_0$

absorption cross section ↑ ↑ threshold

in total : many processes at one frequency

$$\chi_\nu^{bf} = \sum_{\text{elements}} \sum_{\text{ions}} \sum_\ell n_\ell \sigma_{\ell k}(\nu)$$

hydrogenic ions $\sigma_{\ell k}(\nu) = \sigma_0(\ell) \left(\frac{\nu_0}{\nu}\right)^3 \cdot g_{bf}(\nu)$

↑ "gaunt-factor", ≈ 1

EINSTEIN-MILNE relations

$$\chi_\nu^{bf} = \sum_{\substack{\text{elements,}\\ \text{ions}}} \sum_\ell \sigma_{\ell k}(\nu) \left(n_\ell - n_\ell^* e^{-h\nu/kT}\right)$$

↑ stim. emission

$$\eta_\nu^{bf} = \sum \sum_\ell \sigma_{\ell k}(\nu) \frac{2h\nu^3}{c^2} n_\ell^* e^{-h\nu/kT}$$

↑ spontaneous emission

n_ℓ^* = LTE value

NOTE : $n_\ell = n_\ell^* \Rightarrow S_\nu^{bf} = \frac{\eta_\nu^{bf}}{\chi_\nu^{bf}} = B_\nu(T)$!

free-free processes

(emission process: "bremsstrahlung", decelerated charges radiate!)

$$\chi_\nu^{ff} = n_e n_k^{\text{ion}} \sigma_{kk}(\nu) \left(1 - e^{-h\nu/kT}\right)$$

↑ stim. emission

$\sigma_{kk} \sim \frac{\lambda^3}{\sqrt{T}}$, important in IR and radio!

$$\eta_\nu^{ff} = n_e n_k^{\text{ion}} \sigma_{kk}(\nu) \frac{2h\nu^3}{c^2} e^{-h\nu/kT}$$

NOTE $S_\nu^{ff} = B_\nu(T)$ always!

Scattering

1. electron scattering

- important for hot stars
- difference to f-f processes

f-f: photon interacts with e^- in ion's central field
$\Rightarrow$ absorption $\Rightarrow$ photon destruction, i.e. "true" process

scattering: without influence of central field, i.e., no "third" partner in collisional process
$\Rightarrow$ no absorption possible, since energy and momentum conservation cannot be fulfilled simultaneously
$\Rightarrow$ scattering

- very high energies (many MeVs)
  Klein Nishina (Q.E.D.)
- high energies
  Compton / inverse Compton scattering
  $\downarrow$ $\downarrow$
  e^- has low / has high kinetical energy
- low energies (< 12.4 keV ≙ 1 Å)
  Thomson scattering

  classical e^- radius

  $$\sigma^{TH} = n_e \sigma_T ; \quad \sigma_T = \sigma_{class} = \frac{8\pi}{3} r_0^2 = \frac{8\pi}{3} \frac{e^4}{m_e^2 c^4}$$
  $$= 6.65 \cdot 10^{-25}\,\mathrm{cm}^2$$

2. Rayleigh-scattering

actually: line absorption / emission of atoms / molecules far from resonance frequency

$\Rightarrow$ from q.m., Lorentzprofile with $|\nu - \nu_0| \gg \nu_0$

$$\sigma(\nu) = f_{lu} \sigma_T \cdot \left(\frac{\nu}{\nu_0}\right)^4 \sim \lambda^{-4}$$ for $\nu \ll \nu_0$

- if line transition strong, λ^{-4} decrease of far wins can be of major importance

example: Rayleigh wings *of Ly-alpha* in metal-poor, cool stars (G/K-type, few electrons, thus few H^-, see next paragraph) become important opacity source, even in the optical

The H^- ion

- for cool stars (e.g., the sun), one bound state of H^- ($1p + 2e^-$)

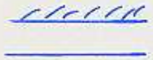

} 0.75 eV ≙ 16550 Å

- dominant bf-opacity (also ff component)
- only by inclusion of H^- (Pannekoek + Wildt, 1939) the solar continuum could be explained

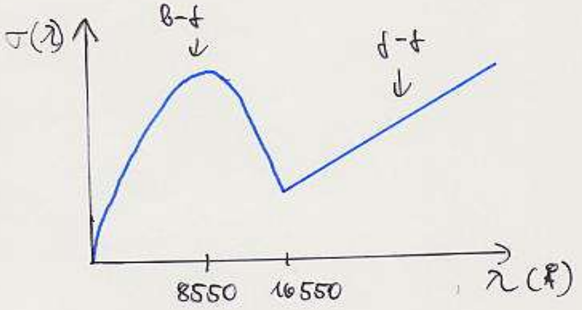

Total opacities and emissivities

$$\chi_\nu^{tot} = \chi^{Line}\phi(\nu) + \Sigma \chi_\nu^{bf} + \Sigma \chi_\nu^{ff} + n_e \sigma_T$$
$$\eta_\nu^{tot} = \chi^{Line}\phi(\nu) S_L + \Sigma \eta_\nu^{bf} + \Sigma \eta_\nu^{ff} + n_e \sigma_T J_\nu$$

NOTE: for LTE ($n_i = n_i^*$) and $J_\nu = B_\nu$

we have always

$$\frac{\eta_\nu^{tot}}{\chi_\nu^{tot}} = B_\nu(T)$$, good test!

Ionization and Excitation

Ionization and Excitation

had $\chi_\nu^{Line} = \frac{\pi e^2}{m_e c} g f_{lu} \left(\frac{n_l}{g_l} - \frac{n_u}{g_u}\right) \phi(\nu)$

$\chi_\nu^{bf} = \sum_l (n_l - n_l^* \, e^{-h\nu/kT}) \sigma_{lk}(\nu)$

$\sigma^{TH} = n_e \sigma_T$

How to determine occupation numbers and electron densities?

Local Thermodynamic Equilibrium (LTE)

- each volume element in TE, with temperature $T_e(r)$

Hypothesis: collisions ($e^- \Leftrightarrow$ ions) adjust equilibrium

problem: interaction with non-local photons

LTE valid, if

- influence of photons small or
- radiation field Planckian at $T_e(r)$ (and isotropic)

Excitation

- Fermi statistics → low density, high temperat.
  → Boltzmannstatistics
- distribution of level occupation n_{ij} (per dV, ionizationstage j)

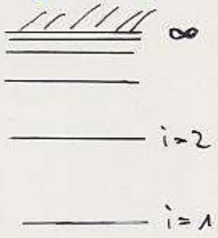

$$\frac{n_{ij}}{n_{1j}} = \frac{g_{ij}}{g_{1j}} e^{-E_{ij}/kT}$$

(if $E_1 = 0$)

- g_i statistical weights (number of degen. states)
- for hydrogen $g_i = 2 i^2$, i = princ. quant. number
  " LS coupling $g = (2S+1)(2L+1)$
- if E_i excitation energy with resp. to ground state

$$\boxed{\frac{n_u}{n_l} = \frac{g_u}{g_l} e^{-E_{ul}/kT}}$$ with $E_{ul} = E_u - E_l$

Ionization

- from generalization of Boltzmann formula for ratio of two (neighbouring) ionic species j and $j+1$

$$n_{1j} \text{ with } g_{1j} \Rightarrow \underset{+\text{free } e^-}{n_{1j+1}} \text{ with } \underbrace{g_{1j+1}\cdot g_{el}}_{\text{weight of final state}}$$

g_{el}: Number of available elements in phase space for free e^-,

$$\frac{d^3\underline{r}\, d^3\underline{p}}{h^3}\cdot \underset{\overset{\uparrow}{\text{spin}}}{2}, \quad d^3\underline{r} = dV = \underset{\overset{\uparrow}{1e^- \text{ per } dV}}{\frac{1}{n_e}}$$

$$\Rightarrow \frac{n_{1j+1}}{n_{1j}} = \frac{1}{n_e}\, 2\, \frac{g_{1j+1}}{g_1}\left(\frac{2\pi mkT}{h^2}\right)^{3/2} e^{-E_{ion}/kT}$$

Saha eq., 1920

- ratio (i.e., ionization) grows with T (clear!)
  falls with n_e (recomb.!)

- generalization for arbitrary levels:
  calcultate n_{1j}, then $n_{ij} = n_{1j}\frac{g_{ij}}{g_{1j}} e^{-E_{ij}/kT}$

- all levels

$$N_j = \sum_{i=1}^{\infty} n_{ij}, \quad N_{j+1} = \sum_{i=1}^{\infty} n_{ij+1}$$

- Boltzmann excitation

$$\sum_{i=1}^{\infty} n_{ij} = \frac{n_{1j}}{g_{1j}} \underbrace{\sum_{i=1}^{\infty} g_{ij}\, e^{-E_{ij}/kT}}_{U_j(T) \text{ partition function}} = N_j$$

$$\Rightarrow \frac{n_{1j}}{g_{1j}} = \frac{N_j}{U_j(T)}, \quad \frac{n_{1j+1}}{g_{1j+1}} = \frac{N_{j+1}}{U_{j+1}(T)}$$

$$\Rightarrow \boxed{\frac{N_{j+1}\cdot n_e}{N_j} = \left(\frac{2\pi mkT}{h^2}\right)^{3/2} 2\, \frac{U_{j+1}(T)}{U_j(T)}\, e^{-E_{ion}/kT}}$$

Note: Summation in partition function until finite maximum, to account for extent of atom

$$\frac{4\pi}{3} r_{MAX}^3 = \Delta V = \frac{1}{N}$$

example hydrogen $r_i = a_0 i^2 = r_{MAX} \Rightarrow i_{MAX}$

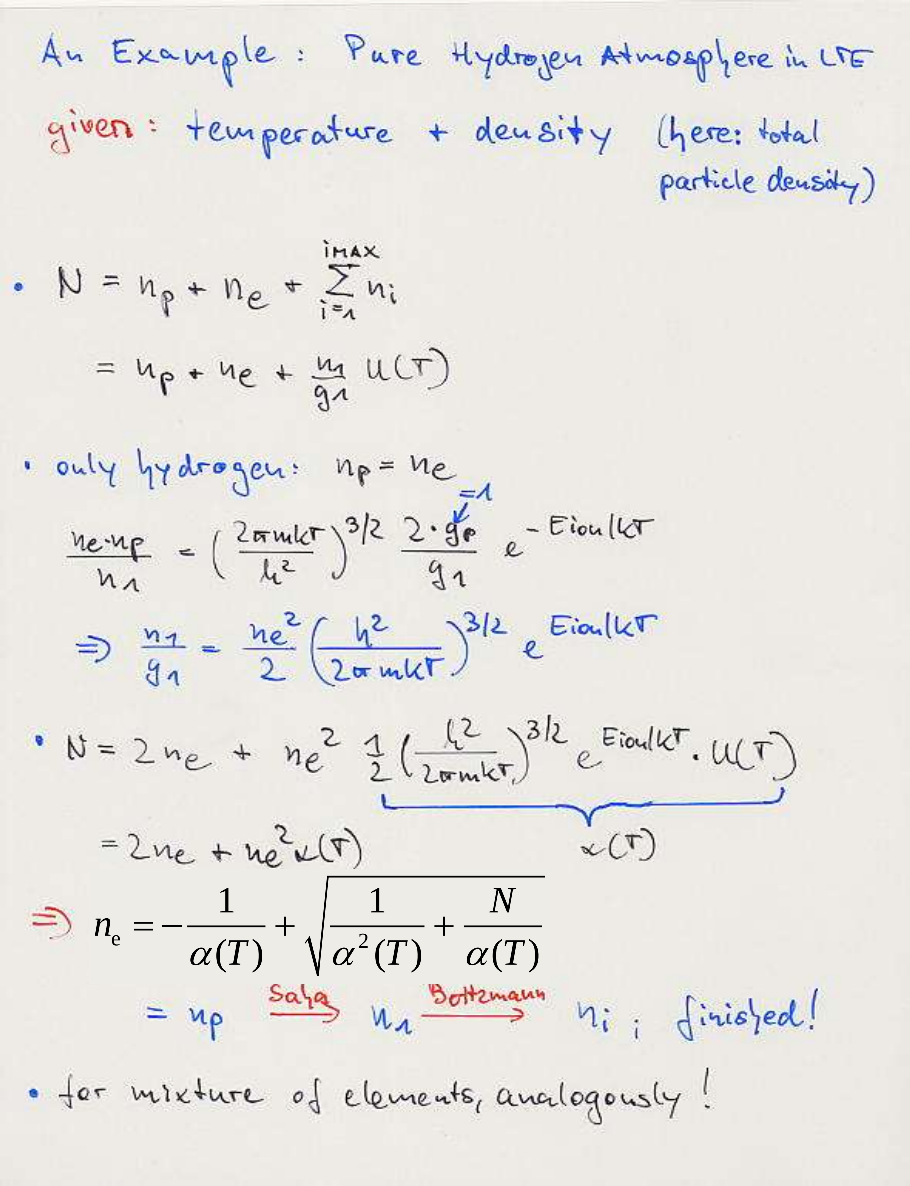

An Example: Pure Hydrogen Atmosphere in LTE

given: temperature + density (here: total particle density)

- $$N = n_p + n_e + \sum_{i=1}^{i\text{MAX}} n_i$$
  $$= n_p + n_e + \frac{n_1}{g_1} U(T)$$

- only hydrogen: $n_p = n_e$
  $$\frac{n_e \cdot n_p}{n_1} = \left(\frac{2\pi m k T}{h^2}\right)^{3/2} \frac{2 \cdot \overset{=1}{g_p}}{g_1} e^{-E_{ion}/kT}$$
  $$\Rightarrow \frac{n_1}{g_1} = \frac{n_e^2}{2}\left(\frac{h^2}{2\pi m k T}\right)^{3/2} e^{E_{ion}/kT}$$

- $$N = 2n_e + n_e^2 \underbrace{\frac{1}{2}\left(\frac{h^2}{2\pi m k T}\right)^{3/2} e^{E_{ion}/kT} \cdot U(T)}_{\alpha(T)}$$
  $$= 2n_e + n_e^2 \alpha(T)$$

$$\Rightarrow n_e = -\frac{1}{\alpha(T)} + \sqrt{\frac{1}{\alpha^2(T)} + \frac{N}{\alpha(T)}}$$

$$= n_p \xrightarrow{\text{Saha}} n_1 \xrightarrow{\text{Boltzmann}} n_i \; ; \text{ finished!}$$

- for mixture of elements, analogously!

LTE bf and ff opacities for hydrogen

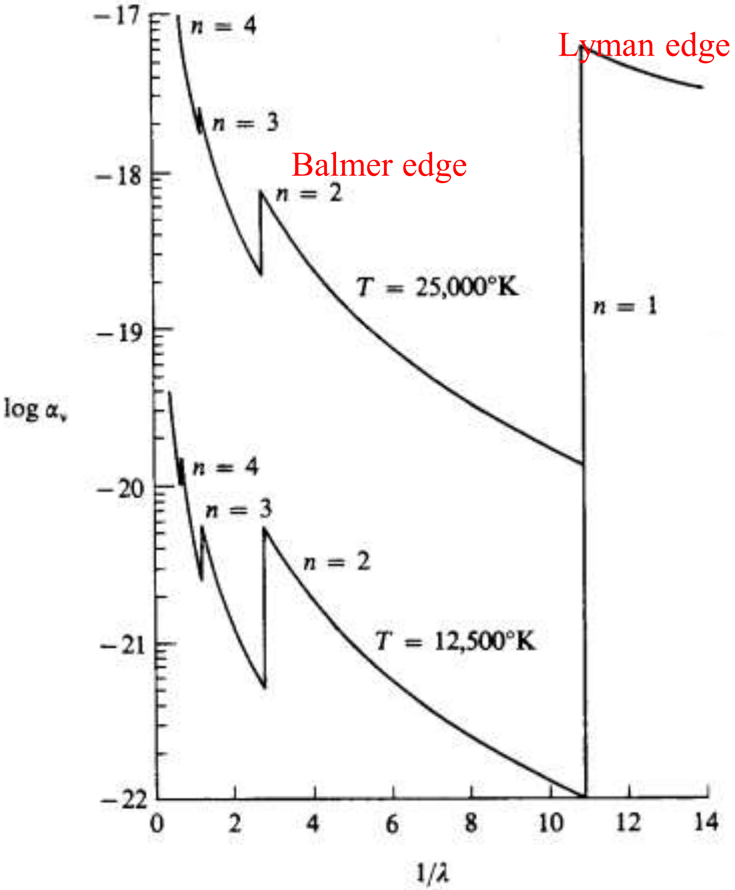

FIGURE 4-1
Opacity from neutral hydrogen at $T = 12{,}500$°K and $T = 25{,}000$°K, in LTE; photoionization edges are labeled with the quantum number of state from which they arise/neutral atom
Ordinate: sum of bound–free and free–free opacity in cm^2/atom; *abscissa*: $1/\lambda$ where λ is in microns.

LTE and NLTE

(L)TE: for **each process**, there exists an inverse process with **identical transition rate**

LTE = ‘detailed balance’ for all processes!

processes = radiative + collisional

- **collisional** processes (and those which are essentially collisional in character, e.g., radiative recombination, ff-emission) in detailed balance, if velocity distribution of colliding particles is **Maxwellian** **(valid in stellar atm., see below)**
- **radiative** processes: photoionization, photoexcitation (= bb absorption) in detailed balance only if radiation field **Planckian** and **isotropic** **(approx. valid only in innermost atmosphere)**

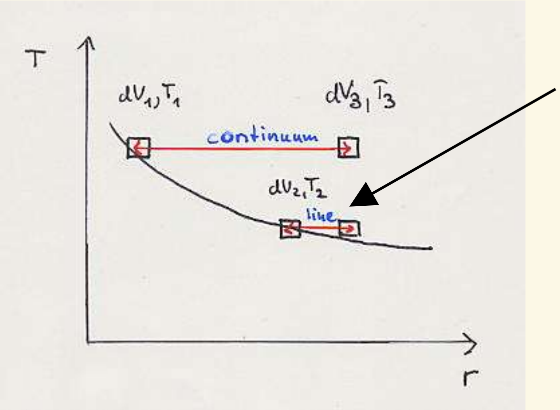

$J_\nu(r) = W(r)\, B_\nu$

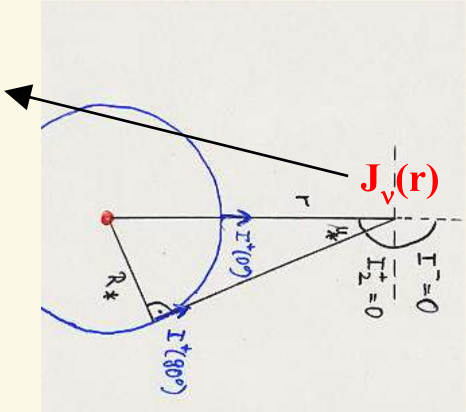

radiative processes couple regions with different temperatures, as a function of frequency: $\Delta\tau_\nu \le 1$

anisotropy

Question: is f(v) dv Maxwellian?

- elastic collisions -> establish equilibrium
- inelastic collisions/recombinations disturb equilibrium
  inelastic collisions: involve electrons only in certain velocity ranges, tend to shift them to lower velocities
  recombinations : remove electrons from the pool, prevent further elastic collisions

- can be shown: in *typical* stellar plasmas, t_{el} / t_{rec} ≈ $10^{-5} \ldots 10^{-7}$ ≈ t_{el} / t_{inel}
  => Maxwellian distribution

- under certain conditions (solar chromosphere, corona), certain deviations in high-energy tail of distribution possible

Question: is T(electron) = T(atom/ion)?

- equality can be proven for stellar atmospheres with 5,000 K < Te < 100,000 K

When is LTE valid???

roughly: electron collisions $\propto n_e T^{1/2}$ >> photoabsorption rates $\propto I_\nu (T) \propto T^x,\ x \geq 1$

LTE: T low, n_e high dwarfs (giants), late B and cooler
NLTE: T high, n_e low all supergiants + rest

however: NLTE-effects also in cooler stars, e.g.. iron in sun

TE – LTE – NLTE : a summary

	TE	LTE	NLTE
velocity distribution of particles **Maxwellian (T_e=T_i)**	✓	✓	✓
excitation **Boltzmann**	✓	✓	no
ionization **Saha**	✓	✓	no
source function	$B_\nu(T)$	$B_\nu(T)$, except scattering component	only $S_\nu^{ff} = B_\nu(T)$
radiation field	$J_\nu = B_\nu(T)$	$J_\nu \neq B_\nu(T)$, equality only for $\tau_\nu \geq \left(\frac{1}{\varepsilon_\nu}\right)^{1/2}$	$J_\nu \neq B_\nu(T)$ dito

Kinetic equilibrium

NLTE – Kinetic equilibrium (or statistical equilibrium)

- do NOT use Saha-Boltzmann, however calculate occupation numbers by assuming statistical equilibrium
- for stationarity ($\partial/\partial t = 0$) and as long as kinematic time-scale >> atomic transition time scales (usually valid)

$$\boxed{\sum_{j\neq i} n_i P_{ij} = \sum_{j\neq i} n_j P_{ji}} \qquad \forall i$$

n_i: occupation number (atomic species, ionization stage, level)

P_{ij} transitionrate from level $i \rightarrow j$ (dim $P_{ij} = s^{-1}$)

- in words: the number of all possible transitions from level i into other states j is balanced by the number of transitions from all other states j into level i.

⇒ linear equation system for n_i, has to be closed by abundance equation

$$\sum n_{ik} = n_k$$

if n_{ik} the occupation numbers of species k and n_k the total particle density of k

Transition rates

- collisional processes bb, ionization/rec.
- radiative processes bb, ionization/rec.

Radiative processes depend on radiation field
radiation field depends on opacities
opacities depend on occupation numbers

Iteration required!

... no so easy, however possible

Note: to obtain reliable results, order of

30 species
3-5 ionizationstages / species
20...1000 level / ion
100,000... some 10^6 transitions
to be considered in parallel

requires large data base of atomic quantities (energies, transitions, cross sections)
fast algorithm to calculate radiative transfer!

Solution of the rate equations – a simple example

HAD: for each atomic level, the sum of all populations must be equal to the sum of all depopulations (for stationary situations)

example: 3-niveau atom with continuum

assume: all rate coefficients are known (i.e., also the radiation field)

=> rate equations (equations of statistical equilibrium)

$$-n_1\left[R_{1k}+C_{1k}+R_{12}+C_{12}+R_{13}+C_{13}\right]+n_2(R_{21}+C_{21})+n_3(R_{31}+C_{31})+n_k(R_{k1}+C_{k1})=0$$

$$n_1(R_{12}+C_{12})-n_2\left[R_{2k}+C_{2k}+R_{21}+C_{21}+R_{23}+C_{23}\right]+n_3(R_{32}+C_{32})+n_k(R_{k2}+C_{k2})=0$$

$$n_1(R_{13}+C_{13})+n_2(R_{23}+C_{23})-n_3\left[R_{3k}+C_{3k}+R_{31}+C_{31}+R_{32}+C_{32}\right]+n_k(R_{k3}+C_{k3})=0$$

$$n_1(R_{1k}+C_{1k})+n_2(R_{2k}+C_{1k})+n_3(R_{3k}+C_{1k})-n_k\left[R_{k1}+C_{k1}+R_{k2}+C_{k2}+R_{k3}+C_{k3}\right]=0$$

with

R_{ij},	radiative bound-bound transitions (lines!)	C_{ij}	collisional bound-bound transitions
R_{ik}	radiative bound-free transitions (ionizations)	C_{ik}	collisional bound-free transitions
R_{ki}	radiative free-bound transitions (recombinations)	C_{ki}	collisonal free-bound transitions

in matrix representation =>

$$P = \underbrace{\begin{pmatrix} -(R_{1k}+C_{1k}+R_{12}+C_{12}+R_{13}+C_{13}) & (R_{21}+C_{21}) & (R_{31}+C_{31}) & (R_{k1}+C_{k1}) \\ (R_{12}+C_{12}) & -(R_{2k}+C_{2k}+R_{21}+C_{21}+R_{23}+C_{23}) & (R_{32}+C_{32}) & (R_{k2}+C_{k2}) \\ (R_{13}+C_{13}) & (R_{23}+C_{23}) & -(R_{3k}+C_{3k}+R_{31}+C_{31}+R_{32}+C_{32}) & (R_{k3}+C_{k3}) \\ (R_{1k}+C_{1k}) & (R_{2k}+C_{2k}) & (R_{3k}+C_{3k}) & -(R_{k1}+C_{k1}+R_{k2}+C_{k2}+R_{k3}+C_{k3}) \end{pmatrix}}_{\text{rate matrix, diagonal elements sum of all depopulations}}$$

$$P * \begin{pmatrix} n_1 \\ n_2 \\ n_3 \\ n_4 (= n_k) \end{pmatrix} = \begin{pmatrix} 0 \\ 0 \\ 0 \\ 0 \end{pmatrix}$$

Rate matrix is singular, since, e.g., last row linear combination of other rows (negative sum of all previous rows)

THUS: LEAVE OUT arbitrary line (mostly the last one, corresponding to ionization equilibrium) and REPLACE by inhomogeneous, linearly independent equation for all n_i, to obtain unique solution

particle number conservation for considered atom:

$$\sum_{i=1}^{N} n_i = \alpha_k N_{\mathrm{H}},$$ with α_{k} the abundance of element k

NOTE 1: numerically stable equation solver required, since typically hundreds of levels present, and (rate-) coefficients of highly different orders of magnitude

NOTE 2: occupation numbers n_i depend on radiation field (via radiative rates),
and radiation field depends (non-linearly) on n_i (via opacities and emissivities)
=> Clever iteration scheme required!!!!

Example for extreme NLTE condition
Nebulium (= [OIII] 5007, 4959) in Planetary Nebulae

mechanism suggested by *I. Bowen* (1927):

- low-lying meta-stable levels of OIII(2.5 eV) **collisionally excited** by free electrons (resulting from photoionization of hydrogen via "hot", *diluted* radiation field from central star)
- Meta-stable levels become **strongly populated**
- **radiative decay** results in **very strong** [OIII] emission lines
- impossible to observe suggested process in laboratory, since *collisional deexitation* (no photon emitted)) *much stronger than radiative decay under terrestrial conditions.*
- Thus, after detection new element proposed , "nebulium"

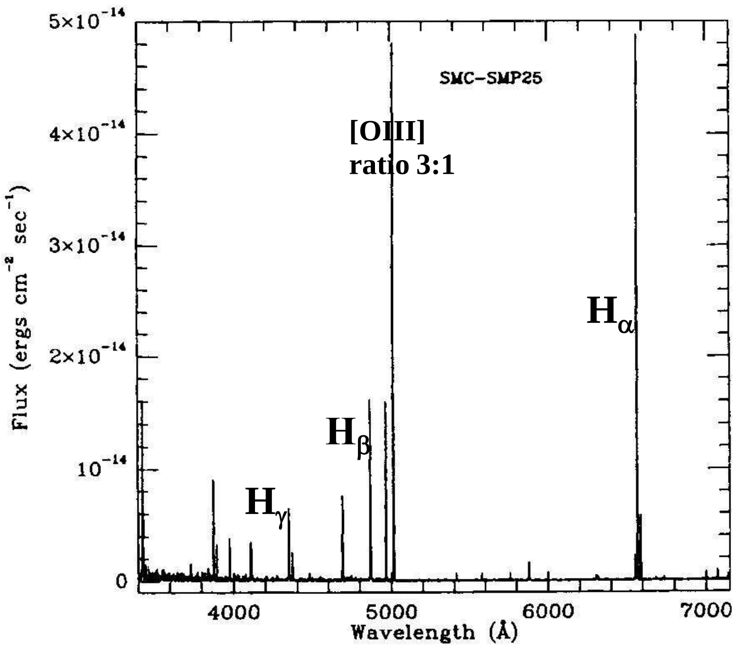

FIG. 1a

Condition for radiative decay

NOTE: $\mathrm{A_{ml}} \le 10^{-2}$ (typical values are 10^7)

$n_m A_{ml} \gg n_m n_e q_{ml}(T_e)$, with metastable level m

$\rightarrow n_e \ll n_e(\text{crit})$,

$$n_e(\text{crit}) = \frac{A_{ml}}{q_{ml}(T_e)}, \quad \mathrm{q_{ml}} = 8.63 \cdot 10^{-6} \frac{\Omega(l,m)}{g_m \sqrt{T_e}}$$

$\Omega(l,m)$ collisional strength, order unity

for typical temperatures $T_e \approx 10{,}000\mathrm{K}$ and [OIII] 5007,

we have $n_e(\text{crit}) \approx 4.9 \cdot 10^5 \mathrm{cm}^{-3}$,

much larger than typical nebula densities

Intermezzo: Stellar Atmospheres in practice

A tour de modeling and analysis of stellar atmospheres throughout the HRD

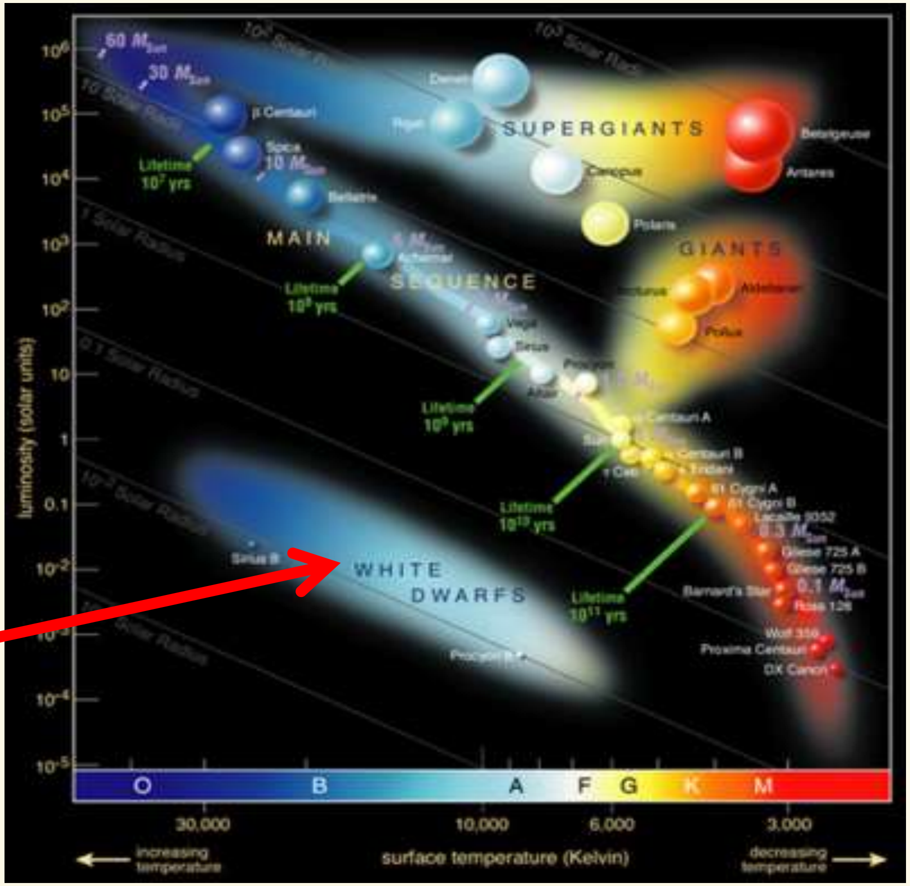

except for
white dwarfs

Stellar Atmospheres in practice

Some different types of stars…

Hot luminous stars:
Massive, main-sequence (MS, ~10 R_{sun}) or evolved, (~20 … 100 R_{sun}).
Strong, fast stellar winds

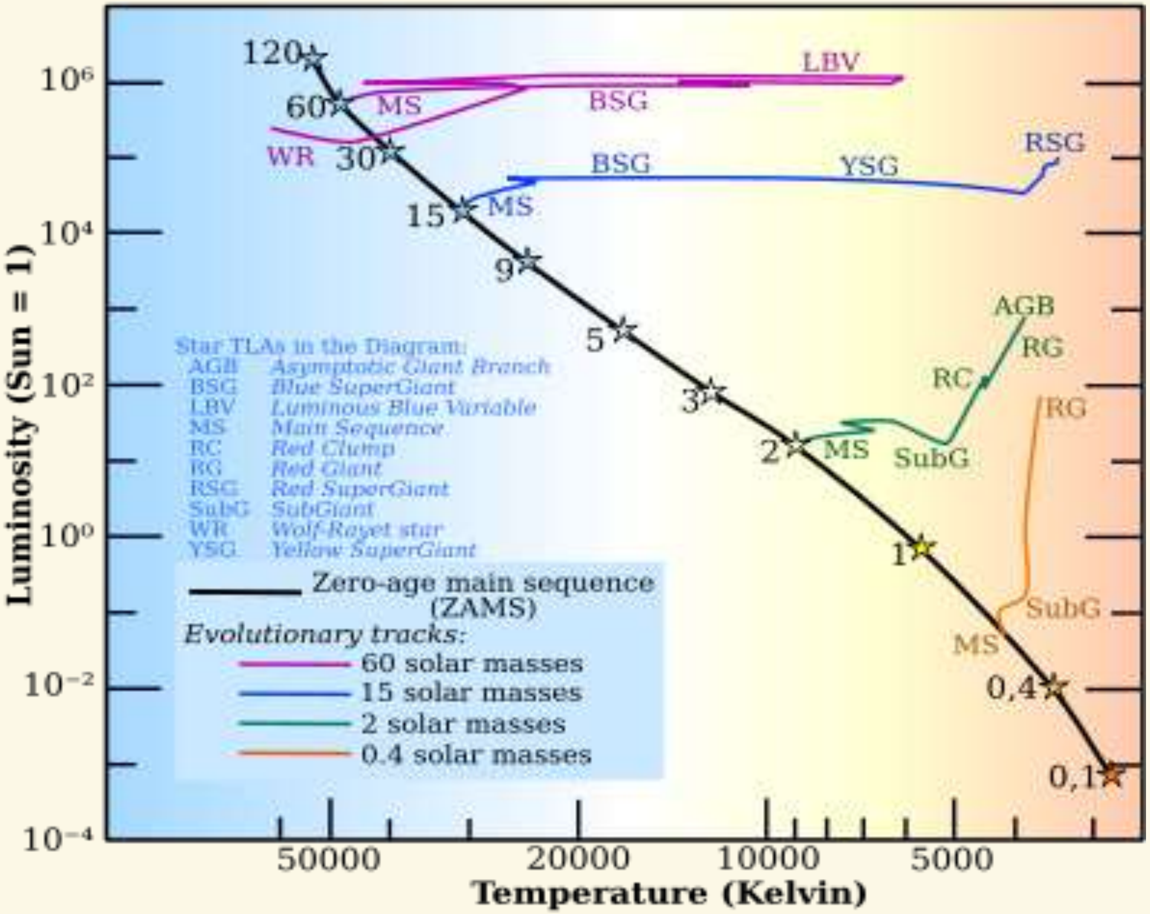

Cool, luminous stars (RSG, AGB):
Massive or low/intermediate mass, evolved, several 100 (!) R_{sun}.
Strong, slow stellar winds

Solar-type stars:
Low-mass, on or near MS, hot surrounding coronae, weak stellar winds
(e.g., solar wind)

Stellar Atmospheres in practice

A tour de modeling and analysis of stellar atmospheres throughout the HRD

Different regimes require different key input physics and assumptions

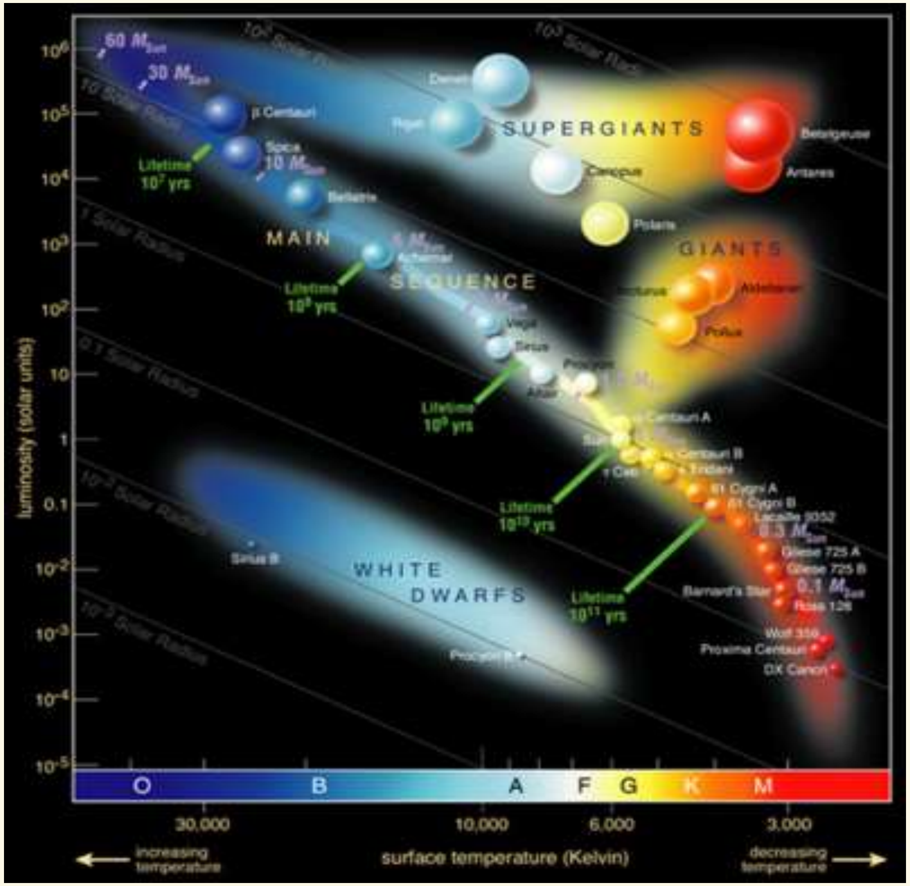

- LTE or NLTE
- Spectral line blocking/blanketing
- (sub-) Surface convection
- Geometry and dimensionality
- Velocity fields and outflows

Stellar Atmospheres in practice

Spectroscopy and Photometry

ALSO:
Analysis
of different
WAVELENGTH
BANDS
is different

(X-ray, UV,
optical, infra-
red...)

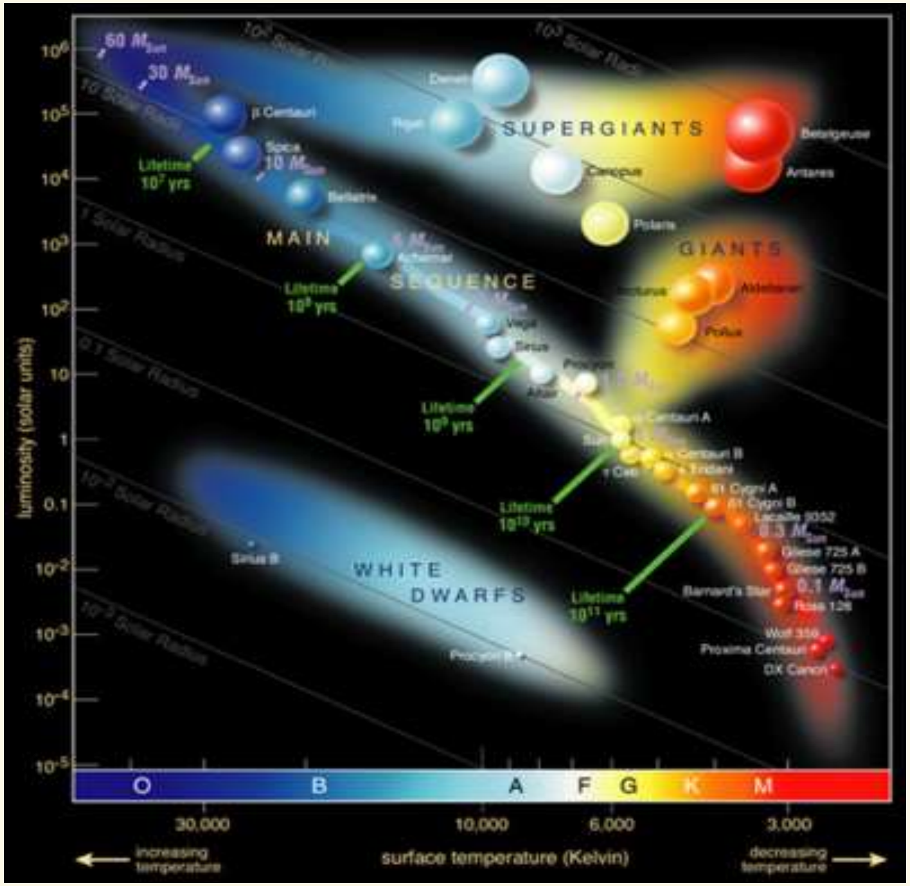

Depends on where in atmosphere light escapes from

Question: Why is this "formation depth" different for different wavebands and diagnostics?

Spectroscopy/photometry (see Chap. 2)

…gives insight into and understanding of our cosmos

- provides
  - stellar properties, mass, radius, luminosity, energy production, chemical composition, properties of outflows
  - properties of (inter) stellar plasmas, temperature, density, excitation, chemical comp., magnetic fields
- INPUT for stellar, galactic and cosmologic evolution and for stellar and galactic structure
- requires
  - plasma physics, plasma is "normal" state of atmospheres and interstellar matter (plasma diagnostics, line broadening, influence of magnetic fields,…)
  - atomic physics/quantum mechanics, interaction light/matter (micro quantities)
  - radiative transfer, interaction light/matter (macroscopic description)
  - thermodynamics, thermodynamic equilibria: TE, LTE (local), NLTE (non-local)
  - hydrodynamics, atmospheric structure, velocity fields, shockwaves,…

Stellar Atmospheres in practice

Spectroscopy (see Chap. 2)

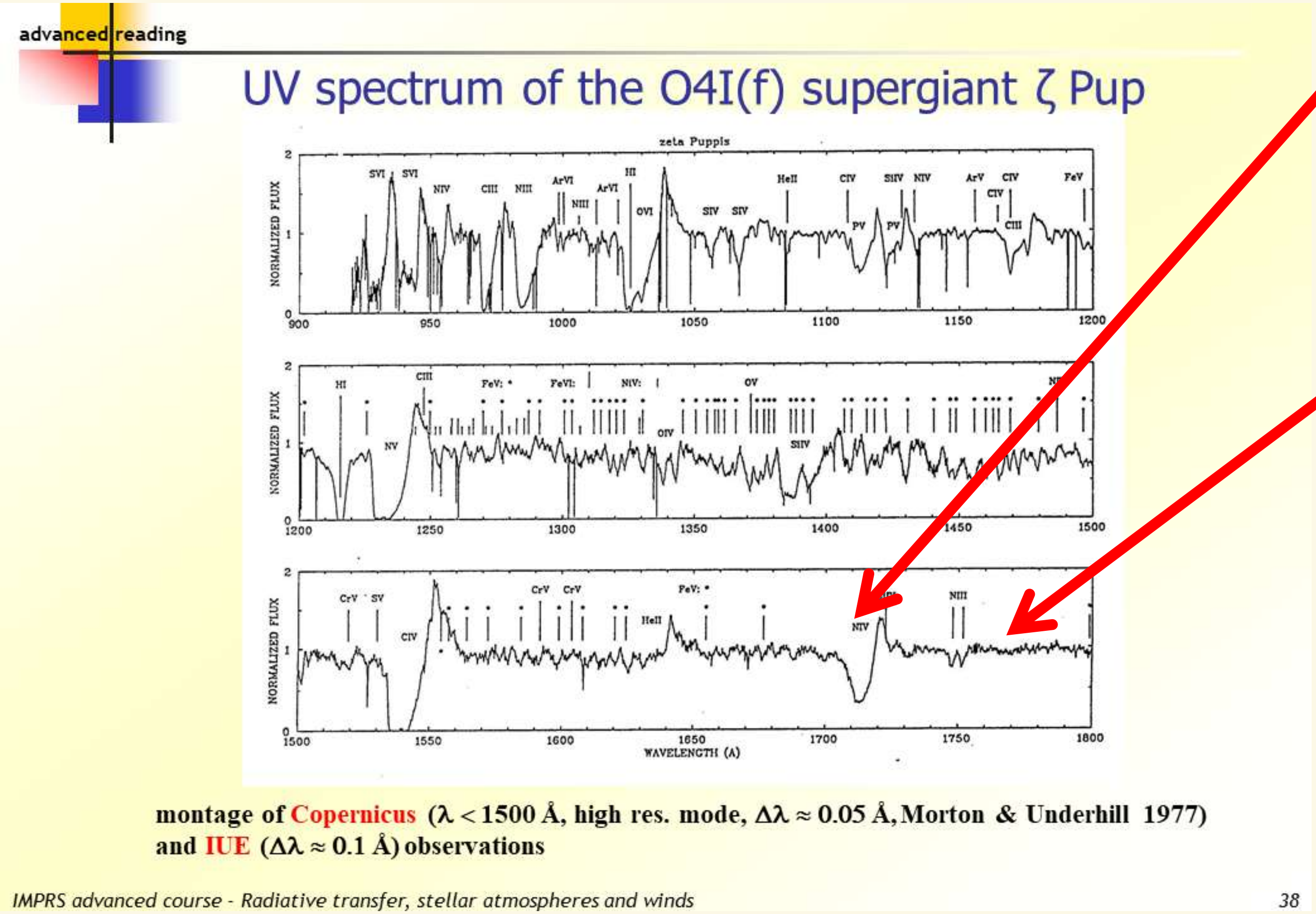

advanced reading

UV spectrum of the O4I(f) supergiant ζ Pup

montage of Copernicus ($\lambda < 1500$ Å, high res. mode, $\Delta\lambda \approx 0.05$ Å, Morton & Underhill 1977) and IUE ($\Delta\lambda \approx 0.1$ Å) observations

IMPRS advanced course - Radiative transfer, stellar atmospheres and winds 38

UV "P-Cygni" lines formed in rapidly accelerating, hot stellar winds

(quasi-) continuum formed in (quasi-) hydrostatic photosphere

Stellar Atmospheres in practice

Spectroscopy

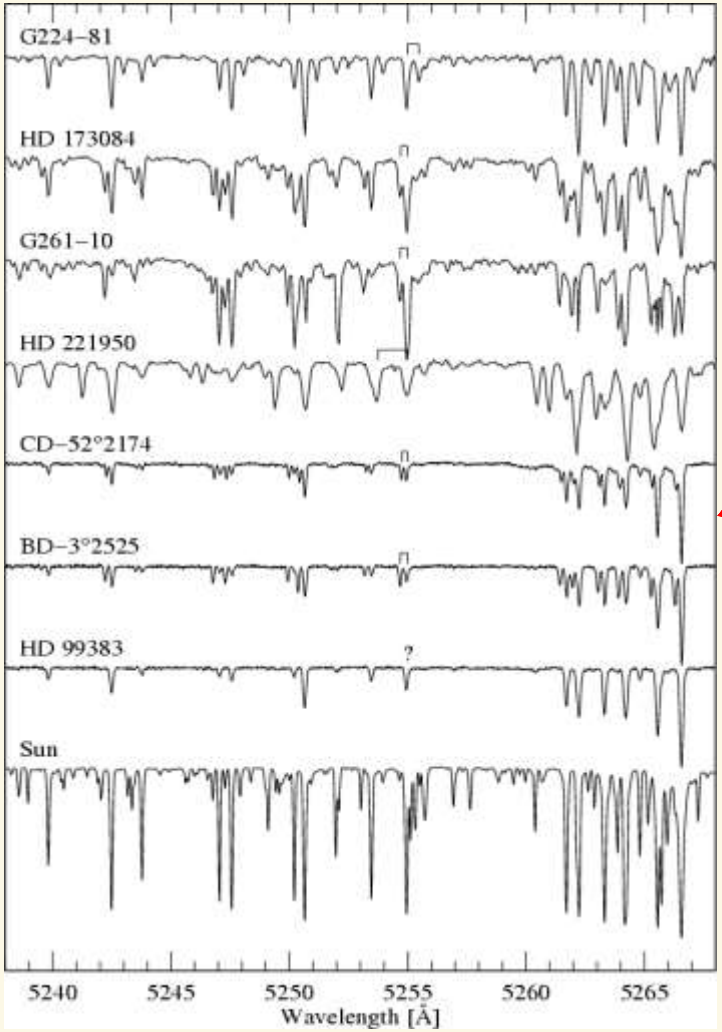

Lines and continuum in the optical around 5200 Å, in cool, solar-type stars, formed in the photosphere

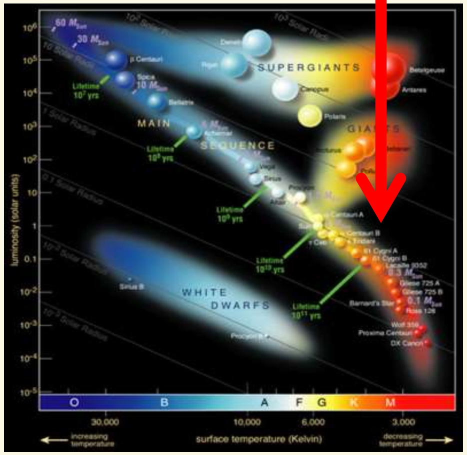

Stellar Atmospheres in practice

Spectroscopy

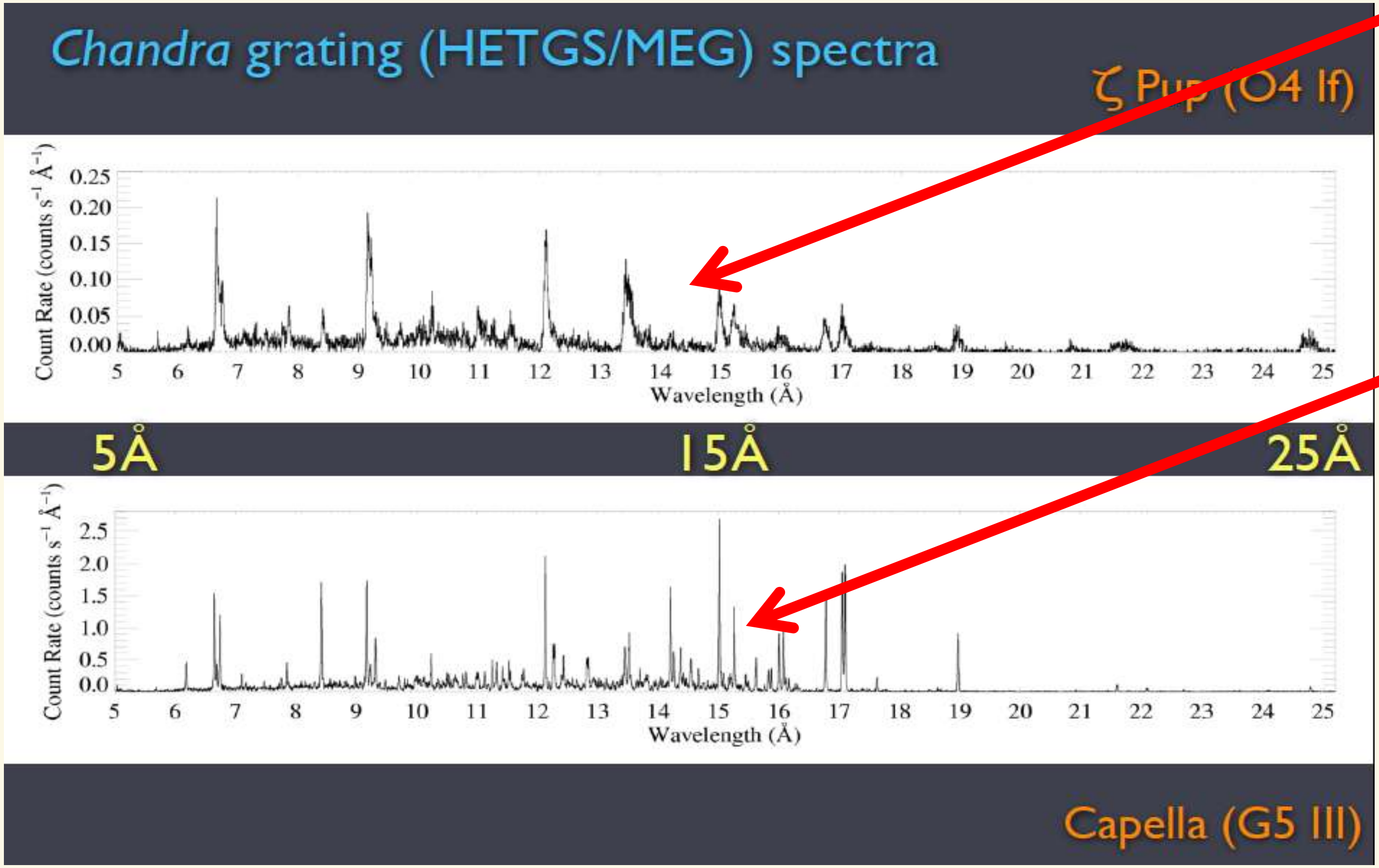

X-rays from hot stars, formed in shocks in stellar wind

X-rays from cool stars, formed in hot coronae

Stellar Atmospheres in practice

A tour de modeling and analysis of stellar atmospheres throughout the HRD

Stellar Winds (see Chap. 8)

KEY QUESTION: What provides the force able to overcome gravity?

$$\dot{M} \approx 10^{-4} ... 10^{-8} M_{\odot} / yr$$

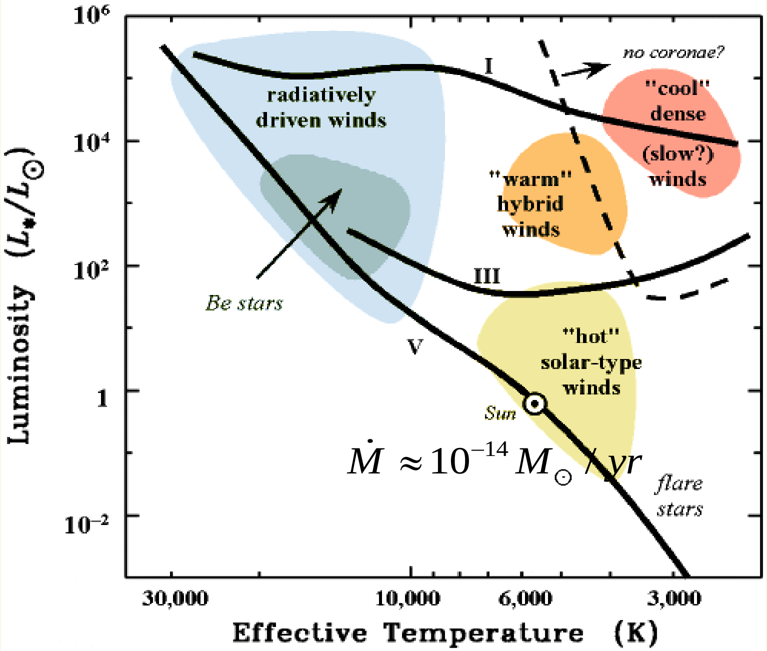

- LTE or NLTE
- Spectral line blocking/blanketing
- (sub-) Surface convection
- Geometry and dimensionality
- Velocity fields and outflows

Stellar Atmospheres in practice

A tour de modeling and analysis of stellar atmospheres throughout the HRD

KEY QUESTION: What provides the force able to overcome gravity?

Pressure gradient
in hot coronae of solar-type stars

Radiation force:
Dust scattering
(in pulsation-levitated material, see Chap. 8)
in cool AGB stars
(e.g., S. Höffner+)

Same mechanism in cool RSGs?

$$\dot{M} \approx 10^{-4} \ldots 10^{-8} M_{\odot} / yr$$

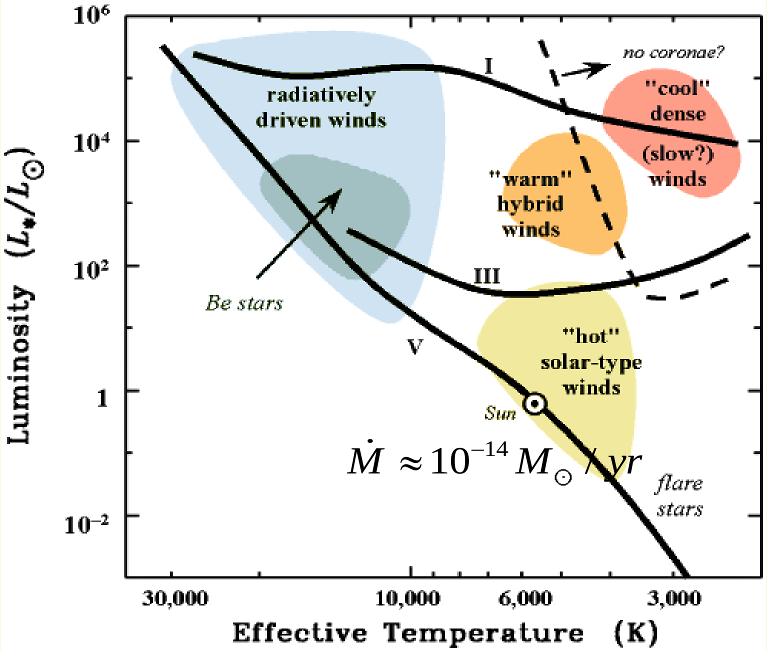

- LTE or NLTE
- Spectral line blocking/blanketing
- (sub-) Surface convection
- Geometry and dimensionality
- Velocity fields and outflows

Stellar Atmospheres in practice

A tour de modeling and analysis of stellar atmospheres throughout the HRD

KEY QUESTION: What provides the force able to overcome gravity?

Radiation force:

line scattering in hot, luminous stars (e.g., J. Sundqvist+, A. Sander+)
more to follow in Chap. 8

$$\dot{M} \approx 10^{-4} \ldots 10^{-8} M_{\odot} / yr$$

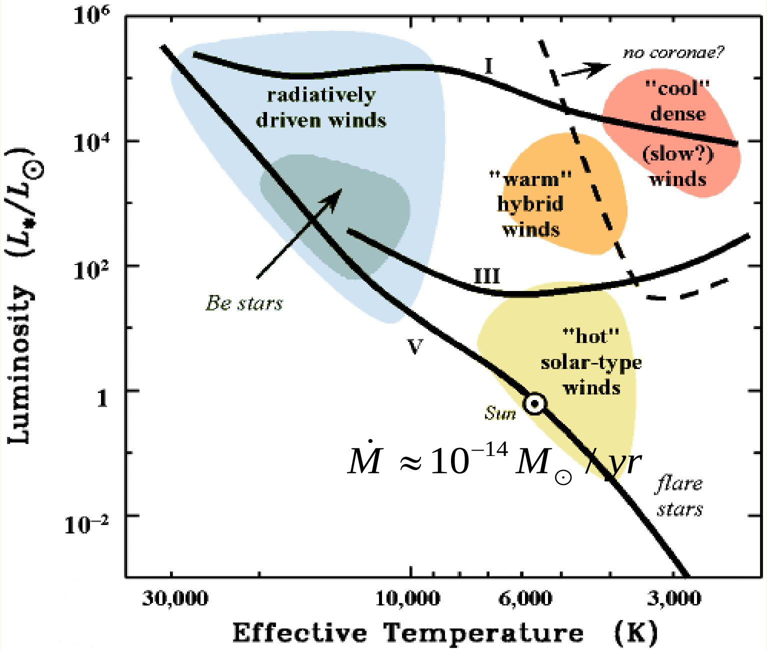

$$\dot{M} \approx 10^{-14} M_{\odot} / yr$$

- LTE or NLTE
- Spectral line blocking/blanketing
- (sub-) Surface convection
- Geometry and dimensionality
- Velocity fields and outflows

Question: How do you think the high mass loss of stars with high luminosities affects the evolution of the star and its surroundings?

Stellar Atmospheres in practice

from introductory slides …

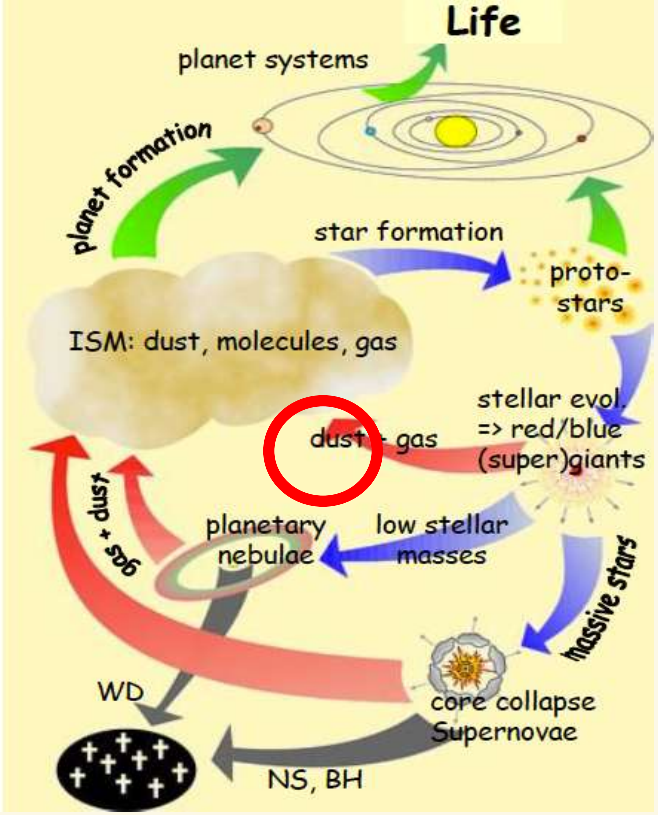

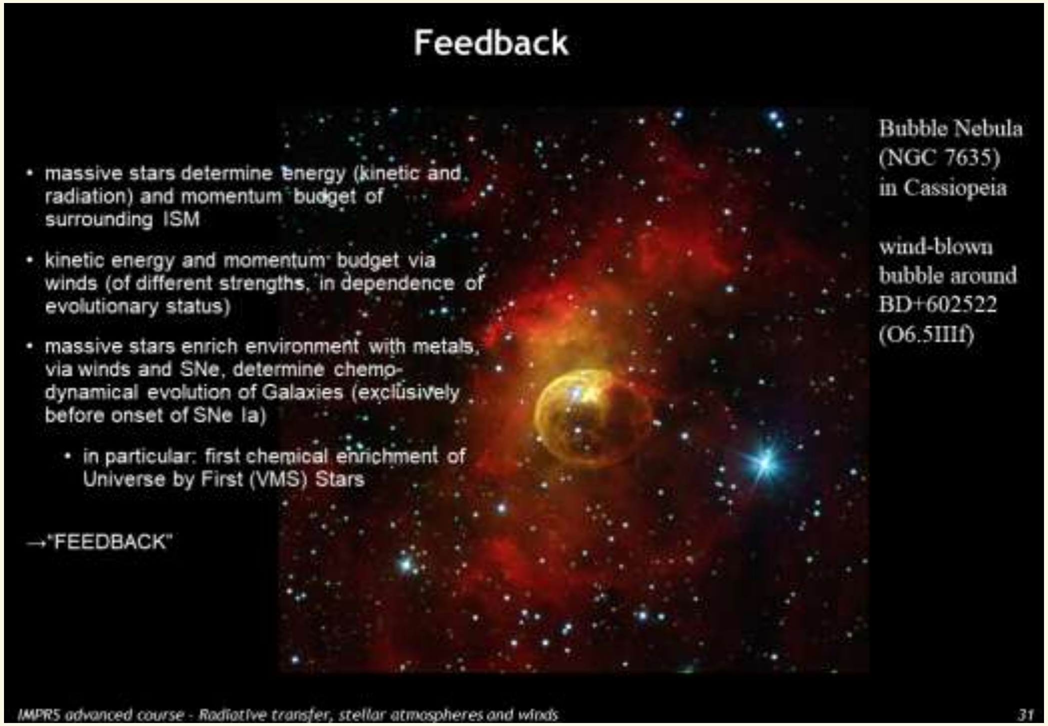

Feedback

- massive stars determine energy (kinetic and radiation) and momentum budget of surrounding ISM
- kinetic energy and momentum budget via winds (of different strengths, in dependence of evolutionary status)
- massive stars enrich environment with metals, via winds and SNe, determine chemo-dynamical evolution of Galaxies (exclusively before onset of SNe Ia)
  - in particular: first chemical enrichment of Universe by First (VMS) Stars

→"FEEDBACK"

Bubble Nebula (NGC 7635) in Cassiopeia

wind-blown bubble around BD+602522 (O6.5IIIf)

IMPRS advanced course - Radiative transfer, stellar atmospheres and winds 31

Stellar Winds from hot/evolved cool stars control evolution/late evolution, and feed the ISM with nuclear processed material

Stellar Atmospheres in practice

A tour de modeling and analysis of stellar atmospheres throughout the HRD

In the following,
we focus on stellar
photospheres

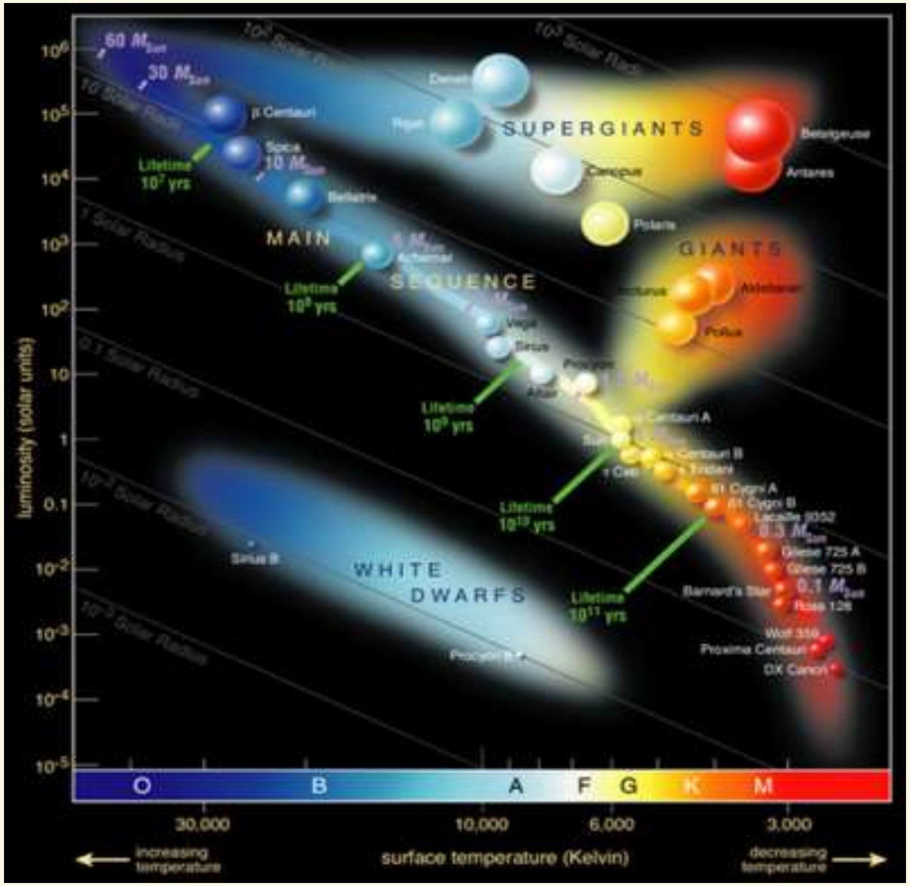

Stellar Atmospheres in practice

From Chap. 6

OBSERVATIONS!!!

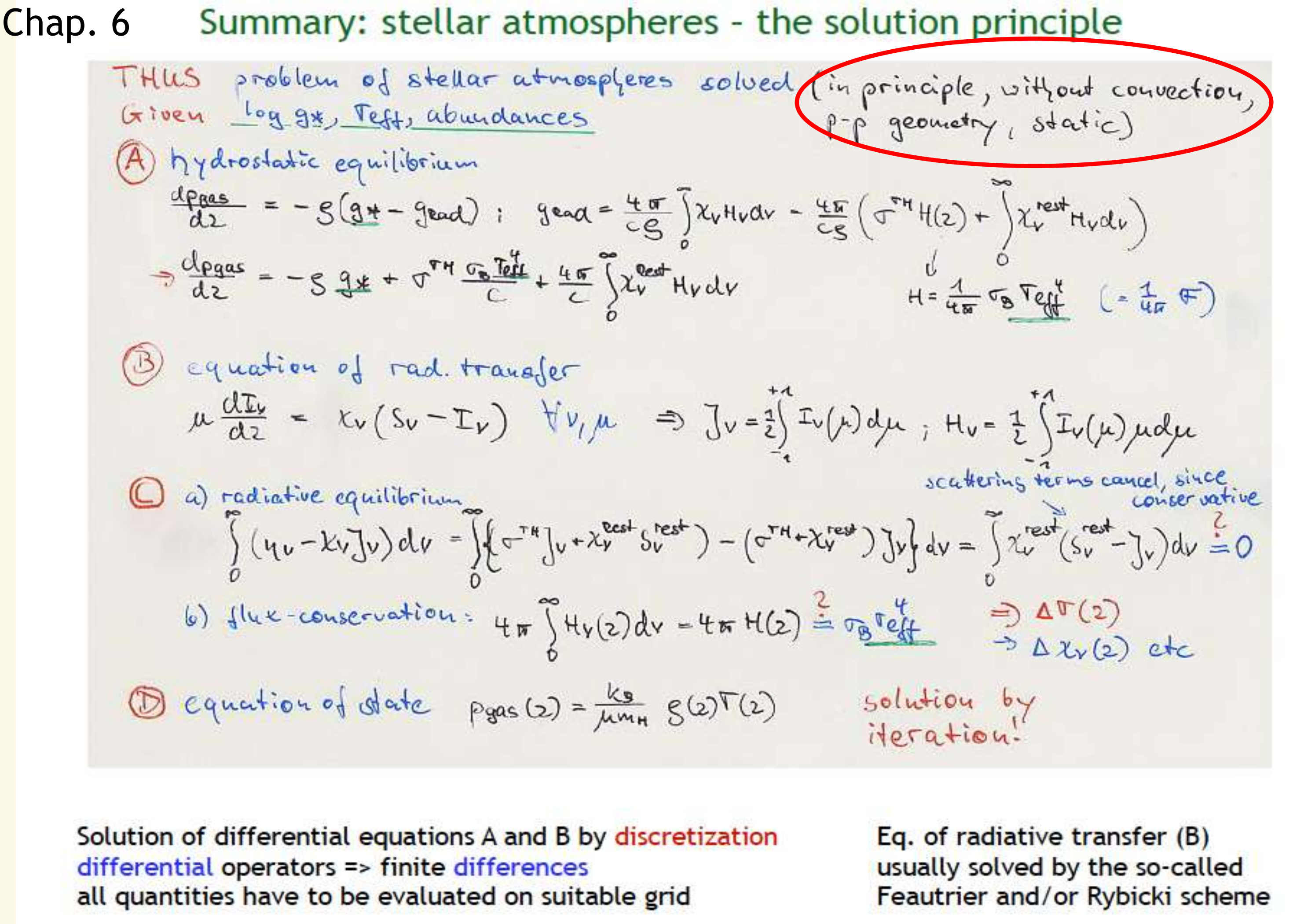

Summary: stellar atmospheres - the solution principle

THUS problem of stellar atmospheres solved (in principle, without convection, p-p geometry, static)

Given log g_*, $T_{\rm eff}$, abundances

Ⓐ hydrostatic equilibrium

$$\frac{dp_{\rm gas}}{dz} = -\rho(g_* - g_{\rm rad})\ ;\quad g_{\rm rad} = \frac{4\pi}{c\rho}\int_0^\infty \chi_\nu H_\nu d\nu = \frac{4\pi}{c\rho}\Big(\sigma^{\rm TH} \underset{\displaystyle\downarrow}{H(z)} + \int_0^\infty \chi_\nu^{\rm rest} H_\nu d\nu\Big)$$

$$\Rightarrow \frac{dp_{\rm gas}}{dz} = -\rho\, g_* + \sigma^{\rm TH}\frac{\sigma_B T_{\rm eff}^4}{c} + \frac{4\pi}{c}\int_0^\infty \chi_\nu^{\rm rest} H_\nu d\nu \qquad H = \frac{1}{4\pi}\sigma_B T_{\rm eff}^4 \quad \Big(= \frac{1}{4\pi}\mathcal{F}\Big)$$

Ⓑ equation of rad. transfer

$$\mu\frac{dI_\nu}{dz} = \chi_\nu(S_\nu - I_\nu) \quad \forall \nu, \mu \quad \Rightarrow J_\nu = \frac{1}{2}\int_{-1}^{+1} I_\nu(\mu)d\mu\ ;\ H_\nu = \frac{1}{2}\int_{-1}^{+1} I_\nu(\mu)\mu d\mu$$

Ⓒ a) radiative equilibrium

scattering terms cancel, since conservative

$$\int_0^\infty (\eta_\nu - \chi_\nu J_\nu)d\nu = \int_0^\infty \{(\sigma^{\rm TH} J_\nu + \chi_\nu^{\rm rest} S_\nu^{\rm rest}) - (\sigma^{\rm TH} + \chi_\nu^{\rm rest}) J_\nu\} d\nu = \int_0^\infty \chi_\nu^{\rm rest}(S_\nu^{\rm rest} - J_\nu)d\nu \overset{?}{=} 0$$

b) flux-conservation:

$$4\pi\int_0^\infty H_\nu(z)d\nu = 4\pi H(z) \overset{?}{=} \sigma_B T_{\rm eff}^4 \qquad \Rightarrow \Delta T(z) \rightarrow \Delta\chi_\nu(z) \text{ etc}$$

Ⓓ equation of state

$$p_{\rm gas}(z) = \frac{k_B}{\mu m_H}\rho(z)T(z)$$

solution by iteration!

Solution of differential equations A and B by discretization
differential operators => finite differences
all quantities have to be evaluated on suitable grid

Eq. of radiative transfer (B)
usually solved by the so-called
Feautrier and/or Rybicki scheme

Stellar Atmospheres in practice

A tour de modeling and analysis of stellar atmospheres throughout the HRD

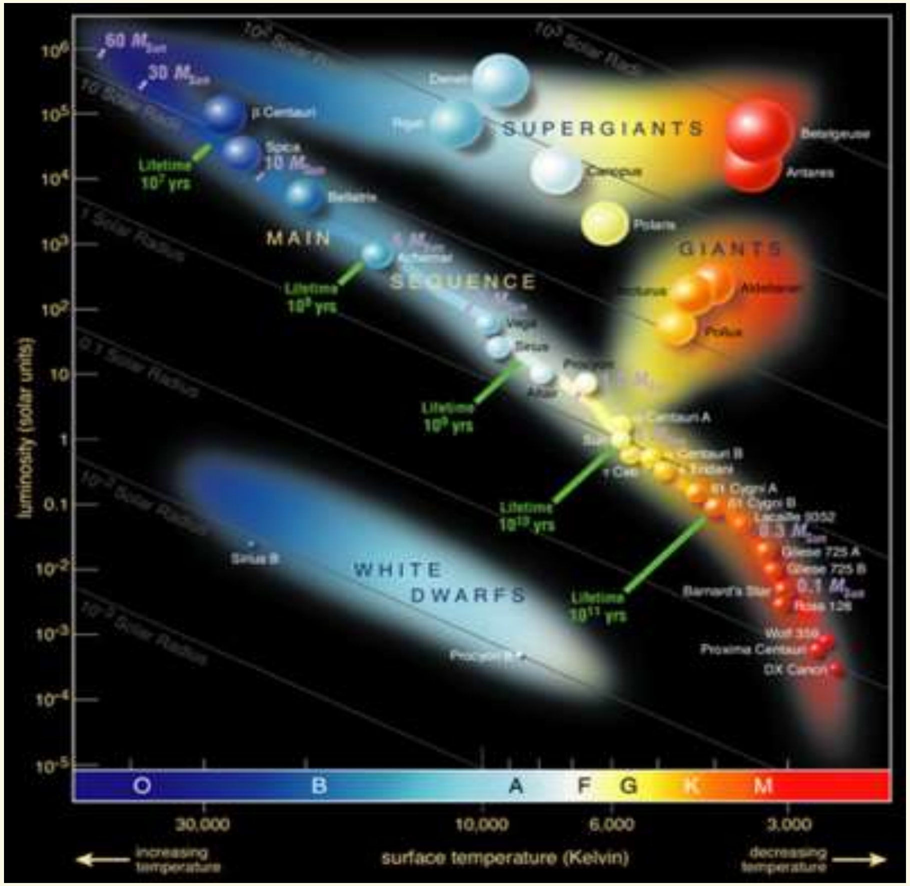

- LTE or NLTE
- Spectral line blocking/blanketing
- (sub-) Surface convection
- Geometry and dimensionality
- Velocity fields and outflows

Stellar Atmospheres in practice

LTE or NLTE? (see Chap. 7)

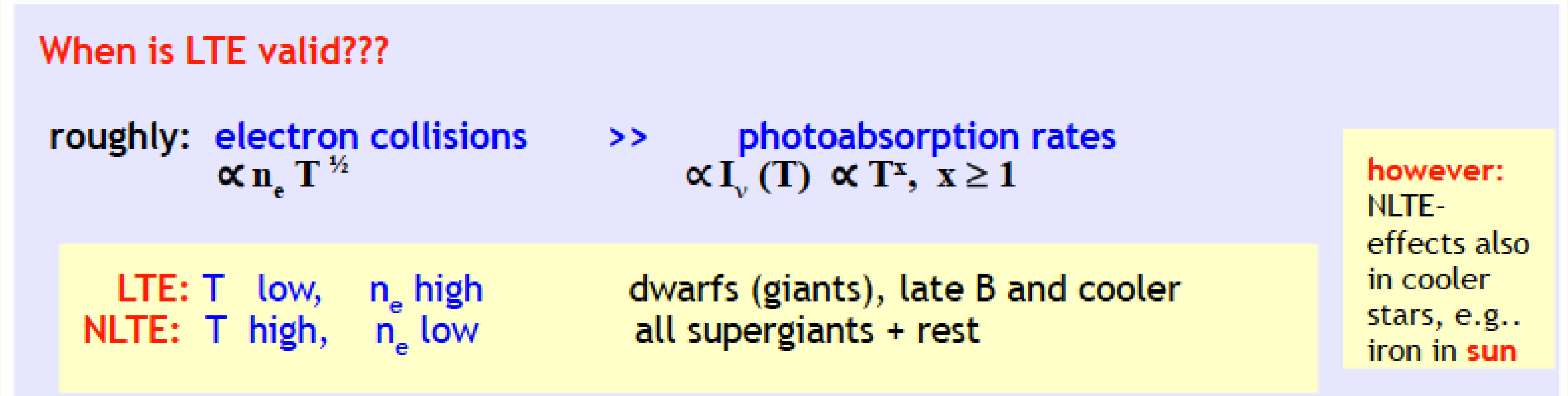

When is LTE valid???

roughly: electron collisions >> photoabsorption rates

$\propto n_e T^{1/2}$ $\propto I_\nu(T) \propto T^x$, $x \geq 1$

LTE: T low, n_e high dwarfs (giants), late B and cooler
NLTE: T high, n_e low all supergiants + rest

however:
NLTE-effects also in cooler stars, e.g.. iron in sun

HOT STARS:

Complete model atmosphere and synthetic spectrum must be calculated in NLTE

NLTE calculations for various applications (including Supernovae remnants) within the expertise of USM

COOL STARS:

Standard to neglect NLTE-effects on atmospheric structure, might be included when calculating line spectra for individual “trace” elements (typically used for chemical abundance determinations), e.g., work by Bergemann+

ALSO: RSGs still somewhat open question

Stellar Atmospheres in practice

A tour de modeling and analysis of stellar atmospheres throughout the HRD

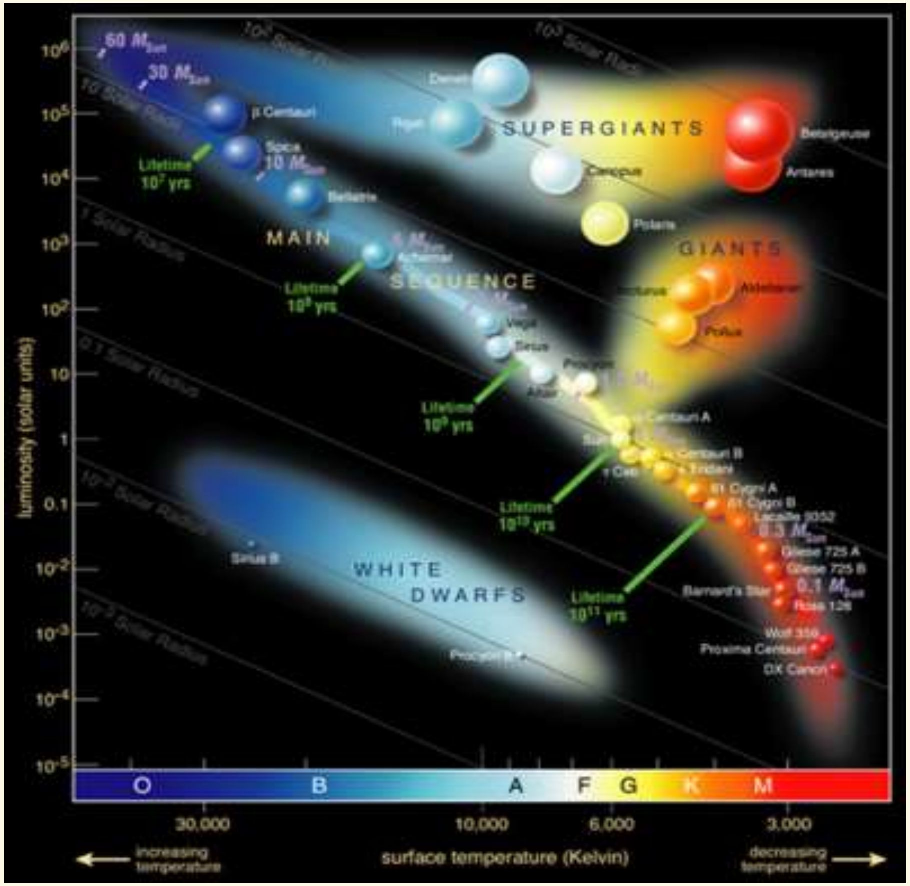

- LTE or NLTE
- Spectral line blocking/blanketing
- (sub-) Surface convection
- Geometry and dimensionality
- Velocity fields and outflows

Stellar Atmospheres in practice

Spectral line blocking/blanketing

- Effects of numerous -- literally millions -- of (primarily metal) spectral lines upon the atmospheric structure and flux distribution
- Q: Why is this tricky business?

Spectral line blocking/blanketing

- Effects of numerous -- literally millions -- of (primarily metal) spectral lines upon the atmospheric structure and flux distribution
- Q: Why is this tricky business?

- Lots of atomic data required (thus atomic physics and/or experiments)
- LTE or NLTE?
- What lines are relevant?
  (i.e., what ionization stages? Are there molecules present?)

Techniques:

Opacity Distribution Functions
Opacity-Sampling
Direct line by line calculations

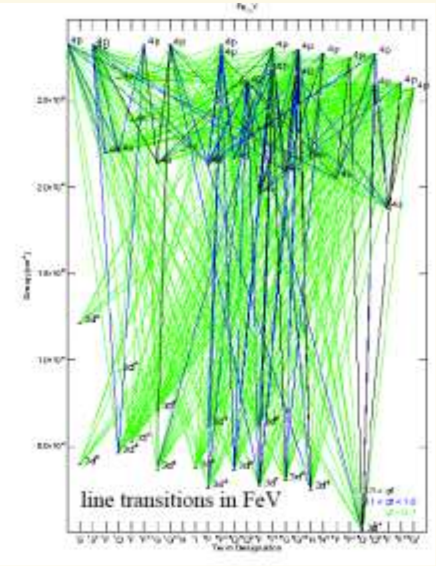

Spectral line blocking/blanketing

Back-warming (and surface-cooling)

Numerous absorption lines
"block" (E)UV radiation flux

Total flux conservation demands
these photons be emitted
elsewhere → redistributed
to optical/infra-red

Lines act as "blanket", whereby
back-scattered line photons
are (partly) thermalized and
thus heat up deeper layers

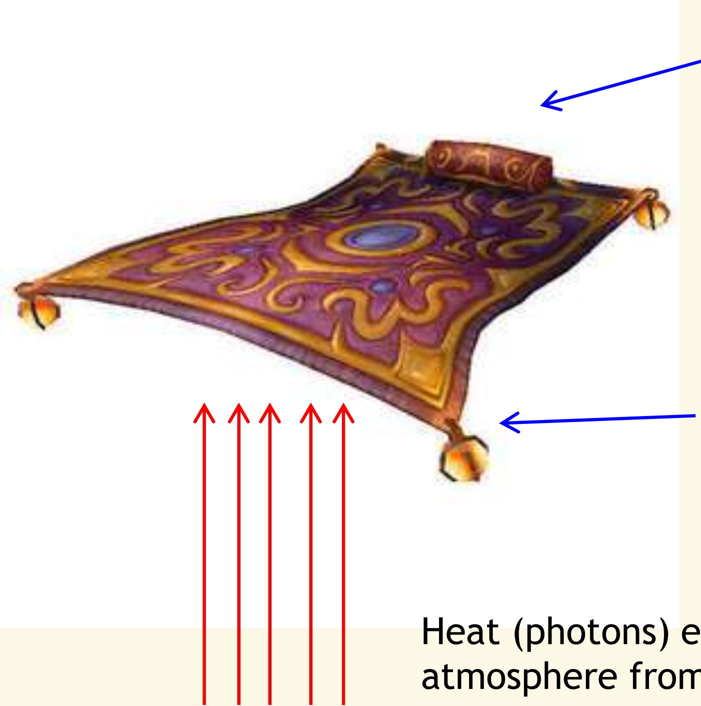

"Blanket" typically cools
uppermost layers

"Blanket" warms deep
layers

Heat (photons) enters
atmosphere from
sub-photospheric layers

Spectral line blocking/blanketing

Back-warming and flux redistribution

…occur in stars of all spectral types

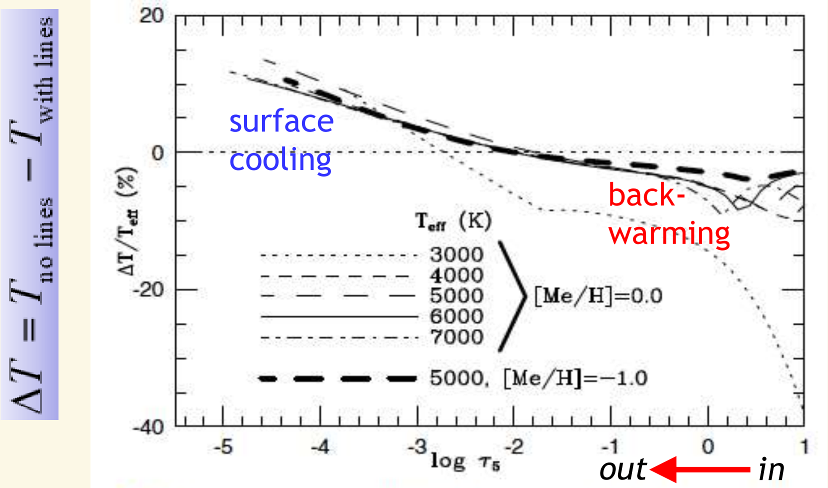

surface cooling

back-warming

out ← in

Fig. 4. The effects of switching off line absorption on the temperature structure of a sequence of models with $\log g = 3.0$ and solar metallicity. Note that $\Delta T \equiv T(\text{nolines}) - T(\text{lines})$. It is seen that the blanketing effects are fairly independent of effective temperature for models with $T_{\text{eff}} \geq 4000$.

Back warming in cool stars
(from Gustafsson et al. 2008)

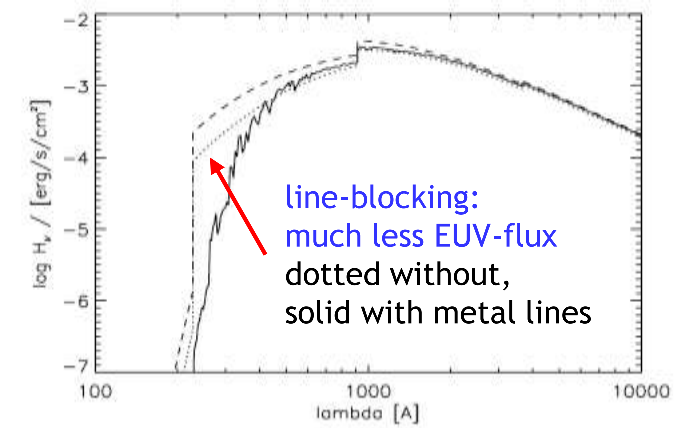

line-blocking:
much less EUV-flux
dotted without,
solid with metal lines

Fig. 10. Emergent Eddington flux H_ν as function of wavelength. Solid line: Current model of HD 15629 (O5V((f)) with parameters from Table 1 ($T_{\text{eff}} = 40\,500$ K, $\log g = 3.7$, "model 1"). Dotted: Pure H/He model without line-blocking/blanketing and negligible wind, at same T_{eff} and $\log g$ ("model 2"). Dashed: Pure H/He model, but with $T_{\text{eff}} = 45\,000$ K and $\log g = 3.9$ ("model 3").

UV to optical flux redistribution in hot stars
(from Repolust, Puls & Hererro 2004)

Spectral line blocking/blanketing

Back-warming and flux redistribution

…occur in stars of all spectral types

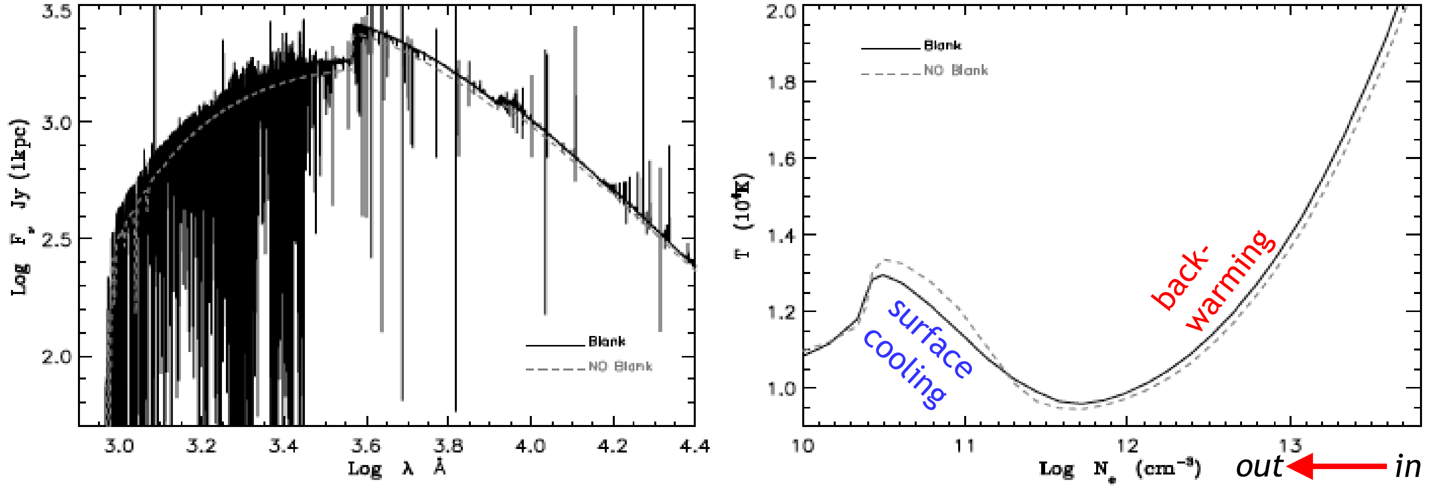

From Puls et al. 2008

Fig. 9 Effects of line blanketing (solid) vs. unblanketed models (dashed) on the flux distribution ($\log F_\nu$ (Jansky) vs. $\log \lambda$ (Å), left panel) and temperature structure ($T\,(10^4$ K) vs. $\log n_e$, right panel) in the atmosphere of a late B-hypergiant. Blanketing blocks flux in the UV, redistributes it towards longer wavelengths and causes back-warming.

Stellar Atmospheres in practice

Spectral line blocking/blanketing

in line/continuum forming regions, blanketed models at a certain $T_{\rm eff}$ have a plasma temperature corresponding to an unblanketed model with higher $T'_{\rm eff}$

Back-warming – effect on effective temperature

RECALL: $T_{\rm eff}$ -- or total flux (plane-parallel) -- fundamental input parameter in model atmosphere!

$$F = \sigma_{\rm B} T_{\rm eff}^4$$

From Gustafsson et al. 2008: Estimate effect by assuming a blanketed model with $T_{\rm eff}$ such that the deeper layers correspond to an unblanketed model with effective temperature $T'_{\rm eff} > T_{\rm eff}$

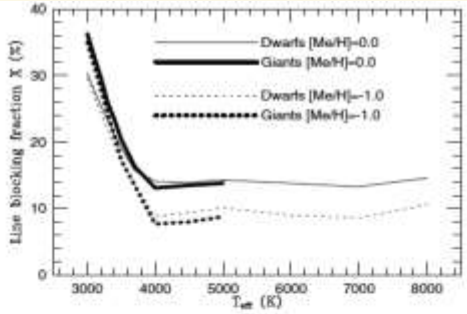

Fig. 3. The blocking fraction X in percent for models in the grid with two different metallicities. The dwarf models all have $\log g = 4.5$ while the giant models have $\log g$ values increasing with temperature, from $\log g = 0.0$ at $T_{\rm eff} = 3000$ K to $\log g = 3.0$ at $T_{\rm eff} = 5000$ K.

Question: Why does the line blocking fraction increase for very cool stars?

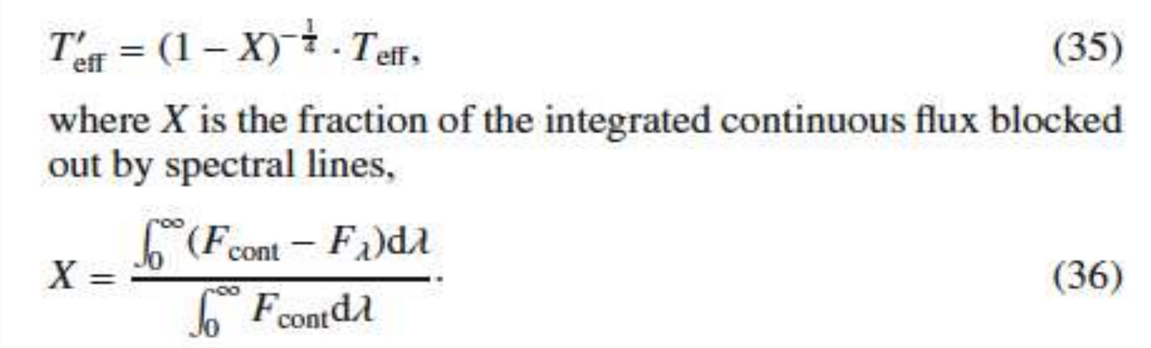

$$T'_{\rm eff} = (1 - X)^{-\frac{1}{4}} \cdot T_{\rm eff}, \qquad (35)$$

where X is the fraction of the integrated continuous flux blocked out by spectral lines,

$$X = \frac{\int_0^\infty (F_{\rm cont} - F_\lambda) {\rm d}\lambda}{\int_0^\infty F_{\rm cont} {\rm d}\lambda}. \qquad (36)$$

$T_{\rm eff}$ in cool stars derived, e.g., by optical photometry

Stellar Atmospheres in practice

Spectral line blocking/blanketing

Back-warming – effect on effective temperature

RECALL: $T_{\rm eff}$ -- or total flux (plane-parallel) -- fundamental input parameter in model atmosphere!

Previous slide were LTE models. In hot stars, everything has to be done in NLTE…

$$F = \sigma_{\rm B} T_{\rm eff}^4$$

Question: Why is optical photometry generally NOT well suited to derive Teff in hot stars?

Stellar Atmospheres in practice

Spectral line blocking/blanketing

Instead, He ionization-balance is typically used
(or N for the very hottest stars, or, e.g., Si for B-stars)

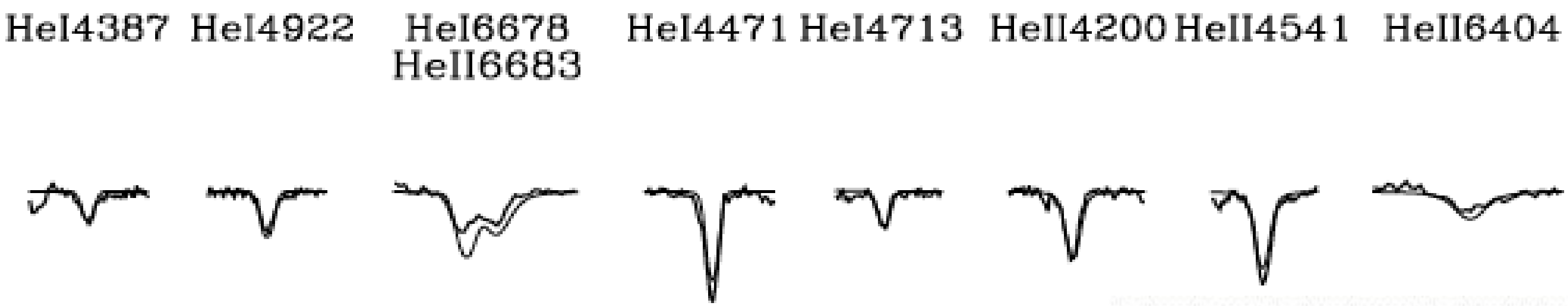

Simultaneous fits to observed HeI and HeII lines
-– from Repolust, Puls, Hererro (2004)

- Back-warming shifts ionization balance toward more completely ionized Helium in blanketed models

→ thus fitting the same observed spectrum requires lower T_{eff} than in unblanketed models

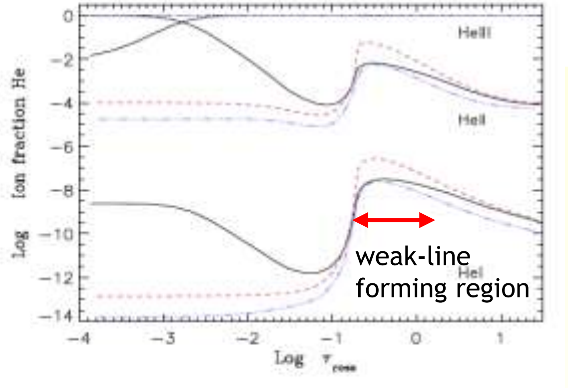

- black – blanketed Teff=45 kK
- red – unblanketed Teff=45 kK
- blue – unblanketed Teff= 50 kK

black and blue have similar (low) HeI/II ionization fractions in weak-line forming region, thus similar line profiles

Stellar Atmospheres in practice

Spectral line blocking/blanketing

Instead, He ionization-balance is typically used
(or N for the very hottest stars, or, e.g., Si for B-stars)

Result: In hot O-stars with Teff~40,000 K, back-warming can lower the derived T_{eff} as compared to unblanketed models by several thousand degrees! (~ 10 %)

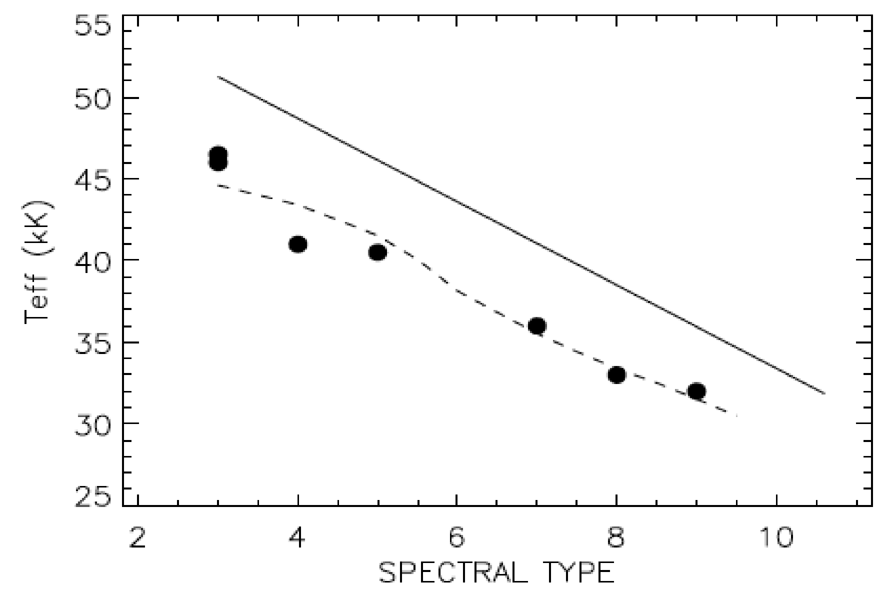

New T_{eff} scale for O-dwarf stars. Solid line – unblanketed models. Dashed – blanketed calibration, dots – observed blanketed values (from Puls et al. 2008)

Stellar Atmospheres in practice

A tour de modeling and analysis of stellar atmospheres throughout the HRD

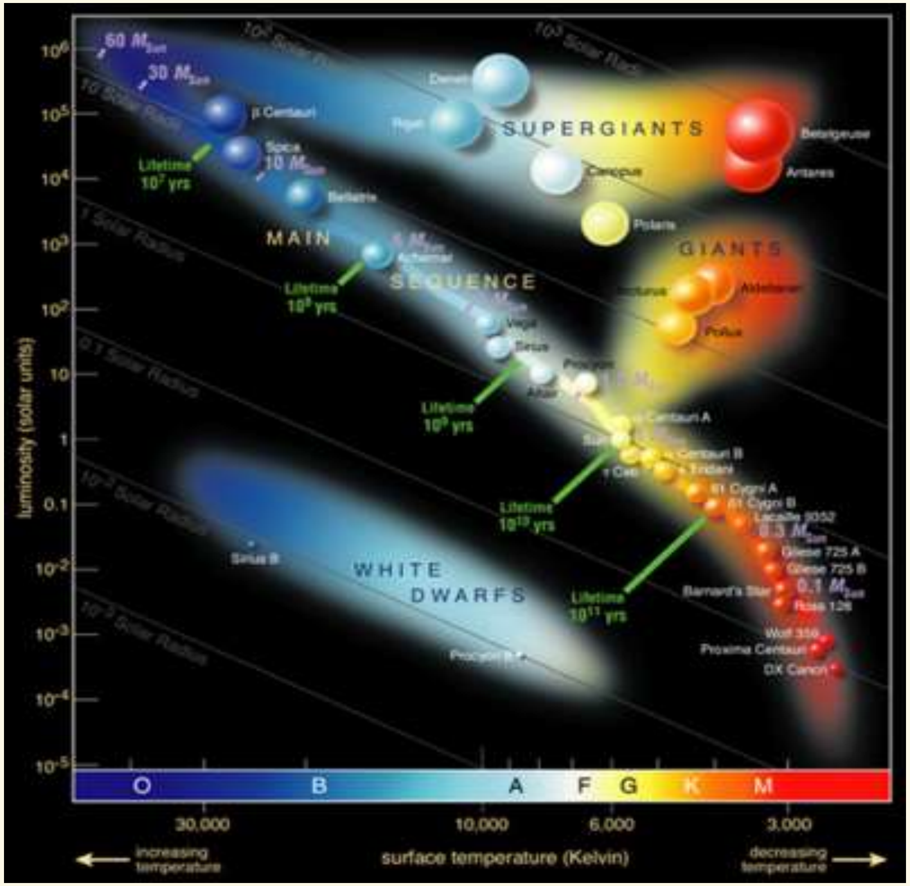

- LTE or NLTE
- Spectral line blocking/blanketing
- (sub-) Surface convection
- Geometry and dimensionality
- Velocity fields and outflows

Surface Convection

from Chap. 6

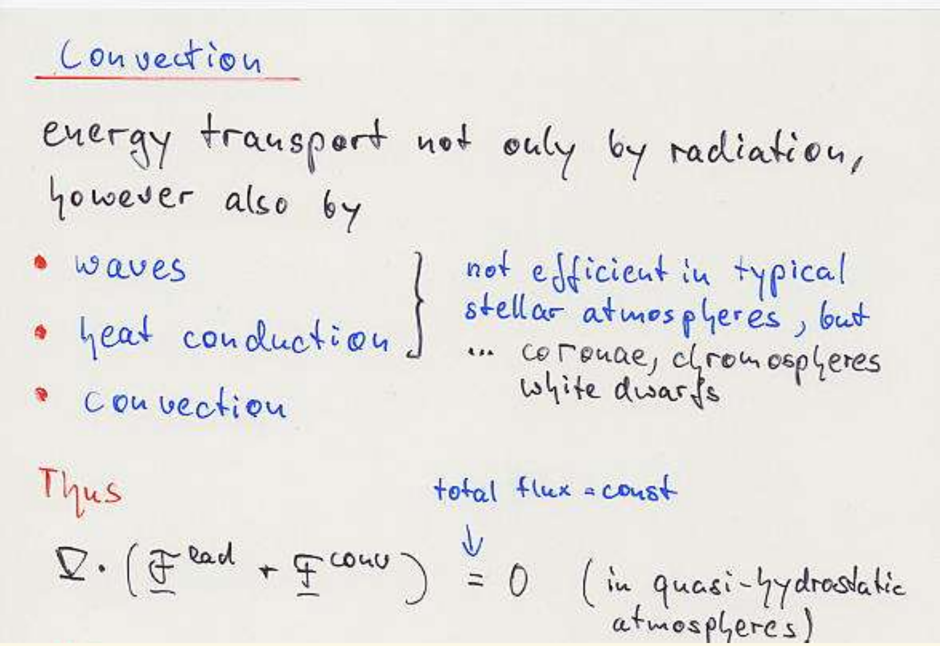

Convection

energy transport not only by radiation, however also by

- waves
- heat conduction
- convection

} not efficient in typical stellar atmospheres, but … coronae, chromospheres white dwarfs

Thus

$$\nabla \cdot \left(\underline{F}^{\mathrm{rad}} + \underline{F}^{\mathrm{conv}}\right) \overset{\overset{\text{total flux = const}}{\downarrow}}{=} 0 \quad \text{(in quasi-hydrostatic atmospheres)}$$

Surface Convection

OBSERVATIONS:
“Sub-surface convection” in layers T~160,000 K (due to iron-opacity peak) currently discussed also in hot stars

Debnath+ 2024:
Convection seems to be inefficient, but supersonic turbulence in/above/below photospheric regions might be initiated

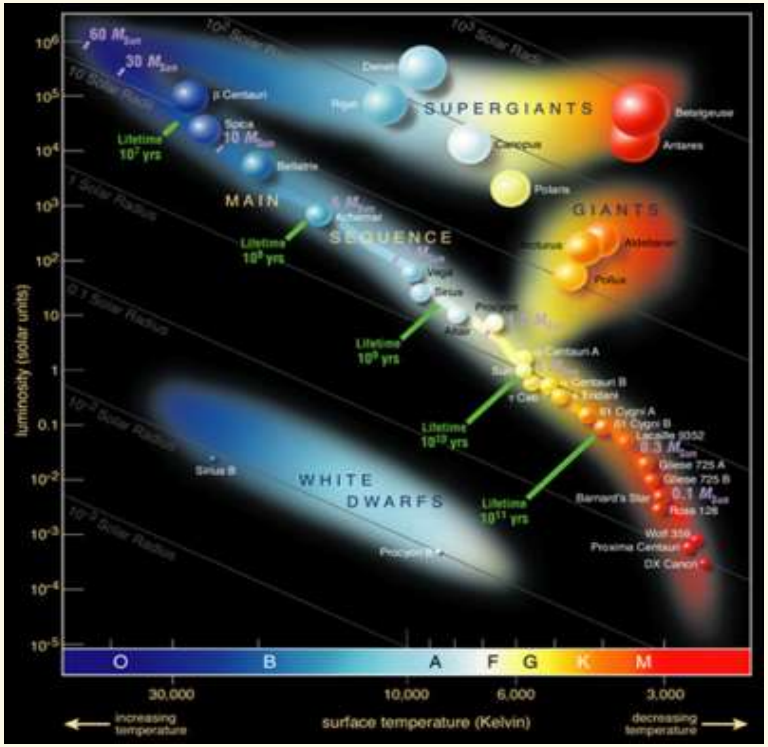

- H/He recombines in atmospheres of cool stars
→ Provides MUCH opacity
→ (page 116) Convective Energy transport

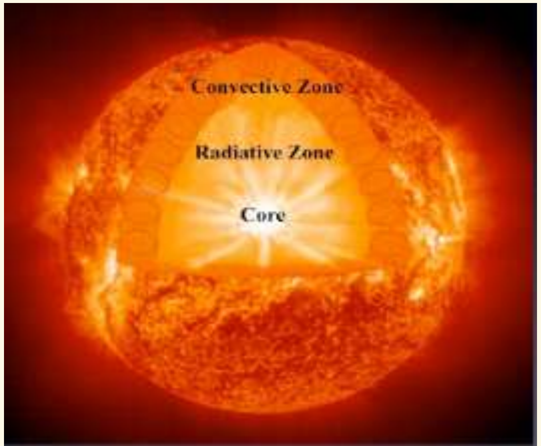

Image: SOHO (ESA/NASA)

Surface Convection

Traditionally accounted for by rudimentary "mixing-length theory" (see Chap. 6) in 1-D atmosphere codes

BUT:
- Solar observations show very dynamic structure
- Granulation and lateral inhomogeneity

→ Need for full 3-D radiation-hydrodynamics simulations in which convective motions occur spontaneously if required conditions fulfilled (all physics of convection 'naturally' included)


Emergent intensity in a 1D model of a stellar atmosphere


Observed and computed solar granulation

Credit: B. Stein

Surface Convection

Solar-type stars:
Photospheric extent << stellar radius
Small granulation patterns

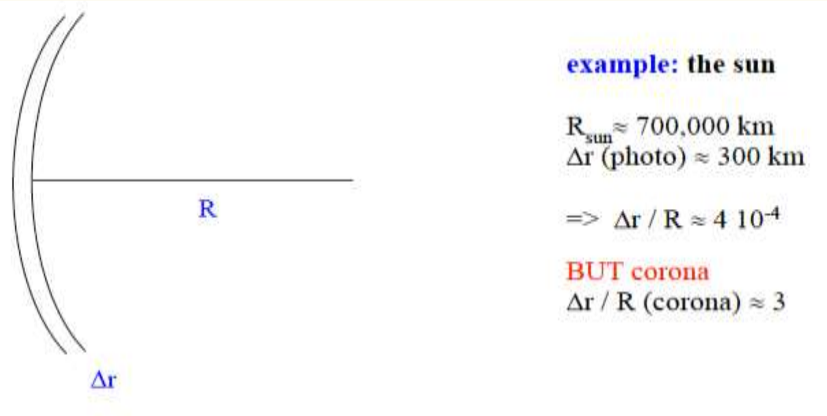

example: the sun

$R_{sun} \approx 700{,}000$ km
Δr (photo) ≈ 300 km

=> $\Delta r / R \approx 4\ 10^{-4}$

BUT corona
$\Delta r / R$ (corona) ≈ 3

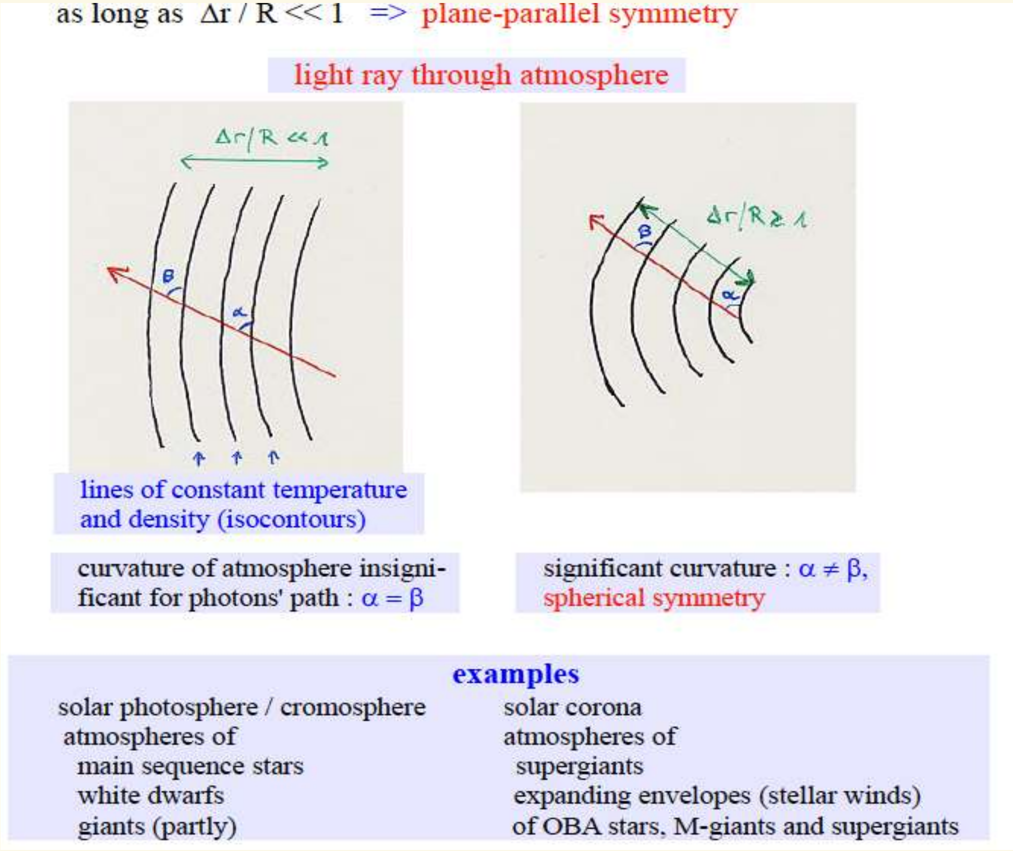
as long as $\Delta r / R << 1$ => plane-parallel symmetry

light ray through atmosphere

lines of constant temperature and density (isocontours)

curvature of atmosphere insignificant for photons' path : $\alpha = \beta$

significant curvature : $\alpha \neq \beta$, spherical symmetry

examples

solar photosphere / cromosphere	solar corona
atmospheres of	atmospheres of
main sequence stars	supergiants
white dwarfs	expanding envelopes (stellar winds)
giants (partly)	of OBA stars, M-giants and supergiants

from Chap. 3

Surface Convection

Solar-type stars:
Atmospheric extent << stellar radius
Small granulation patterns

→

Box-in-a-star Simulations

(cmp. plane-parallel approximation)

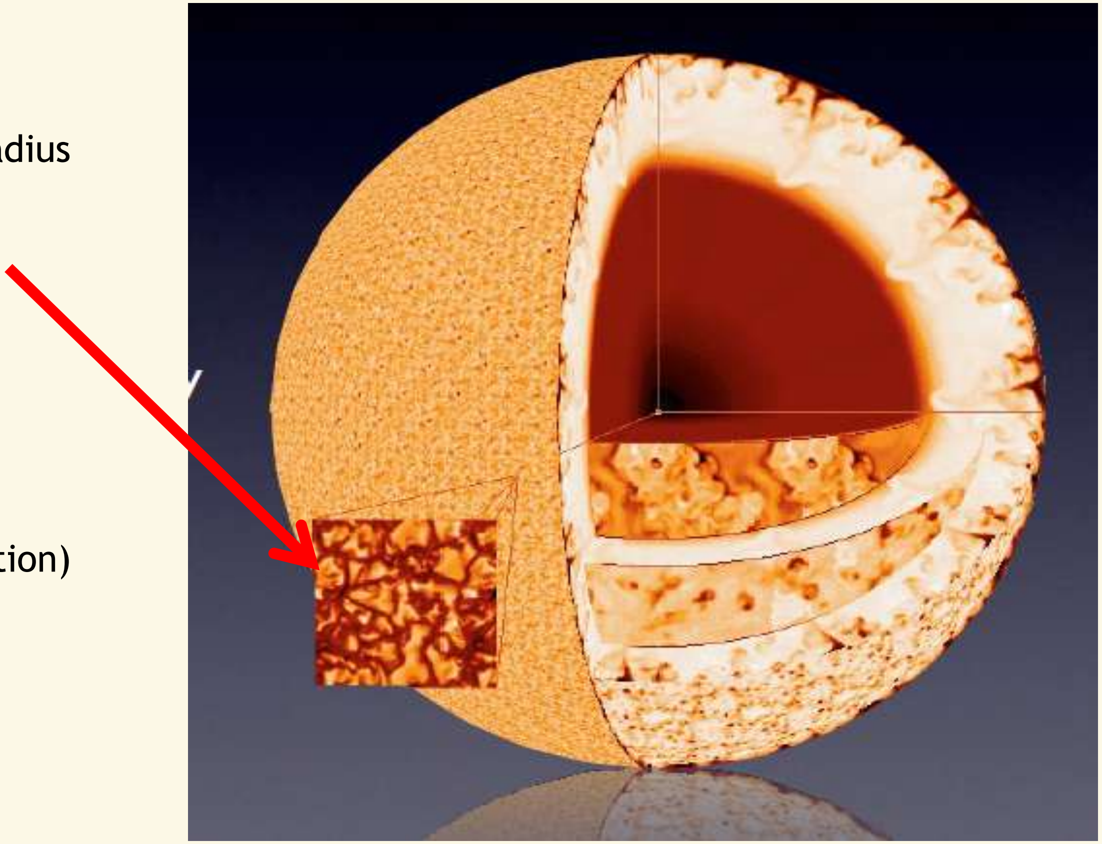

From Wolfgang Hayek

Surface Convection

Approach
(teams by Nordlund, Steffen):

Solve radiation-hydrodynamical conservation equations of mass, momentum, and energy (closed by equation of state).

3-D radiative transfer included to calculate net radiative heating/cooling q_{rad} in energy equation, typically assuming LTE and a very simplified treatment of line-blanketing

$$q_{\rm rad} = 4\pi\rho \int_\lambda \kappa_\lambda (J_\lambda - S_\lambda)\, d\lambda,$$

(= 0 in case of radiative equilibrium)

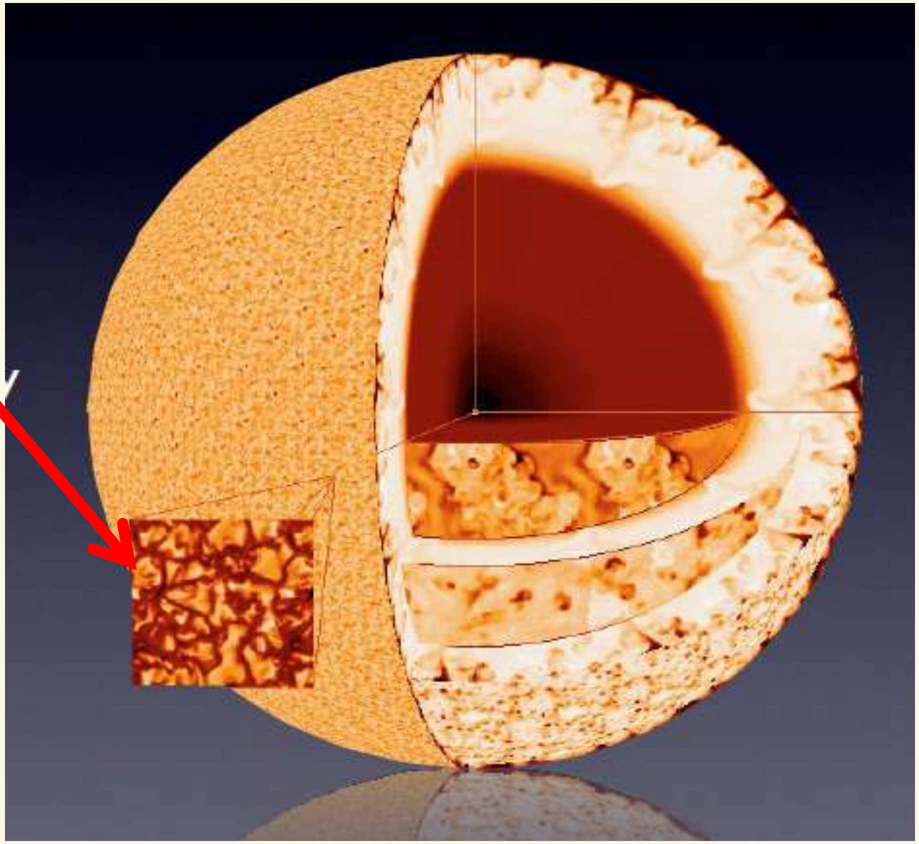

From Wolfgang Hayek

Surface Convection

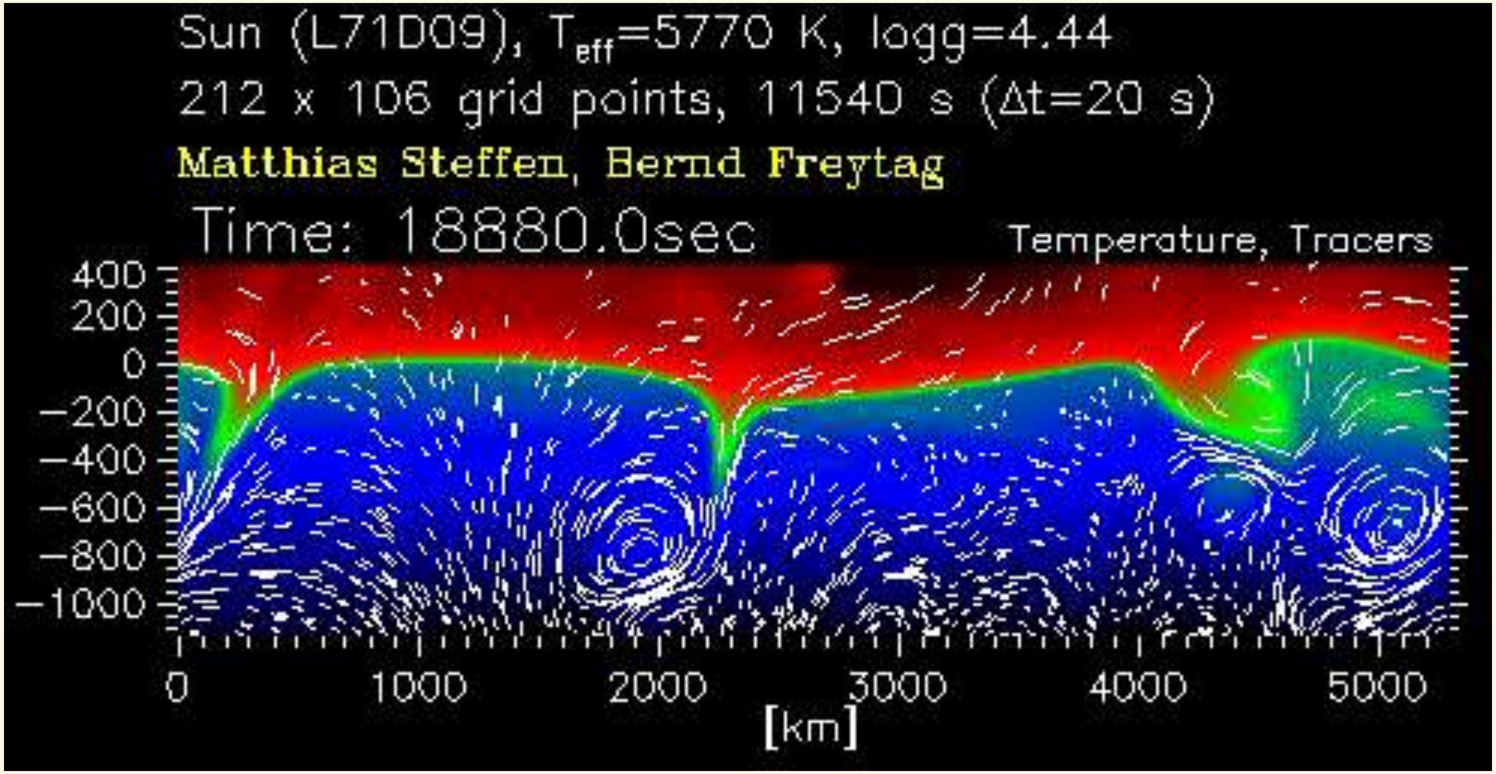

From Berndt Freytag's homepage: http://www.astro.uu.se/~bf/

Stellar Atmospheres in practice

Surface Convection

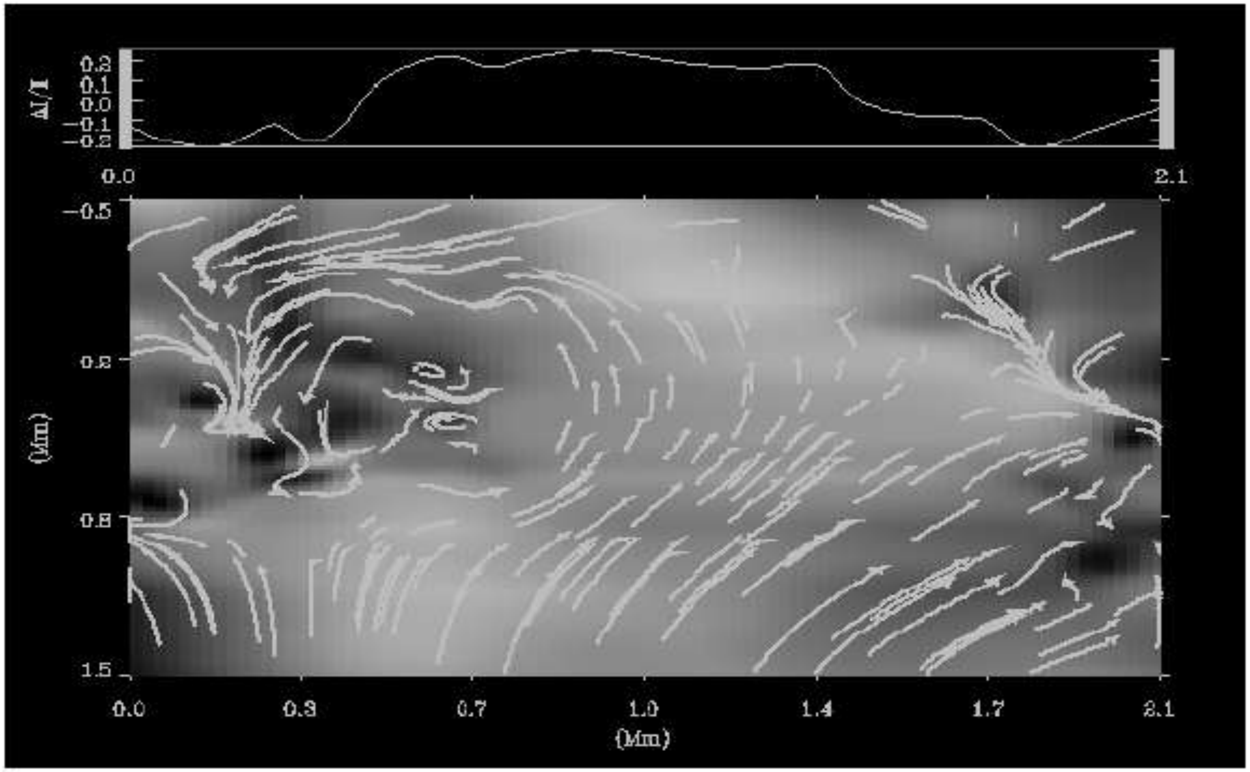

FIG. 4.—Pressure fluctuations about the mean hydrostatic equilibrium and the velocity field in an xz slice through a granule. The pressure is high above the centers of granules, which decelerates the warm upflowing fluid and diverts it horizontally. High pressure also occurs in the intergranular lanes where the horizontal motions are halted and gravity pulls the now cool, dense fluid down into the intergranular lanes. Horizontal rolls of high vorticity occur at the edges of the intergranular lanes. The emergent intensity profile across the slice is shown at the top.

From Stein & Nordlund (1998)

Surface Convection

Some key features:

Slow, broad upward motions, and faster, thinner downward motions

Non-thermal velocity fields

Overshooting from zone where convection is efficient according to stability criteria (see Chap. 6)

Energy balance in upper layers not only controlled by radiative heating/cooling, but also by cooling from adiabatic expansion

See Stein & Nordlund (1998); Collet et al. (2006), etc.

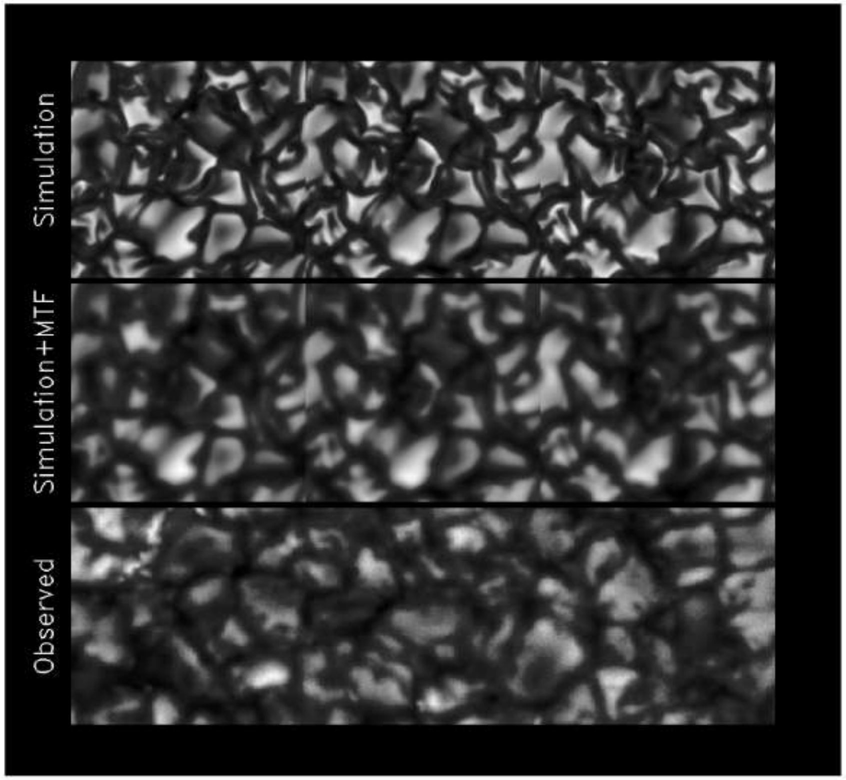

Fig. 19.—Comparison of granulation as seen in the emergent intensity from the simulations and as observed by the Swedish Vacuum Solar Telescope on La Palma. The top row shows three simulation images at 1 minute intervals, which together make a composite image 18 × 6 Mm in extent. The middle row shows this image smoothed by an Airy plus exponential point-spread function. The bottom row shows an 18 × 6 Mm white-light image from La Palma. Note the similar appearance of the smoothed simulation image and the observed granulation. The common edge brightening in the simulation is reduced when smoothed. Images by (Title 1996, private communication) taken in the CH G-band have much more contrast than white light and clearly reveal the edge brightening of granules.

Question: This does not look much like the traditional 1-D models we’ve discussed during the previous lecture! – Do you think we should throw them in the garbage?

Surface Convection

blue: mean temperature from 3D hydro-model (scatter = dashed)
red: from 1D semi-empirical model (Holweger & Müller, see Chap. 5)
green: from 1D theoretical model atmospheres (MARCS)

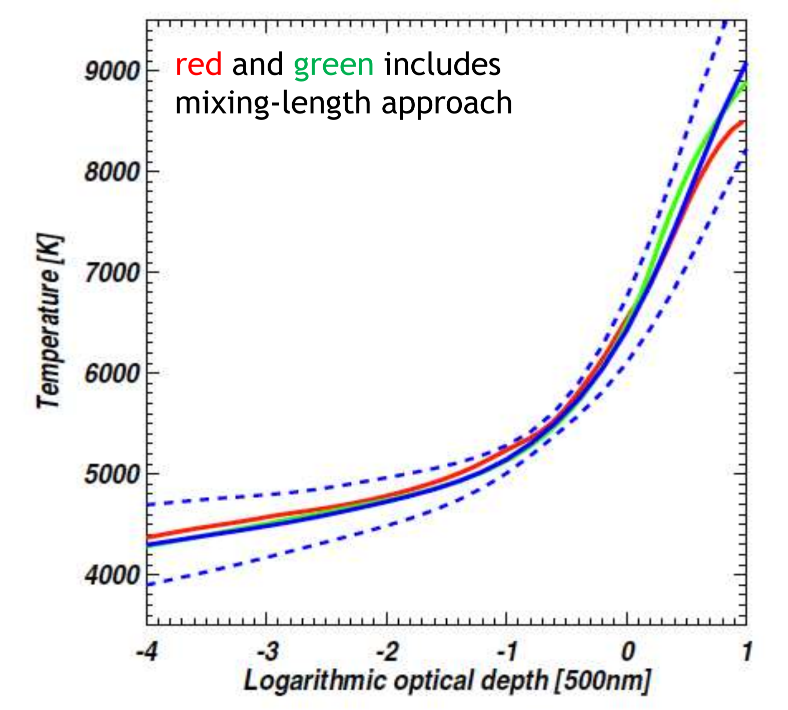

Figure 1: The mean temperature structure of the 3D hydrodynamical model of Trampedach et al. (2009) is shown as a function of optical depth at 500 nm (blue solid line). The blue dashed lines correspond to the spatial and temporal rms variations of the 3D model, while the red and green curves denote the 1D semi-empirical Holweger & Müller (1974) and the 1D theoretical MARCS (Gustafsson et al. 2008) model atmospheres, respectively.

In many (though not all) cases, AVERAGE properties still quite OK:

Convection in energy balance approximated by "mixing-length theory"
Non-thermal velocity fields due to convective motions included by means of so-called "micro-" and "macro-turbulence"

BUT quantitatively we always need to ask:
To what extent can average properties be modeled by traditional 1-D codes?

Unfortunately, a general answer very difficult to give, need to be considered case by case

Stellar Atmospheres in practice

Surface Convection

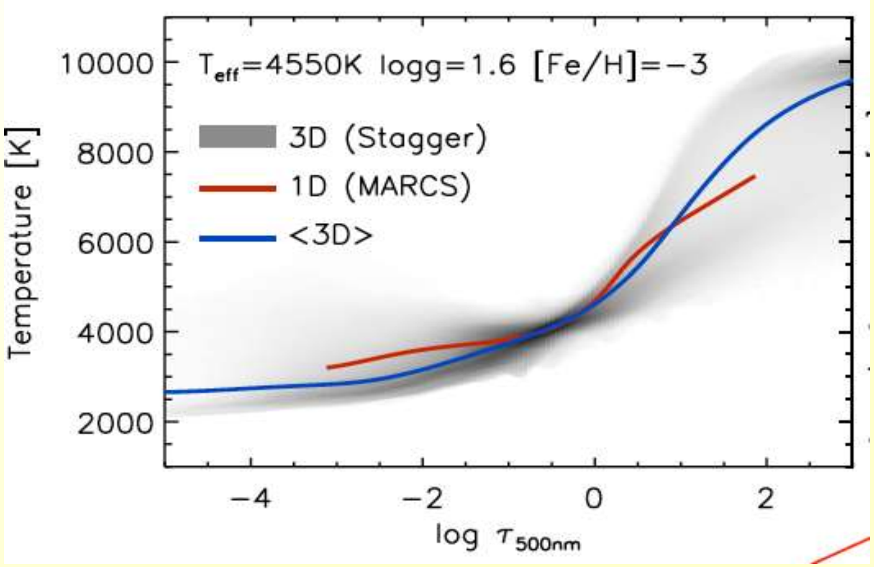

Metal-poor red giant, simulation by Remo Collet,
figure from talk by M. Bergemann

For example:

In metal-poor cool stars spectral lines are scarce (Question: Why?), and energy balance in upper photosphere controlled to a higher degree by adiabatic expansion of convectively overshot material.

In classical 1-D models though, these layers are convectively stable, and energy balance controlled only by radiation (radiative equilibrium, see Chap. 4).

Stellar Atmospheres in practice

Surface Convection

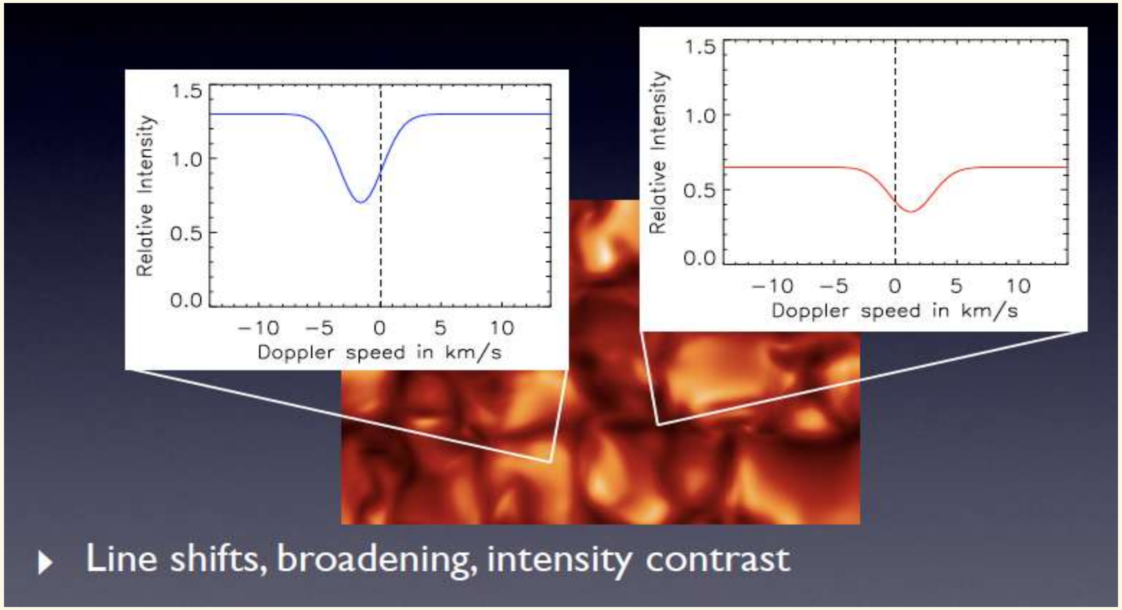

- Line shifts, broadening, intensity contrast

From talk by Hayek

3-D radiation-hydro models successful in reproducing many solar features (see overview in Asplund et al. 2009), e.g:

Center-to-limb intensity variation

Line profiles and their shifts and variations (without micro/macroturbulence)

Observed granulation patterns

Surface Convection

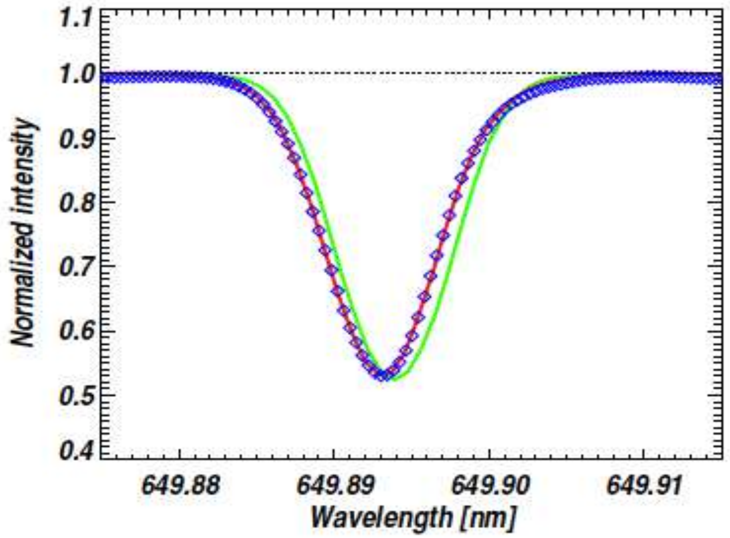

Figure 3: The predicted spectral line profile of a typical Fe I line from the 3D hydrodynamical solar model (red solid line) compared with the observations (blue rhombs). The agreement is clearly very satisfactory, which is the result of the Doppler shifts arising from the self-consistently computed convective motions that broaden, shift and skew the theoretical profile. For comparison purposes also the predicted profile from a 1D model atmosphere (here Holweger & Müller 1974) is shown; the 1D profile has been computed with a microturbulence of 1 km s^{-1} and a tuned macroturbulence to obtain the right overall linewidth. Note that even with these two free parameters the 1D profile can neither predict the shift nor the asymmetry of the line.

affects chemical abundance (determined by means of line profile fitting to observations)

One MAJOR result:
Effects on line formation has led to a downward revision of the CNO solar abundances and the solar metallicity, and thus to a revision of the *standard cosmic chemical abundance scale*

Fig. from Asplund et al. (2009) – “The Chemical Composition of the Sun”

Stellar Atmospheres in practice

Surface Convection

Also potentially critical for Galactic archeology…

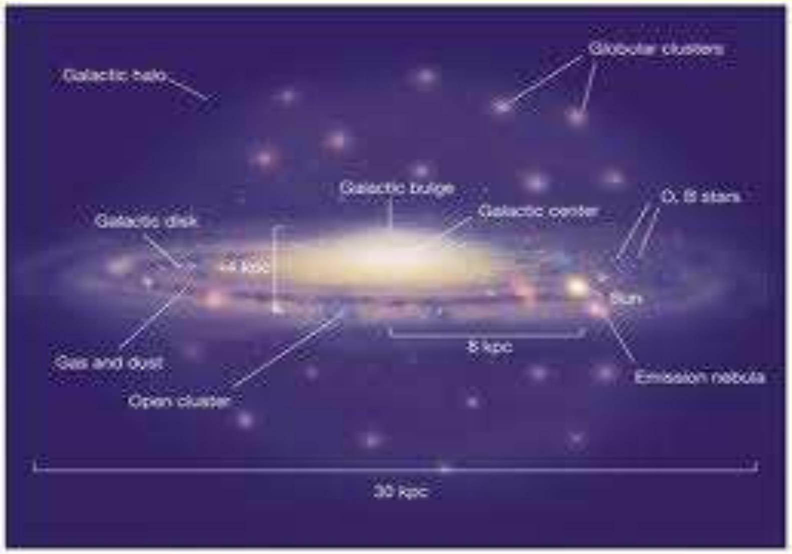

…which traces the chemical evolution of the Universe by analyzing VERY old, metal-poor Globular Cluster stars –- relics from the early epochs (e.g., A. Frebel and collaborators)

Surface Convection

Out to Jupiter…

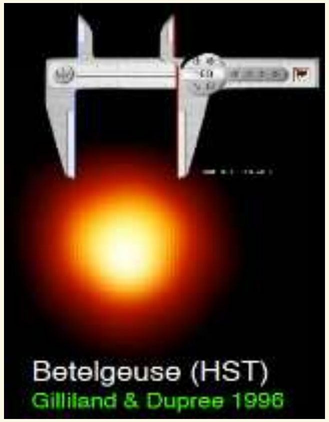

Betelgeuse (HST)
Gilliland & Dupree 1996

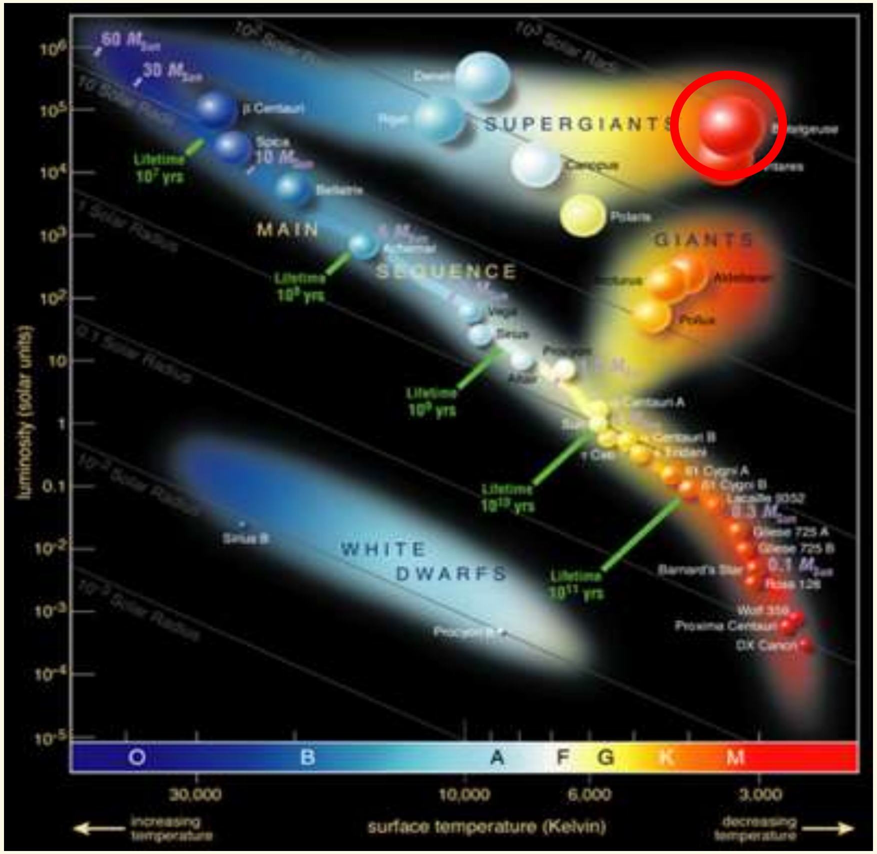

- giant convection cells in the low-gravity, extended atmospheres of Red Supergiants
- Question: Why extended?

$H = a^2 / g$ (with $a = \mathrm{v_s}$ the isothermal speed of sound)

$a^2_{\mathrm{RSG}} / a^2_{\mathrm{sun}} \approx T_{\mathrm{RSG}} / T_{\mathrm{sun}} = 0.5 \ldots 0.6$

$g_{\mathrm{RSG}} / g_{\mathrm{sun}} \approx 10^{-4}$!

(see Chap. 6)

Surface Convection

Supergiants (or models including a stellar wind):
Atmospheric extent > stellar radius:

Box-in-a-star → Star-in-a-box

(1D: Plane-parallel → Spherical symmetry,
see Chap. 3)

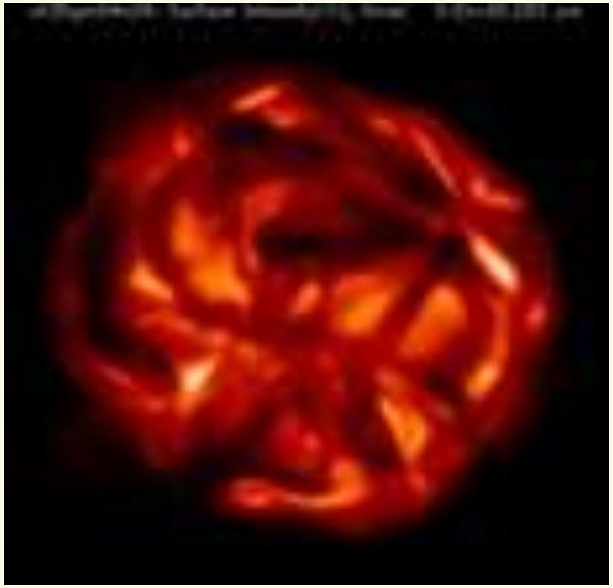

Star to model: Betelgeuse
Mass: 5 solar masses
Radius: 600 R_{sun}
Luminosity: 41400 L_{sun}
Grid: Cartesian cubical grid with 171^3 points
Edge length of box 1674 solar radii

Model by Berndt Freytag, note the HUGE convective cells visible in the emergent intensity map!!

Surface Convection

Star to model: Betelgeuse
Mass: 5 solar masses
Radius: 600 R_{sun}
Luminosity: 41400 L_{sun}
Grid: Cartesian cubical grid with 171^3 points
Edge length of box 1674 solar radii
Movie time span: 7.5 years

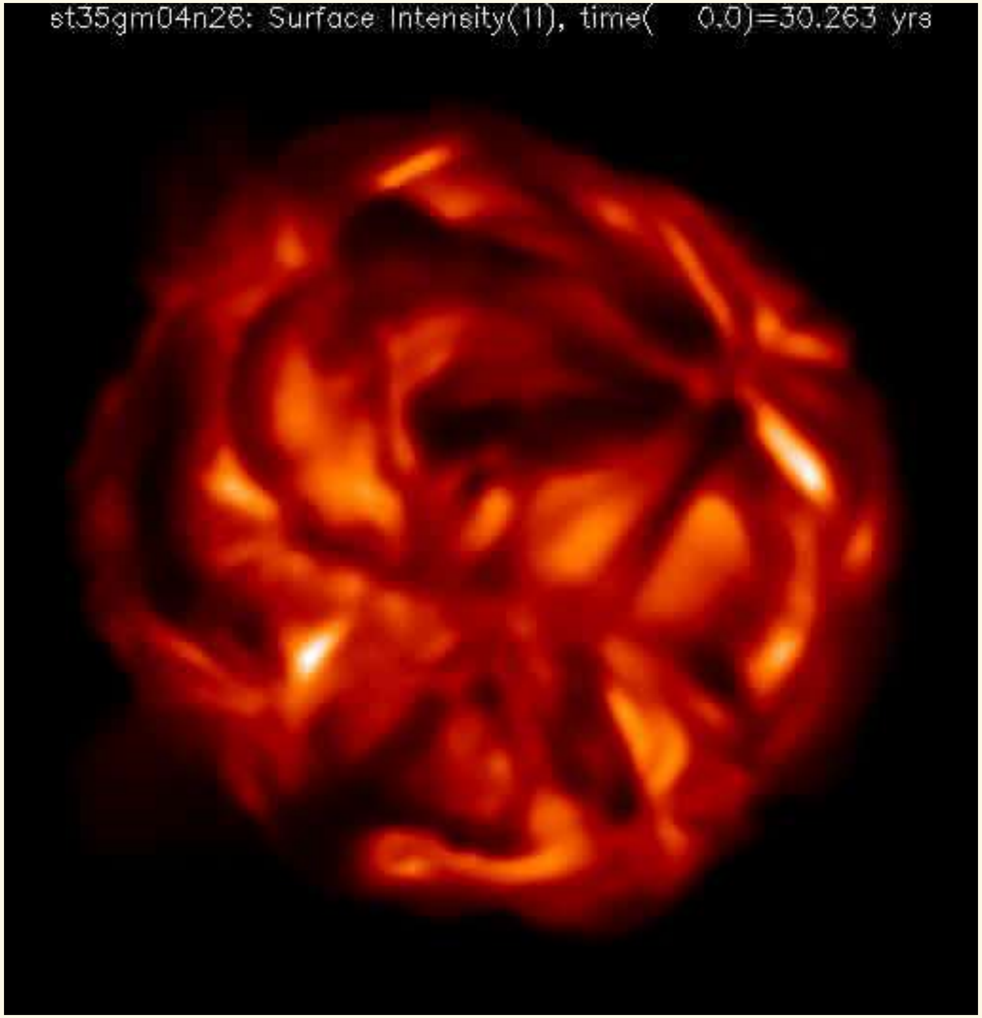

http://www.astro.uu.se/~bf/movie/dst35gm04n26/movie.html

Surface Convection

Extremely challenging,
models still in their infancies.
LOTS of exciting physics to explore, like

Pulsations
Convection
Numerical radiation-hydrodynamics
Role of magnetic fields
Stellar wind mechanisms

Also, to what extent can main effects
be captured by 1-D models?
For quantitative applications like….

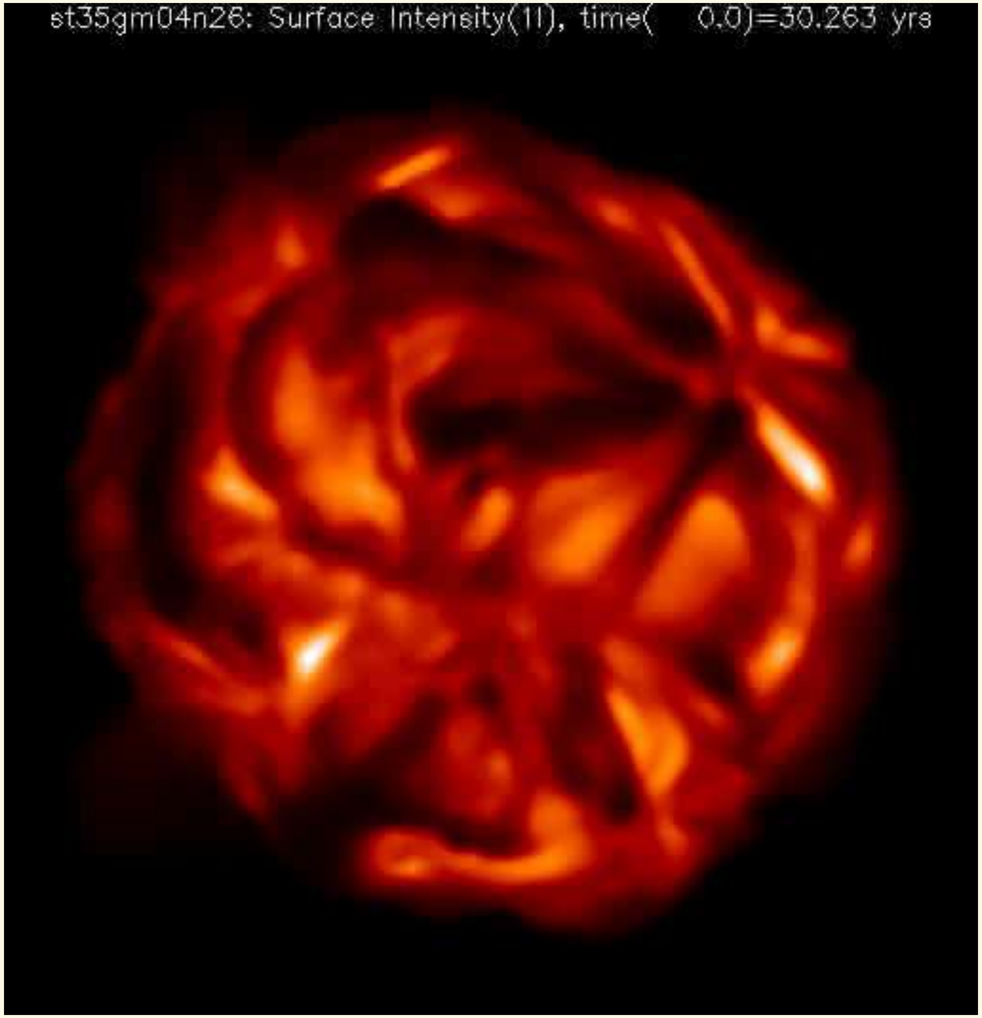

Stellar Atmospheres in practice

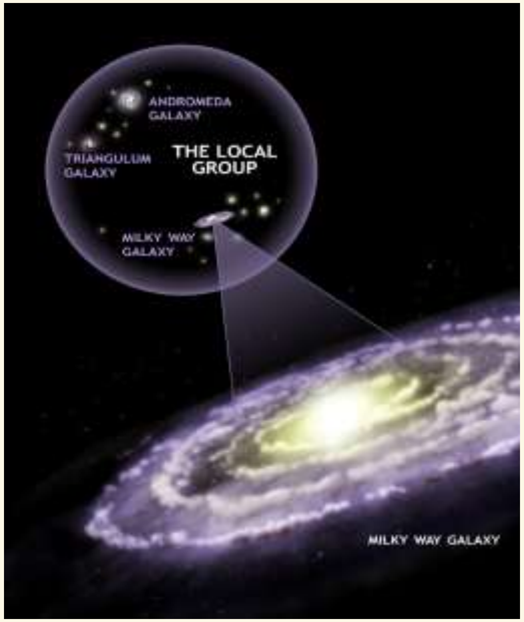

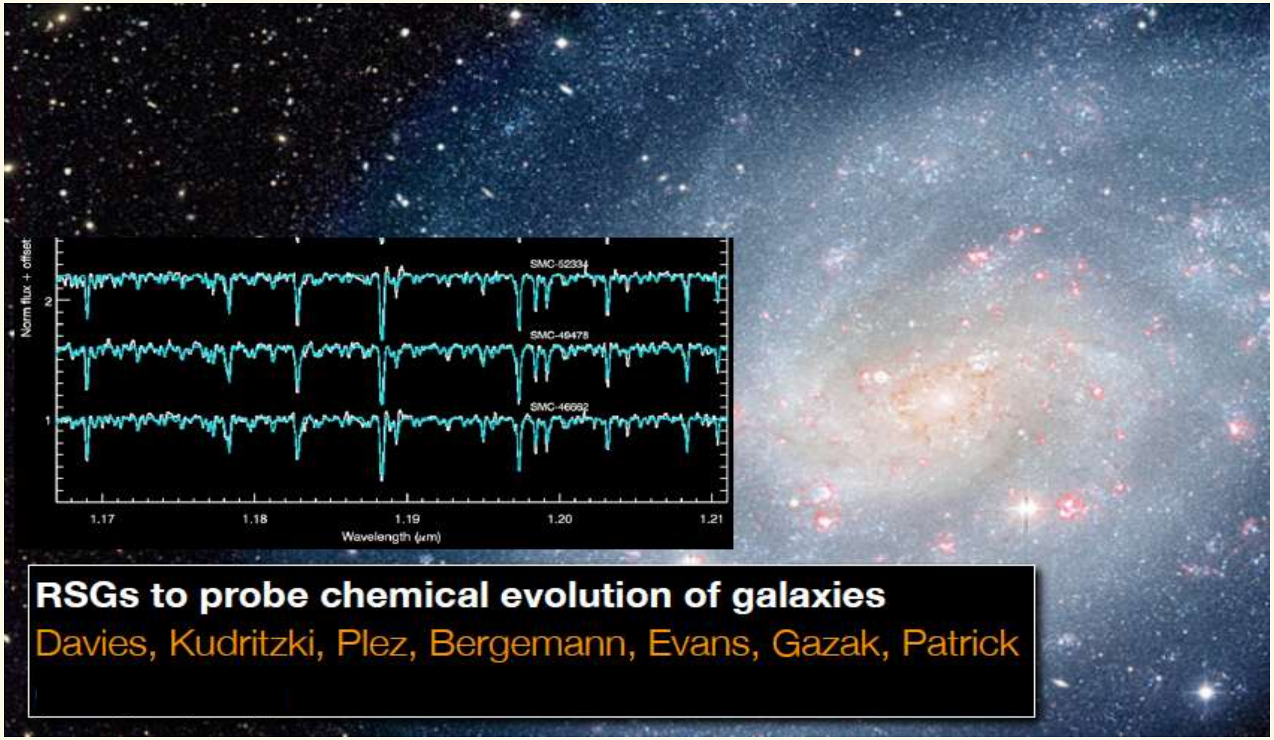

RSGs to probe chemical evolution of galaxies

Davies, Kudritzki, Plez, Bergemann, Evans, Gazak, Patrick

Question: Why are RSGs ideal for observational extragalactic stellar astrophysics, particularly in the near future?

Stellar Atmospheres in practice

important codes (not complete) and their features ….

Codes	FASTWIND CMFGEN PoWR	WM-basic	TLUSTY Detail/Surface	Phoenix	MARCS Atlas	CO^{5}BOLD[*] STAGGER
geometry	1-D spherical	1-D spherical	1-D plane-parallel	1-D/3-D spherical/ plane-parallel	1-D plane-parallel (MARCS also spherical)	3-D Cartesian
LTE/NLTE	NLTE	NLTE	NLTE	NLTE/LTE	LTE	LTE simplified
dynamics	quasi-static photosphere + prescribed supersonic outflow	time-independent hydrodynamics	hydrostatic	hydrostatic or allowing for supersonic outflows	hydrostatic	hydrodynamic
stellar wind	yes	yes	no	yes	no	no
major application	hot stars with winds	hot stars with dense winds, ion. fluxes, SNRs	hot stars with negligible winds	cool stars, brown dwarfs, SNRs	cool stars	cool stars
comments	CMFGEN also for SNRs; FASTWIND using approx. line-blocking	line-transfer in Sobolev approx. (see part 2)	Detail/Surface with LTE-blanketing	convection via mixing-length theory	convection via mixing-length theory	very long execution times, but model grids start to emerge

[*] COnservative COde for the COmputation of COmpressible COnvection

Stellar Atmospheres in practice

And then there are, e.g.,

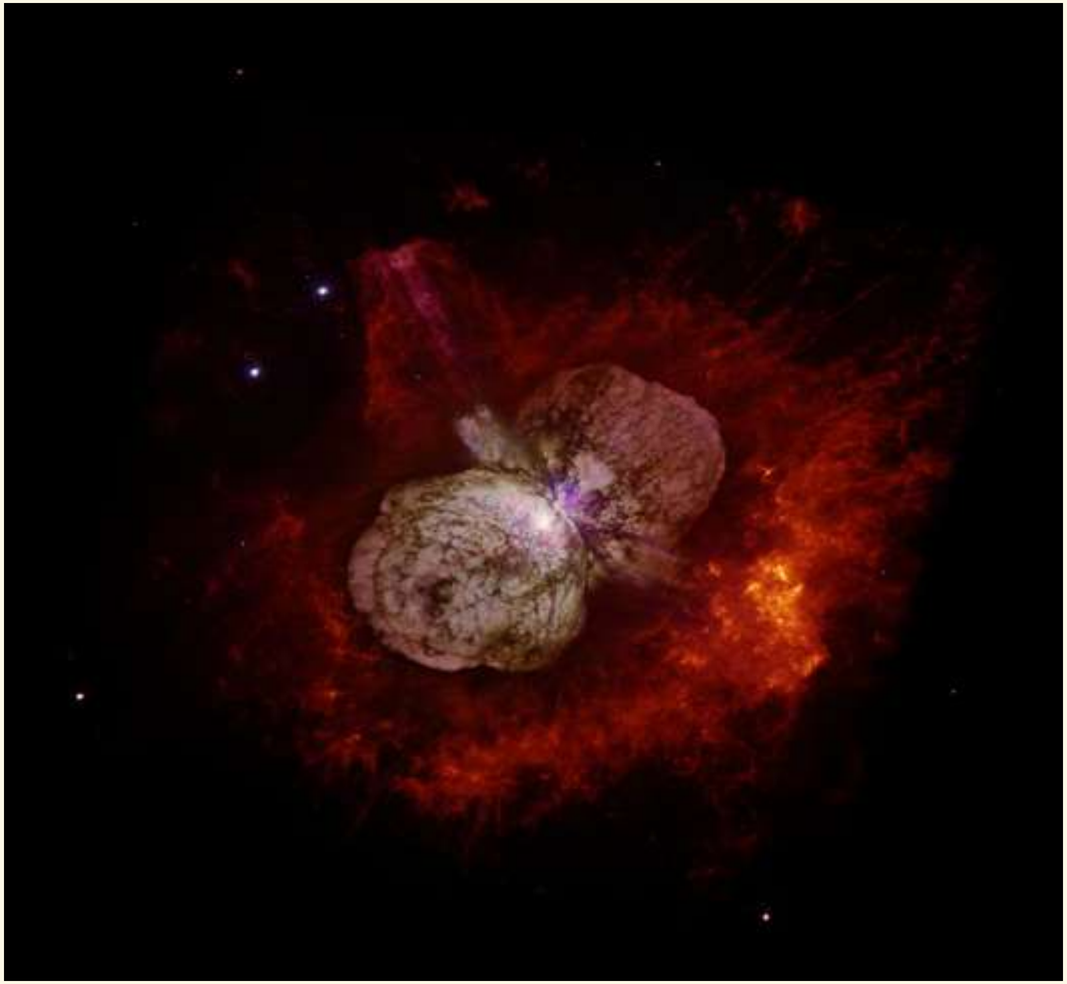

- Luminous Blue Variables (LBVs) like Eta Carina,
- Wolf-Rayet Stars (WRs)
- Planetary Nebulae (and their Central Stars)
- Be-stars with disks
- Brown Dwarfs
- Pre main-sequence T-Tauri and Herbig stars

…and many other interesting objects

Stellar astronomy alive and kicking! Very rich in both

Physics
Observational applications

A first application –
The D4000 break in early type galaxies

- spectroscopic study of region around 4000 Å: useful tool to investigate stellar populations in composite stellar systems

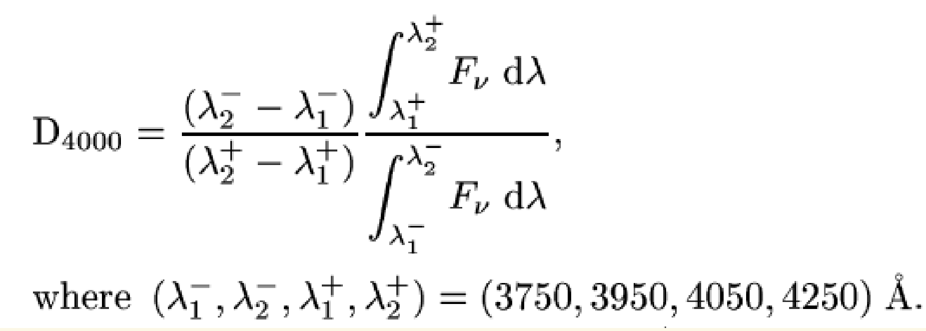

$$\mathrm{D}_{4000} = \frac{(\lambda_2^- - \lambda_1^-)}{(\lambda_2^+ - \lambda_1^+)} \frac{\displaystyle\int_{\lambda_1^+}^{\lambda_2^+} F_\nu \, \mathrm{d}\lambda}{\displaystyle\int_{\lambda_1^-}^{\lambda_2^-} F_\nu \, \mathrm{d}\lambda},$$

where $(\lambda_1^-, \lambda_2^-, \lambda_1^+, \lambda_2^+) = (3750, 3950, 4050, 4250)$ Å.

definition by Bruzual (1983)

D4000 pseudo color
(combination of λ and ν,
not logarithmically defined

- star formation history (e.g., easy detection of young populations “contaminating” the break)
- distinct indicator of stellar population ages (Kauffmann, 2003) and metallicities (Maraston 2005)
- Balmer decrement (“jump”, “break”) and D4000 break often used as a single feature to detect high redshift “quiescent” galaxies

- D4000 break in early type galaxies
    - only low signal to noise required
    - only weakly contaminated by reddening
    - no absolute fluxes required
    - same def. for red-shifted objects, only int. range has to be modified → photometric parallaxes
    - BUT: many lines contribute to break, complex behavior

Spectral energy distribution of A-K stars

1992ApJS...79..255K

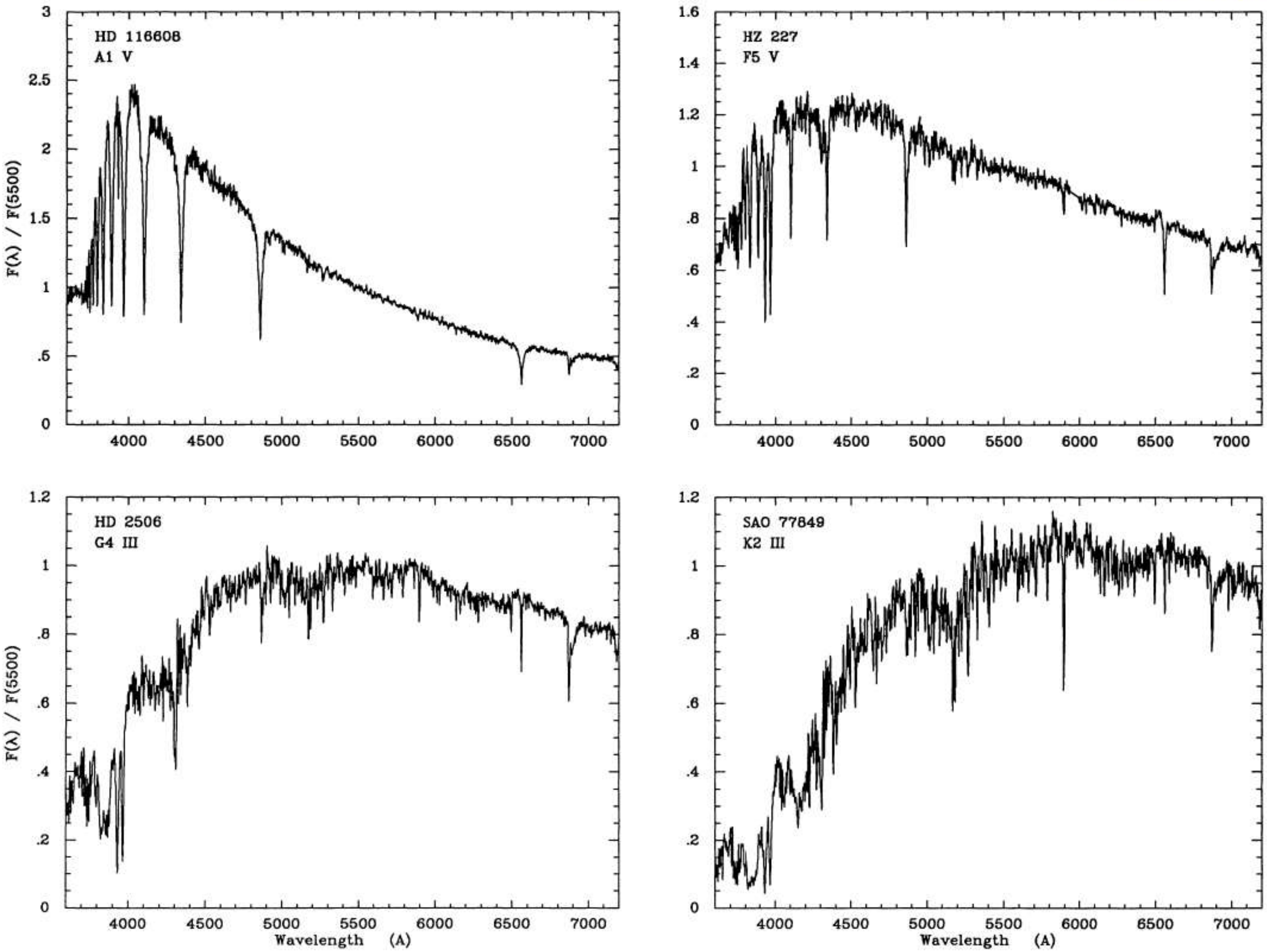

FIG. 4.—Spectra of four Galactic stars, taken from the spectral library of Jacoby et al. (1984). These spectra can be used to identify some of the major stellar absorption features in the galaxy spectra.

Note the change in the energy distribution as a function of spectral type (Teff)

Spectral energy distribution of elliptical galaxies

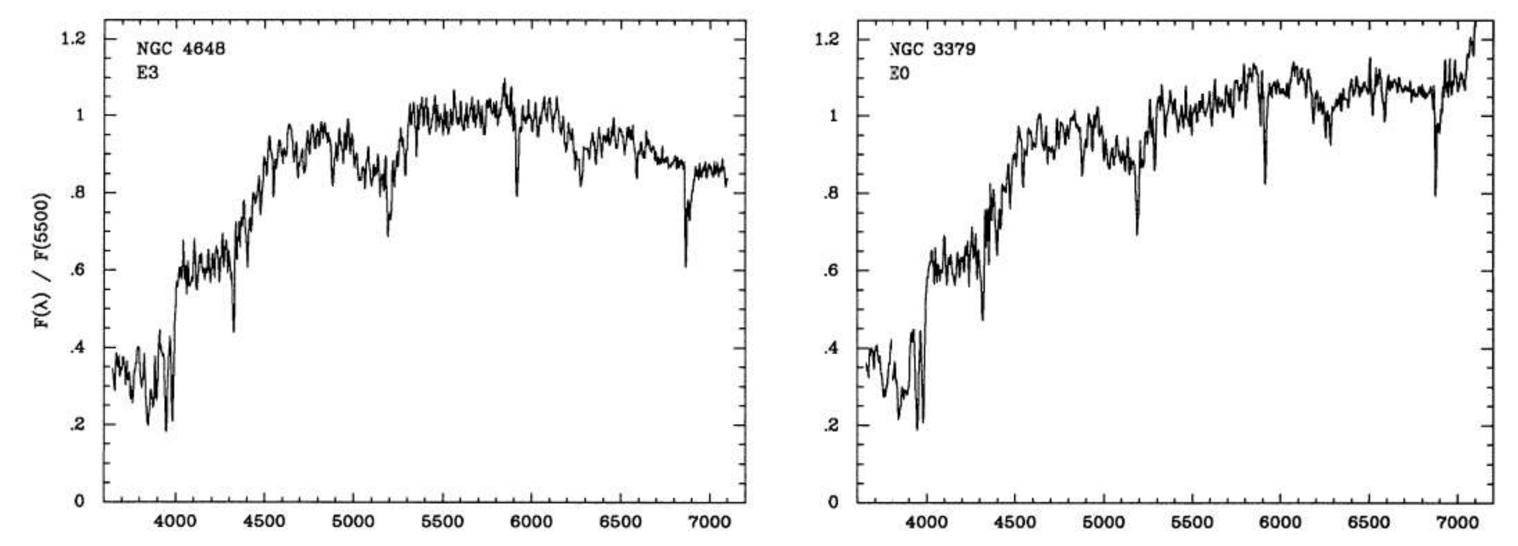

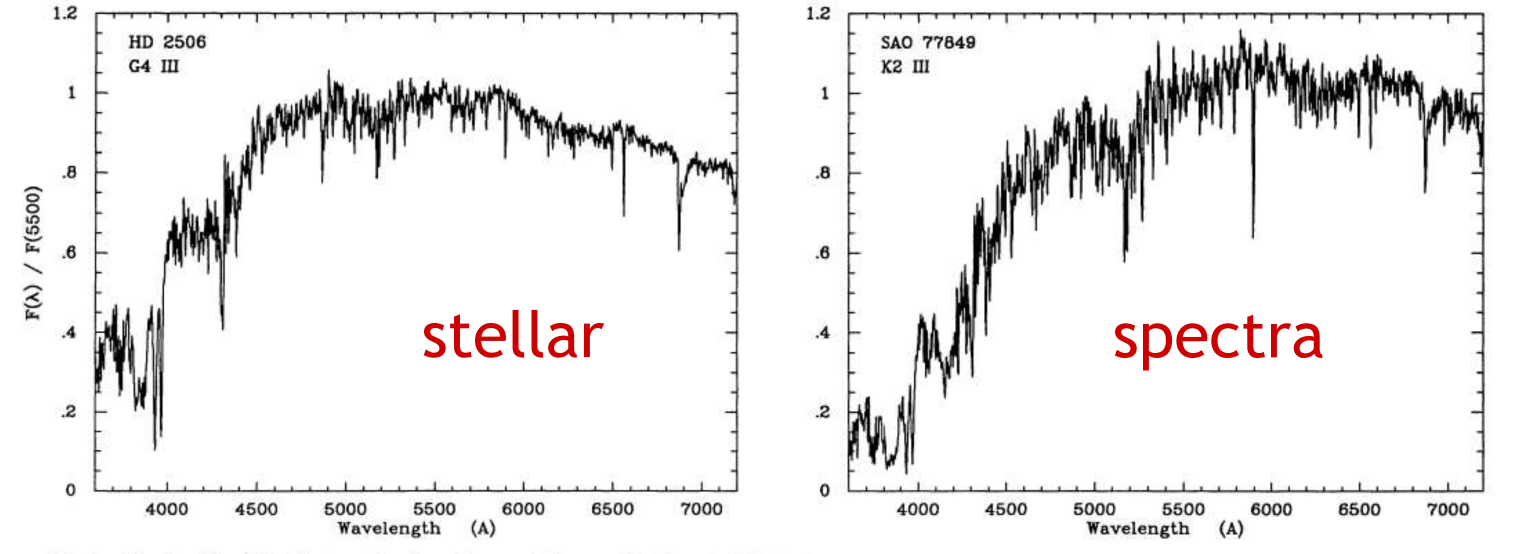

stellar spectra

D4000 break clearly visible, Mg/MgH (5000-5500 Å) complex strong
$\Rightarrow$dominated by G/K-giants

from Kennicutt, 1992, ApJS 79

Spectral energy distribution of spiral galaxies

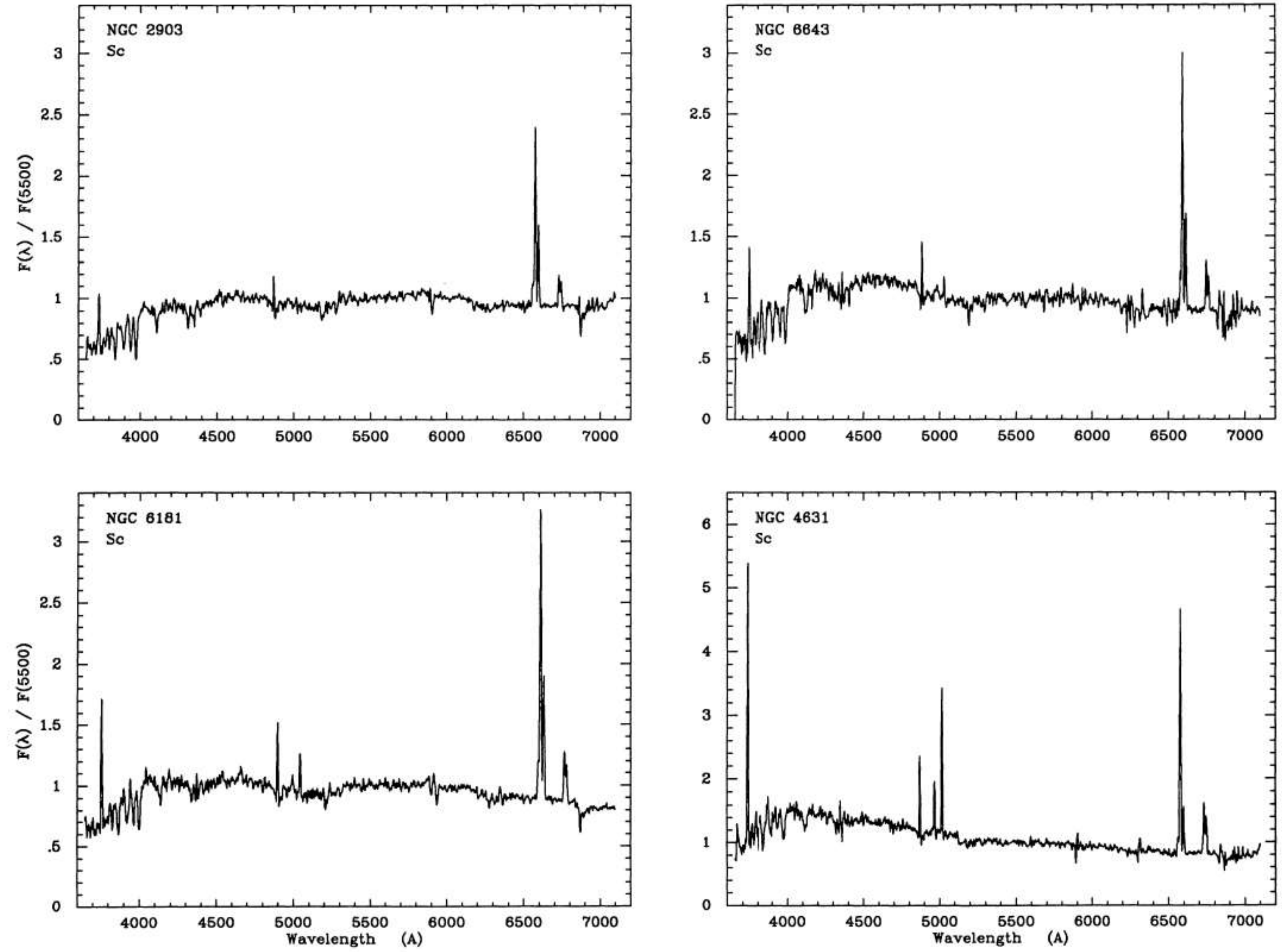

FIG. 10.—Integrated spectra of four Sbc–Sc galaxies, selected to illustrate the range in excitation in the emission-line spectra. See Fig. 9 for other examples.

no break,
Balmer decrement,
nebular emission lines (Halpha, Hbeta, [OIII 4959, 5007],…)

⇒presence of
early type stars
plus HII-regions

The 4000 Å region: a closer inspection

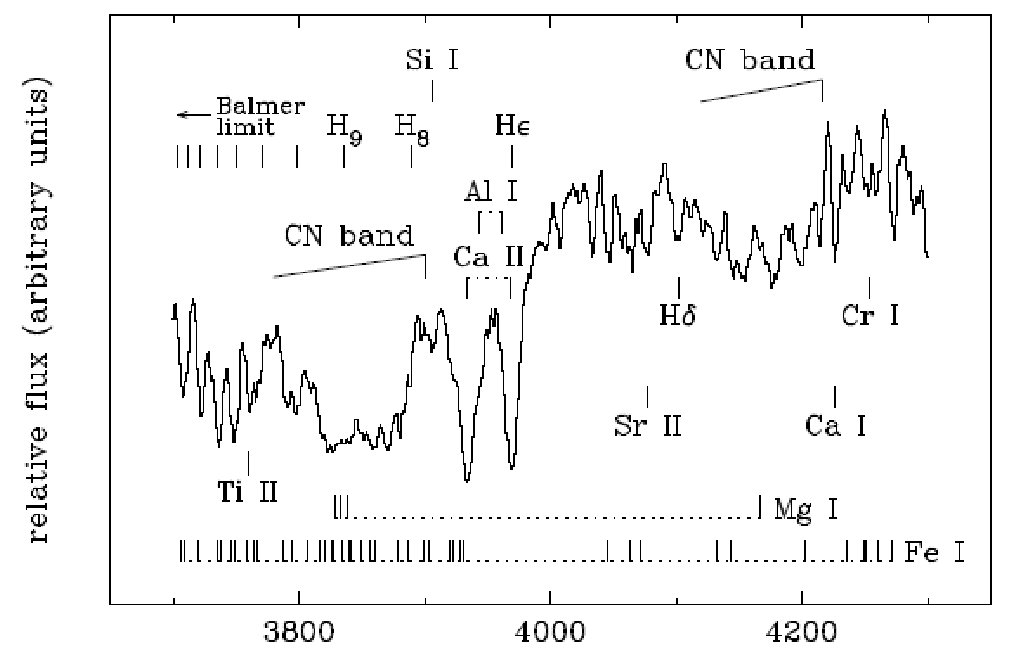

From Gorgas et al., 1999, A&A

spectrum of HD72324(G9 III)

- very strong CaII H/K lines
  - major ion, resonance lines (almost all Ca-atoms are in ground-state of CaII)
    => very strong lines
- weaker Balmer lines (almost all hydrogen in ground-state)
- multitude of FeI and MgI lines
- + CN band lines

=> Strong D4000 break

Theoretical energy distributions of (super)giants

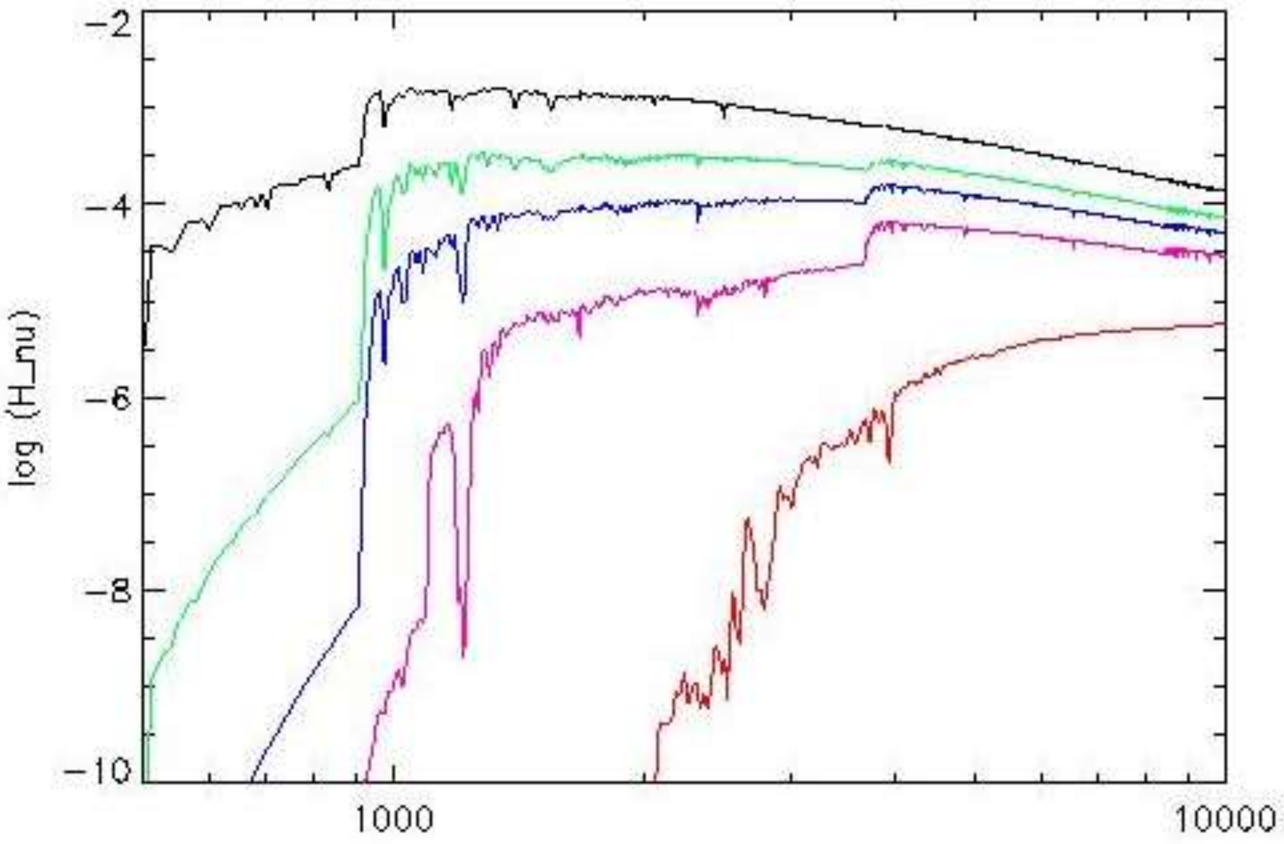

Teff [K] =

30000
20000
15000
10000
5000

calculated by
means of
‘Atlas’ (Kurucz)
model atmospheres
(LTE)

Theoretical energy distributions of (super)giants: zoom into the 4000 Å region

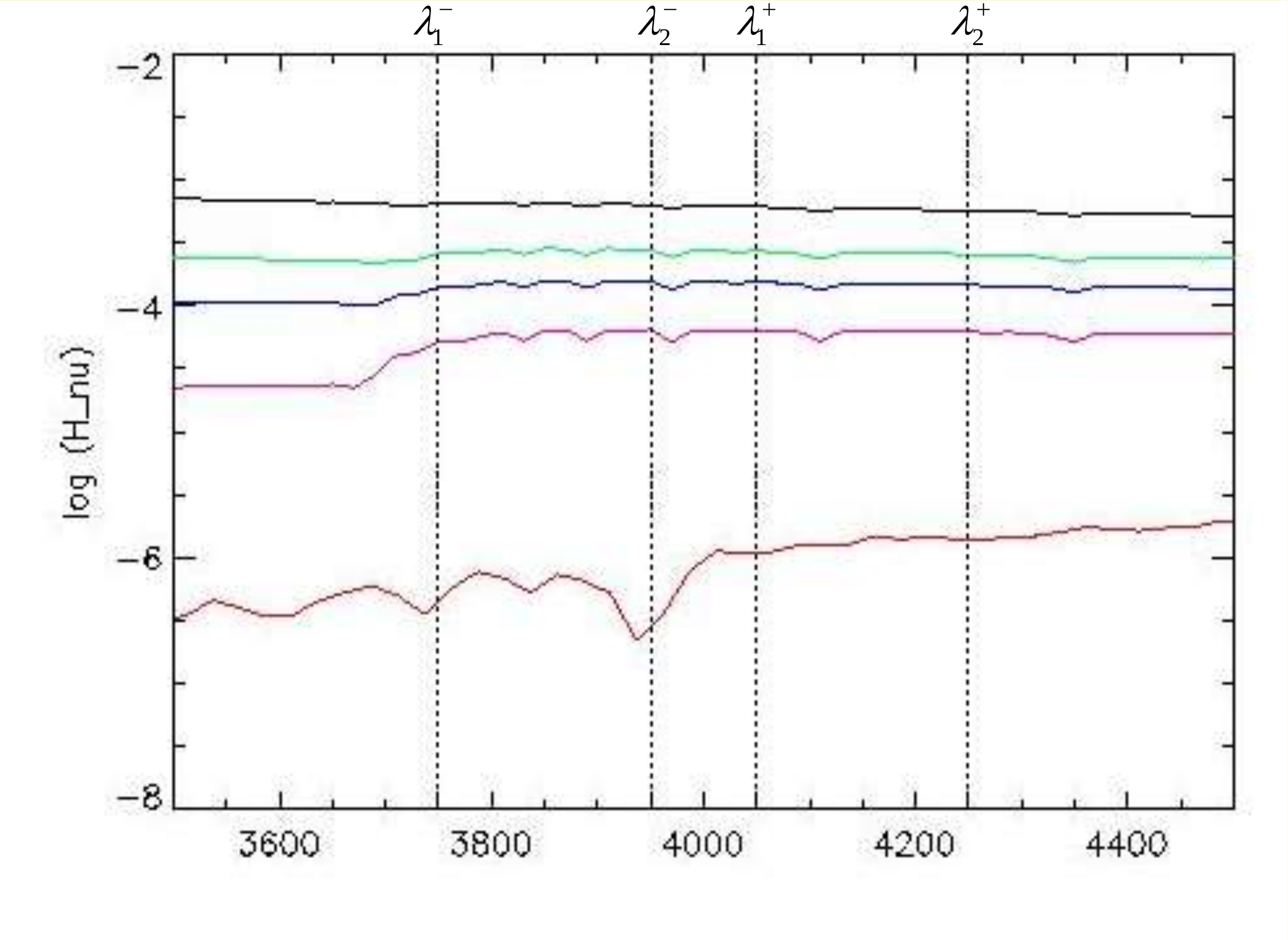

Teff [K] =

30000
20000
15000
10000
5000

calculated by means of ‘Atlas’ (Kurucz) model atmospheres (LTE)

The D4000 break: consequence of line-blocking

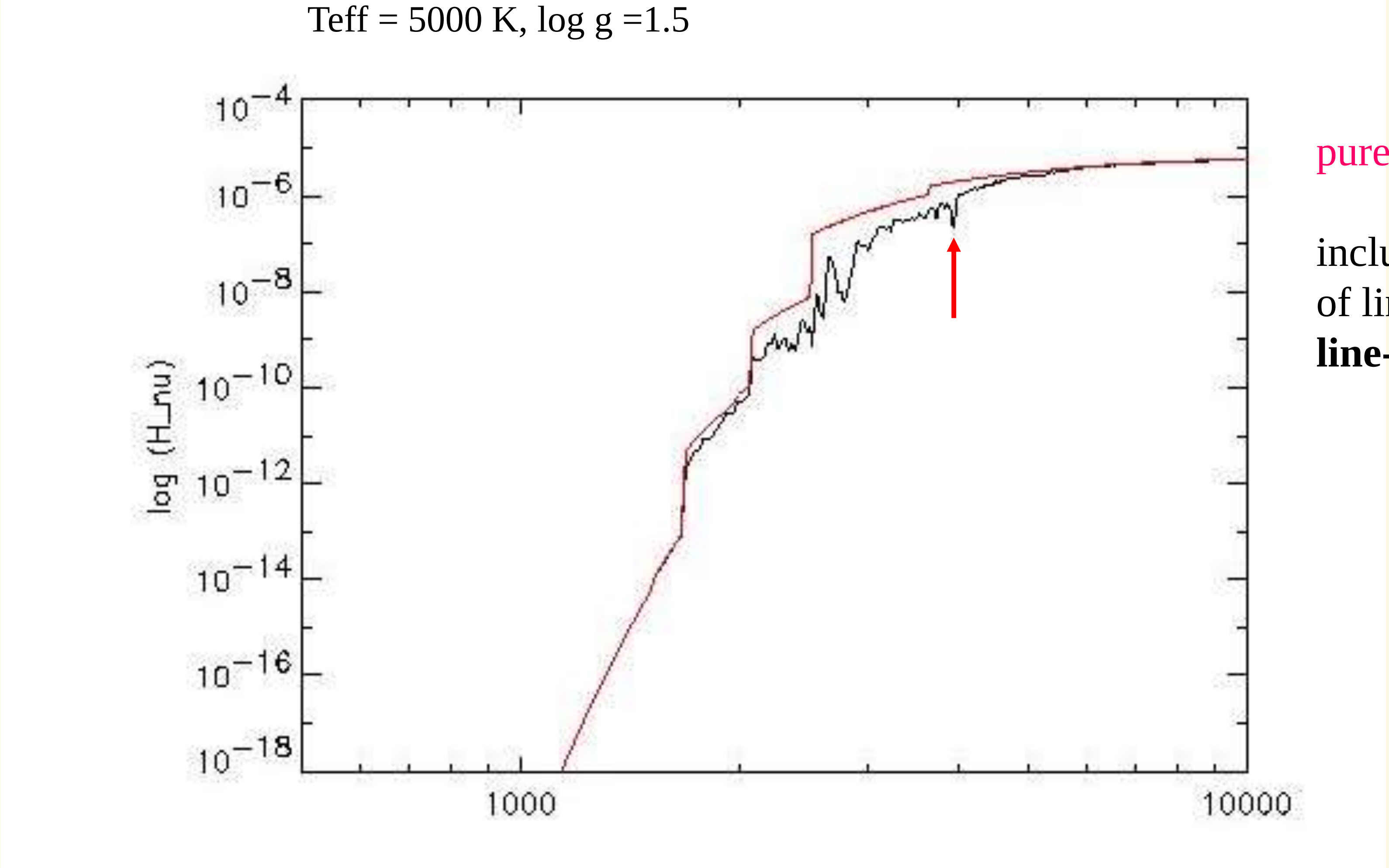

pure continuum

including multitude of lines:
line-blocking

The D4000 break: dependence on parameters

supergiants,
Teff [K] =

6000
5000
4000

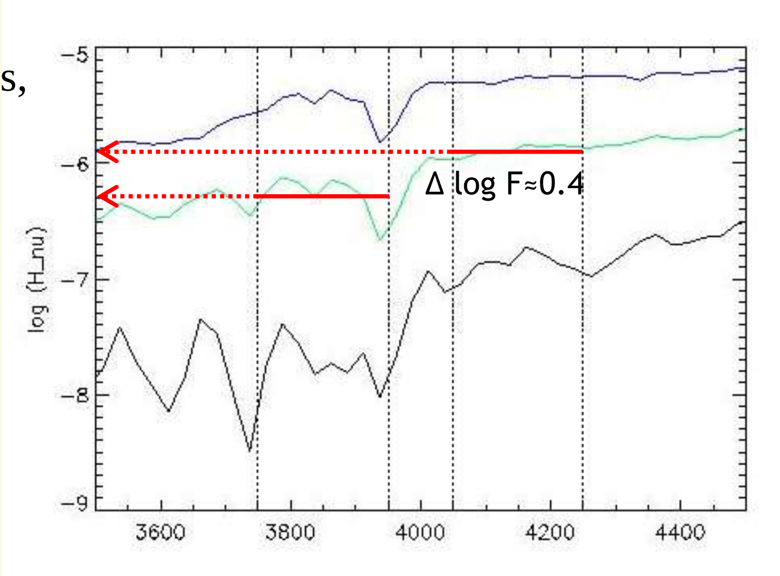

Teff [K] =
5000

log g =
1.50
2.25
3.00
4.50

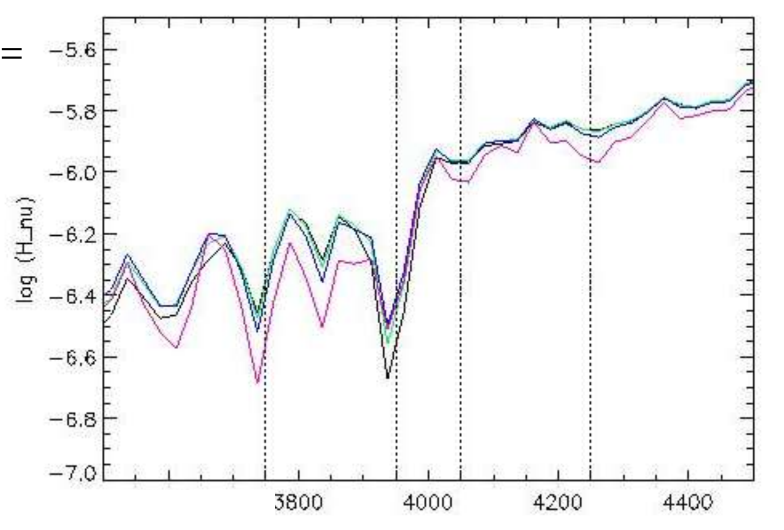

- ✓ dependence on T_{eff}: strong
- ✓ dependence on log g: weak
- ✓ dependence on Z: strong

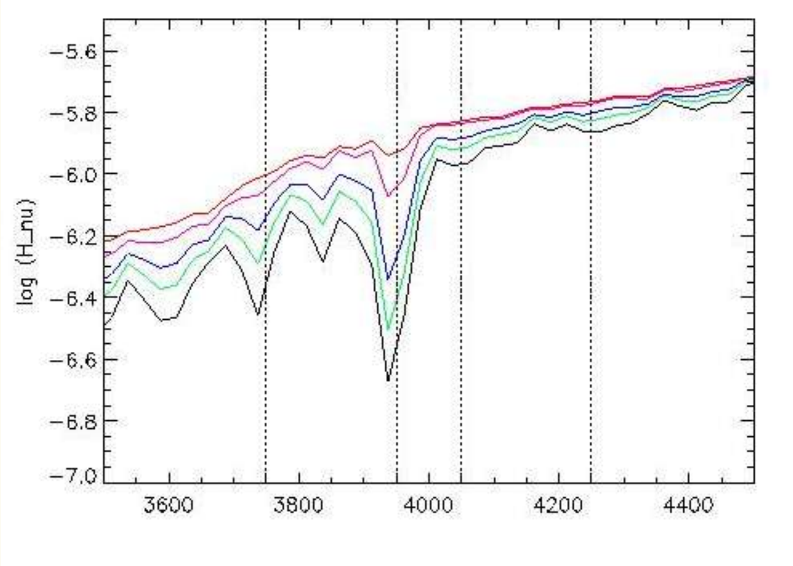

Teff [K] = 5000
log g = 1.50

metallicity (log Z/Z_{sun})
0.00
-0.50
-1.00
-2.00
-3.00

The D4000 break: empirical calibration

factor 2.5
corresponds to
Δ log F=0.4
(see previous
slide)

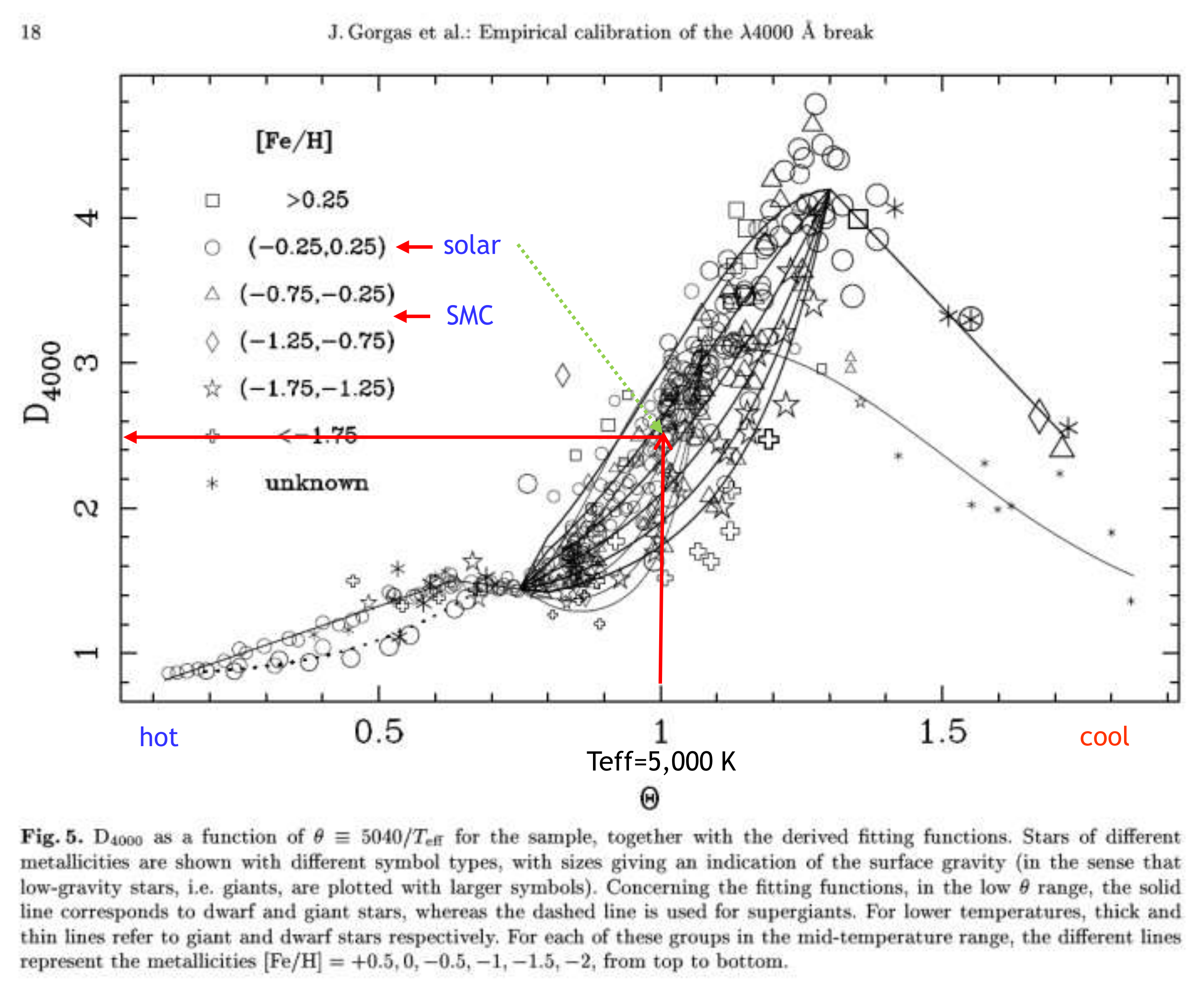

18 J. Gorgas et al.: Empirical calibration of the λ4000 Å break

Fig. 5. D_{4000} as a function of $\theta \equiv 5040/T_{\rm eff}$ for the sample, together with the derived fitting functions. Stars of different metallicities are shown with different symbol types, with sizes giving an indication of the surface gravity (in the sense that low-gravity stars, i.e. giants, are plotted with larger symbols). Concerning the fitting functions, in the low θ range, the solid line corresponds to dwarf and giant stars, whereas the dashed line is used for supergiants. For lower temperatures, thick and thin lines refer to giant and dwarf stars respectively. For each of these groups in the mid-temperature range, the different lines represent the metallicities [Fe/H] = +0.5, 0, −0.5, −1, −1.5, −2, from top to bottom.

Chap. 8 – Stellar winds

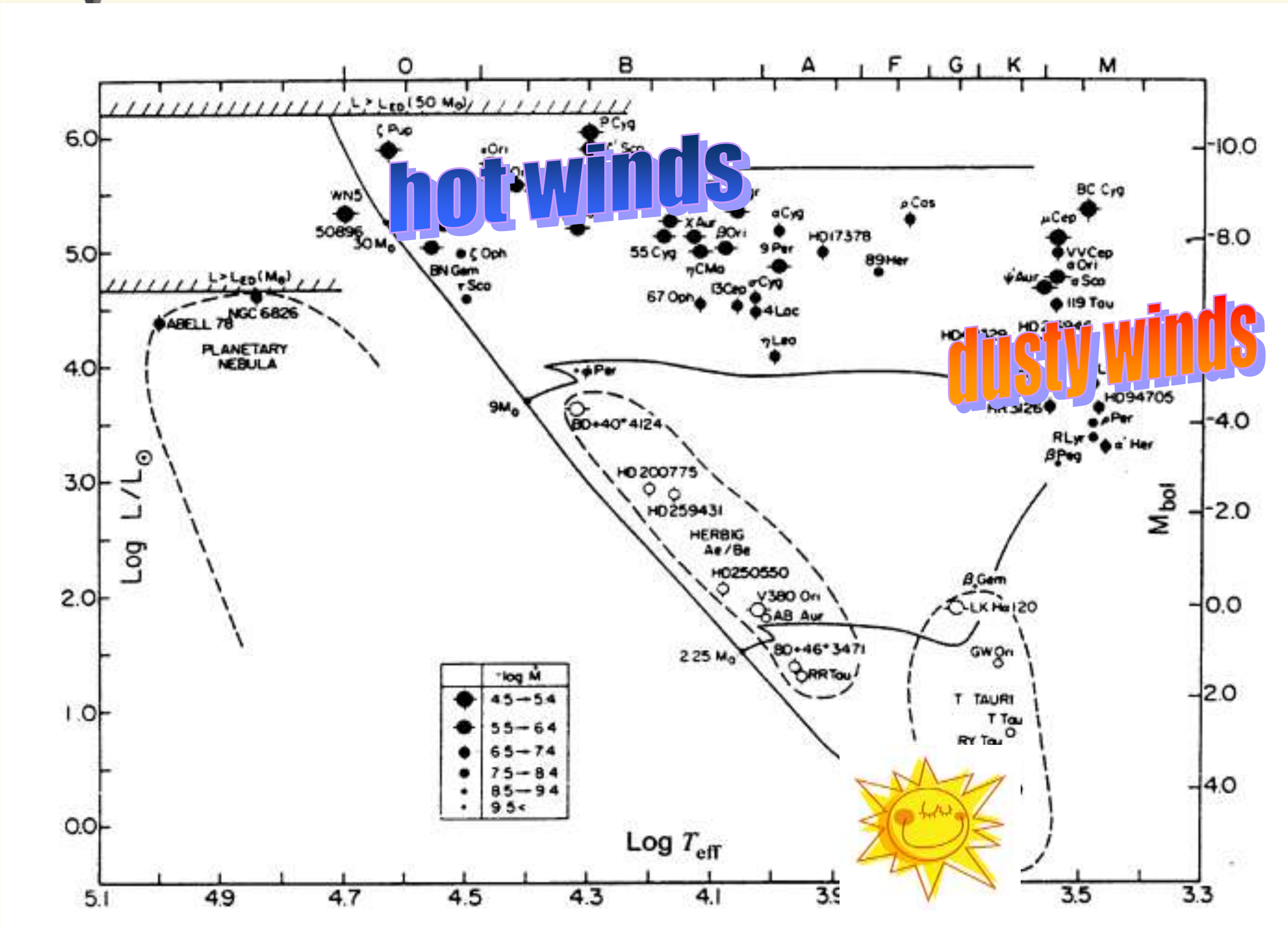

ubiquitous phenomenon

- solar type stars (incl. the sun)
- red supergiants/AGB-stars ("normal" + Mira Variables)
- hot stars (OBA supergiants, Luminous Blue Variables, OB-dwarfs, Central Stars of PN, sdO, sdB, Wolf-Rayet stars)
- T-Tauri stars
- and many more

The solar wind - a suspicion

comet Halley,
with „kink“ in
tail

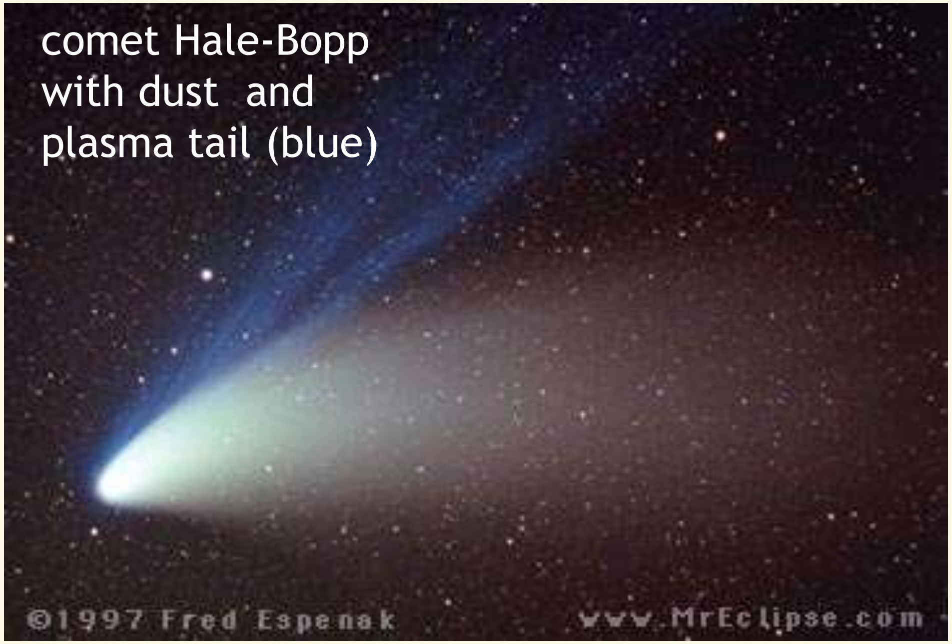

comet Hale-Bopp
with dust and
plasma tail (blue)

©1997 Fred Espenak www.MrEclipse.com

- comet tails *directed away from the sun*
- **Kepler:** influence of solar radiation pressure (-> radiation driven winds)
- *Ionic tail*: emits own radiation, sometimes different direction
- **Hoffmeister** (1943, subsequently Biermann): *solar particle radiation* different direction, since **v** (particle) comparable to **v** (comet)

The solar wind – the discovery

- **Eugene Parker (1958):** theoretical(!) investigation of coronal equilibrium:
  high temperature leads to (solar) wind (more detailed later on)
- **confirmed by**
  - Soviet measurements (Lunik2/3) with “ion-traps” (1959)
  - Explorer 10 (1961)
  - Mariner II (1962): measurement of fast and slow flows
    (27 day cycle -> co-rotating, related “coronal holes” and sun spots)

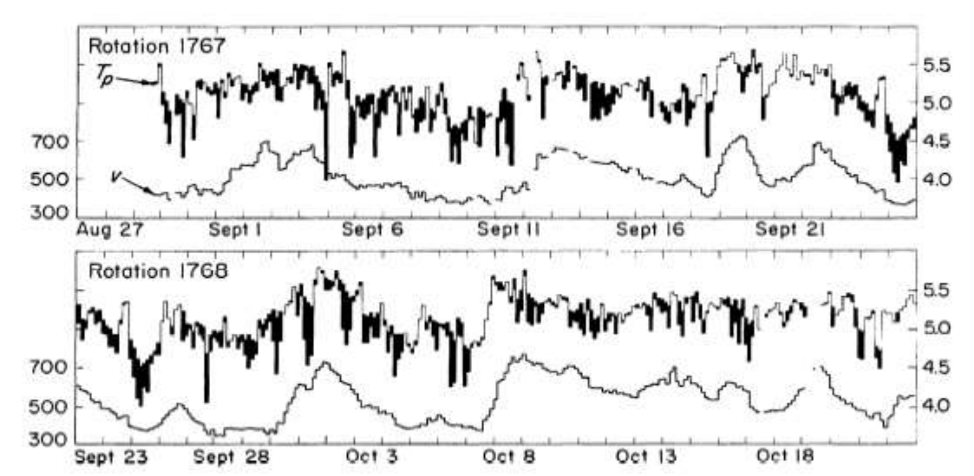

The solar wind – Ulysses ...

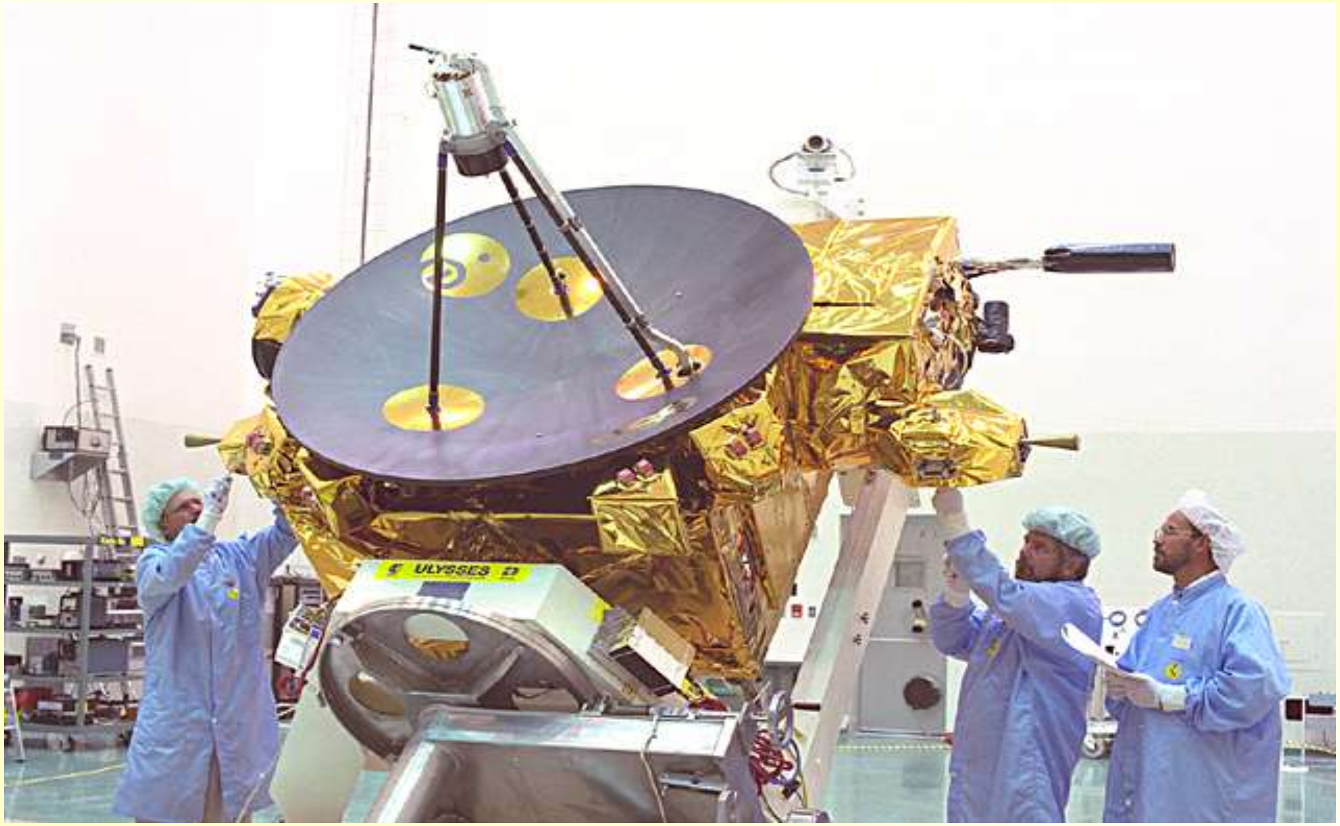

… surveying the polar regions

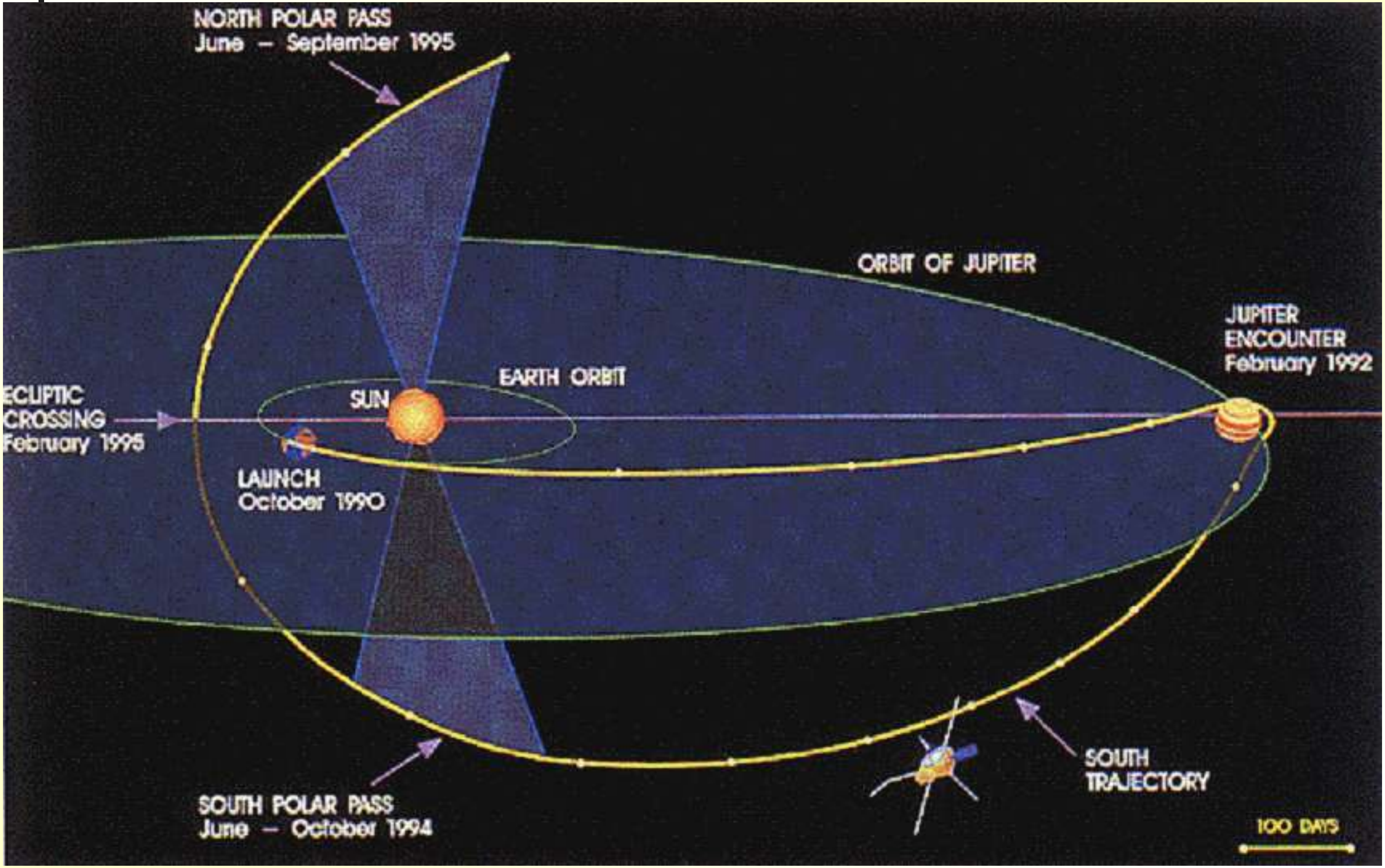

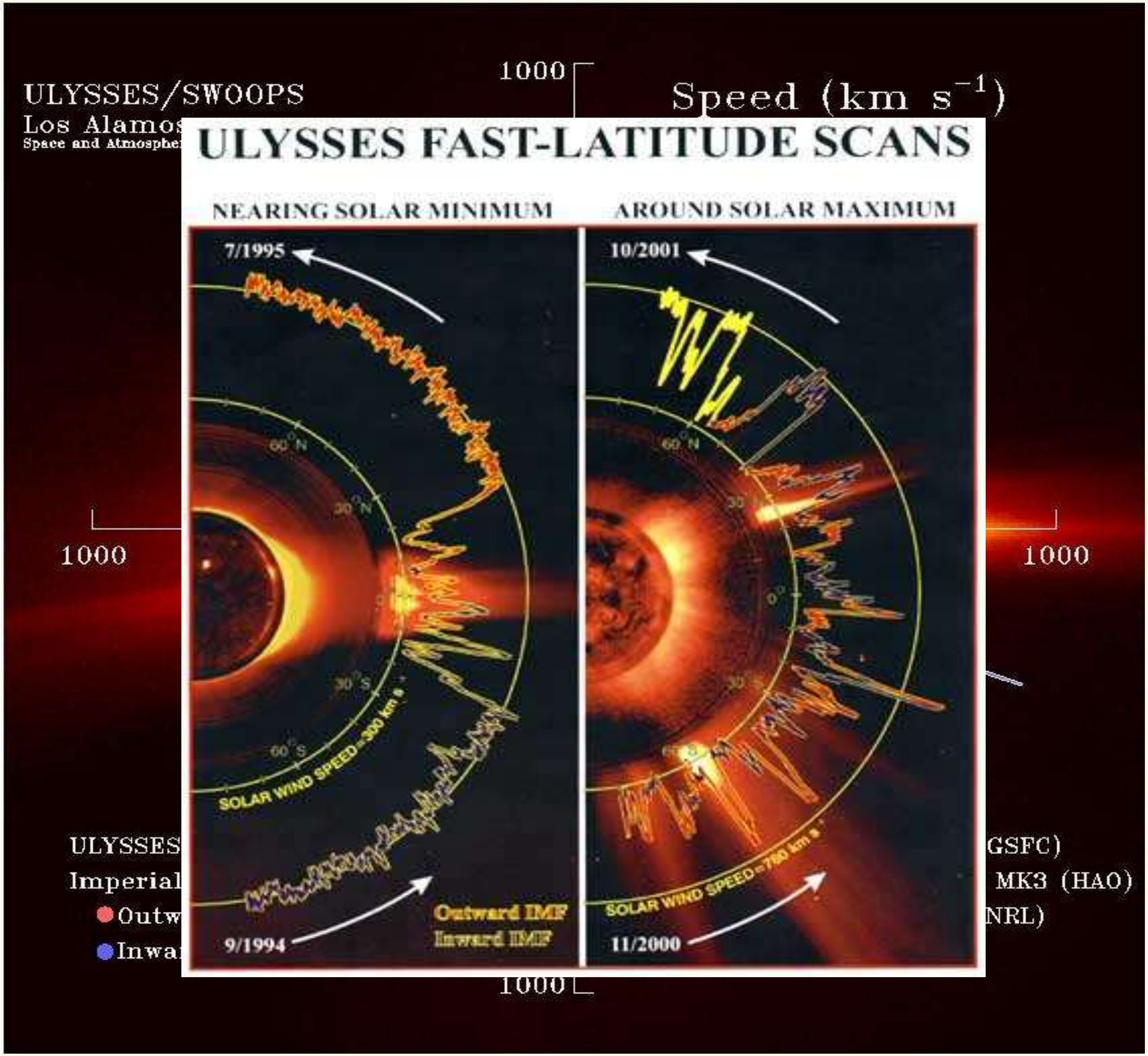

polar wind:
fast and thin

equatorial wind:
slow and dense

The solar wind - coronal holes

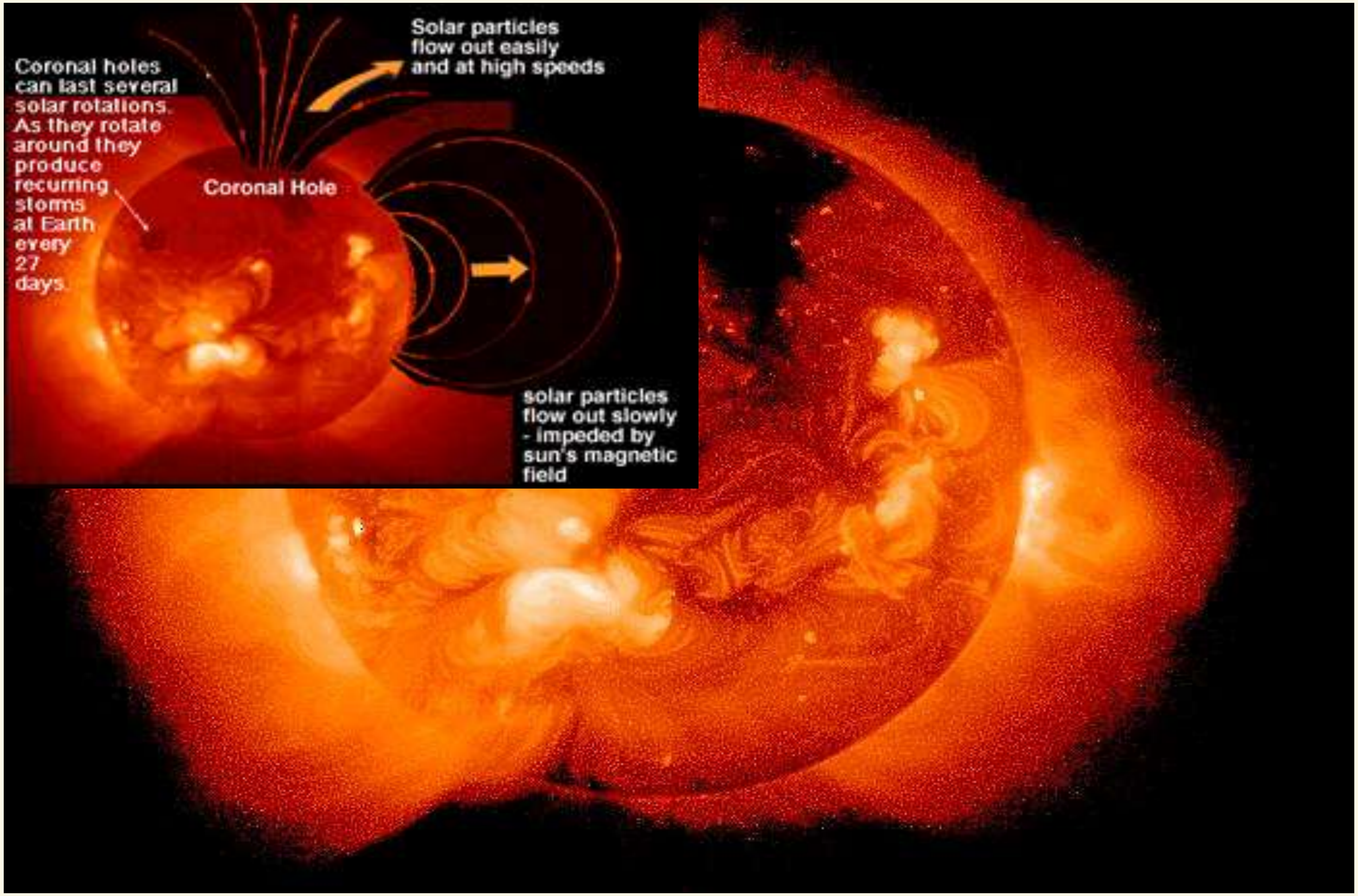

fast wind:
over coronal holes (dark corona, "open" field lines, e.g., in polar regions)

coronal X-ray emission

⇒

very high temperatures

(Yohkoh Mission)

Parker Solar Probe

Primary objectives for the mission

- trace the energy flow, understand heating of the solar corona, study the outer corona.
- determine the structure and dynamics of the plasma and magnetic fields
- explore solar wind driving, and mechanisms that accelerate and transport energetic particles.

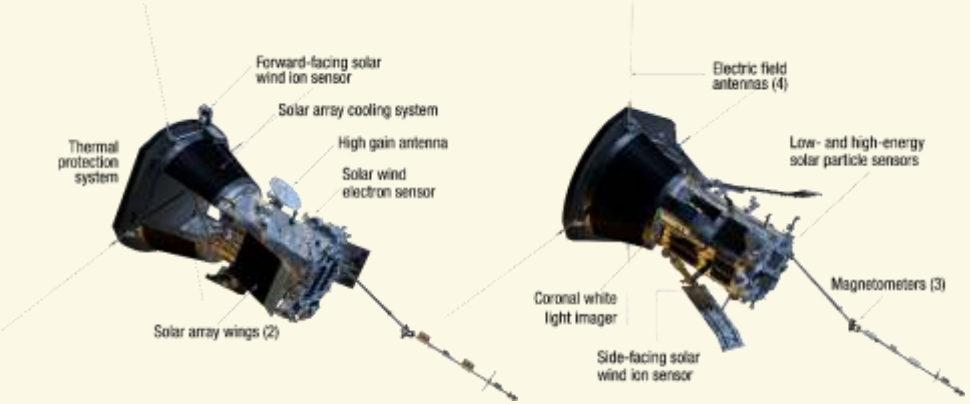

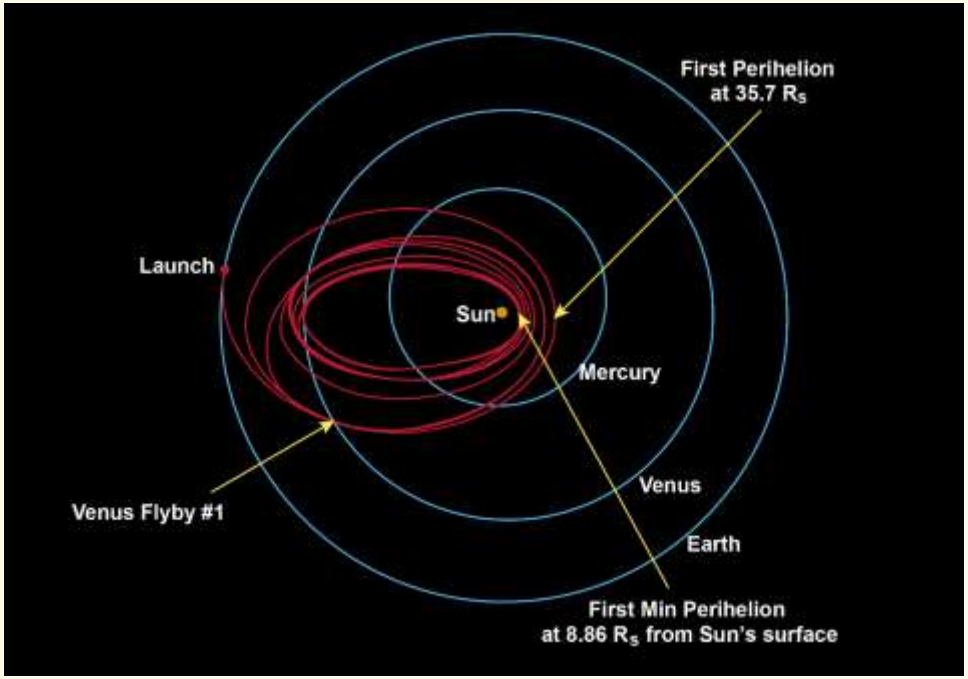

planned: 24 orbits, first perihelion on Nov. 5, 2018;
seven Venus-flybys over 7 years, to decrease perihelion distance from 36 to 8.9 R_{sun} (6 Millionen km, with $T\sim1100$ K)

First results (Nov. 2019)

- wind rotates, but up to 10 times faster than expected
- high speed plasma waves, up to c/6, can revert direction of B-field → "switchbacks": coherent (wind) structures
- coronal mass ejections much more irregular than expected
- dust cleared by solar wind

closest distance reached Dec. 24. 2024 all instruments in operation!

Credit: NASA's Goddard Space Flight Center/Conceptual Image Lab/Adriana Manrique Gutierrez

all material from: parkersolarprobe.jhuapl.edu

The sun and its wind: mean properties

The sun

radius = 695,990 km = 109 terrestrial radii
mass = 1.989 10^{30} kg = 333,000 terrestrial masses
luminosity = 3.85 10^{33} erg/s = 3.85 10^{20} MW $\approx$ 10^{18} nuclear power plants
effective temperature = 5770 °K
central temperature = 15,600,000 °K
life time approx. 10 10^9 years
age = 4.57 10^9 years
distance sun earth approx. 150 10^6 km $\approx$ 400 times earth-moon

The solar wind

temperature when leaving the corona: approx.1 10^6 K
average speed approx. 400-500 km/s (travel time sun-earth approx. 4 days)
particle density close to earth: approx. 6 cm^{-3}
temperature close to earth: $\lesssim 10^5$ K
mass-loss rate: approx 10^{12} g/s (1 Megaton/s) $\approx$ 10^{-14} solar masses/year
$\approx$ one Great-Salt-Lake-mass/day $\approx$ one Baltic-sea-mass/year
$\Rightarrow$ no consequence for solar evolution, since only 0.01% of total mass lost over total life time

Stellar winds – hydrodynamic description

Need mechanism which accelerates material beyond escape velocity:

- **pressure** driven winds
- **radiation** driven winds

Note: red giant winds still not understood,
only scaling relations available ("Reimers-formula")

remember equation of motion (conservation of momentum + stationarity, cf. Chap. 6, page 96)

$$v\frac{dv}{dr} = -\frac{1}{\rho}\frac{dp}{dr} + g^{ext} \text{ (in spherical symmetry), and } p = \rho a^2 \text{ (equation of state, with isothermal sound-speed } a\text{)}$$

$\Rightarrow$ with mass-loss rate $\dot{M}$, radius r, density ρ and velocity v

$$\dot{M} = 4\pi \mathrm{r}^2 \rho v,$$

equation of continuity:
conservation of mass

$$\left(1 - \frac{a^2}{v^2}\right) v\frac{dv}{dr} = -\frac{GM}{r^2} + g_{rad} + \frac{2a^2}{r} - \frac{da^2}{dr}$$

equation of motion:
from conservation of momentum

vel. field	grav. accel.	radiative accel.	(part of) accel. by pressure gradient
	inwards	outwards	outwards

positive for v > a
negative for v < a

Pressure driven winds

$$\left(1-\frac{a^2}{v^2}\right) v\frac{dv}{dr} = -\frac{GM}{r^2} + \cancel{g_{rad}} + \frac{2a^2}{r} - \cancel{\frac{da^2}{dr}}$$

vel. field

grav. accel.

radiative accel.

“pressure”

The solar wind as a proto-type for pressure driven winds

- present in stars which have an (extremely) hot corona (T ≈ 10^6 K)
- with $g_{rad} \approx 0$ and T ≈ const, the rhs of the equation of motion changes sign at

$$r_c = \frac{GM}{2a^2}; \quad \text{with a (T=1.5}\cdot 10^6 \text{ K)} \approx 160 \text{ km/s},$$

we find for the sun $r_c \approx 3.9 R_{sun}$

and obtain four possible solutions for v/v_c ("c" = critical point)

- only one (the "transonic") solution compatible with observations
- pressure driven winds as described here rely on the presence of a hot corona (large value of a!)
- Mass-loss rate $\dot{M} \approx 10^{-14}$ M_{sun} / yr, terminal velocity $v_\infty \approx 500$ km/s
- has to be heated (dissipation of acoustic and magneto-hydrodynamic waves)
- not completely understood so far

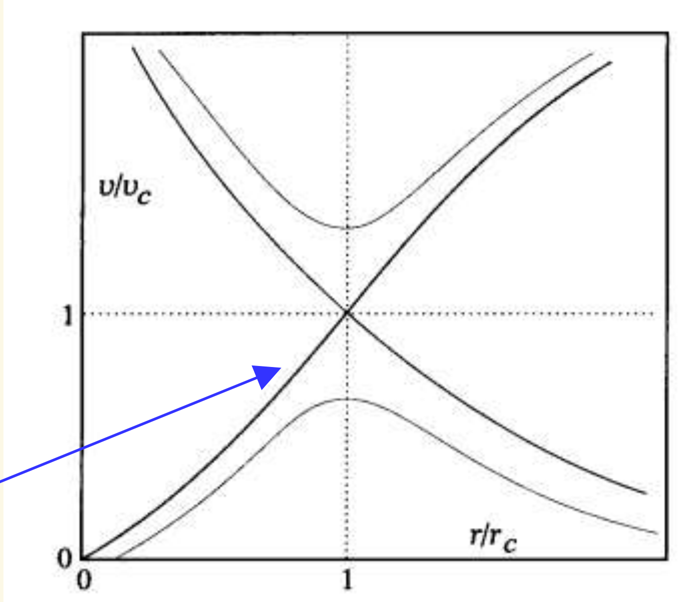

Radiation driven winds

accelerated by radiation pressure:

$$\left(1-\frac{a^2}{v^2}\right)v\frac{dv}{dr} = -\frac{GM}{r^2} + g_{rad} + \underbrace{\frac{2a^2}{r}-\frac{da^2}{dr}}_{\text{important only in lowermost wind}}$$

pressure terms only of secondary order
(a ≈ 20 km/s for hot stars,
≈ 3 km/s for cool stars)

- cool stars (AGB): major contribution from **dust** absorption;
  coupling to “gas” by viscous drag force (gas – grain collisions)

  $\dot{M} \approx 10^{-6} \mathrm{M_{sun}} / \mathrm{yr},\ \mathrm{v}_\infty \approx 20\ \mathrm{km/s}$

- hot stars: major contribution from **metal line** absorption;
  coupling to bulk matter (H/He) by Coulomb collisions

  $\dot{M} \approx 10^{-6} ... 10^{-5}\ \mathrm{M_{sun}} / \mathrm{yr},\ \mathrm{v}_\infty \approx 2{,}000\ \mathrm{km/s}$

dusty winds

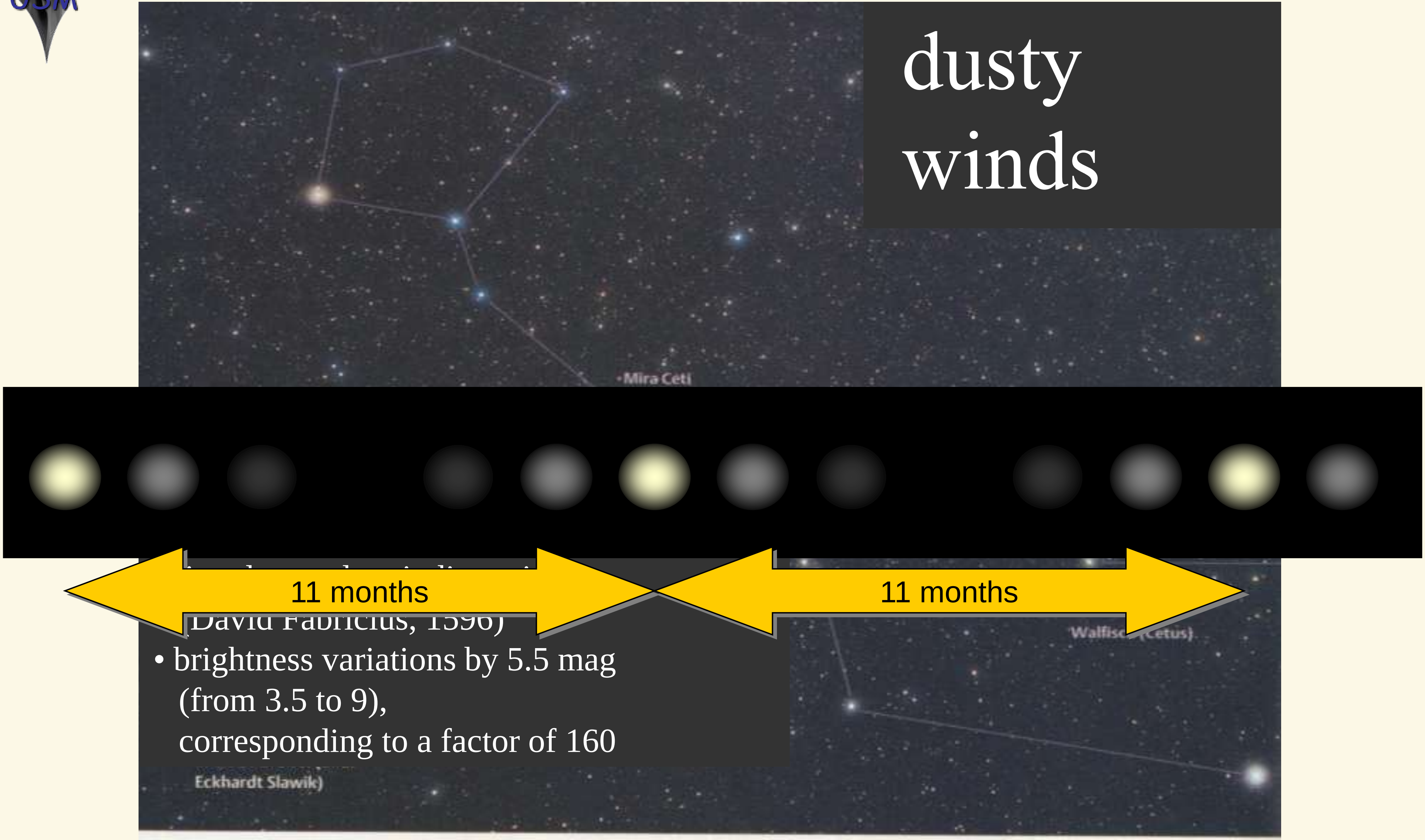

(David Fabricius, 1596)

- brightness variations by 5.5 mag (from 3.5 to 9), corresponding to a factor of 160

Cool supergiants: The dust-factories of our Universe

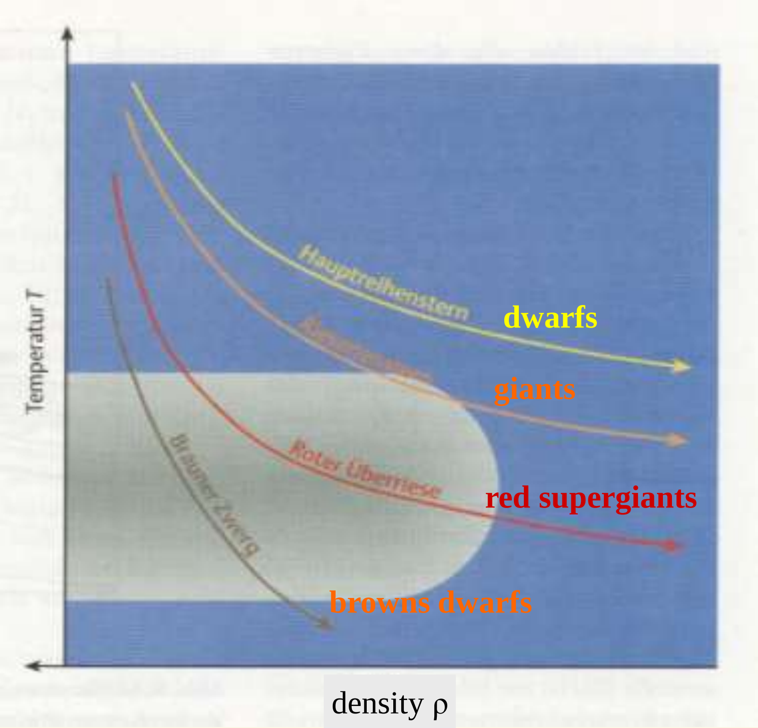

Material on this and following pages from Chr. Helling, *Sterne und Weltraum*, Feb/March 2002

dust: approx. 1% of ISM, 70% of this fraction formed in the winds of AGB-stars (cool, low-mass supergiants)

Red supergiants are located in dust-forming “window”

transition from gaseous phase to solid state possible only in **narrow range of temperature and density:**

gas density must be high enough and temperature low enough to allow for the chemical reactions:

- sufficient number of dust forming molecules required
- the dust particles formed have to be thermally stable

Growth of dust in matter outflow

- decrease of density and temperature
- more and more complex structures are forming
- dust: macroscopic, solid state body, approx. 10^{-7} m (1000 Angstrom), 10^9 atoms

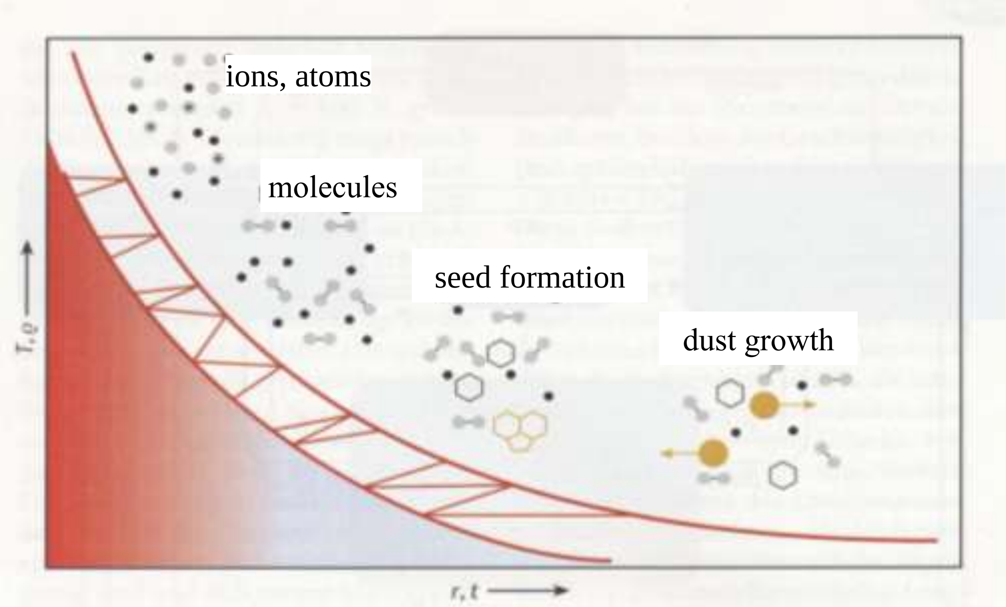

terrestrial, macroscopic rutile crystal (TiO_2, yellowish)

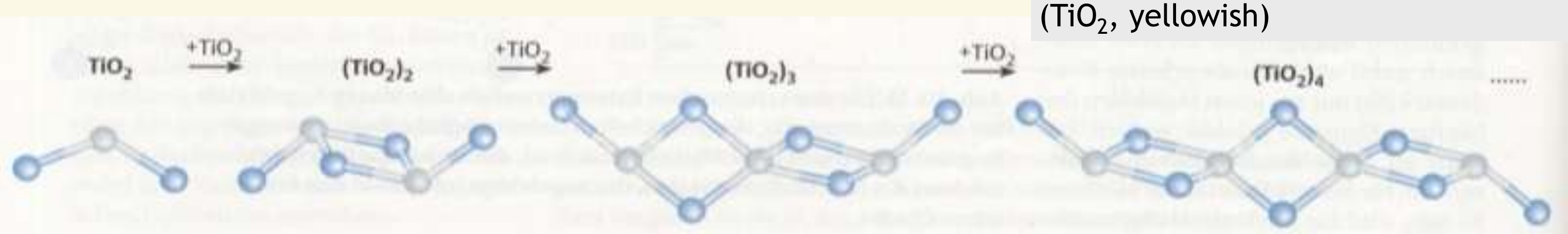

first steps of a linear reaction chain, forming the seed of $(TiO_2)_N$

Dust-driven winds: the principle

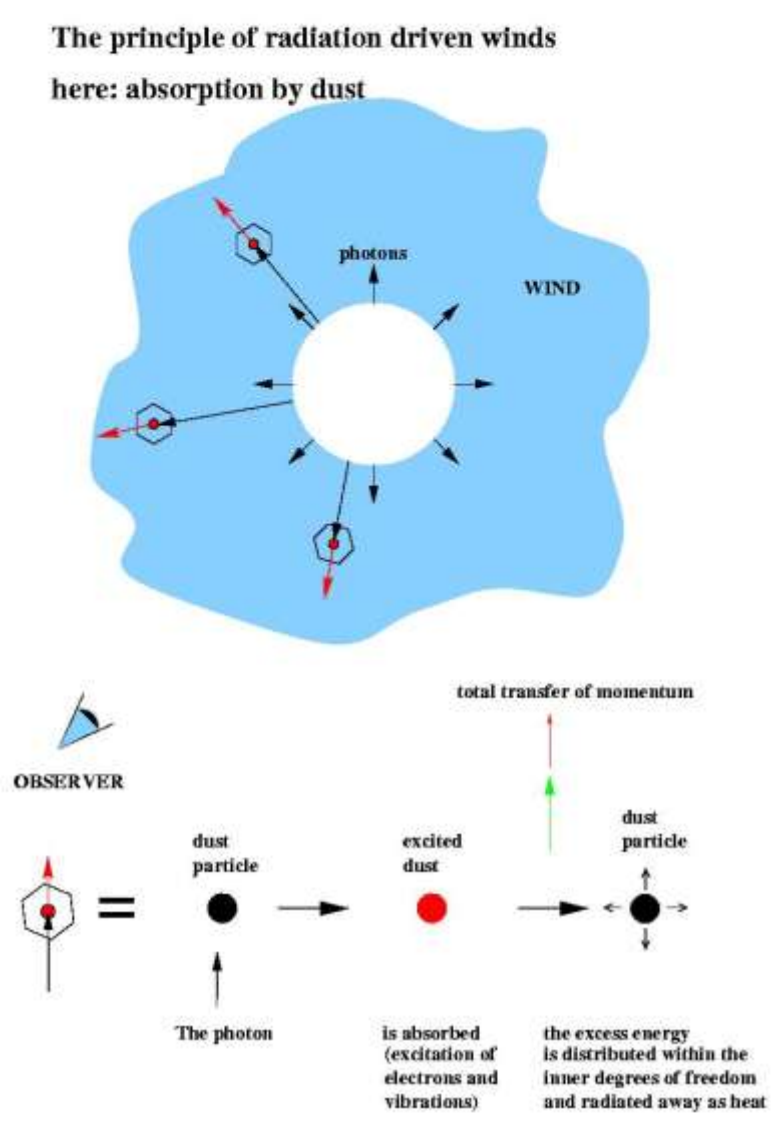

- star emits photons
- photons absorbed (or scattered) by dust
- momentum transfer accelerates dust
- gas accelerated by viscous drag force due to gas-dust collisions

acceleration
proportional to number of photons, i.e.,
proportional to *stellar luminosity **L***

$\Rightarrow$ mass-loss rate $\propto$ ***L***

dust driven winds at tip of AGB responsible for ejection of envelope
$\Rightarrow$ Planetary Nebulae

winds from massive red supergiants still not explained, but maybe similar mechanism

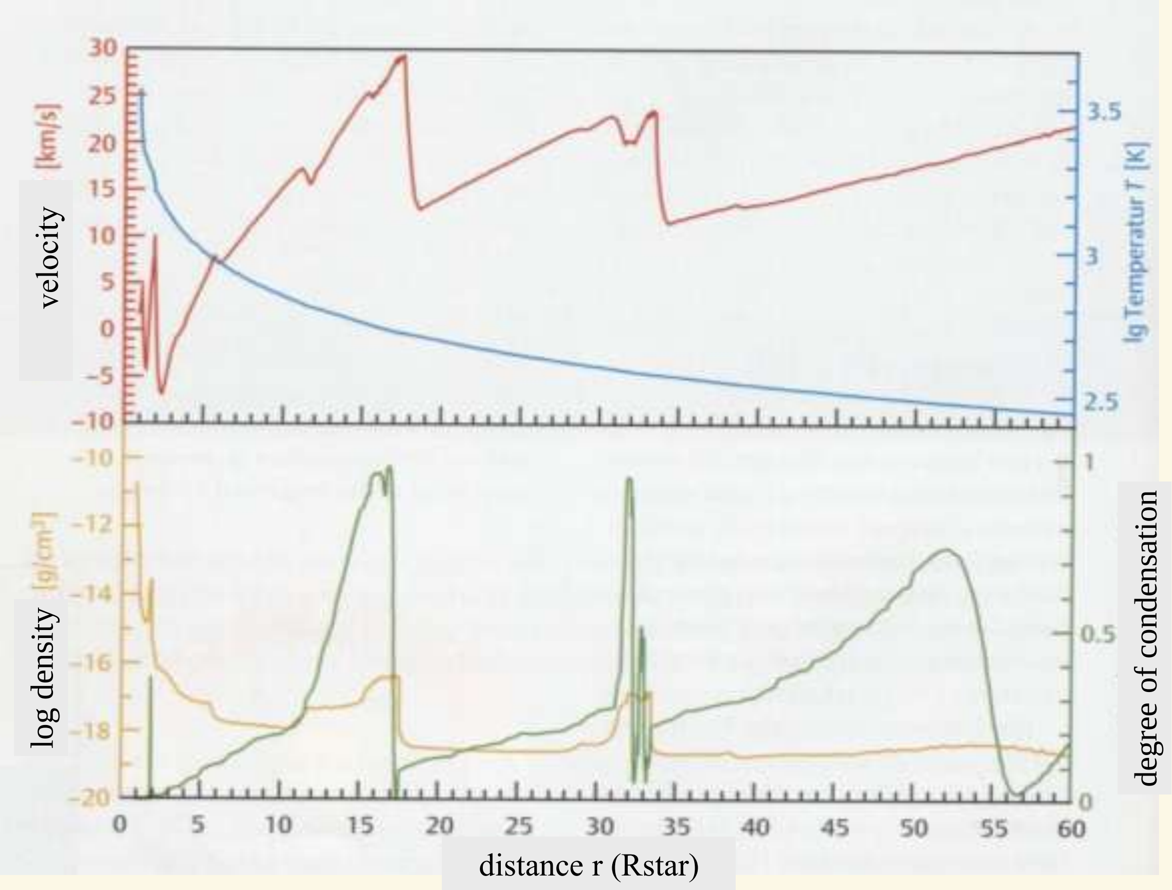

snapshot of a time-dependent hydro-simulation of a carbon-rich circumstellar envelope of an AGB-star. Model parameters similar to next slide.

- star (“surface”) pulsates,
- sound waves are created,
- steepen into shocks;
- matter is compressed,
- dust is formed
- and accelerated by radiation pressure

dust shells are blown away, following the pulsational cycle

⇒ periodic darkening of stellar disc
⇒ **brightness variations**

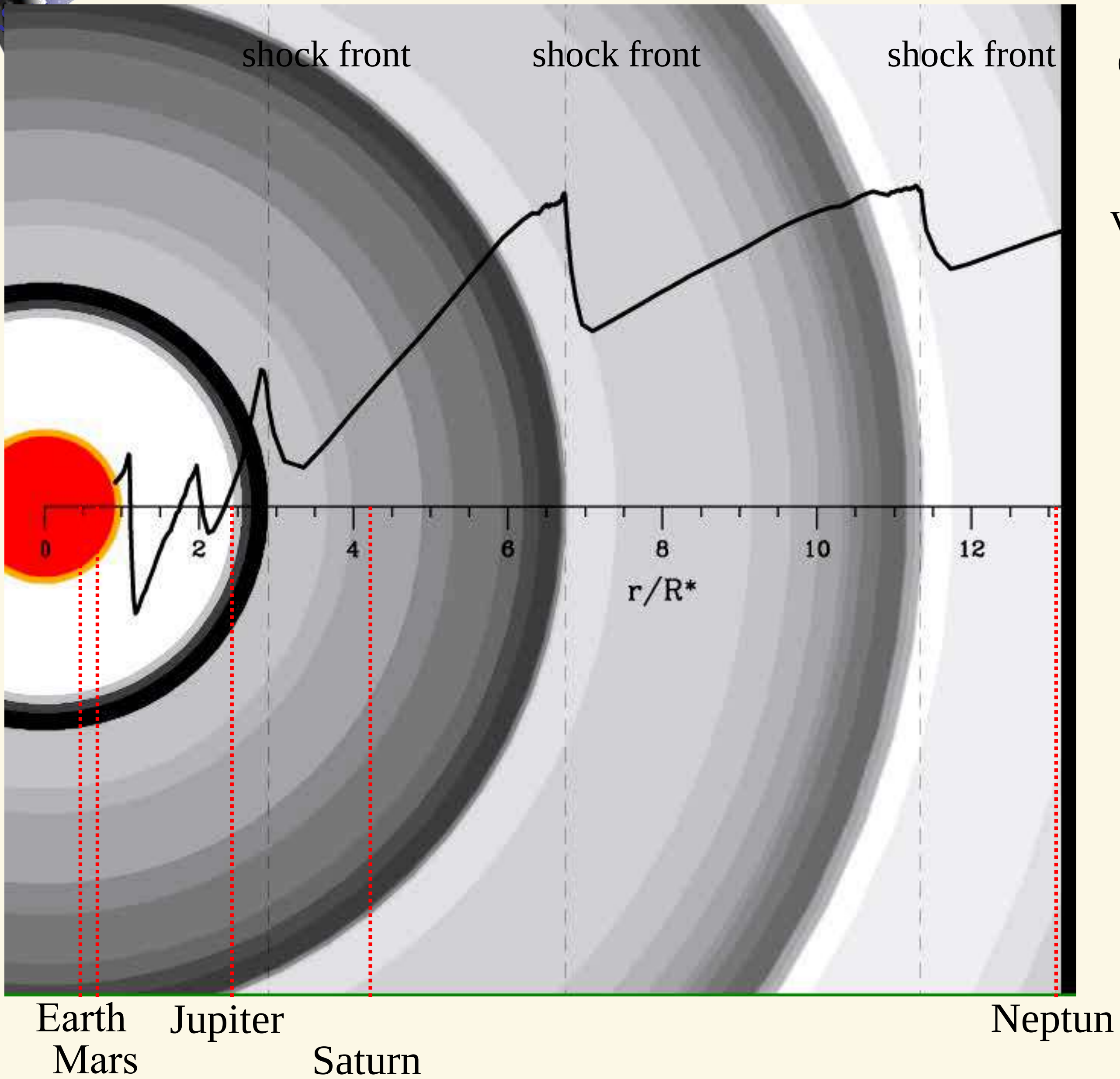

dark colors: dust shells

velocity

simulation of a
dust-driven wind
(*previous working group*
E. Sedlmayr, TU Berlin)

$T = 2600$ K, $L = 10^4\ L_{sun}$,
$M = 1\ M_{sun}$, $\Delta v = 2$ km/s

Stars and their winds - typical parameters

	The sun	Red AGB-stars	Blue supergiants
mass [$M_\odot$]	**1**	**1 … 3**	**10…100**
luminosity [$L_\odot$]	**1**	**10^4**	**$10^5 \ldots 10^6$**
stellar radius [$R_\odot$]	**1**	**400**	**10…200**
effective temperature [K]	**5570**	**2500**	**$10^4 \ldots 5\cdot10^4$**
wind temperature [K]	**10^6**	**1000**	**8000…40000**
mass loss rate [$M_\odot$ /yr]	**10^{-14}**	**$10^{-6} \ldots 10^{-4}$**	**10^{-6} … few 10^{-5}**
terminal velocity [km/s]	**500**	**30**	**200…3000**
life time [yr]	**10^{10}**	**10^5**	**10^7**
total mass loss [$M_\odot$]	**10^{-4}**	**$\gtrsim 0.5$**	**up to 90% of total mass**

massive stars determine energy (kinetic and radiation) and momentum budget of surrounding ISM

Bubble Nebula
(NGC 7635)
in Cassiopeia

wind-blown
bubble around
BD+602522
(O6.5IIIf)

Line-driven winds: basics

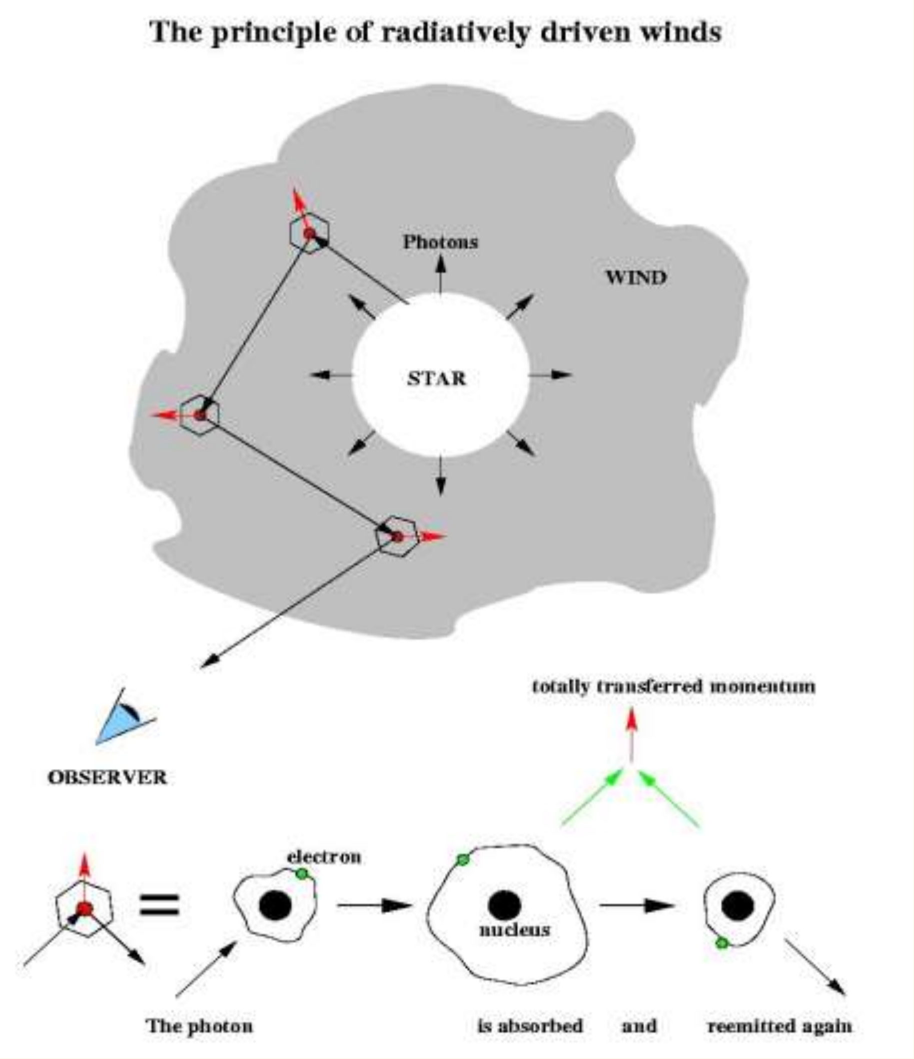

- accelerated by radiation pressure in **lines**
  $M \approx 10^{-7}...10^{-5}\ \mathrm{M_{sun}}\ /\ \mathrm{yr},\ \mathrm{v}_\infty \approx 200\ ...\ 3{,}000\ \mathrm{km/s}$
- momentum transfer from accelerated species (ions) to bulk matter (H/He) via Coulomb collisions

Prerequesites for radiative driving

- large number of photons => high luminosity
  $L \propto R_*^2\ T_{\mathrm{eff}}^4$ => supergiants or hot dwarfs
- line driving:
  large number of lines close to flux maximum
  (typically some 10^4...10^5 lines relevant)
  with high interaction probability
  (=> mass-loss dependent on metal abundances)

- line driven winds important for chemical evolution of (spiral) Galaxies, in particular for starbursts
- transfer of momentum (=> induces *star formation*, hot stars mostly in *associations)*, energy and nuclear processed material to surrounding environment
- dramatic impact on stellar evolution of massive stars (mass-loss rate vs. life time!)

pioneering investigations by
Lucy & Solomon, 1970, ApJ 159
Castor, Abbott & Klein, 1975, ApJ 195 (CAK)
reviews by Kudritzki & Puls, 2000, ARAA 38
Puls et al. 2008 A&Arv 16, issue 3,
Vink, 2020, ARAA 60

Radiative line driving and the Doppler effect

$g_{rad} \propto N$ (number of absorbed photons)

LINE absorption

absorption only if frequency close to a possible line transition,

$$\kappa_\nu \propto \kappa_0 \text{ if } \nu_0 \pm \delta\nu \text{ (thermal width)}$$
$$\kappa_\nu = 0 \quad \text{else}$$

- absorption always at *line frequency* ν_0 $(\pm\delta\nu)$ *in frame of matter*
- matter moves at certain velocity with respect to stellar frame
- matter "sees" stellar photons at different frequency than star itself (Doppler-effect)

$$\nu_{\mathrm{CMF}} = \nu_{\mathrm{obs}} - \frac{\nu_0 \mathrm{v}(r)}{c} =: \nu_0 \quad \text{(radial photons, } \mu\text{=1, assumed)}$$

- the larger the velocity of matter, the larger the photon's stellar frame frequency must be in order to become absorbed at ν_0 (in frame of matter)

$$\left.\begin{aligned} \nu_0 &= \nu_1^{\mathrm{obs}} - \frac{\nu_0}{c}\mathrm{v}_1(r) \\ \nu_0 &= \nu_2^{\mathrm{obs}} - \frac{\nu_0}{c}\mathrm{v}_2(r) \end{aligned}\right\} \text{if } \mathrm{v}_2(r) > \mathrm{v}_1(r), \text{ then } \nu_2^{\mathrm{obs}} > \nu_1^{\mathrm{obs}}$$

⇒accelerated matter "sees" photons from a considerably larger band-width than static matter, $\Delta\nu_{\mathrm{obs}} = \frac{\nu_0}{c}\Delta\mathrm{v} \gg \delta\nu$

shell of matter with spatial extent Δr,

and velocity $\mathrm{v}_0 + \left(\frac{\mathrm{dv}}{\mathrm{dr}}\right)_1 \Delta r$

absorption of photons at $\nu_0 \pm \delta\nu$

in frame of matter

photons must start at higher (stellar) frequencies, are "seen" at $\nu_0 \pm \delta\nu$ in frame of matter because of Doppler-effect.

Let $\Delta\nu$ be frequency band contributing to acceleration of matter in Δr

The larger $\frac{\mathrm{dv}}{\mathrm{dr}}$,

- the larger $\Delta\nu$
- the more photons can be absorbed
- the larger the acceleration

$$\boxed{g_{\mathrm{rad}} \propto \frac{\mathrm{dv}}{\mathrm{dr}}}$$

(assuming that each photon is absorbed, i.e., acceleration from optically thick lines)

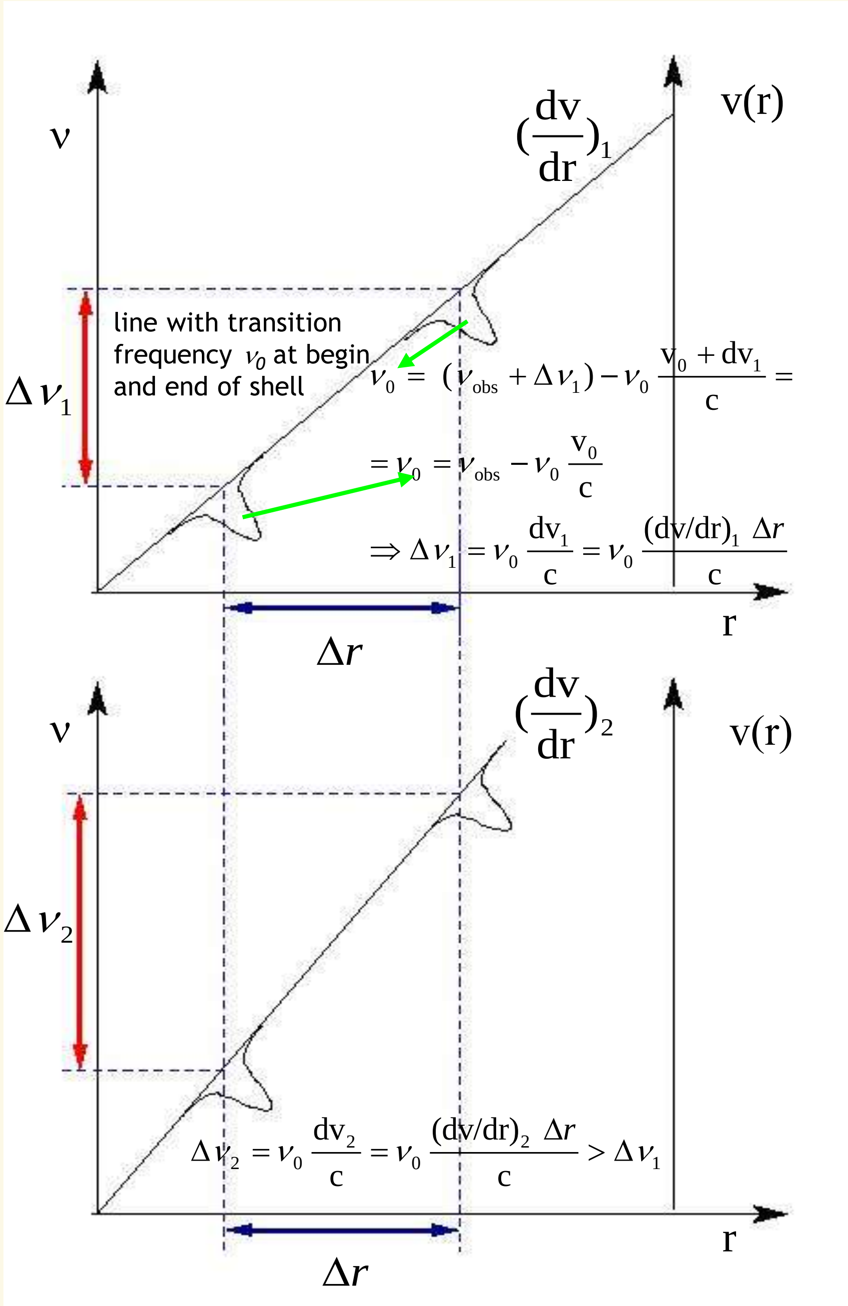

Millions of lines ....

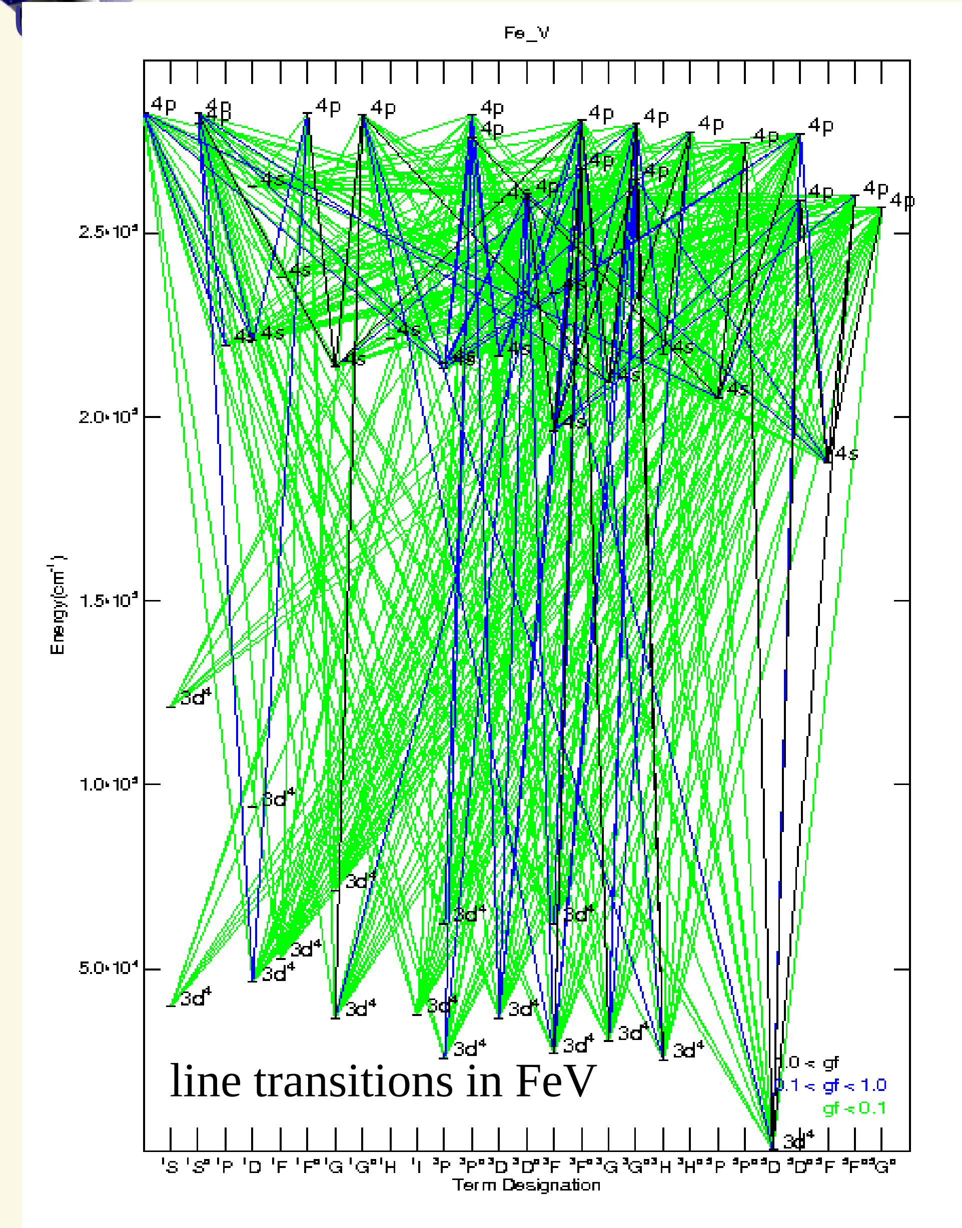

line transitions in FeV

... are present
... and needed!

Remember (Chapt. 4)

$$g_{rad} = \frac{1}{c\rho}\int \kappa_\nu \mathscr{F}_\nu d\nu \qquad \text{with opacity } \kappa_\nu$$

and radiative flux $\mathscr{F}_\nu$

summing up the individual contributions from optically thin and thick lines,

$$g_{rad}^{tot} = \sum_{\text{all lines}} g_{rad}^{i},$$

$$g_{rad}^{thin} \propto L_\nu^i k^i, \quad k^i \propto \frac{\kappa^i}{\rho} \text{ (line-strength)}$$

$$g_{rad}^{thick} \propto L_\nu^i \frac{\mathrm{dv}/dr}{\rho}$$

when accounting for interaction probability $(1-\exp(-\tau^i))$

The line distribution function

- pioneering work by Castor, Abbott & Klein (1975) and by Abbott (1982)
- first realistic line-strength distribution function by Kudritzki et al. (1988)
- NOW: 4.2 Ml (Mega lines), 150 ionization stages (H – Zn), NLTE

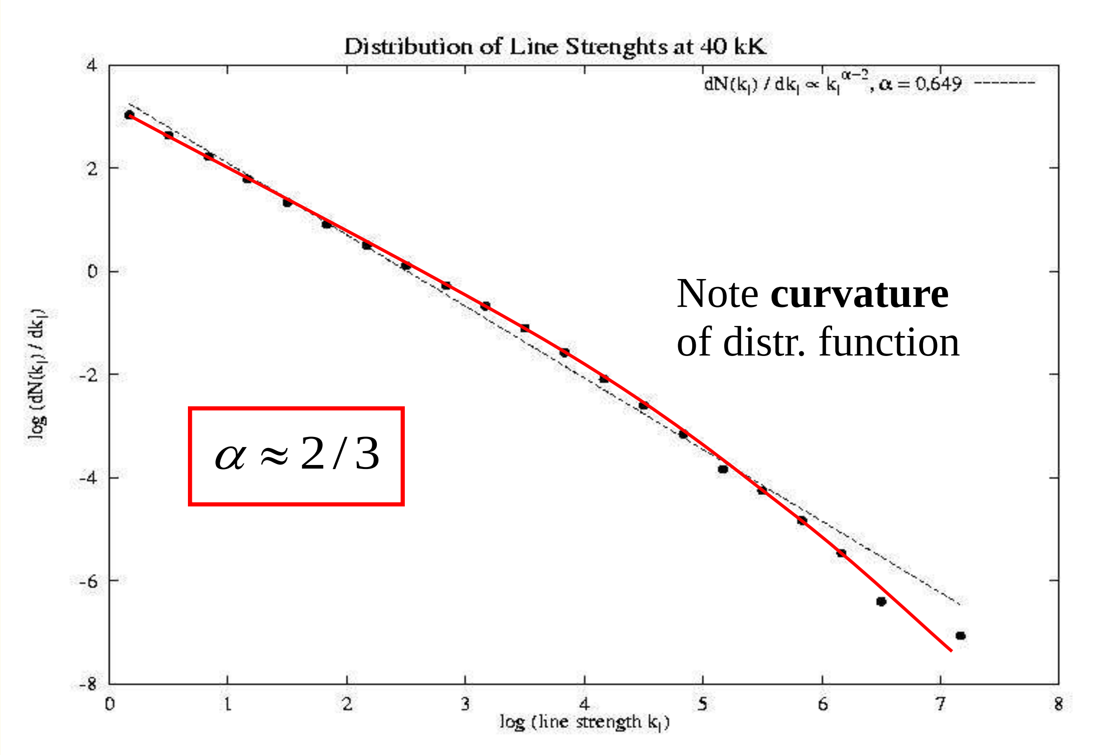

Note **curvature** of distr. function

$$\alpha \approx 2/3$$

Logarithmic plot of line-strength distribution function for an O-type wind at 40,000 K and corresponding power-law fit
(see Puls et al. 2000, A&AS 141)

$$\frac{dN(k)}{dk} = k^{\alpha-2}, \quad \alpha \approx 0.6 \ldots 0.7$$

+ 2nd empirical finding:
valid in *each* frequential subinterval

$$dN(k,\nu) = -N_0 f(\nu) d\nu \, k^{\alpha-2} dk$$

$$g_{rad}^{tot} = \sum_{\text{all lines}} g_{rad}^{i} \quad \Rightarrow \iint g_{rad}^{i}(\nu,k)\, dN(\nu,k) \quad \propto N_{\text{eff}}\, L \left(\frac{\mathrm{d}v/dr}{\rho} \right)^{\alpha},$$

N_{eff} "effective" number of lines

α exponent of line-strength distr. function, also: $\alpha = \dfrac{g_{rad}^{thick}}{g_{rad}^{tot}}$

Hydrodynamical descri

mass-loss rate $\dot{M}$, radi

$\dot{M} = 4\pi \mathrm{r}^2 \rho v,$ n of continuity

vation of mass-flux

isothermal soundspeed

with

$$g_{rad} = g_{\text{cont}} + g_{\text{lines}}, \quad g_{\text{lines}} \propto N_{\text{eff}}\, L \left(\frac{\mathrm{d}v/dr}{\rho} \right)^{\alpha},$$

(approximate) analytical solution possible

$$\left(1 - \frac{a^2}{v^2}\right) v \frac{dv}{dr} = -\frac{GM}{r^2} + g_{rad} + \frac{2a^2}{r} - \frac{da^2}{dr}$$

equation of motion
conservation of momentum-flux

velocity field	grav. accel.	radiative accel.	“pressure”
positive for v > a	inwards	outwards	outwards
negative for v < a			

Scaling relations for line-driven winds (without rotation)

$$\dot{M} \propto N_{\mathrm{eff}}^{1/\alpha'} L^{1/\alpha'} \left(M(1-\Gamma)\right)^{1-1/\alpha'}$$

$$v_\infty \approx 2.25 \frac{\alpha}{1-\alpha} v_{\mathrm{esc}}, \quad v_{\mathrm{esc}} = \left(\frac{2GM(1-\Gamma)}{R_*}\right)^{\frac{1}{2}}$$

$$v(r) = v_\infty \left(1 - \frac{R_*}{r}\right)^\beta, \quad \beta = 0.8 \text{ (O-stars) ... 2 (BA-SG)}$$

Γ Eddington factor, accounting for acceleration by Thomson-scattering, diminishes effective gravity

N_{eff} number of lines effectively driving the wind, corrected for ionization effects, dependent on metallicity and spectral type

α exponent of line-strength distribution function, $0 < \alpha < 1$
large value: more optically thick lines

$\alpha' = \alpha - \delta$, with δ ionization parameter, typical value for O-stars: $\alpha' \approx 0.6$

The wind-momentum luminosity relation (WLR)

- use scaling relations for $\dot{M}$ and v_∞, calculate modified wind-momentum rate

$$\dot{M}\, v_\infty R_*^{1/2} \propto N_{\text{eff}}^{1/\alpha'} L^{1/\alpha'} \left(M(1-\Gamma)\right)^{1-1/\alpha'} \left(M(1-\Gamma)\right)^{1/2}$$

$$(\alpha' \approx \frac{2}{3}) \propto N_{\text{eff}}^{1/\alpha'} L^{1/\alpha'}, \text{ independent of } M \text{ and } \Gamma$$

$$\Rightarrow \log(\dot{M}\, v_\infty R_*^{1/2}) \approx \frac{1}{\alpha'} \log L + const(z, \text{ sp.type})$$

(Kudritzki, Lennon & Puls 1995)

- (at least) two applications

(1) construct observed WLR, calibrate as a function of
spectral type and metallicity (N_{eff} and α’ depend on both parameters)
independent tool to measure extragalactic distances
from *wind-properties*, T_{eff} and metallicity

(2) compare with theoretical WLR to test validity of radiation driven wind theory

Determination of wind-parameters: v_∞

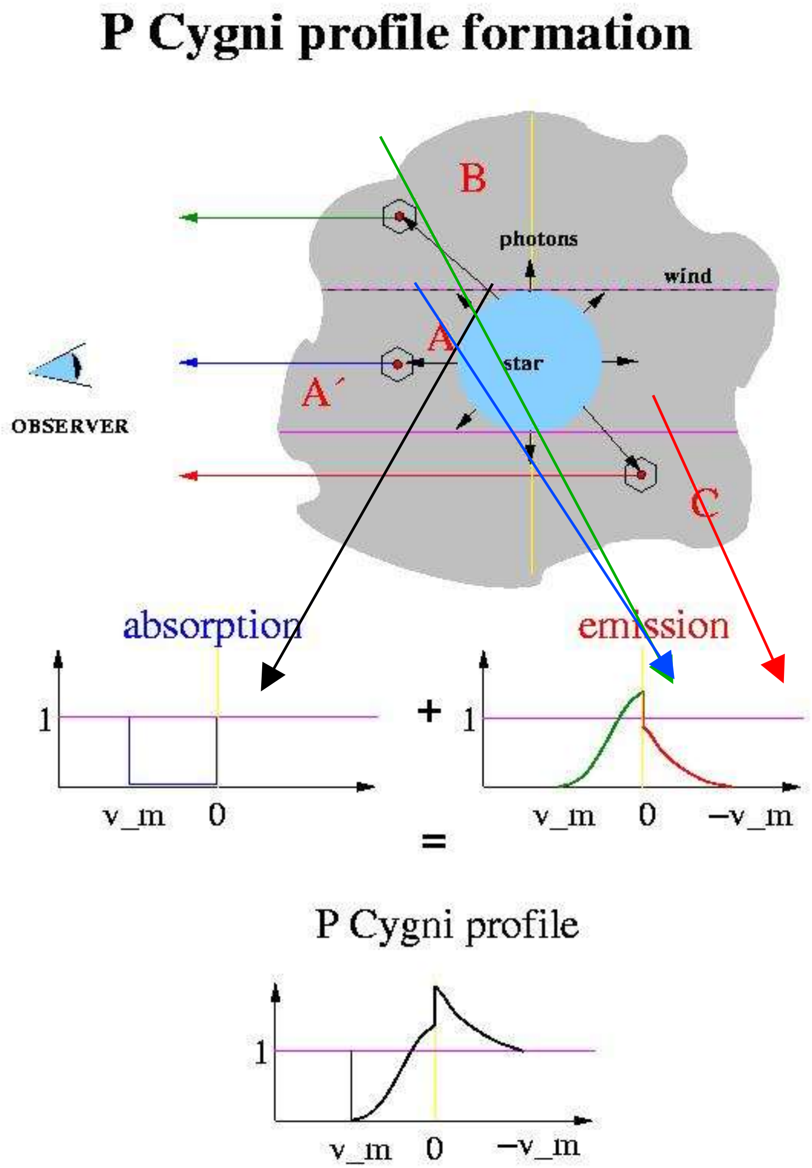

$$\nu_{\rm obs} = \nu_0\left(1+\frac{\mu v(r)}{c}\right); \quad \nu_0 \ \text{line frequency in CMF}$$

$$\mu v(r) > 0: \quad \nu_{\rm obs} > \nu_0 \quad \text{blue side}$$

$$\mu v(r) < 0: \quad \nu_{\rm obs} < \nu_0 \quad \text{red side}$$

$$\frac{v_{\rm m}}{\rm c} = \frac{\nu_{\max}-\nu_0}{\nu_0} = 1 - \frac{\lambda_{\min}}{\lambda_0}$$

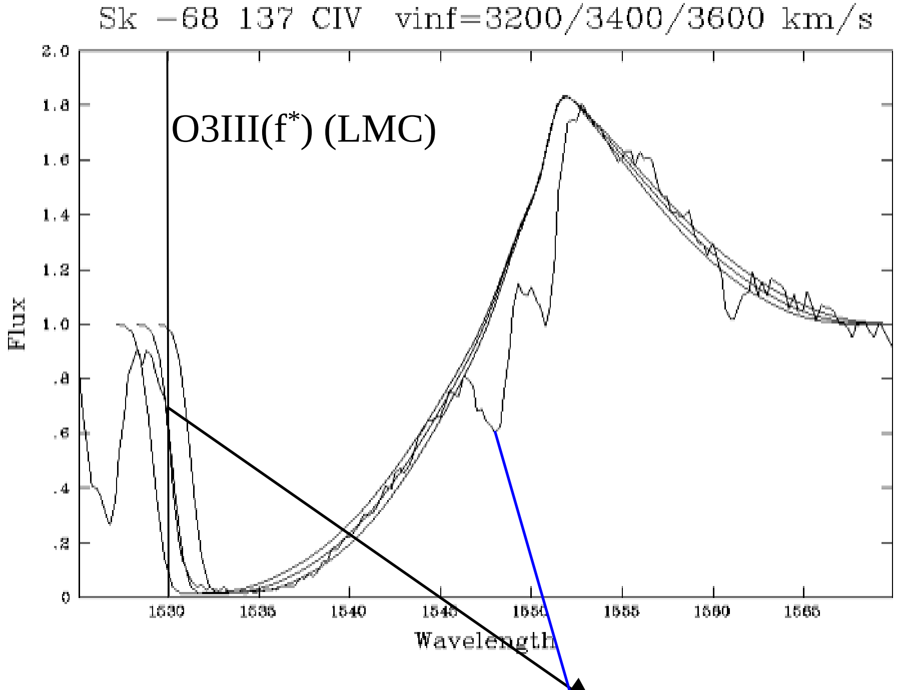

$$v_{\rm m} \approx 2.998\cdot 10^5\left(1-\frac{1530}{1548}\right) \approx 3,480 \text{ km/s}$$

Determination of mass-loss rate from H_α

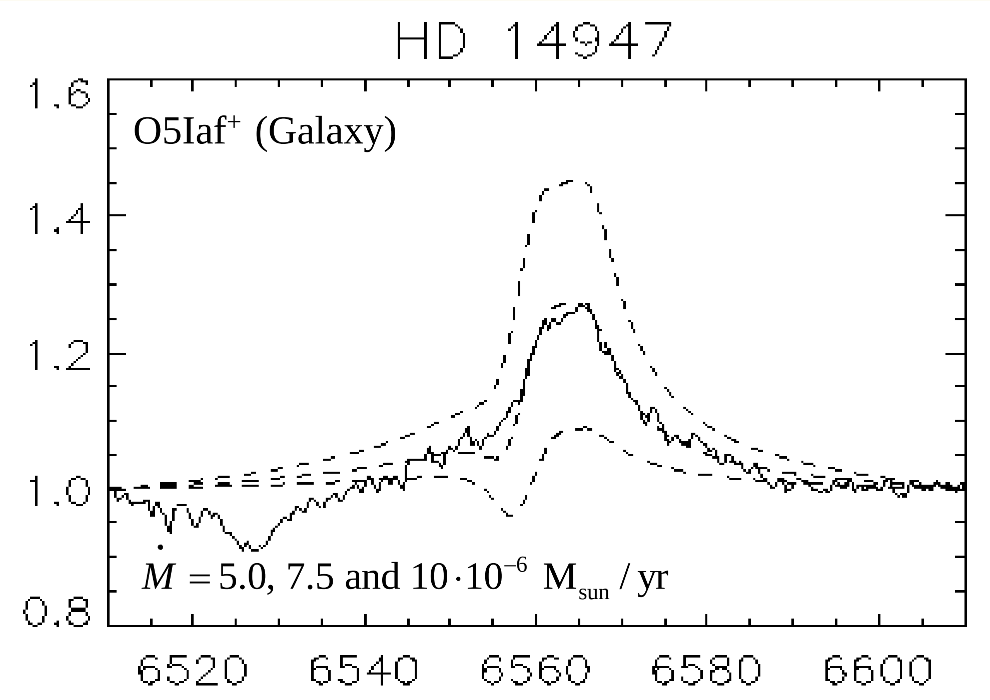

Note: Wind parameters can be cast into one quantity

$$Q = \frac{\dot{M}}{(R_* v_\infty)^{1.5}} \quad \text{or} \quad Q' = \frac{\dot{M}}{R_*^{1.5}}$$

For same values of $Q^{(')}$ (albeit different combinations of Mdot, v_∞ and R_*), profiles look almost identical!

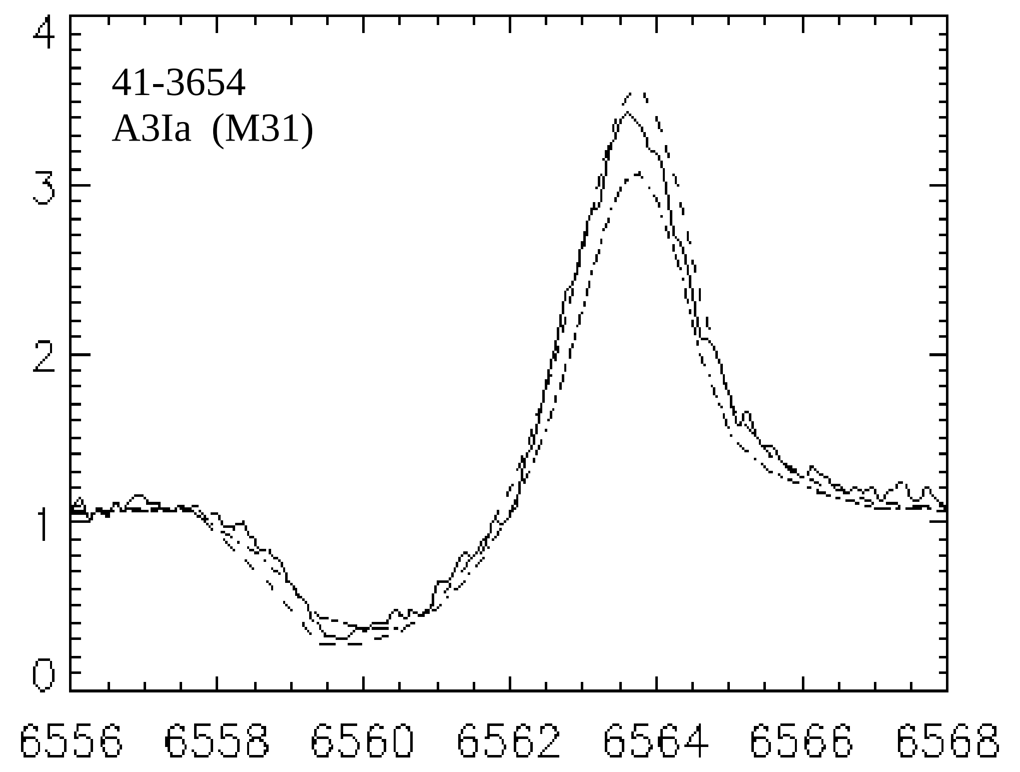

H_α taken with the Keck HIRES spectrograph, compared with two model calculations adopting $\beta = 3$, $v_\infty = 200$ km/s and *Mdot* = 1.7 and 2.1 $\times 10^{-6}\ \mathrm{M_{sun}/yr}$.

Observed WLR

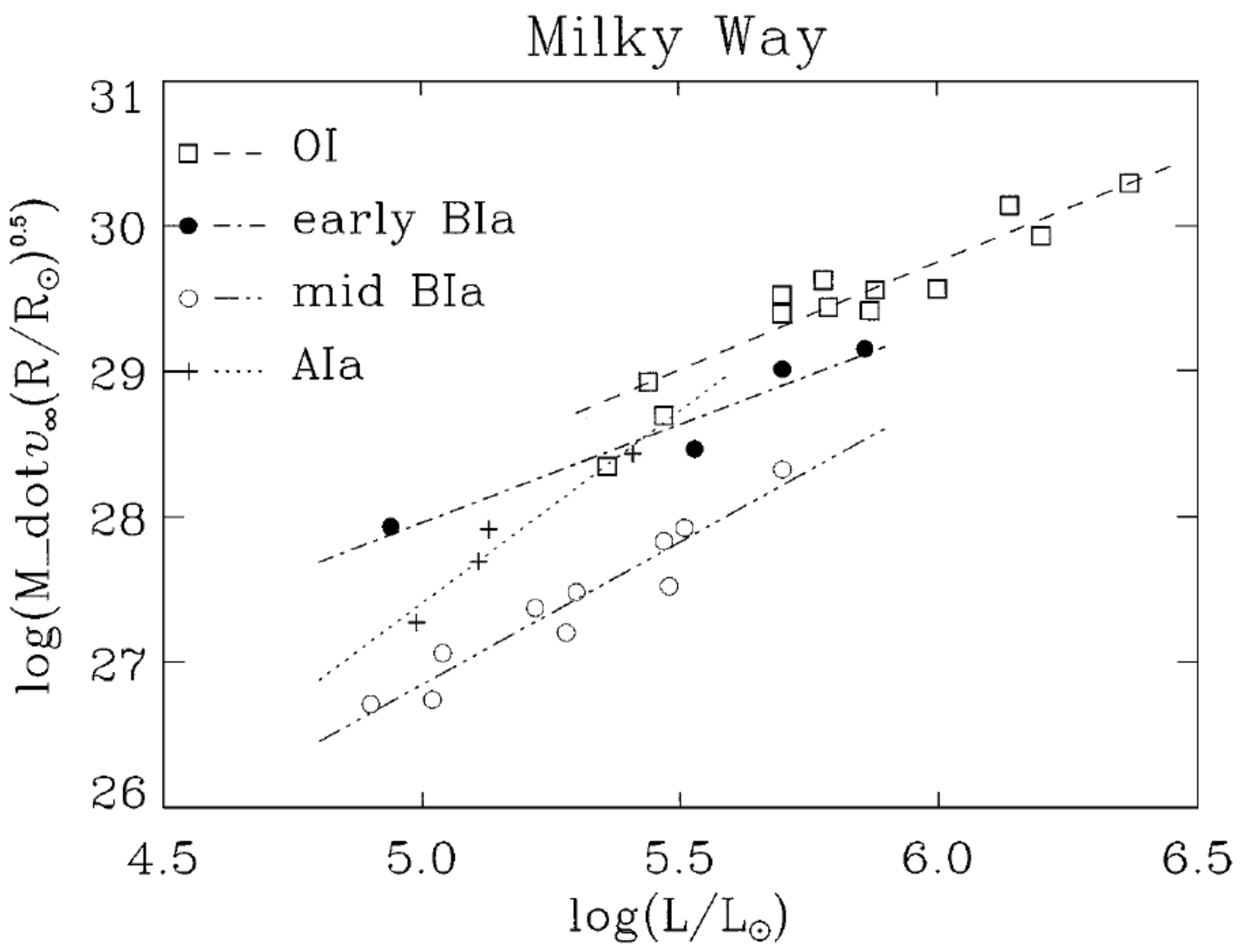

Modified wind momenta of Galactic O-, early B-, mid B- and A-supergiants as a function of luminosity, together with specific WLR obtained from linear regression. (From Kudritzki & Puls, 2000, ARAA 38).

η Car: Aspherical ejecta

image by HST

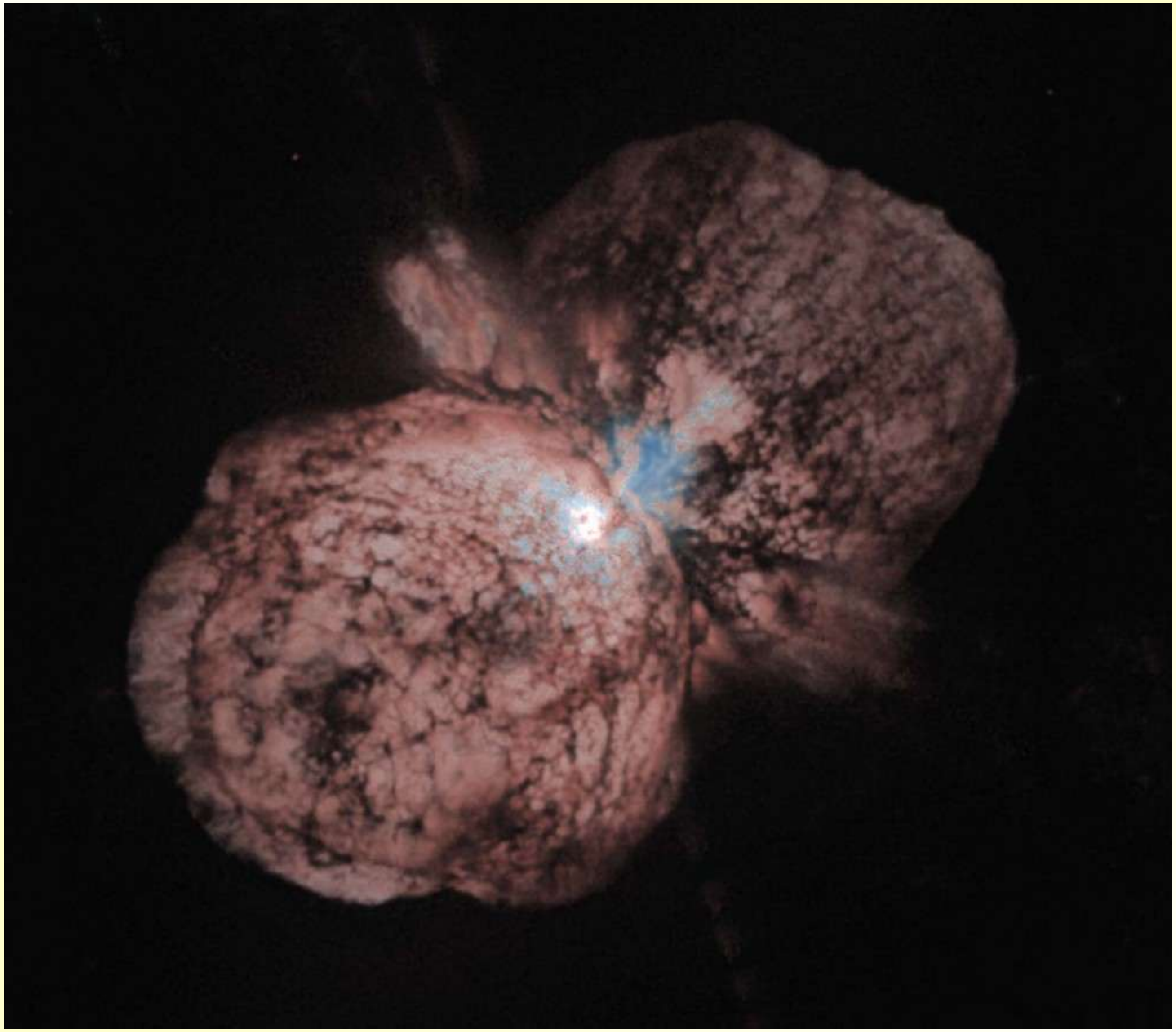

Influence of rotation

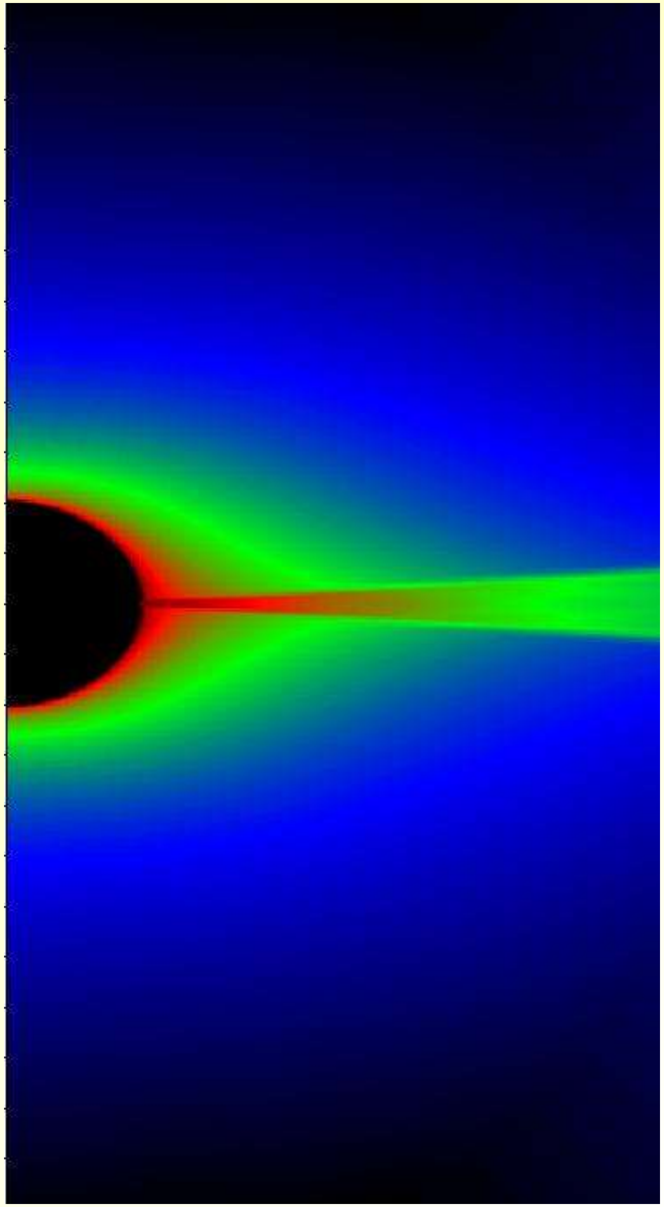

hot, massive stars = young stars

rapidly rotating (up to several 100 km/s)

twofold effect
- star becomes “oblate”
- wind has to react on additional centrifugal acceleration, large in equatorial, small in polar regions

Prolate or oblate wind structure?

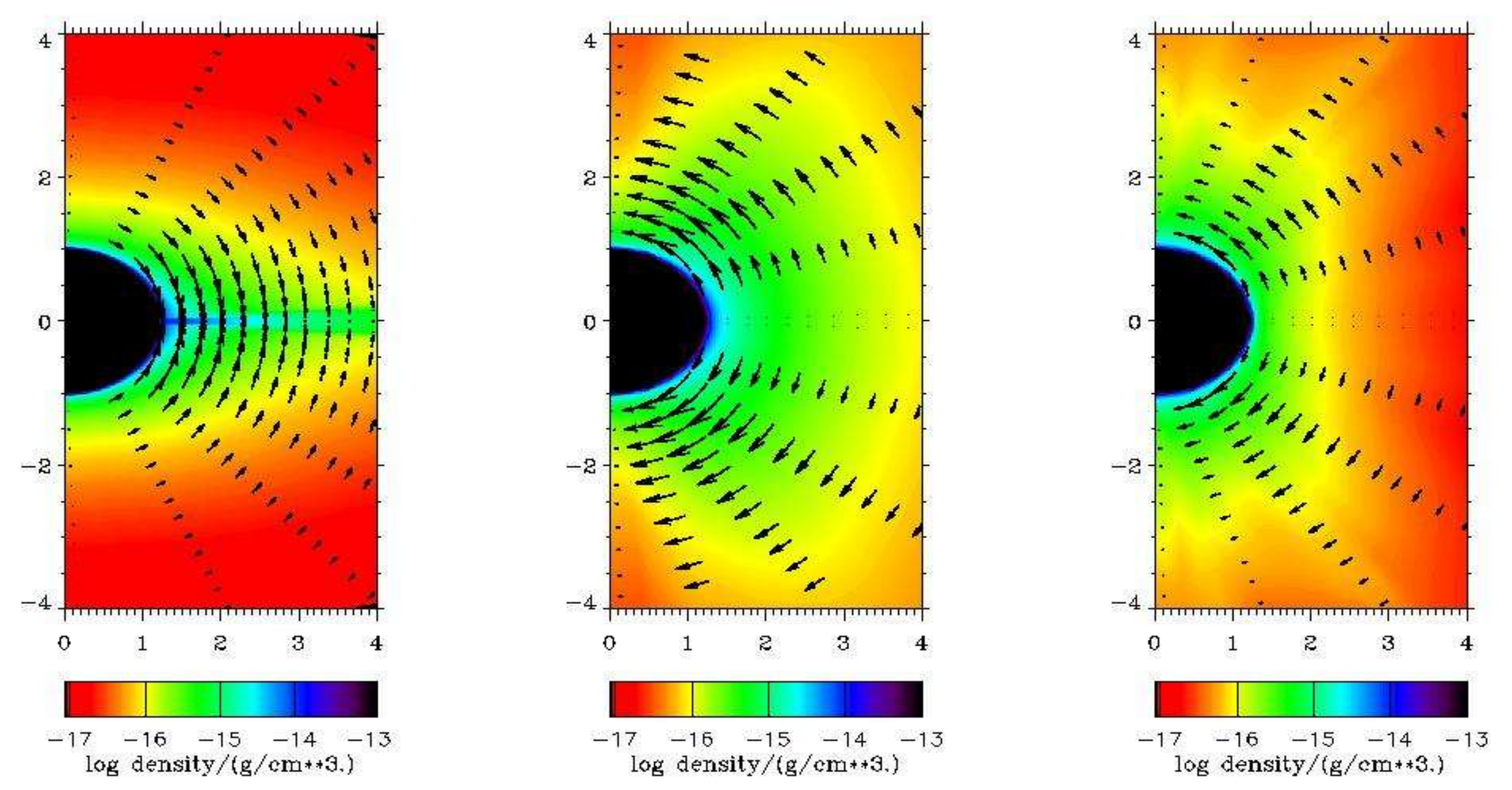

purely radial radiative acceleration:
wind-compressed disk

inclusion of non-radial component of line-acceleration (rotation breaks symmetry)

non-radial line-acceleration plus „gravity darkening“:
prolate geometry

The line-driven instability

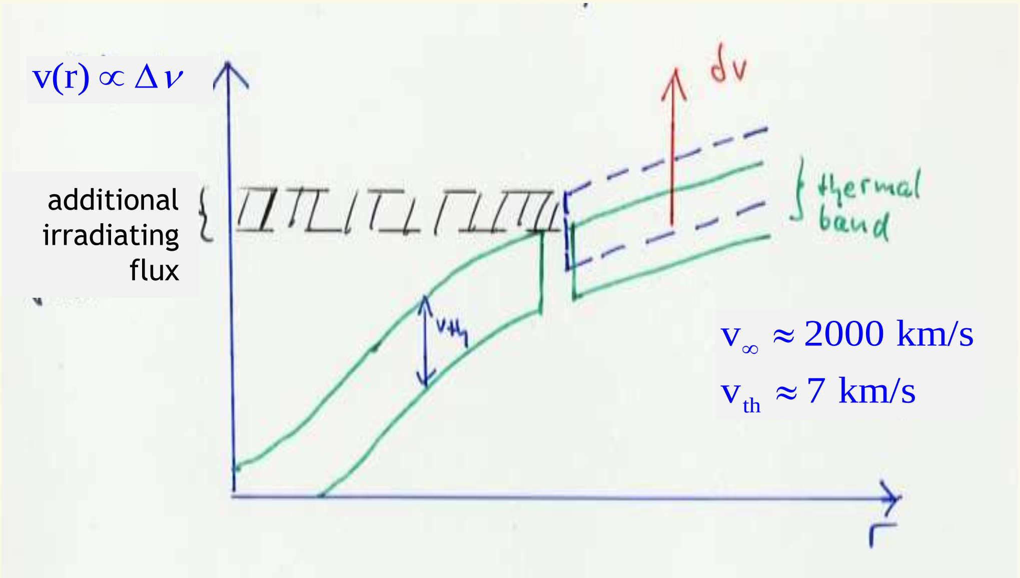

perturbation δv ↑

→ profile shifted to higher freq.

→ line 'sees' more stellar flux

→ line force grows δg ↑

→ additional acceleration δv ↑

exponential growth of perturbation

$\delta g_{Rad} \propto \delta v$

[for details, see MacGregor et al.1979 and Carlberg 1980]

Time dependent hydro-simulations of line-driven winds: Snapshot of density, velocity and temperature structure

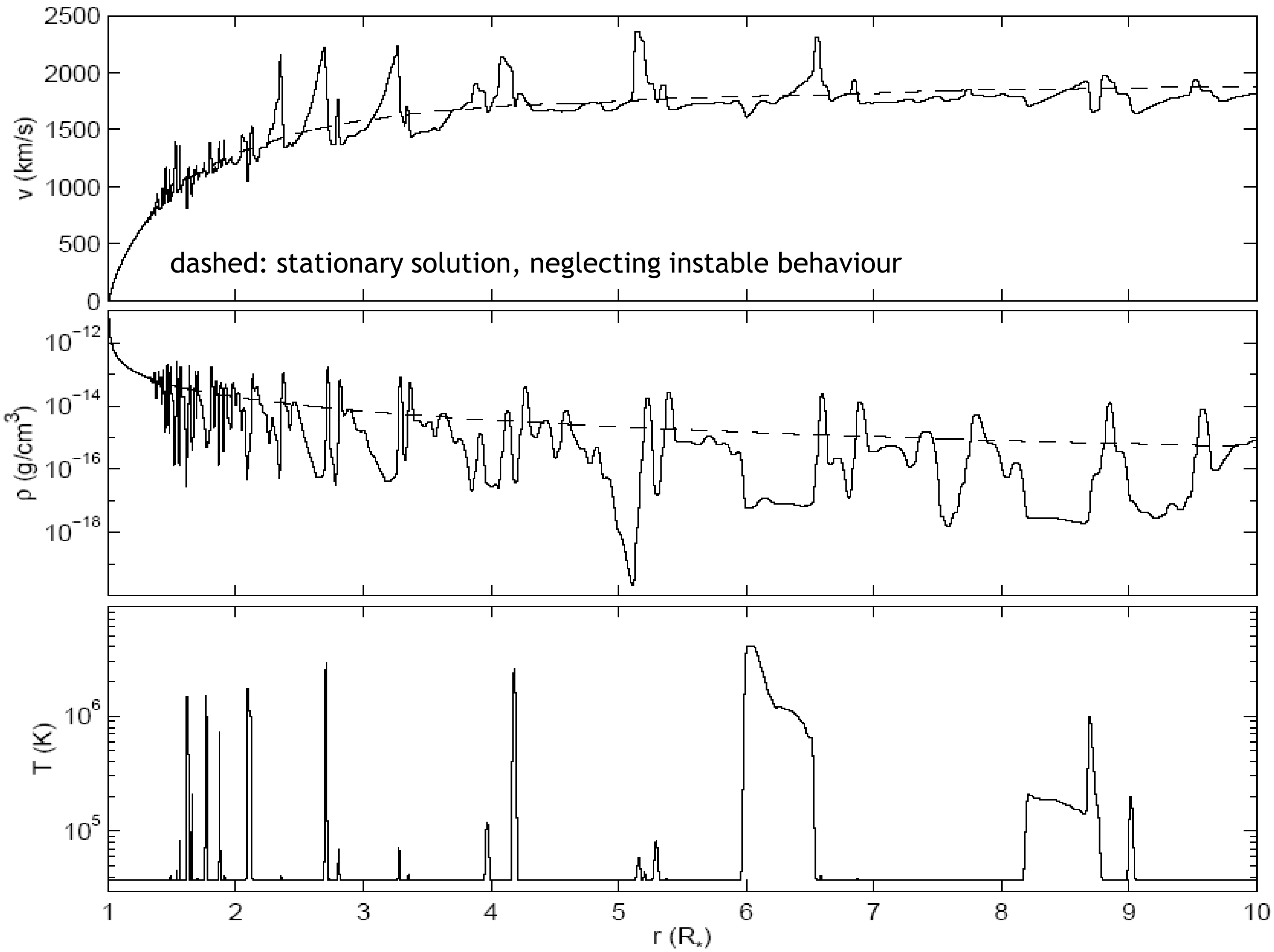

dashed: stationary solution, neglecting instable behaviour

average hydro-structure not too different from stationary approx.: Most line profiles fairly similar, but effect ("clumping") needs to be accounted for in analysis

(very) hot gas
→ X-ray emission
(observed!)

From Runacres & Owocki, 2002, A&A 381

The clumping factor

$$f_{\mathrm{cl}} = \frac{\langle \rho^2 \rangle}{\langle \rho \rangle^2} \geq 1 \text{ always! } (= 1 \text{ only for smooth flows})$$

brackets denote temporal averages

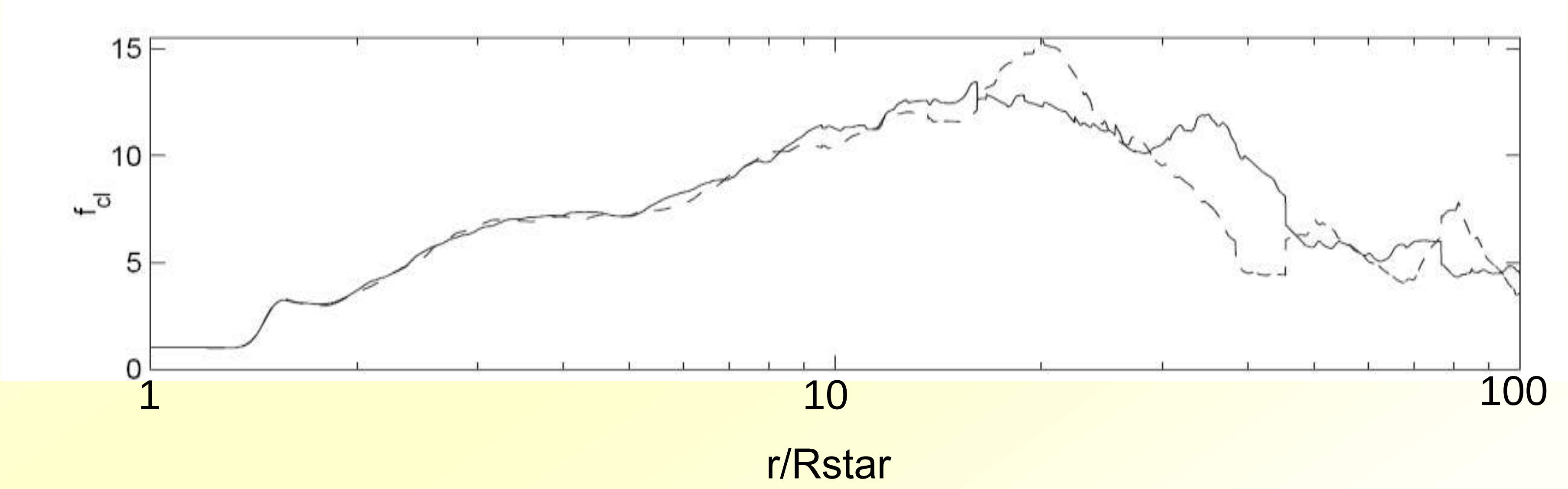

Inhomogeneities have to be accounted for in model atmospheres/spectrum synthesis!

Clumping and X-ray emission in hot stars

density and temperature evolution
as a function of time

(very) hot gas
→ X-ray emission
(observed!)

hydrodynamical simulations of unstable hot star winds, from Feldmeier et al., 1997, A&A 322

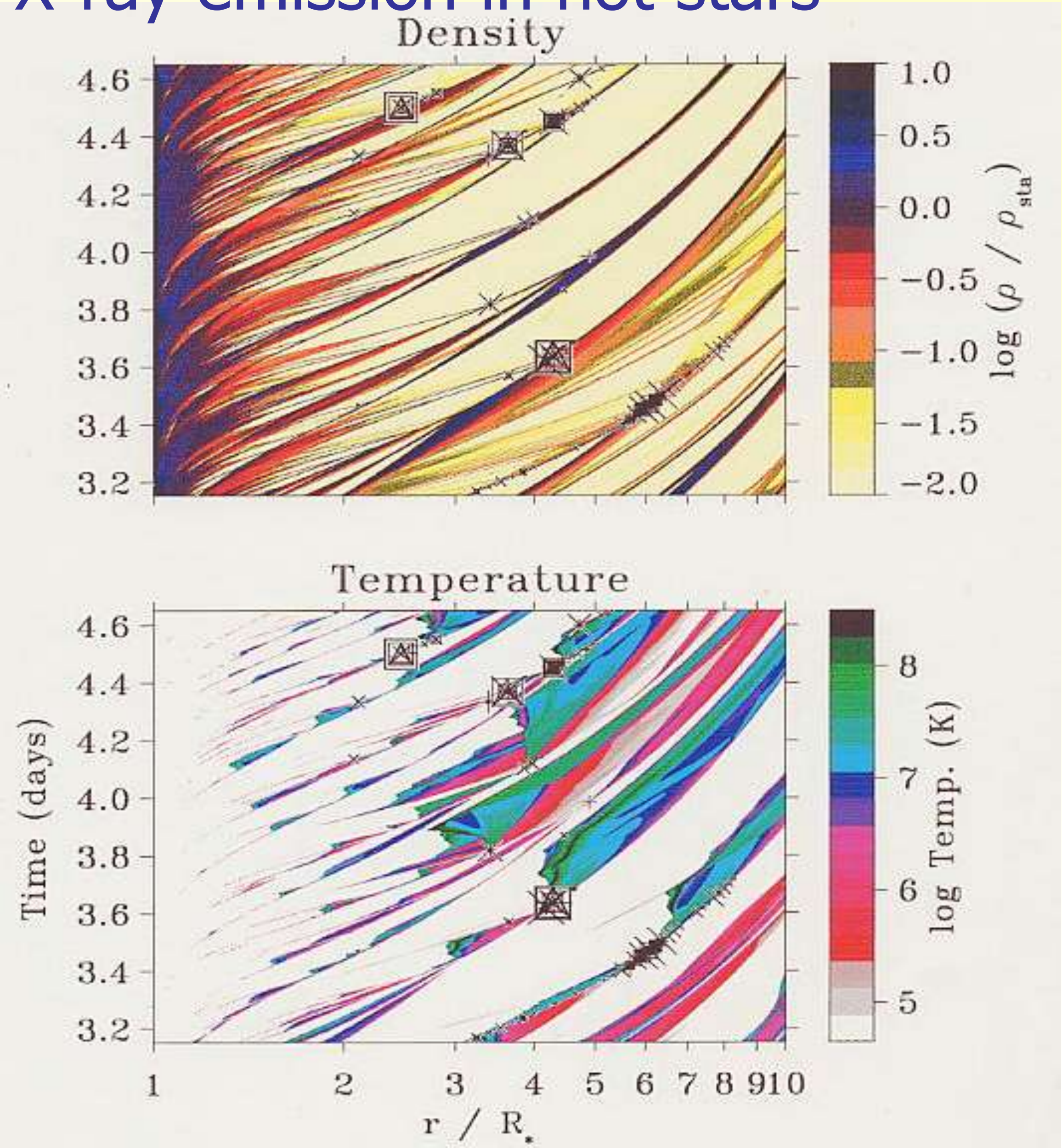

Density evolution in an unstable wind

x

X-ray "flash"

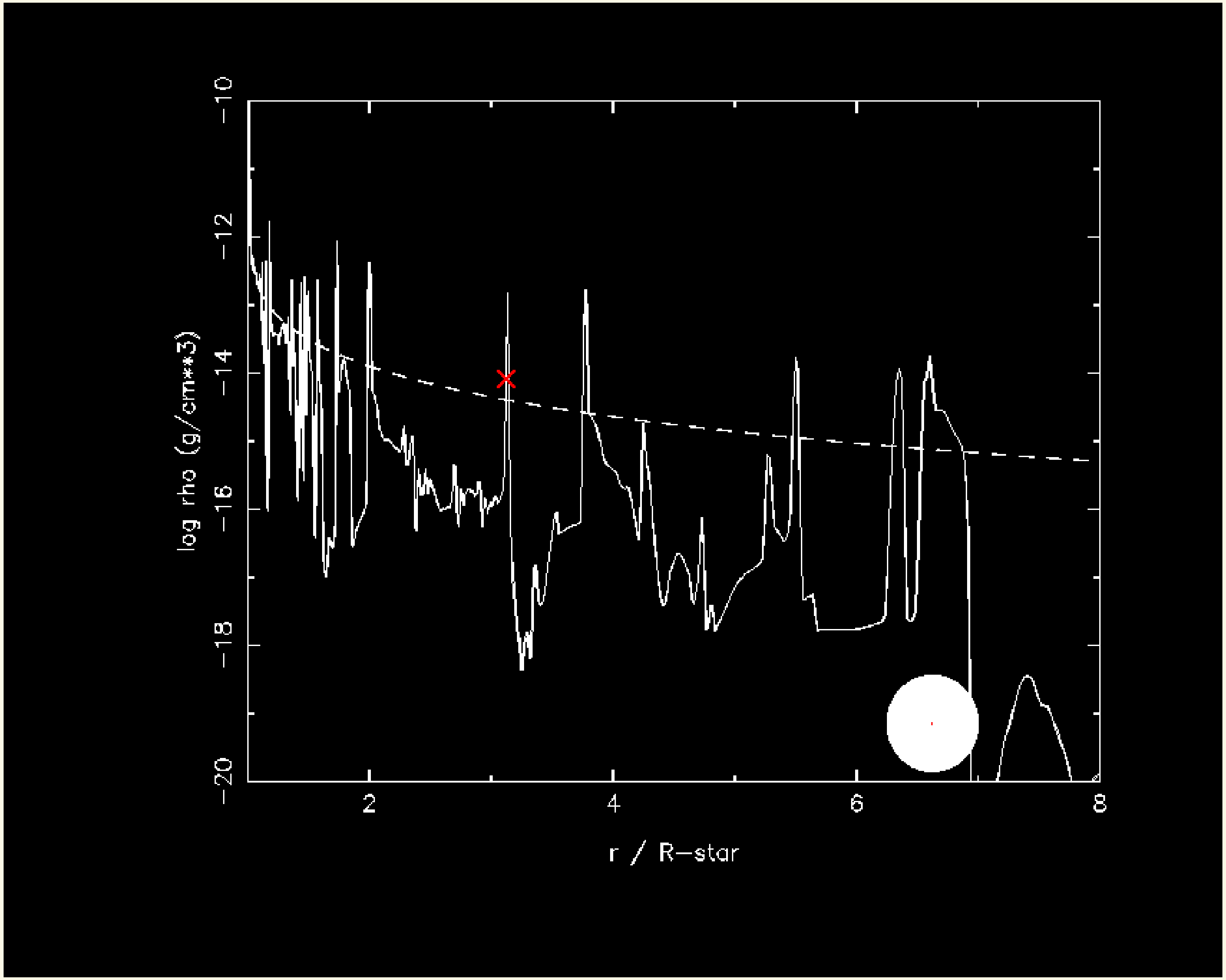

Chap. 9 Quantitative spectroscopy
The exemplary case of hot stars

Determine atmospheric parameters from observed spectrum

Required

$T_{\rm eff}$, log g, R, $Y_{\rm He}$, Mdot, v_∞, β (+ metal abundances)
(R stellar radius at $\tau_{\rm R} = 2/3$)

also necessary

$v_{\rm rad}$ (radial velocity)
v sin i (projected rotational velocity)

Given

- *reduced* optical spectra (eventually +UV, +IR, +X-ray)
- λ/Δλ, resolution of observed spectrum
- Visual brightness V
- distance d (from cluster/association membership), partly rather insecure
- NLTE-code(s), "model grid"

1. Rectify spectrum, i.e. divide by continuum (experience required)
2. Shift observed spectrum to lab wavelengths (use narrow **stellar** lines as reference):

$$\lambda_{\rm lab} \approx \lambda_{\rm obs}\left(1-\frac{v_{\rm rad}}{\rm c}\right),\quad v_{\rm rad} \text{ assumed as positive if object moves away from observer}$$

- **Alternative set of parameters**

L, M, R *or*
L, M, $T_{\rm eff}$ *or*
$T_{\rm eff}$, log g, R …

- **interrelations**

$$L = 4\pi R_*^2 \sigma_B T_{\rm eff}^4$$

$$g = \frac{GM}{R_*^2}$$

- **Useful scaling relations**

If L, M, R in *solar units*, then

$$R_* = \frac{L^{0.5}}{T_{\rm eff}^2}\cdot 3.327\cdot 10^7$$

$$\log g = \log\left(\frac{M}{R_*^2}\cdot 2.74\cdot 10^4\right)$$

$$v_{\rm esc} = \sqrt{R_* g(1-\Gamma)\cdot 1.392\cdot 10^{11}}$$

$$\Gamma = s_{\rm e} T_{\rm eff}^4 / g \cdot 1.8913\cdot 10^{-15}$$

$$s_{\rm e} = 0.4\frac{1+I_{\rm He}Y_{\rm He}}{1+4Y_{\rm He}},$$ cf. page 103

with $I_{\rm He}$ number of free electrons per Helium atom (e.g.,=2, if completely ionized) rectified **optical spectrum,** ("blue" and "red") corrected for v_{rad}, of the late O-SG *19 Cep*

___ Hydrogen
...... Helium I
- - - Helium II

in "red":
"strategic" lines to derive atmospheric parameters in hot stars

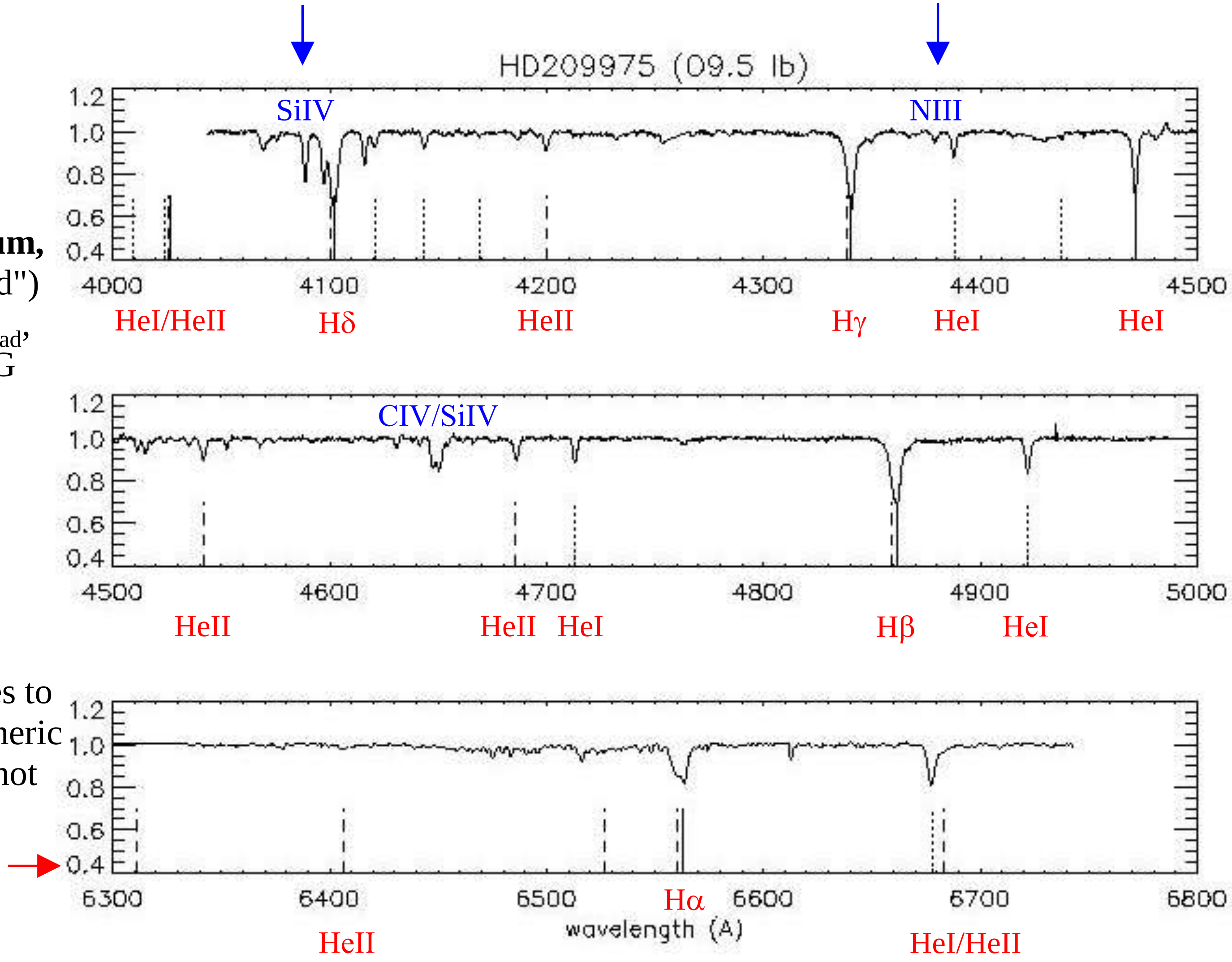

Equivalent width $W_\lambda = \int\limits_{\text{line}} \frac{H_{\text{cont}} - H_{\text{line}}(\lambda)}{H_{\text{cont}}} d\lambda = \int\limits_{\text{line}} \left(1 - R(\lambda)\right) d\lambda,$

area of profile under continuum, $\dim[W_\lambda]$ = Angstrom or milliAngstrom, mÅ

corresponds to width of saturated profile $(R(\lambda) = 0)$ with same area

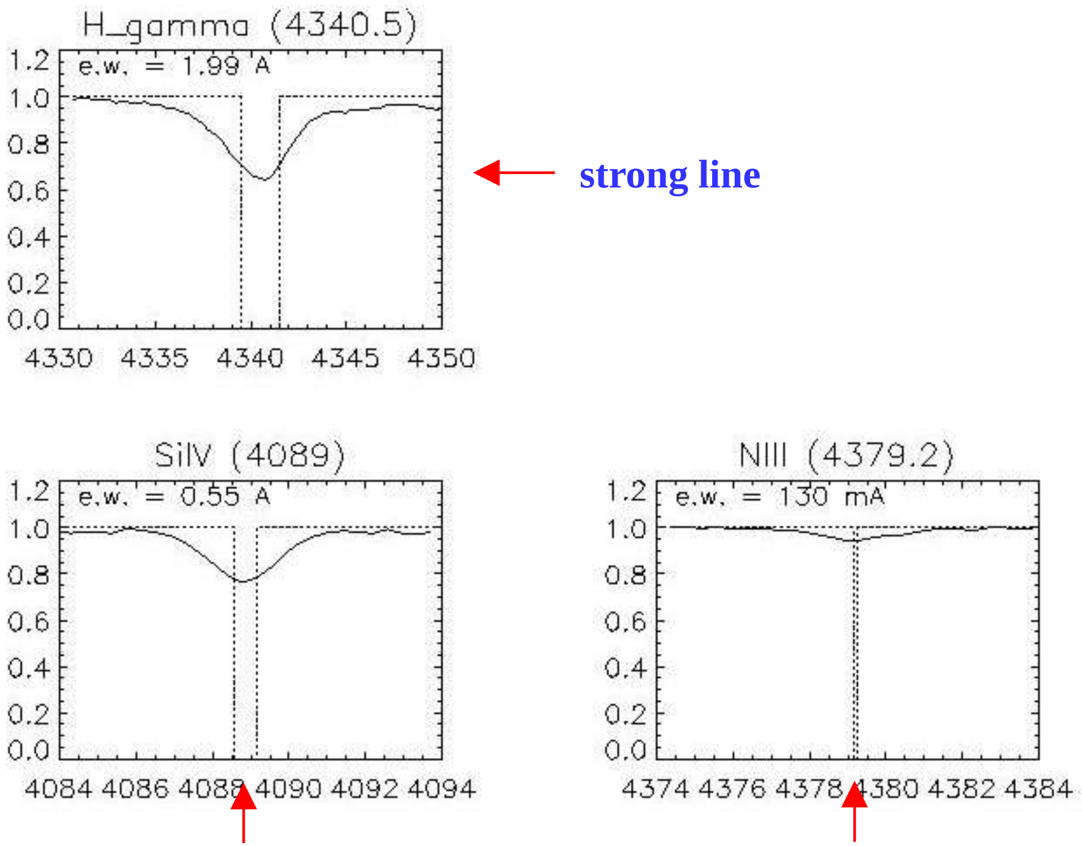

strong line

intermediate line

weak line

Determine projected rotational speed v sin i

Use weak metal lines
to derive v sin i:
Convolve theoretical line
with rotational profile.

Convolve finally with
instrumental profile
(~ Gauss) according
to spectral resolution

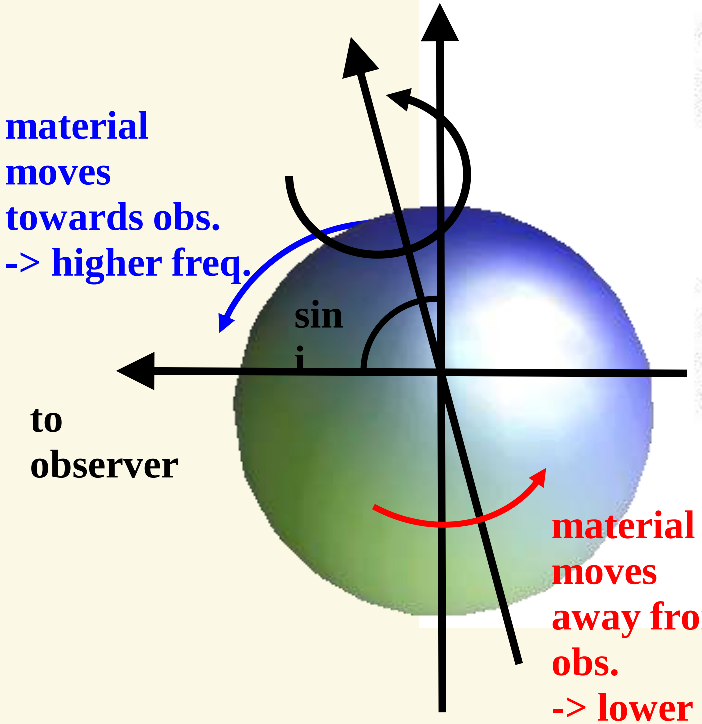

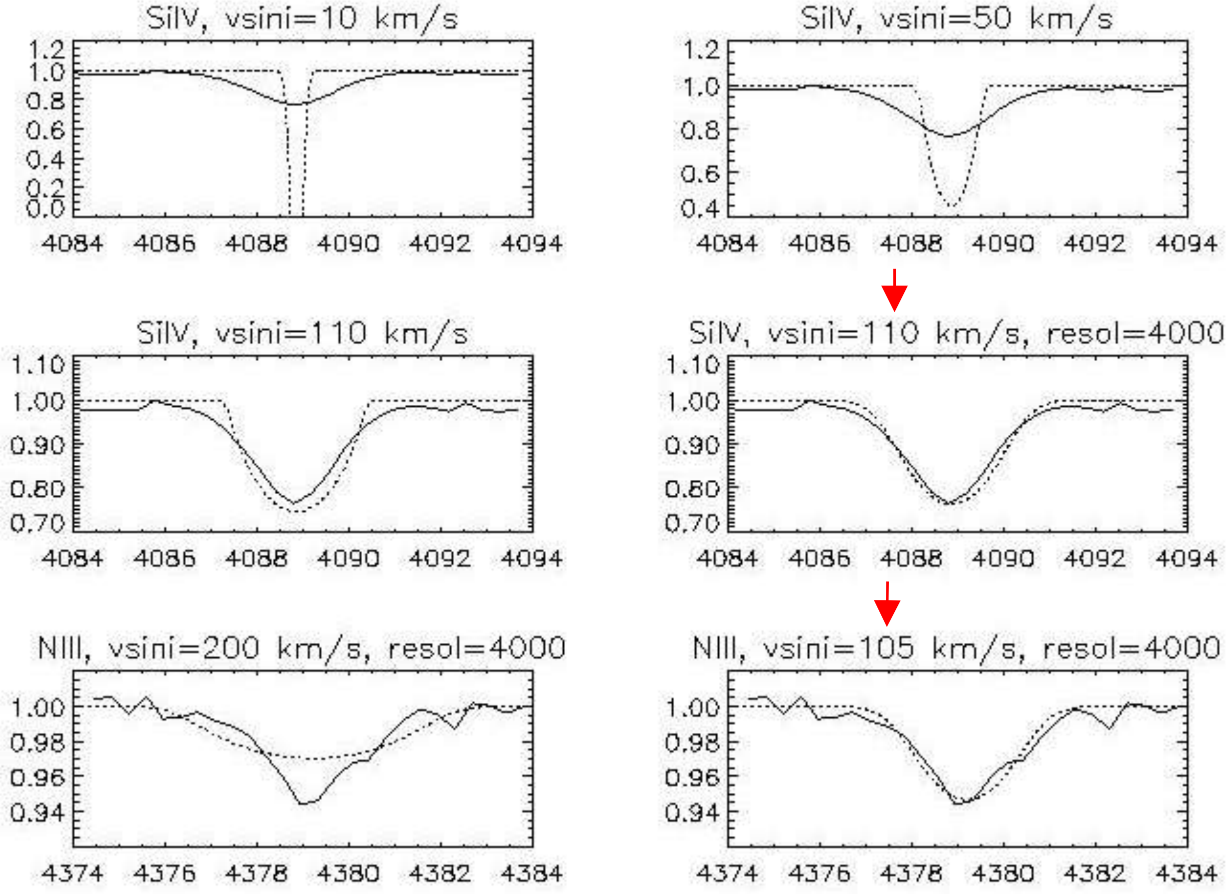

Convolution with rotational and instrumental profile conserves equivalent width!!!

Recent methods use a Fourier technique to infer vsini

Hγ - log g and T_{eff}

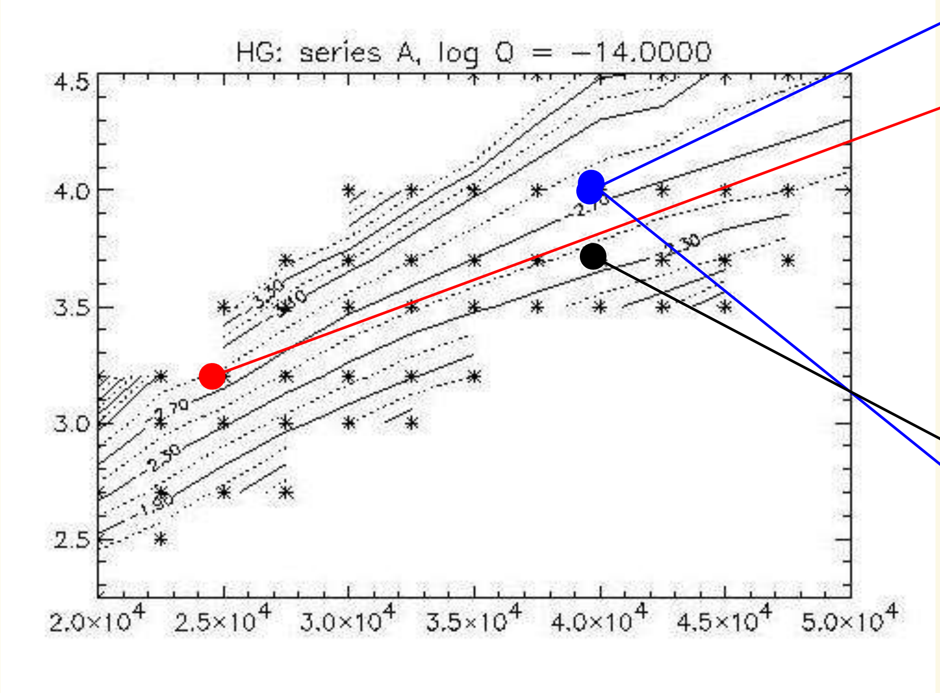

Iso-contours of equiv. widths for Hγ (from model grid), for solar Helium abundance and (very) thin winds

to derive T_{eff}, log g and Y_{He},
at least 3 lines have to be fitted in parallel
(if no wind is present):

Hγ defines **log g** (for given T_{eff})
HeII/HeI define $\mathbf{T_{eff}}$ (for given log g)
absolute **strength of He lines** define $\mathbf{Y_{He}}$

usually, wind emission has to be accounted for (profiles shallower)

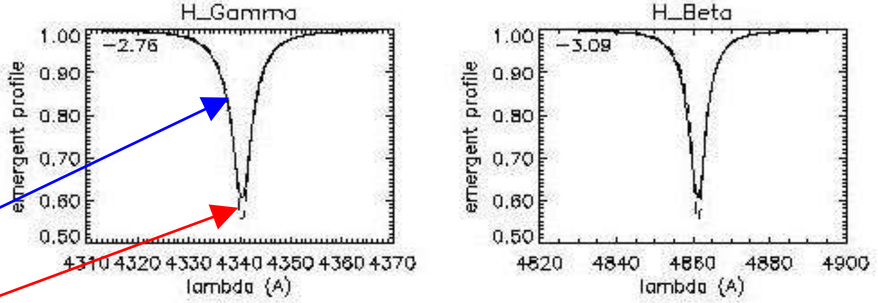

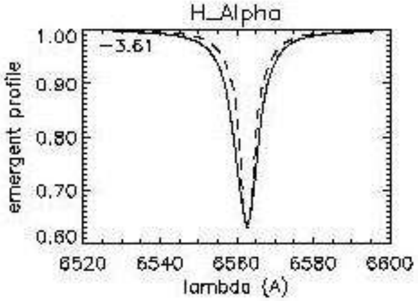

degeneracy of profiles:
(almost) identical lines for
T_{eff} =40,000 and log g=4.0
and
T_{eff} =25,000 and log g=3.2

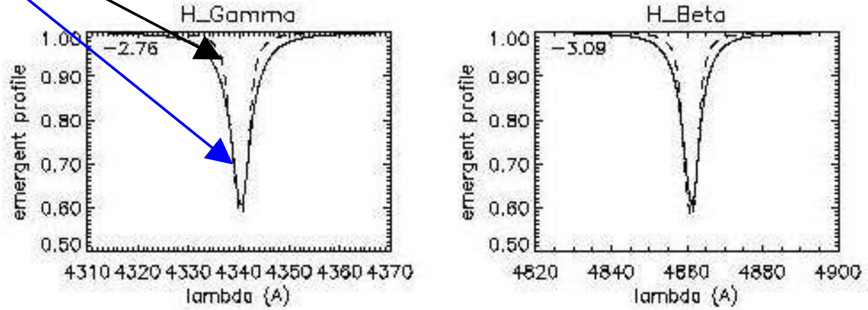

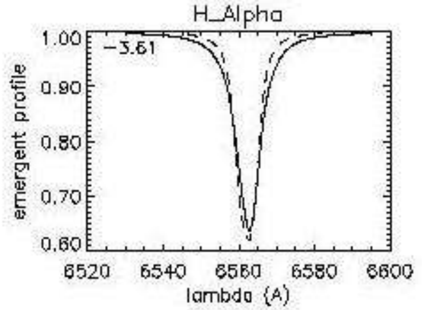

wings of Balmer lines
(Stark-broadened)
react strongly on electron-density (as a function of τ)
=> perfect gravity indicator

Coarse fit - analysis of equivalent widths

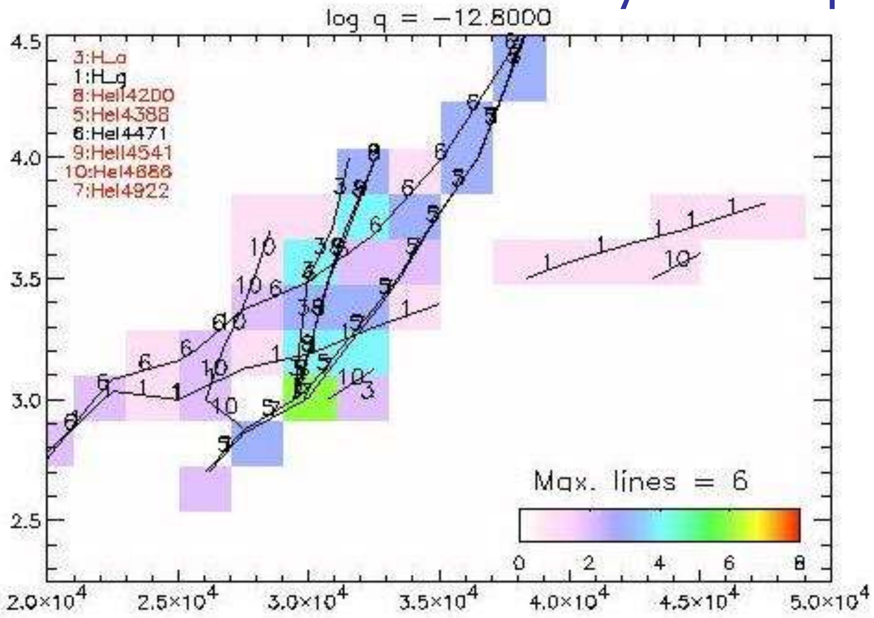

Fit diagram for Y_{He} = 0.1 (best fit at log Q = -12.8)

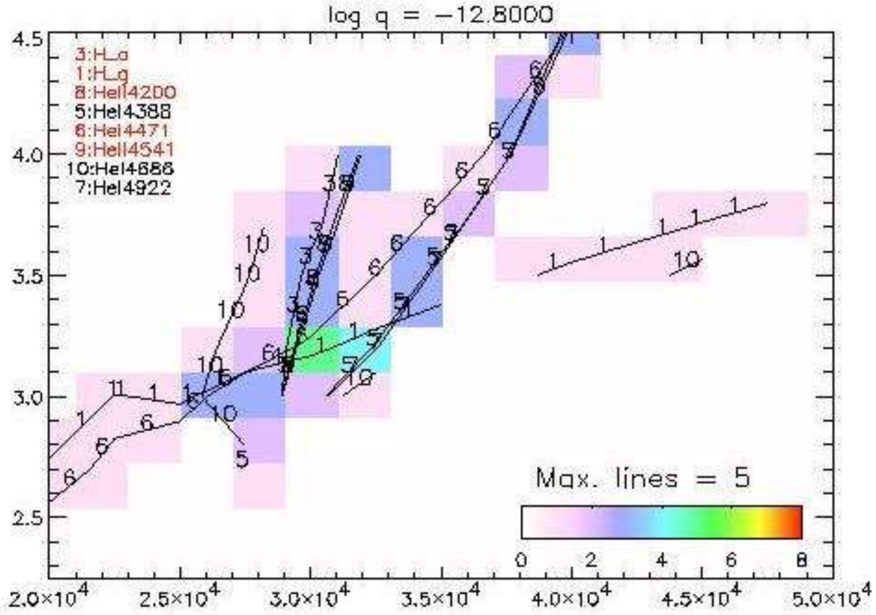

Fit diagram for Y_{He} = 0.15 (best fit at log Q = -12.8)

Measured equivalent widths

Balmer lines	**HeI**	**HeII**
Hγ 1.99	4387 0.32	4200 0.25
Hα 1.33	4471 0.86	4541 0.31
	4922 0.46	4686 0.27

Note: Hα and HeII 4686 mass-loss indicators

Result: $T_{eff} \approx$ 30,000 K, log g ≈ 3.0 ...3.2, $Y_{He} \approx$ 0.10 ... 0.15, log Q ≈ -12.8

Fit diagram constructed from model grid with

20,000 K < T_{eff} < 50,000 K with ΔT = 2,500 K

2.2 < log g < 4.5 with Δlog g = 0.25

-14 < log Q < -11 with Δlog Q = 0.3, Y_{He} = 0.10, 0.15, 0.20

Note: Wind parameters can be cast into one quantity

$$Q = \frac{\dot{M}}{(R_* v_\infty)^{1.5}}$$

For same values of Q (albeit different combinations of Mdot, v_∞ and R_*), profiles look almost identical!

Determination of terminal velocity from UV-P Cygni profiles

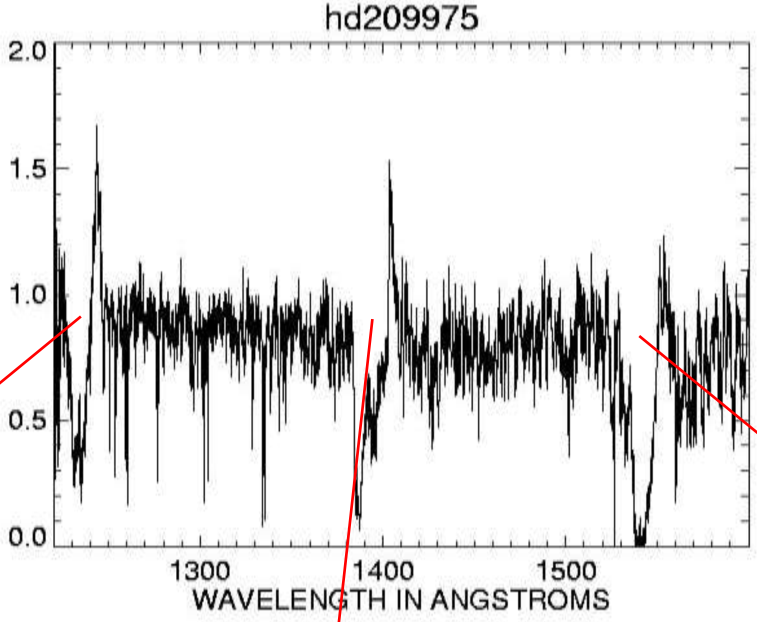

observation with IUE (International Ultra- violet Explorer)
no longer active

recent data (archive!) from HST (λ >1200 Å) and FUSE (λ > 911 Å)

NV

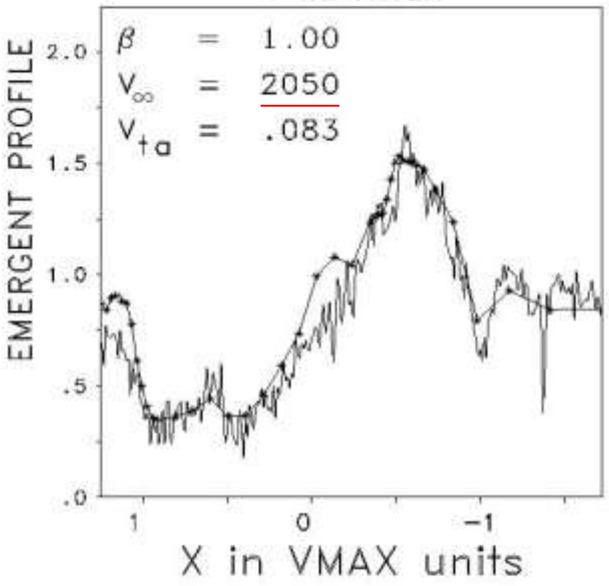

Si IV

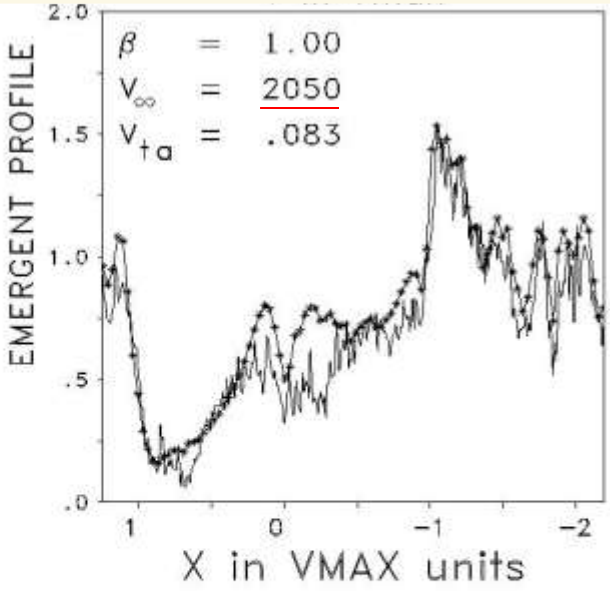

CIV

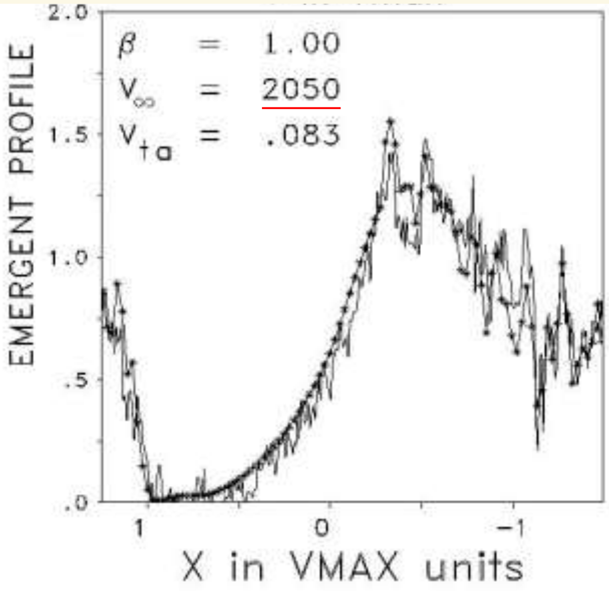

Fine fit - detailed comparison of line profiles

___ Hydrogen
...... Helium I
- - -Helium II

indicated lines used for fits

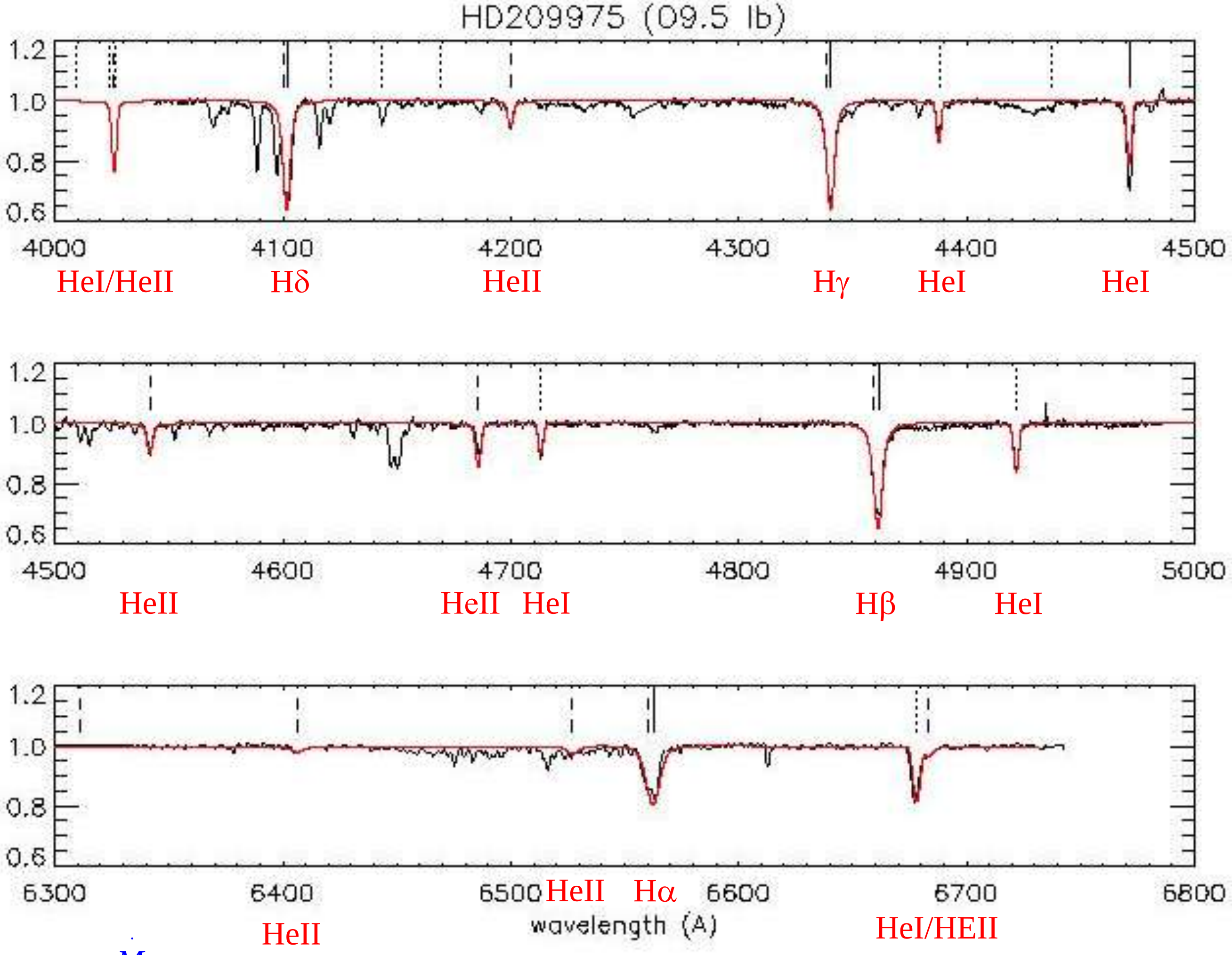

analysis via (semi-) automatic methods, based on high-dimensional model grids or genetic algorithms, to optimize the fit quality for a multitude of lines

derived parameters

T_{eff} = 31,000 K
log g = 3.17
log Q = -12.87
Y_{He} = 0.10
β = 1.0

with v_∞ = 2050 km/ s we have

$$\log(\dot{M}/R_*^{1.5}) = -7.9$$

$$Q = \frac{\dot{M}}{(R_* v_\infty)^{1.5}}$$

Determination of stellar radius – if it cannot be resolved

- **IF** *you believe in stellar evolution*
  - use **evolutionary tracks** to derive M from (measured) T_{eff} and log g **=> R**
  - transformation of conventional HRD into log T_{eff} - log g diagram required
  - for many massive objects, "mass discrepancy": “spectroscopic masses” and “evolutionary masses” not consistent, discrepancy presumably related to photospheric turbulence pressure and mass-loss rates (Markova et al. 2018)

- **IF** *you know the distance* (e.g., from GAIA) **and** *have theoretical fluxes* (from model atmospheres):

- **IF** *you believe in radiation driven wind theory*
  - use **wind-momentum luminosity relation**

$$V = -2.5\log \int_{\text{filter}} \mathcal{F}_\lambda S_\lambda d\lambda + \text{const}$$

S_λ spectral response of photometric system

absolute flux calibration

$V = 0$ corresponds to $\mathcal{F}_\lambda = 3.66 \cdot 10^{-9}$ erg s^{-1} cm^{-2} Å^{-1} at $\lambda_0 = 5{,}500$ Å outside earth's atmosphere

λ_0 *isophotal* wavelength such that $\int_{\text{filter}} \mathcal{F}_\lambda S_\lambda d\lambda \approx \mathcal{F}(\lambda_0) \int_{\text{filter}} S_\lambda d\lambda$, $\int_{\text{filter}} S_\lambda d\lambda \approx 2895$ for Johnson V-filter

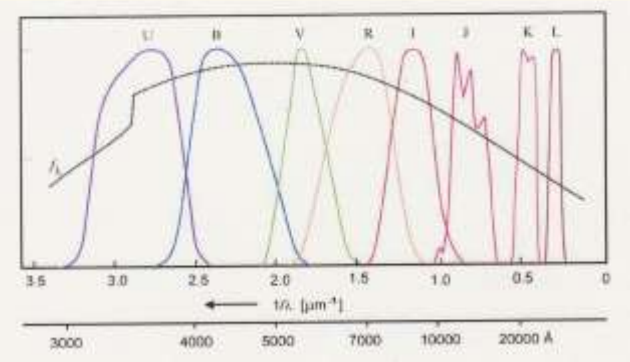

$\Rightarrow$

$$\text{const} = -2.5\log(3.66 \cdot 10^{-9} \cdot 2895) = -12.437$$

$$M_V = -2.5\log\left[\left(\frac{R_* R_{\text{sun}}}{10\text{ pc}}\right)^2 \int_{\text{filter}} \mathcal{F}_\lambda S_\lambda d\lambda\right] + \text{const}$$

$$5\log R_* = 29.553 + (V_{\text{theo}} - M_V)$$

if R_* in solar units, M_V the absolute visual brightness (from V(observed), distance and reddening) and

$V_{\text{theo}} - 2.5\log \int_{\text{filter}} 4H_\lambda S_\lambda d\lambda$ with H_λ the *theoretical* Eddington flux in units of [erg s^{-1} cm^{-2} Å^{-1}]

Alternatively, use bolometric correction (BC)

Calibration for Galactic O-stars:

$$BC = M_{\rm Bol} - M_V \approx 27.58 - 6.8\log(T_{\rm eff}) \quad \text{(see Martins et al. 2005, A\&A 436)}$$

and definition of $M_{\rm Bol}$

$$\log\frac{L}{L_\odot} = 4\log\frac{T_{\rm eff}}{T_{\rm eff,\odot}} + 2\log\frac{R_*}{R_\odot} = 0.4(M_{\rm Bol,\odot} - M_{\rm Bol})$$

$$\log\frac{R_*}{R_\odot} = 0.2(4.74 - M_{\rm Bol}) - 2\log\frac{T_{\rm eff}}{5770} =$$

$$= 0.2(4.74 - M_{\rm V} - 27.58 + 6.8\log(T_{\rm eff})\ ) - 2\log\frac{T_{\rm eff}}{5770} =$$

$$= 2.954 - 0.2M_{\rm V} - 0.64\log(T_{\rm eff})$$

[valid only for O-stars with $Z \approx Z_\odot$]

remember relation between M_V and V (distance modulus)

$\boxed{M_V = V + 5(1 - \log d) - A_V}$, d distance in pc, A_V reddening

d from parallaxes (GAIA) or cluster/ association/ galaxy membership (hot stars)
(note: clusters/ assoc. radially extended!)

For Galactic objects, use compilation by
Roberta Humphreys, 1978, ApJS 38, 309 *and/or*
Ian Howarth & Raman Prinja, 1989, ApJS 69, 527

Back to our example

HD 209975 (19 Cep): $M_v = -5.7$
check: belongs to Cep OB2 Assoc., d ≈ 0.83 kpc
$V = 5.11$, $A_V = 1.17$ => $M_V = -5.65$, OK

From our final model, we calculate $V_{theo} = -29.08$ => $R = 17.4\ R_{sun}$
(Alternatively, by using BC, M_V and $T_{eff} = 31$kK, we would obtain $R = 16.6\ R_{sun}$)

Finally, from the result of our fine fit, $\log(\dot{M} / R_*^{1.5}) = -7.9$, we find $\dot{M} = 0.91 \cdot 10^{-6}\ M_{sun}$ / yr

Finished, **determine metal abundances if required,**
next star ....

… but end of lecture!!!